University of Montana

ScholarWorks at University of Montana

2021

FUN CTIONAL IMPLICATIONS OF DUAL TRANSMITTING NEURONS ON AGGRESSION

Lewis Michael Sherer II

Follow this and additional works at: https://scholarworks.umt.edu/etd

Let us know how access to this document benefits you.

FUNCTIONAL IMPLICATIONS OF DUAL TRANSMITTING NEURONS ON AGGRESSION

By

LEWIS MICHAEL SHERER II

Bachelor of Science, Texas A&M University, College Station, TX, 2014

Dissertation

presented in partial fulfillment of the requirements
for the degree of

Doctor of Philosophy
in Cellular, Molecular, and Microbial Biology

The University of Montana
Missoula, MT

August 2021

Approved by:

Scott Whittenburg,
Graduate School Dean

Sarah Certel, Chair
Division of Biological Sciences

Ekaterina Voronina
Division of Biological Sciences

Jesse Hay
Division of Biological Sciences

Mark Grimes
Division of Biological Sciences

R. Steven Stowers
Department of Microbiology and Immunology

Table of Contents

Acknowledgements

I've always found it odd that in scientific writing, the convention is to include the acknowledgements at the very end. I find this odd because I think it does an incredible disservice to the environment from which the intellectual achievement sprang. A feat such as an academic paper (or indeed, a dissertation) is never the work of one person, or even a few. It is the culmination of a society that provides the infrastructure, friends and family who provide support, and the general intellectual milieu in which an individual stews. I would like to thank every workman who paved the roads that I rode my bike to the lab on every day, every acquaintance who offered a passing word of support, every scholar whose shoulders I stand on, if only I had the space and time. I will settle for taking the time to recognize some important influences here.

Words are insufficient to express my gratitude to my thesis advisor, Dr. Sarah Certel, but I will make an effort regardless. Thank you for your guidance when things were going well and patience when they were not. Thank you for your understanding and assistance with the financial concerns of graduate life. Thank you for your knowledgeable and diligent mentorship in improving my experiments, presentations, and writing. And of course, thank you for great and thought-provoking discussions on the issues of the day. I have tried to remember each day the kindness you showed me by accepting me into your lab as a master's, and later doctoral, student and consider myself incredibly lucky to have had a fantastic advisor for my graduate years. I sincerely hope my work in your lab has been sufficient to justify your faith in me. Thank you for everything.

I would like to thank my committee members, Dr. Ekaterina Voronina, Dr. Mark Grimes, Dr. Jesse Hay, and Dr. Steve Stowers for your support, encouragement, ideas, critiques, and input throughout the years.

I would like to thank our collaborators in the Stowers lab at Montana State University, especially Dr. Hannah McKinney, for such a fruitful collaboration which I count myself lucky to have been a part of. I would also like to thank Lou Herritt, Director of the Histology & Imaging Core, and David Xing, Manager of the Genomics Core, for technical expertise, Dr. Budha Chowdhury for

invaluable assistance with automating behavioral analysis, and the Hay lab and the Voronina lab for sharing reagents and general helpfulness.

I would like to thank the bright undergraduate and high school students that I have had the privilege of working with over the years, including Ned Brewer, Sammy Clark, Lucy Sirrs, Tait Kuchenbrod, Samantha Chong, and Raegan Hauschildt for their diligence in data collection and valuable discussions about what these piles of graphs actually mean.

I would like to thank my undergraduate research mentor Dr. Spencer Behmer for getting me started in *Drosophila* research and additionally Dr. Laura Beaster-Jones and Dr. Bill Rixey for writing my recommendation letters for graduate school.

I would like to thank Dr. Rebecca Clark for being quite possibly the greatest postdoc mentor an undergraduate researcher could have asked for, and later an incredible resource about the process and pitfalls of applying to graduate school.

I would like to thank the Division of Biological Sciences office, especially Jill Burke for being a ray of light at the front desk and Zooey Zephyr, Janean Clark, and Ruth Johnson for being incredibly helpful with payroll issues, employment contracts, trip reimbursements, and course registration.

I would like to thank my parents, Bill and Shira Sherer, for always encouraging me to follow my interests, no matter which strange direction they led. I would like to thank my brother, Joseph Sherer, for being a friend and sharing in intellectual and recreational pursuits growing up. I would also like to thank my grandparents Lew and Stella Sherer for teaching me the importance of financial stewardship and for providing the means for my undergraduate education via the Texas Tomorrow fund, Joe and Joy Leyh for teaching patience and good humor, and Dr. Harvey and Jossie Huddleston, for fostering a love of seeking wisdom.

I would like to thank the friends that I made in Missoula or who took the time to visit me here from elsewhere, especially Hannah Morgan, Ashley Bielawski, Kacie Gries, Gered Wallace,

Sherer, Lewis, Ph.D., Summer 2021 *Cellular, Molecular, and Microbial Biology*

Functional Implications of Dual Transmitting Neurons on Aggression

Chairperson: Sarah Certel

Abstract

The phenomenon of dual transmission, or the ability of neurons to release more than one neurotransmitter, has become increasingly recognized as a fundamental mechanism of neuron communication within the nervous system. The release of multiple transmitters from a single neuron can generate diverse non-linear and novel consequences in downstream circuits, adding a layer of complexity to both the mechanisms that neurons use to communicate and the functional outputs of neurons. In this dissertation I characterize a set of dual transmitting neurons that express octopamine (the invertebrate norepinephrine analog) and glutamate and examine the functional implications of octopamine/glutamate dual transmission using two behaviors (aggression and courtship) as a readout. In chapter II, our collaborators and I characterize the expression patterns of octopamine α- and β-adrenergic-like receptors using MiMIC-converted Gal4 lines. We demonstrate that octopamine receptors are widely expressed within octopaminergic neurons and identify subsets of octopamine receptor expressing neurons that also express the glutamate receptor GluRIA. These findings suggest that octopamine/glutamate dual transmitting neurons can use octopamine and/or glutamate autoreceptors to promote or inhibit neurotransmitter release. In chapter III, I examined within VPM4, a single octopamine/glutamate dual transmitting neuron. I characterize VPM4 as an octopamine/glutamate dual transmitting neuron that expresses the glutamate autoreceptor mGluR and the octopamine autoreceptor OAα2R. I determine that both mGluR and OAα2R are required to constrain high-level aggressive behavior, but not mid-level aggressive behavior. Additionally, I identify a role for octopamine release from VPM4 in inhibiting courtship and determine that OAα2R expression is required octopamine-mediated courtship inhibition. These findings suggest a mechanism by which dual transmitting neurons may modulate their own activity to inhibit the release of neurotransmitters to downstream circuits.

Abbreviations

>	Drives expression of
5-HT	Serotonin
A1	Noradrenergic Cell Group A1
AD	Activation Domain
AL	Antennal Lobe
AMPA	α-amino-3-hydroxy-5-methyl-4-isoxazolepropionic acid
AMPH	Amphetamine
ASMP	Anterior Superior Medial Protocerebrum
ATP	Adenosine Triphosphate
B3RT	B3 Recombination Target Site
Brp	*bruchpilot*
C1	Adrenergic Cell Group C1
C2	Adrenergic Cell Group C2
C3	Adrenergic Cell Group C3
Ca2+	Calcium Ion
cAMP	Cyclic Adenosine Triphosphate
CG	*Drosophila* Protein-Coding Gene
ChI	Cholinergic Interneuron
Cl-	Chloride Ion
CNS	Central Nervous System
D2	Dopamine Receptor D2
DA	Dopamine Receptor D2
DBD	DNA-binding Domain
EAAT	Excitatory Amino Acid Transporter
EKAR	Eye-enriched Kainate Receptor
FFN206	Fluorescent False Neurotransmitter 206 (Fluorescent VMAT2 Substrate)
FruM	Male-Specific fruitless Isoform
GABA	γ-aminobutyric acid
GFP	Green Fluorescent Protein
Glu/Glut	Glutamate
GluClα	Glutamate-gated Chloride Channel
GluN/NMDAR	Glutamate Ionotropic Receptor NMDA Type
GluR	Glutamatergic Receptor
GPCR	G-Protein Coupled Receptor
Gr	Gustatory Receptor
GRIA	Glutamate Ionotropic Receptor AMPA Type
GRIK	Glutamate Ionotropic Receptor Kainate Type

GRP	Gastrin-releasing Peptide
HA	Hemagglutinin
HEK 293	Human Embryonic Kidney 293 (Immortalized Cell Line)
iGluR	Ionotropic Glutamate Receptor
JAABA	Janelia Automatic Animal Behavior Annotator
K+	Potassium Ion
KaiR1D	Kainate-type Ionotropic Glutamate Receptor Subunit 1D
KDRT	KD Recombination Target Site
LDCV	Large Dense-Core Vesicle
lexAop	lexA Operon
LNvs	Lateral-Ventral Pacemaker Neurons
mAb	Monoclonal Antibody
MB112C	MBON11-Gal4
MB113C	VPM4-Gal4
MB-MV1	Dopamine Neurons in Protocerebral Posterior Lateral Cluster
MBON	Mushroom Body Output Neuron
mEPSP	Miniature Excitatory Postsynaptic Potential
mGluR	Metabotropic Glutamate Receptor
MiMIC	Minos-Mediated Integration Cassette
MPN	Modulatory Proctolin Neuron
Na+	Sodium Ion
NAc	Nucleus Accumbens
NE/NA	Norepinephrine
NMDA	N-methyl-d-aspartic acid
NMJ	Neuromuscular Junction
NPY	Neuropeptide Y
nsyb/n-syb	Neuronal-synaptobrevin
OA/Oct	Octopamine
OAMB	Octopamine in Mushroom Bodies (α1 Adrenergic-like Receptor)
OAR/OctR	Octopaminergic Receptor
OAα2R	α2 Adrenergic-like Receptor
OAβ1R	β1 Adrenergic-like Receptor
OAβ2R	β2 Adrenergic-like Receptor
OAβ3R	β3 Adrenergic-like Receptor
oes	Esophagus
OGN	Octopamine-Glutamate Neuron
pb	Protocerebral Bridge
PDF	Pigment-dispersing Factor
PDFR	Pigment-dispersing Factor Receptor

PENP	Periesophageal Neuropil
PI3K	Phosphatidylinositol 3-kinase
PSMP	Posterior Superior Medial Protocerebrum
RSRT	RS Recombination Target Site
SEM	Standard Error of the Mean
SEZ	Subesophageal Zone
SMP	Superior Medial Protocerebrum
SNRI	Serotonin–norepinephrine Reuptake Inhibitor
SV	Clear Synaptic Vesicle
Syt/SYN	Synaptotagmin
TDC	Tyrosine Decarboxylase
tsh	Teashirt
TβH	Tyramine-β-Hydroxylase
UAS	Upstream Activating Sequence
UTR	Untranslated Region
UWE	Unilateral Wing Extension
VAChT	Vesicular Acetylcholine Transporter
VGLUT	Vesicular Glutamate Transporter
VL	Ventrolateral
VM	Ventromedial
VMAT	Vesicular Monoamine Transporter
VNC	Ventral Nerve Cord
VNS	Ventral Nervous System
VNUT	Vesicular Nucleotide Transporter
VPM	Ventral Paired Medial
ΔpH	Acidity
ΔμH+	Electrochemical Gradient
ΔΨ	Electric Potential

Figures

Introduction

Dual transmission

History and principles of dual transmission

The assertion known as "Dale's Principle" (named for English physiologist Sir Henry Dale) states, in its most common formulation, that all synapses of any given neuron release the same set of transmitters (Eccles *et al.* 1954). At the time Dale formulated his principle in 1934, only two neurotransmitters were known: acetylcholine and norepinephrine (Dale 1935). However, as the diverse suite of neurotransmitters, neuromodulators, and neuropeptides began to be appreciated within the nervous system, the question was asked as to whether this diverse suite could also be reflected within single neurons (Eccles 1976; Burnstock 1976, 2004; Hökfelt *et al.* 1977; Svensson *et al.* 2019). Indeed, even Dale himself recognized the possibility that neurons could express and release more than one transmitter (Dale 1935). This possibility was ultimately recognized as the phenomenon of dual transmission, by which neurons are able to release more than one neurotransmitter, neuromodulator, or neuropeptide (Burnstock 2004; Vaaga *et al.* 2014; Trudeau and El Mestikawy 2018; Svensson *et al.* 2019).

The first colocalization experiments identifying mammalian nerve cells that did not conform to Dale's Principle were performed by Hokfelt *et al.* Hokfelt's studies identified of the neuropeptide somatostatin and the biogenic amine norepinephrine within sympathetic nerves of the guinea pig (Hökfelt *et al.* 1977). However, in order to be classified as a transmitter, a neuronal substance must both be released from the neuron and detected by postsynaptic receptors, which must subsequently lead to a postsynaptic response (Kandel *et al.* 2012). Co-immunolabeling does not necessarily indicate co-transmission, as both substances may not be released or have functional effects on postsynaptic targets (Burnstock 2004; Breedlove and Watson 2013).

The existence of colocalized neurotransmitters within single neurons raised the question of whether multiple neurotransmitters were stored in neurons to save space or whether the release of multiple neurotransmitters from a neuron served to expand a neuron's functionality (Jaim-Etcheverry and Zieher 1973; Brownstein *et al.* 1974; Cottrell 1976). Carefully-controlled early

studies in coexpressing neurons described the release of multiple neurotransmitters from small neuronal subsets as critical in regulating the pacemaker complexes required for autosomal behaviors such as the gastric mill in the crustacean stomatogastric ganglion and the pyloric rhythm in the vertebrate gut (Katz and Harris-Warrick 1990; Blitz and Nusbaum 1999; Nusbaum et al. 2001; Hökfelt et al. 2002; Burnstock 2004). Significantly, these early studies identified key mechanisms, such as the release of alternate transmitters in response to stronger excitation and the trafficking of different transmitters to distinct downstream targets, that expanded the functionality of neurons (Harris-Warrick *et al.* 1995; Blitz and Nusbaum 1999; Swensen and Marder 2000). Such studies confirmed that coexpression of multiple transmitters in a single neuron serves a functional purpose and paved the way for the study of dual transmission, or the ability of a neuron to release multiple neurotransmitters, neuromodulators, and/or neuropeptides (Burnstock 2004; Vaaga *et al.* 2014; Trudeau and El Mestikawy 2018; Svensson *et al.* 2019; Okaty *et al.* 2019).

Functional implications of dual transmission

While early studies of dual transmission focused on describing the colocalization of neurotransmitters, neuromodulators, and neuropeptides, in neuronal subsets, current research focuses on describing the mechanisms of dual transmission in the central nervous system (Burnstock 1976; Osborne 1983; Kupfermann 1991; Lundberg 1996). Far from being only a means of compacting neuronal circuitry, there is now ample evidence that dual transmission can serve a variety of functional roles across the central and peripheral nervous system (Burnstock 2004; Trudeau 2004; El Mestikawy *et al.* 2011; Vaaga *et al.* 2014; Trudeau and El Mestikawy 2018; Svensson *et al.* 2019). The functional outcome of dual transmission adds a layer of complexity to neuron communication, expanding a neuron's signaling capabilities by enabling it to modulate the spatial and temporal aspects of neurotransmitter release, enhance packaging of transmitters in synaptic vesicles to modulate signal strength, and even regulate its own activity via negative feedback (Vaaga *et al.* 2014; Svensson *et al.* 2019).

Three classes of dual transmitting neurons have been convincingly demonstrated: those that release two fast small-molecule neurotransmitters (i.e. glutamate, GABA, acetylcholine, and histamine), those that release a fast small-molecule neurotransmitter and a monoamine (i.e.

noradrenaline/octopamine, serotonin, or dopamine) and those that release a small-molecule neurotransmitter (i.e. either a fast neurotransmitter or a monoamine) and a neuropeptide (Vaaga *et al.* 2014). Within these classes of dual transmitting neurons, intrinsic differences in vesicular loading, localization, and release between neurotransmitters, neuromodulators, and neuropeptides allows dual transmitting neurons a great degree of control over transmitter release at the presynaptic level (Nässel 2018). Additionally, postsynaptic expression of one or more different receptors that can distinguish between, amplify, or inhibit transmitter release from dual transmitting neurons grants an additional layer of control over any postsynaptic response (Nusbaum *et al.* 2001; Svensson *et al.* 2019).

In the presynaptic neuron, small-molecule neurotransmitters are packaged into clear synaptic vesicles (SVs), which localize to the presynaptic active zone and are released in response to a single action potential (Hökfelt *et al.* 2003; Svensson *et al.* 2019). In contrast, neuropeptides are exclusively stored within large dense-core vesicles (LDCVs), which can localize to either the active zone, the soma, or the dendrites and are usually released in response to multiple, prolonged action potentials, though the release mechanisms for LDCVs are still poorly understood (Hökfelt *et al.* 2003; Grygoruk *et al.* 2010; Bulgari *et al.* 2018; Nässel 2018; Tao *et al.* 2019). Monoamines can be packaged into either SVs or LDCVs, which grants them versatility as potential co-transmitters with either small-molecule neurotransmitters or neuropeptides (Svensson *et al.* 2019; Zhang *et al.* 2019). Packaging of co-transmitters in SVs versus LDCVs influences the localization and sensitivity of neurotransmitter release and thus provides spatial and temporal control over specific neurotransmitters (Hökfelt *et al.* 2003; Vaaga *et al.* 2014; Svensson *et al.* 2019). Additionally, postsynaptic responses to specific neurotransmitters can be modulated by receptor expression within the postsynaptic neuron (Sengupta *et al.* 2017). The release of fast small-molecule neurotransmitters from a presynaptic neuron activates ligand-gated ion channels on a postsynaptic neuron which act on a scale of milliseconds, while the release of monoamines and neuropeptides activate G-protein coupled receptors (GPCRs), which act on a scale of seconds to minutes (Kandel *et al.* 2012; Svensson *et al.* 2019). By expressing (or not expressing) receptors that respond to different neurotransmitters within different postsynaptic terminals, postsynaptic neurons are able to mediate both fast and

slow responses to dual transmitting neurons (Nusbaum *et al.* 2001; Vaaga *et al.* 2014; Sengupta *et al.* 2017).

The differences between neurotransmitters, neuromodulators, and neuropeptides described above allow dual transmitting neurons and their postsynaptic partners much more precise control over their outputs and inputs, respectively. They also indicate functional mechanisms of dual transmission by which individual neurotransmitters are packaged into the same SVs or LDCVs and released together (i.e. both transmitters are released at the same time and in the same location) (Zhang *et al.* 2019), packaged into either SVs or LDCVs and released in response to different signal strengths (i.e. both neurotransmitters are released in the same location but not necessarily at the same time) (Pagani *et al.* 2019), or packaged into either SVs or LDCVs and trafficked to different areas within the neuron (i.e. both neurotransmitters are released at the same time but not necessarily in the same location) (Silm *et al.* 2019). These dual transmission mechanisms can generally be grouped into two categories: co-release (Figure 1A) and co-transmission (Figure 1B).
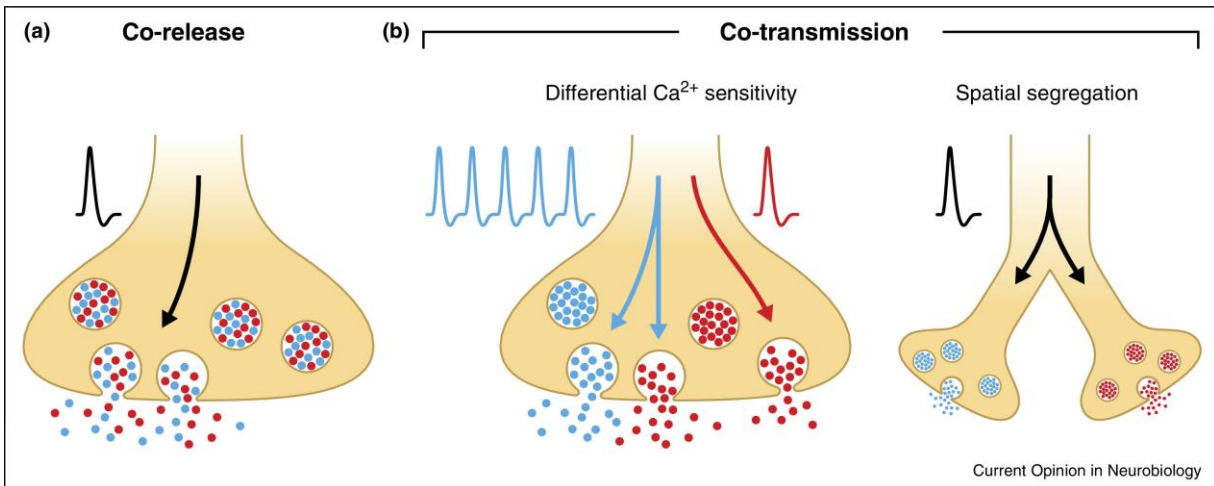
Figure 1 Mechanisms of Dual Transmission (**A**) During co-release, individual neurotransmitters are packaged into the same vesicles and released together. (**B**) During co-transmission, individual neurotransmitters are packaged into different vesicles that are either released from the same location in response to different signal strengths or trafficked to and released from different locations. Image from Vaaga C. E., M. Borisovska, and G. L. Westbrook, 2014 Dual-transmitter neurons: functional implications of co-release and co-transmission. Curr. Opin. Neurobiol. 29: 25–32. https://doi.org/10.1016/j.conb.2014.04.010

Co-release

Co-release is defined as the simultaneous release of two small-molecule transmitters from the same vesicle (Trudeau and El Mestikawy 2018). Co-released transmitters are transported and stored within the same vesicle and are released onto the same downstream target in response to the same stimulus (Figure 1A). Functionally, co-release can serve to produce varying degrees of postsynaptic response based on the distribution of postsynaptic receptors for either neurotransmitter (Nässel 2018; Brewer *et al.* 2019). A postsynaptic neuron might also express only one receptor, leading to detection of one co-released neurotransmitter but not the other (Nusbaum *et al.* 2001). An example of this occurs in two sets of downstream partners of glycine/GABA inhibitory interneurons in the cerebellar granular layer (Dugué *et al.* 2005). While both sets form synapses downstream of the inhibitory interneurons, one set of downstream neurons, the granule cells express only GABA$_A$ receptors while the other, the unipolar brush cells, express only glycine receptors. Thus, co-release provides a means for targeted signaling to postsynaptic neurons based on parsimonious expression of downstream receptors.

Co-release could also produce both fast-acting responses (mediated by postsynaptic ion channels) and slow-acting responses (mediated by postsynaptic GPCRs) simultaneously (Nusbaum *et al.* 2001; Vaaga *et al.* 2014; Sengupta *et al.* 2017; Svensson *et al.* 2019). This has been observed in the dopamine midbrain, where dopaminergic neurons of the ventral tegmental area express VGLUT2 and are able to emit fast glutamatergic excitatory postsynaptic currents in response to stimulation (Silm *et al.* 2019). Functional effects of co-release of fast and slow transmitters include motivational salience, maintenance of internal states, and reward learning (Mingote *et al.* 2017, 2019; Hutchison *et al.* 2018; Alcedo and Prahlad 2020).

Another possible interpretation of co-release (though not a mutually exclusive one) is that the loading of an auxillary neurotransmitter into an SV enhances SV packaging of the primary transmitter, a process known as vesicular synergy (El Mestikawy *et al.* 2011; Münster-Wandowski *et al.* 2016; Okaty *et al.* 2019). In this interpretation, release of the auxillary neurotransmitter may serve a secondary role to transmit a downstream signal, but the presence of the auxillary neurotransmitter in SVs serves principally to enhance the signal strength of the primary transporter through increased vesicle quanta (El Mestikawy *et al.* 2011; Trudeau and El Mestikawy 2018; Okaty *et al.* 2019). This increase in loading efficacy is due to the reliance of vesicular neurotransmitter transporters on the vesicular ATPase, which creates an electrochemical gradient ($\Delta\mu H^+$) and increases the acidity of SVs (ΔpH) by pumping in protons, resulting in an electric potential ($\Delta\Psi$) against the cytosol (Münster-Wandowski *et al.* 2016; Aguilar *et al.* 2017). Changes in ΔpH and/or $\Delta\Psi$ subsequently allow for increased activity of the vesicular neurotransmitter transporter, depending on its substrate. VAChT (acetylcholine) and VMAT (dopamine, serotonin, noradrenaline/octopamine) activity requires a high ΔpH, while VGLUT (glutamate) and VNUT (ATP) require high $\Delta\Psi$ (El Mestikawy *et al.* 2011; Münster-Wandowski *et al.* 2016). Since $\Delta\mu H^+ = \Delta pH + \Delta\Psi$, a transporter whose activity lowers $\Delta\Psi$ by raising ΔpH can enhance the loading of the neurotransmitter associated with the ΔpH-dependent transporter. Vesicular synergy was in fact first described between the high $\Delta\Psi$ VNUT and the high ΔpH VAChT and has subsequently been demonstrated between high $\Delta\Psi$ and high ΔpH transporters, though the most frequent combination involve an isoform of VGLUT and VAChT/VMAT (Münster-Wandowski *et al.* 2016).

Co-transmission

While co-release is characterized by a lack of spatial or temporal synchronicity between two neurotransmitters due to their presence in the same vesicle, co-transmission is characterized by the separation of transmitter release either spatially or temporally (Vaaga *et al.* 2017; Trudeau and El Mestikawy 2018). Thus, co-transmission gives neurons the ability to modulate transmitter release as more than just a response to a single action potential. Functionally, co-release could occur as a result of transmitters being packaged within separate SVs/LDCVs within the same terminal (resulting in temporal segregation of release) (Vaaga *et al.* 2014; Svensson *et al.* 2019; Silm *et al.* 2019), or from separately packaged transmitters trafficked to separate terminals or released through volume transmission (resulting in spatial segregation) (Blitz and Nusbaum 1999; Hökfelt *et al.* 2003; Vaaga *et al.* 2014).

Co-transmission allows dual transmitting neurons to encode different responses in response to the strength of signal input, particularly in the case of neurons that transmit both fast-acting and slow-acting substances (Figure 1B). One example of differential release based on signal strength occurs in the interneurons of the spinal cord dorsal horn, which gate both nociceptive (pain) and pruritoceptive (itch) responses (Pagani *et al.* 2019). While the physical sensations of pain and itch are superficially similar, the timescales and localization of pain and itch differ significantly, and thus evoke vastly different behavioral responses (Liu *et al.* 2010; Lagerström *et al.* 2011). Pagani *et al* show that spinal dorsal horn neurons are able to mediate between pain versus itch as a consequence of differential release sensitivity between glutamate and gastrin-releasing peptide (GRP) from GRP-glutamate neurons in response to signal input strength (Pagani *et al.* 2019). Pain is a hyperlocalized sensation that occurs on quick timescales. As such, pain is mediated by the spinal dorsal horn through the release of glutamate onto ionotropic receptors in response to single action potential pulses (Liu *et al.* 2010; Lagerström *et al.* 2011). In contrast, itch is a diffuse sensation that occurs on a relatively slower time scale, often in response to a continual stimulus. Burst firing onto spinal dorsal horn neurons is sufficient to induce both glutamate release from SVs and volume transmission of GRP from LDCVs, which evokes an itch response. The difference in transmitter release between pain and itch thus demonstrates co-transmission between transmitters with different release thresholds.

Co-transmission can also result from dual transmitting neurons segregating the release of neurotransmitters by transporting them to different locations within the neuron, allowing each transmitter to exert its function separately (Figure 1B). One of the most carefully-controlled studies of spatial segregation to date has been of the modulatory proctolin neuron (MPN) in the stomatogastric ganglion of the crab *Cancer borealis* (Blitz and Nusbaum 1999). MPN is a single dual transmitting neuron that expresses the neuropeptide proctolin and the inhibitory fast small-molecule neurotransmitter GABA. MPG releases proctolin onto the stomatogastric ganglion to promote gastric mill rhythm and GABA onto the commissural ganglia to suppress gastric mill rhythm. Blitz *et al* pharmacologically inhibited GABA release from the MPN and observed no activity in the commisural ganglia upon MPN stimulation, even though commissural ganglia neurons express proctolin receptors. This was an elegant and early demonstration of spatially segregated co-transmission in invertebrates. In mammalian neurons, separation of vesicles has been directly observed through immunohistochemistry for neuropeptide Y (NPY), VMAT2, and VAChT in cultured sympathetic ganglionic neurons, finding distinctly co-localized NPY/VMAT2 and VAChT/VMAT2 terminals (Vega *et al.* 2010). Spatial segregation has also been observed *in vivo* through immunohistochemistry experiments between VAChT and methionine enkephalin in rat superior cervical ganglion neurons (Vega *et al.* 2016) and by structured illumination microscopy between VGLUT2 and VMAT2 in mouse midbrain dopamine neurons (Silm *et al.* 2019). Spatial segregation of glutamate and acetylcholine has been demonstrated to increase in rat superior cervical ganglion neurons in response to external factors such as stress, hypertension, and aging suggesting a role for spatial segregation in mediating differential transmitter release in response to environmental factors (Merino-Jiménez *et al.* 2018).

An interesting presynaptic mechanism that could occur as a result of either co-release or co-transmission is autoreception, which could serve to enhance or attenuate the further release of neurotransmitter(s) through the activation of presynaptic GPCRs (Langer 2008; Niswender and Conn 2010; Vaaga *et al.* 2014, 2017; McKinney *et al.* 2020). While autoreception as a regulatory mechanism and the function of specific autoreceptors in transmitter release have been very well-characterized (Swanson *et al.* 2005; Langer 2008, 2015; Brady and Conn 2008; Niswender and Conn 2010), the role of autoreception in regulating the activity of dual transmitting neurons is not well understood. However, one tantalizing study suggests a functional requirement for the

co-transmission of small-molecule neurotransmitters for the proper function of neuropeptide-mediated autoreceptor activity (Choi *et al.* 2012). The lateral-ventral pacemaker neurons (LN$_{VS}$) are a subset of *Drosophila* circadian clock neurons that express both Pigment Dispersing Factor (PDF) and its receptor, PDFR. Activation of PDFR in LN$_{VS}$ as a result of PDF release from LN$_{VS}$ is required for maintaining morning activity. However, when SV release in LN$_{VS}$ is disrupted by expression of tetanus toxin light chain, the maintenance of morning activity is disrupted even as PDF release and PDFR autoreception remains functional. This result indicates a role for PDFR-mediated autoreception within LN$_{VS}$ in regulating co-transmission of PDF and small-molecule neurotransmitter(s), and suggests that autoreception is critical for the activity of key subsets of dual transmitting neurons.

Glutamate and biogenic amines in dual transmission

Glutamate is the major excitatory neurotransmitter in both vertebrate and invertebrate nervous systems (Kandel *et al.* 2012). Because of the prominent role of glutamate in transmitting excitatory signals, dual transmitting neurons expressing vesicular glutamate transporters (VGLUTs) are among the most well-studied (Bérubé-Carrière *et al.* 2009; Noh *et al.* 2010; Liu *et al.* 2010; Lagerström *et al.* 2011; Zhang *et al.* 2015; Fortin *et al.* 2019). There are three VGLUTs in the vertebrate nervous system, mainly differing in their distribution (El Mestikawy *et al.* 2011; Trudeau and El Mestikawy 2018). While the VGLUTs are expressed in a large number of neuron types, this section will focus exclusively on VGLUT expression in aminergic neurons. VGLUT expression within aminergic neurons varies based on the subpopulation of neurons and their developmental stage, but a glutamatergic phenotype within aminergic neurons is common (Mendez *et al.* 2008). It has been estimated that over 80% of dopamine neurons in the ventral tegmantal area and the substantia nigra pars compacta express VGLUT2 at some point in their development (Dal Bo *et al.* 2008; Steinkellner *et al.* 2018). Adrenergic neurons are just as likely to be glutamatergic, with over 80% of neurons in the C1, C2, C3, and A2 groups expressing VGLUT2 (Stornetta *et al.* 2002; DePuy *et al.* 2013). The co-expression of glutamate in dopamine and noradrenaline/octopamine neurons makes them extremely versatile, both because glutamate and monoamines can stimulate activity over short and long time periods, respectively (Vaaga *et al.* 2014; Zhang *et al.* 2019; Okaty *et al.* 2019; Mongia *et al.* 2019), and because monoamines can be transported into both SVs and LDCVs (Hökfelt *et al.* 2003; Grygoruk *et al.*

9

2010; Svensson *et al.* 2019). Thus, almost all of the co-release and co-transmission mechanisms described previously have been described in monoaminergic-glutamatergic neurons.

The monoamine transporter VMAT2 and VGLUT2 are commonly found to colocalize within synaptic terminals, but whether monoamines and glutamate are co-released from these terminals or are co-transmitted from separate vesicles remains a subject of investigation (Trudeau and El Mestikawy 2018). Studies in cultured dopamine-glutamate midbrain neurons identified synaptic terminals containing only glutamate, as well as terminals containing both dopamine and glutamate, suggesting a certain degree of segregation between the transmitters. Determining transporter localization on SVs from monoaminergic-glutamatergic neurons has been inconclusive, with some studies reporting colocalization of VMAT2 and VGLUT2 (Hnasko *et al.* 2010) and others reporting segregation of the transporters to distinct terminals (Zhang *et al.* 2015; Fortin *et al.* 2019). Acidification of SVs in HEK 293 cells co-transfected with VMAT2 and VGLUT2 has been described, indicating vesicular synergy and suggesting co-release (Hnasko *et al.* 2010). Furthermore, Aguilar *et al* directly observed vesicle acidification *in vivo* using the fluorescent indicator FFN206 within *Drosophila* MB-MV1 VMAT/VGLUT neurons (Aguilar *et al.* 2017). These studies provide support for the existence of vesicular synergy and co-release in dual transmitting neurons. However, this investigation was limited to a dopamine-dense region of MB-MV1, and even then estimates for percentages of co-localization ranged from 2%-25% (Aguilar *et al.* 2017). Thus, the prevalence of vesicular synergy and co-release within aminergic-glutamatergic co-releasing neurons as a whole remains an open question.

Outside of co-release, co-transmission of monoamines and glutamate can also result in differential transmitter release based on signal strength, demonstrated in the serotonergic-glutamatergic neurons of the basal amygdala (Sengupta *et al.* 2017). Low-frequency optogenetic stimulation of these neurons evoked release of glutamate, while high-frequency stimulation evoked release of serotonin. This result both demonstrates co-transmission of glutamate and serotonin in response to signal strength and indirectly suggests that monoamines and glutamate can be loaded into different vesicles within some neuronal subsets.

Differences in receptor expression in postsynaptic target neurons can lead to distinct responses to transmitters released from monoaminergic-glutamatergic neurons (Trudeau 2004; Kapoor *et al.* 2016; Trudeau and El Mestikawy 2018; Okaty *et al.* 2019). For example, recent work characterizing dopamine-glutamate co-release from dual transmitting neurons in the dorsolateral striatum onto mGluR-expressing cholinergic interneurons reveals an important role for glutamate co-release in amplifying a postsynaptic response (Cai *et al.* 2021). Cai *et al* describe glutamate-mediated signal amplification from dopamine-glutamate neurons in a mouse model of early Parkinson's. Dopamine release from dorsolateral striatal neurons to cholinergic interneurons (ChIs) results in D2 receptor-mediated silencing, while glutamate release to ChIs results in burst firing due to mGluR1 activation. Reduced DA release as a result of lesioning DA neurons led to reduced mGluR1 expression and altered activity in ChIs, which resulted in Parkinson's-like symptoms. Dopamine denervation, rather than a reduction in presynaptic glutamate release, caused this reduced mGluR1-mediated activity in ChIs, as overexpression of mGluR1 in ChIs neurons rescue motor function in early Parkinson's mice. This result reveals distinct roles for dopaminergic and glutamatergic release in regulating the actiuvity of ChIs and invites further study into the role of monoamine-glutamate dual transmission for neurological disease states.

Octopamine

Octopamine structure and synthesis

Octopamine is a biogenic amine that serves as the invertebrate analog to vertebrate norepinephrine, with which it shares significant structural similarity (Farooqui 2012; Rillich and Stevenson 2015; Blenau *et al.* 2020). The structures of octopamine and norepinephrine differ only in that norepinephrine is a catecholamine, while the benzene ring of octopamine possesses only one hydroxyl group. While octopamine can exist as either an *ortho-, meta-, or para*-isomer (and each with a D(-) or L(+) enantiomer) (Danielson *et al.* 1977; Williams and Couch 1978; Ibrahim *et al.* 1985; Brown *et al.* 1988), the dominant endogenous neuroactive form in invertebrate nervous systems is (-)-*p*-octopamine (Starratt and Bodnaryk 1981; Farooqui 2012). Octopamine is synthesized from L-tyrosine via a two-step process. First, the α-carbon of L-tyrosine is decarboxylated by tyrosine decarboxylase (TDC1 in non-neuronal cells and TDC2 in neurons) to form tyramine (Livingstone and Tempel 1983). The β-carbon of tyramine is

subsequently hydroxylated by tyramine-β-hydroxylase (TβH) (Monastirioti *et al.* 1996). The synthesis of octopamine allows for neurons to synthesize an endogenous ligand able to modulate a variety of processes and behaviors by way of its high-affinity for binding to octopamine receptors.

Octopamine receptors

Octopaminergic receptors (OARs) share structural similarities to their mammalian counterparts, the adrenergic receptors (Blenau *et al.* 2020). OARs are characterized by their high affinity for octopamine relative to other neurotransmitters (Yellman *et al.* 1997; Farooqui 2012; Blenau *et al.* 2020), though *in vitro* activation of specific OARs in response to other monoamines has been described (Qi *et al.* 2017; Xie *et al.* 2018). All known OARs belong to the class A (rhodopsin-like) G-protein coupled receptor family, possessing 7 α-helical transmembrane domains that contain the receptors' ligand-binding sites (Evans and Maqueira 2005; Farooqui 2012; Wu *et al.* 2014). As metabotropic receptors, OARs are able to transduce a signal over relatively long time periods in response to an agonist. Modern classification schemes divide OARs into three groups (Evans and Maqueira 2005; Farooqui 2012; Bayliss *et al.* 2013). The first two groups, the α-adrenergic-like and the β-adrenergic-like receptors, exhibit high affinity for octopamine, while the third group, the octopamine-tyramine receptors, exhibit higher affinity for tyramine. The α-adrenergic-like receptor group has two members: octopamine receptor in mushroom bodies (OAMB) and the α2-adrenergic-like receptor (OAα2R). OAMB is an ortholog to vertebarte α1-adrenergic receptors and is involved in multiple behaviors including sleep, olfactory learning, aggression, gustation, and courtship (Crocker *et al.* 2010; Watanabe *et al.* 2017; Youn *et al.* 2018; Deng *et al.* 2019; Sabandal *et al.* 2020). Like α1-adrenergic receptors, OAMB associates with the G_q heterotrimeric protein and increases intracellular Ca^{2+} via the phospholipase C pathway upon activation, though the OAMB-K3 isoform stimulates an additional increase in cAMP (Han *et al.* 1998; Balfanz *et al.* 2005; Farooqui 2012; Kim *et al.* 2013; Sujkowski *et al.* 2020). OAα2R is the most recently-described octopaminergic receptor and is of particular interest to this dissertation. OAα2R exhibits a high sequence similarity both to other invertebrate α2-receptor orthologues and vertebrate α2-adrenergic receptors, suggesting shared ancestry (Wu *et al.* 2014; Qi *et al.* 2017; Blenau *et al.* 2020). Functional characterization of OAα2R has determined that the receptor shares a conserved role with vertebrate α-adrenergic receptors, as both act as inhibitory

receptors via reducing the activity of the adenylyl cyclase pathway. When expressed in mammalian cell lines, both *Drosophila* and *Apis mellifera* (honeybee) OAα2Rs attenuate cAMP synthesis in a dose-dependent manner upon administration of octopamine (Qi *et al.* 2017; Blenau *et al.* 2020). The β-adrenergic-like receptor group contains three members: OAβ1R, OAβ2R, and OAβ3R. Ligand binding to these receptors results in increased cAMP synthesis as a result of adenylyl cyclase pathway activation (Evans and Maqueira 2005; Farooqui 2012; Wu *et al.* 2012; Sujkowski *et al.* 2020). OAβ1R and OAβ2R also have been shown to serve a role in the plasticity of OAergic synapses, with OAβ1R activity serving as a negative regulator of synaptic bouton development and OAβ2R activity serving as a positive regulator (Koon *et al.* 2010; Koon and Budnik 2012).

Glutamate

Glutamate structure and synthesis

Glutamate is the anion of glutamic acid that serves as the primary excitatory neurotransmitter in both vertebrate and invertebrate nervous systems (Meldrum 2000; Kandel *et al.* 2012). Within the central nervous system, neuroactive glutamate is synthesized from non-neuroactive glutamine through the glutamate-glutamine cycle (Bak *et al.* 2006). In this pathway, glutamate is released into the synaptic cleft by the presynaptic neuron and taken up by astrocytes via excitatory amino acid transporters (Malik and Willnow 2019). Once glutamate has been transported into an astrocyte, the carboxylic acid of carbon-5 is amidated via glutamine synthetase to form glutamine (Norenberg and Martinez-Hernandez 1979). This non-neuroactive glutamine is then released into the extracellular space via solute carrier family 38a member 3 and taken up by the synaptic terminal via solute carrier family 38a member 1 (Melone *et al.* 2004; Rubio-Aliaga and Wagner 2016). Within the synaptic terminal, the amide on carbon-5 of glutamine is carboxylized by the mitochondrial enzyme glutaminase, resulting in glutamate (Kvamme *et al.* 2001). The newly-synthesized glutamate is then repackaged into synaptic vesicles by VGLUTs (Daniels *et al.* 2006), where it is able to be released from synaptic vesicles and bind to postsynaptic glutamate receptors.

Glutamate receptors

Glutamate receptors fall into two general categories: the ionotropic glutamate receptors (iGluRs) and the metabotropic glutamate receptors (mGluRs) (Reiner and Levitz 2018). The iGluRs are glutamate-gated ion channels that form heteromultimers as a result of interactions between iGluR subunit proteins (Traynelis *et al.* 2010). iGluRs can be further subdivided into two major classes: NMDA receptors and non-NMDA receptors (Traynelis *et al.* 2010; Willard and Koochekpour 2013). Pharmacologically, NMDA receptors are characterized by their responsiveness to the agonist N-methyl-D-aspartate, while non-NMDA receptors exhibit no response (Meldrum 2000; Traynelis *et al.* 2010; Reiner and Levitz 2018). Structural characterization of NMDA receptors reveals a heteromeric receptor made up from the subunits GluN1, GluN2, and GluN3 (Salussolia *et al.* 2011). The receptor contains a large N-terminus, three transmembrane domains, a pore loop, and an intracellular C-terminus (Loftis and Janowsky 2003; Limapichat *et al.* 2012). Glutamate binding and glycine modulation results in neuronal depolarization and the initiation of an action potential due to an influx of Na^+ and Ca^{2+} (Furukawa *et al.* 2005). NMDA receptor activity is essential for learning and memory (Loftis and Janowsky 2003; Furukawa *et al.* 2005) and for the maintenance of synaptic plasticity (Loftis and Janowsky 2003; Papathanou *et al.* 2018), especially in conjunction with class I mGluRs (Zhang *et al.* 1999; Meldrum 2000).

In vertebrates, the non-NMDA receptors can be classified further as AMPA receptors and kainate receptors (Zhang *et al.* 1999; Meldrum 2000). AMPA receptors mediate the majority of fast synaptic excitatory transmission (Platt 2007) and form heterotetramers from the subunits GRIA1, GRIA2, GRIA3, and GRIA4 (Shi *et al.* 1999; Song and Huganir 2002). AMPA receptors contain four transmembrane domains containing two loops that coalesce to form a pore (Hollmann *et al.* 1994; Greger *et al.* 2007). Binding of glutamate results in quick opening and closing of an AMPA receptor, making it permeable to Na^+ (Platt 2007). Kainate receptors are formed via the assembly of the subunits GRIK1, GRIK2, GRIK3, GRIK4, and GRIK5 into tetramers (Dingledine *et al.* 1999). Kainate receptors contain an extracellular ligand-binding site and three transmembrane domains (Meldrum 2000). They are similar to AMPA receptors in that glutamate binding results in permeability to Na^+, but they act over a longer timescale (Castillo *et al.* 1997; Huettner 2003).

mGluRs are glutamate-activated GPCRs that form through the dimerization of mGluR subunit proteins (Niswender and Conn 2010; Moustaine *et al.* 2012; Levitz *et al.* 2016). mGluRs make up the class-C GPCR family, which are characterized by a large extracellular domain containing a Venus flytrap module and a cysteine-rich ligand-binding domain, along with the 7 α-helical transmembrane domains typical to GPCRs (Brauner-Osborne *et al.* 2006; Chun *et al.* 2012). Vertebrate mGluRs are subdivided into three groups based on sequence similarity, second-messenger pathway, and pharmacological profile (Ji-Quan Wang and Anna-Liisa Brownell 2007). While these three groups primarily function as subsequently described, specific exceptions to these functions have been identified. Group I mGluRs (consisting of mGluR1 and mGluR5) are excitatory G_q-coupled GPCRs that primarily localize to the postsynapse and act through the phospholipase C pathway to modulate the activity of Na^+, K^+, and Ca^{2+} channels (Swanson *et al.* 2005; Conn *et al.* 2009; Kumari *et al.* 2013). Group II (consisting of mGluR2 and mGluR3) and Group III mGluRs (consisting of mGluR4, mGluR6, mGluR7, and mGluR8) primarily function as negative feedback autoreceptors that inhibit the cAMP-dependent pathway via the release of $G_{i/o}$ protein that negatively regulates adenylyl cyclase activity (Shigemoto *et al.* 1997; Brady and Conn 2008; Niswender and Conn 2010). This inhibition reduces neuron excitability and thus further release of glutamate.

Glutamate in the Drosophila Brain

While glutamate has been identified as the primary motor neurotransmitter in invertebrate nervous systems, it also serves a functional role in the central nervous system as well (Daniels *et al.* 2008). *Drosophila* glutamate receptors are expressed primarily in neurons, indicating a role for glutamate neurotransmission (Xia *et al.* 2005; Devaud *et al.* 2008). The *Drosophila* genome encodes 16 glutamate receptor subunits (Parmentier *et al.* 1996; Xia *et al.* 2005; Lee *et al.* 2009; Croset *et al.* 2010; Han *et al.* 2015). Of these genes, 15 encode iGluR subunits, while only a single gene encodes an mGluR subunit.

The mGluR subunit dimerizes to form the single *Drosophila* mGluR, which shares structural and functional similarities to vertebrate group II mGluRs (Panneels *et al.* 2003; Eroglu *et al.* 2003; Bogdanik *et al.* 2004). When expressed in HEK 293 cells, mGluR suppressed adenylyl cyclase activity (Parmentier *et al.* 1996), indicating that like group II mGluRs it functions as a negative

feedback receptor (Shigemoto *et al.* 1997; Swanson *et al.* 2005; Niswender and Conn 2010). mGluR is expressed widely throughout the *Drosophila* brain, where it is involved in circadian rhythm maintenance, courtship, olfactory learning, sleep modulation, and other behaviors (Hamasaka *et al.* 2007; Devaud *et al.* 2008; Schoenfeld *et al.* 2013; Collins *et al.* 2014; Andlauer *et al.* 2014; Guo *et al.* 2016; Ly *et al.* 2020). It is also expressed in presynaptic terminals at the NMJ, though its mechanistic role here is not clear (Zhang *et al.* 1999; Bogdanik *et al.* 2004). Application of mGluR agonists to the *Drosophila* NMJ was shown to enhance synaptic firing; however, this was attributed to mGluR-mediated activation of adenylyl cyclase, which is the opposite result of class II mGluR activation (Zhang *et al.* 1999). Studies of mGluR at the NMJ as well as more recent studies showing that ligand activation of mGluR mediates PI3K pathway activation (Chun-Jen Lin *et al.* 2011) suggest that mGluR has more diversity of function than group II mGluRs. Although its association with the $G_{i/o}$ α-subunit and its structural similarity to vertebrate group II mGluRs suggests that it functions primarily as an inhibitory autoreceptor (Eroglu *et al.* 2003; Bogdanik *et al.* 2004; Devaud *et al.* 2008; Schoenfeld *et al.* 2013), it is likely that many pre- and postsynaptic functions that in vertebrates would be carried out by different classes of mGluRs are conserved in this single mGluR.

The *Drosophila* genome encodes two NMDA-like proteins, NMDAR1 and NMDAR2. These proteins are orthologs to NMDA receptor subunits and come together to form a heterotetrameric receptor (Ultsch *et al.* 1993; Völkner *et al.* 2000). Like vertebrate NMDARs, the *Drosophila* NMDAR allows for the passage of Na^+ and Ca^{2+} ions into the neuron upon glutamate binding and are modulated by glycine (Xia and Chiang 2009; Chorna and Hasan 2012). Also like vertebrate NMDARs, the *Drosophila* NMDAR is required for learning and memory (Xia *et al.* 2005).

Although attempts have been made to classify the remaining *Drosophila* iGluR receptor subunits as AMPA or kainate (Benton *et al.* 2009; Croset *et al.* 2010), the pharmacological profiles of these receptors is distinct from vertebrate iGluRs and it is not clear whether they can be classified in the same way (Lee *et al.* 2009). To reflect this current debate, I will refer to the remaining *Drosophila* iGluRs simply as non-NMDA receptors.

GluRIIA, GluRIIB, GluRIIC, GluRIID, and GluRIIE are iGluR subunits that form non-NMDARs at the neuromuscular junction (Qin *et al.* 2005; Han *et al.* 2015). These iGluRs are pharmacologically distinct in that they are able to respond to the quisqualate, but not AMPA or kainate (Han *et al.* 2015). They respond to glutamate release from motor neurons and are required for locomotor activity (Lee *et al.* 2009; Han *et al.* 2015).

The remaining excitatory non-NMDA iGluR subunits are GluRIA, GluRIB, *clumsy*, CG11155, EKAR, Grik, and KaiR1D. GluRIA and GluRIB are iGluR subunits that are expressed in the CNS (Ultsch *et al.* 1993; Völkner *et al.* 2000), and have been compared to kainate and AMPA receptors, respectively, in some classification systems (Croset *et al.* 2010; Robinson *et al.* 2016; Li *et al.* 2016). c*lumsy,* EKAR, Grik, and KaiR1D are all iGluRs that are expressed in the visual system and are essential for vision and detection of UV light (Karuppudurai *et al.* 2014; Hu *et al.* 2015; Li *et al.* 2016).

Glutamate-gated chloride channels are unique to invertebrates, though they share structural similarities with vertebrate glycine receptors (Wolstenholme 2012). Unlike most iGluRs which mediate excitatory synaptic transmission, these channels mediate inhibitory synaptic transmission by allowing Cl^- ions to enter the neuron in response to glutamate ligand binding, hyperpolarizing the neuron (Molina-Obando *et al.* 2019). The *Drosophila* genome encodes one glutamate-gated chloride channel subunit (GluClα), which assemble to form homomeric channels (Cully *et al.* 1996).

Drosophila **as a model organism**

Major contributions of Drosophila to neuroscience research

A major unsolved problem in neuroscience is determining the mechanisms through which decisions are made (Adolphs 2015). The fruit fly *Drosophila melanogaster* has proven a powerful model through which such complex questions can be addressed. *Drosophila* is a model organism in which a detailed partial connectome is available, allowing the pre- and postsynaptic connections of many neurons to be identified (Zheng *et al.* 2018). Drosophila exhibit complex yet stereotyped behaviors, allowing for the quantification of aggression, courtship, and other

behaviors (Certel and Kravitz 2012; Berman *et al.* 2014; Youn *et al.* 2018; Zhang *et al.* 2018). Drosophila analogs to mammalian neuropeptides and neuromodulators have been shown to influence aggressive behavior (Hoyer *et al.* 2008; Asahina *et al.* 2014; Zelikowsky *et al.* 2018). Furthermore, the existence and similarity of function of decision-making circuits has been demonstrated in both flies (Certel *et al.* 2010; Koganezawa *et al.* 2016) and vertebrates (Lin *et al.* 2011). By quantifying the frequency and intensity of aggressive behaviors in flies with specific receptor deficits in specific neurons, the circuits and neuronal mechanisms that constrain and promote aggression can be identified, with the results being applicable across systems.

Drosophila aggression

Aggression is an innate and evolutionarily-conserved behavior that animals use to gain access to food, mates, territory, and other resources. Aggressive behaviors expressed in ethological contexts are considered adaptive, as they increase an organism's chances of survival (Cassidy *et al.* 2015; de Boer 2018; Rillich and Stevenson 2019; Covington *et al.* 2019; Kiyose *et al.* 2021). In both animals and humans, aggressive behaviors are considered pathological when they are exaggerated, persistent, or expressed out of context (Nelson and Trainor 2007; Blair 2016; de Boer 2018; Wolf *et al.* 2018).

The occurrence of aggressive behaviors between vastly different organisms indicates a shared functionality in aggression circuitry (Nelson and Trainor 2007; Kennedy *et al.* 2014; Zelikowsky *et al.* 2018, 2019) Determining the circuit-level mechanisms that influence aggressive motivation in any nervous system would therefore provide insight into aggressive motivation. In vertebrates such as rats and primates, sensory information is received by the olfactory bulb and processed by neural circuits in the amygdala before being transmitted to regions that promote aggressive behavior, such as the hypothalamus and the bed nucleus of the stria terminalis (Nelson and Trainor 2007; Lin *et al.* 2011). Insects have an analogous pathway, with sensory information taken in and processed by neural circuits in the antennal lobes and subesophageal ganglion, then transmitted to aggression-promoting regions such as the mushroom body and pars intercerebralis (Aso *et al.* 2014; Hartenstein *et al.* 2018). In any system, then, describing the circuit-level mechanisms that promote aggressive behavior requires identifying (i) the chemical messengers that transmit aggression-promoting information, (ii) the pre- and/or postsynaptic mechanisms

that control the transmission of aggression-promoting information, and (iii) the neuron(s) in which the constraint and release of aggression-promoting information occur.

Aggressive behavior in insects has been a subject of popular fascination for over a millenium (Suga 2006) and a subject of scientific study since at least Darwin, who noted that the internal states that generate aggression might be homologous to those that generate aggression in humans (Darwin 1872). The ethological study of aggression in *Drosophila* began with Sturdevant in 1915, who recorded "tussling" between *Drosophila* males (Sturtevant 1915). Many neural circuits and transmitters are involved in initiating and maintaining aggression, among them octopamine (Rillich and Stevenson 2015; Watanabe *et al.* 2017; Balsam and Stevenson 2020), tachykinin (Asahina *et al.* 2014; Zelikowsky *et al.* 2018), glutamate (Chowdhury *et al.* 2017; Sherer *et al.* 2020), and Gr32a gustatory receptors (Andrews *et al.* 2014). Male conspecifics, including the male-specific hormone *z*-7-tricosene, are also capable of promoting inter-male aggression (Andrews *et al.* 2014; Lin *et al.* 2015). Crucially, failure to recognize male conspecifics will result in male *Drosophila* exhibiting inter-male courtship in the context of an aggression assay, due to the fly being unable to recognize a male opponent (Certel *et al.* 2007; Gupta *et al.* 2017). The performance of inter-male courtship behavior rather than aggression thus provides insight into the decision-making processes that underlie the decision to initiate aggressive behavior (Certel *et al.* 2010). Of particular interest to this dissertation are the behaviors through which we quantify aggressive behavior. Mid-intensity aggressive behaviors consist of the lunge, in which a male fly rears up on his hind legs and snaps his forelegs down on his opponent (Kravitz and Fernández 2015), and the wing threat, in which a fly raises his wings at a 45° angle, assuming an aggressive posture (Duistermars *et al.* 2018). High-intensity aggressive behaviors consist of holding, a one-sided prolonged attack in which a male fly will grab onto his opponents wings (Davis *et al.* 2018), and boxing, an extended period of reciprocal shoving, lunging, and tussling (Penn *et al.* 2010).

The earliest aggression assays involved placing male pairs in aggression chambers and manually quantifying their behavior over a set period of time (Certel and Kravitz 2012; Kravitz and Fernández 2015). As machine learning algorithms have grown more sophisticated, the means by which animal behavior is quantified have shifted from manual annotation to high-throughput,

automated approaches (Dankert *et al.* 2009; Kabra *et al.* 2013; Eyjolfsdottir *et al.* 2014). A significant portion of time during Aim 3 was spent developing an automated aggression analysis pipeline using freely-available and rigorously tested software, including CalTec FlyTracker 1.05 which tracks the position of each male fly within a video (Dankert *et al.* 2009), and the Janelia Automated Animal Behavior Annotator (JAABA) which subsequently quantifies the behavior of the tracked male flies (Kabra *et al.* 2013). I also implemented the Divider assay, a recently published high-throughput assay that allows aggression to be automatically quantified in up to 12 pairs of males at a time (Chowdhury *et al.* 2021).

Significance

This introduction has provided the necessary background information to inform an examination of dual transmission mechanisms within individual neurons and their functional behavioral outputs, from here onward assayed as aggression and courtship. Absent from this background information has been a hypothesis regarding how the mechanisms of dual transmission that promote or inhibit the release of specific neurotransmitters from neurons translate into the promotion or constraint of specific behavioral outputs in organisms. The neurons, neurotransmitters, and receptors that make up dual transmitting circuits have all been well characterized. However, the specific mechanisms that promote or inhibit transmitter release within individual dual transmitting neurons to promote or constrain specific behavioral outputs are not yet understood. It is this gap in knowledge that this dissertation will address. The first two chapters will elaborate on the release of OA and glutamate from OA/glutamate neurons in the *Drosophila* brain, a description of dual transmission mechanisms within these neurons, and how genetic manipulation of these mechanisms reveals a functional role for dual transmission in OA/glutamate neurons specifically and aggression and courtship behavioral output broadly. The third chapter will contain a report on my current investigations, which I am preparing for publication, on the presynaptic and postsynaptic mechanisms used by a single dual transmitting neuron and their functional implications. These chapters will expand upon our understanding of how monoaminergic and glutamatergic signaling from dual transmitting OA/glutamate neurons is able to produce complex behavioral outputs, such as courtship and aggression, and how individual neurons within the OA/glutamate subset are able to modulate these complex outputs through the mechanisms of dual transmission.

References

Adolphs R., 2015 The unsolved problems of neuroscience. Trends Cogn. Sci. 19: 173–175. https://doi.org/10.1016/J.TICS.2015.01.007

Aguilar J. I., M. Dunn, S. Mingote, C. S. Karam, Z. J. Farino, *et al.*, 2017 Neuronal depolarization drives increased dopamine synaptic vesicle loading via VGLUT. Neuron 95: 1074-1088.e7. https://doi.org/10.1016/J.NEURON.2017.07.038

Alcedo J., and V. Prahlad, 2020 Neuromodulators: an essential part of survival. J. Neurogenet. 1–7. https://doi.org/10.1080/01677063.2020.1839066

Andlauer T. F. M., S. Scholz-Kornehl, R. Tian, M. Kirchner, H. A. Babikir, *et al.*, 2014 Drep-2 is a novel synaptic protein important for learning and memory. Elife 3: 1–24. https://doi.org/10.7554/ELIFE.03895

Andrews J. C., M. de la P. Fernández, Q. Yu, G. P. Leary, A. K. Leung, *et al.*, 2014 Octopamine neuromodulation regulates Gr32a-linked aggression and courtship pathways in Drosophila males, (T. Clandinin, Ed.). PLOS Genet. 10: e1004356. https://doi.org/10.1371/journal.pgen.1004356

Asahina K., K. Watanabe, B. J. Duistermars, E. D. Hoopfer, C. R. González, *et al.*, 2014 Tachykinin-expressing neurons control male-specific aggressive arousal in Drosophila. Cell 156: 221–235. https://doi.org/10.1016/j.cell.2013.11.045

Aso Y., D. Hattori, Y. Yu, R. M. Johnston, N. A. Iyer, *et al.*, 2014 The neuronal architecture of the mushroom body provides a logic for associative learning. Elife 3: e04577. https://doi.org/10.7554/eLife.04577

Bak L. K., A. Schousboe, and H. S. Waagepetersen, 2006 The glutamate/GABA-glutamine cycle: aspects of transport, neurotransmitter homeostasis and ammonia transfer. J. Neurochem. 98: 641–653. https://doi.org/10.1111/J.1471-4159.2006.03913.X

Balfanz S., T. Strünker, S. Frings, and A. Baumann, 2005 A family of octapamine receptors that specifically induce cyclic AMP production or Ca2+ release in Drosophila melanogaster. J. Neurochem. 93: 440–451. https://doi.org/10.1111/J.1471-4159.2005.03034.X

Balsam J. S., and P. A. Stevenson, 2020 Pre-adult aggression and its long-term behavioural consequences in crickets, (S. D. Iñiguez, Ed.). PLoS One 15: e0230743. https://doi.org/10.1371/journal.pone.0230743

Bayliss A., G. Roselli, and P. D. Evans, 2013 A comparison of the signalling properties of two tyramine receptors from Drosophila. J. Neurochem. 125: 37–48. https://doi.org/10.1111/JNC.12158

Benton R., K. S. Vannice, C. Gomez-Diaz, and L. B. Vosshall, 2009 Variant Ionotropic
Glutamate Receptors as Chemosensory Receptors in Drosophila. Cell 136: 149–162.
https://doi.org/10.1016/J.CELL.2008.12.001

Berman G. J., D. M. Choi, W. Bialek, and J. W. Shaevitz, 2014 Mapping the stereotyped
behaviour of freely moving fruit flies. J. R. Soc. Interface 11.
https://doi.org/10.1098/RSIF.2014.0672

Bérubé-Carrière N., M. Riad, G. Dal Bo, D. Lévesque, L.-É. Trudeau, *et al.*, 2009 The dual
dopamine-glutamate phenotype of growing mesencephalic neurons regresses in mature rat
brain. J. Comp. Neurol. 517: 873–891. https://doi.org/10.1002/cne.22194

Blair R. J. R., 2016 The Neurobiology of Impulsive Aggression. J. Child Adolesc.
Psychopharmacol. 26: 4–9.

Blenau W., J. A. Wilms, S. Balfanz, and A. Baumann, 2020 AmOctα2R: Functional
Characterization of a Honeybee Octopamine Receptor Inhibiting Adenylyl Cyclase Activity.
Int. J. Mol. Sci. 2020, Vol. 21, Page 9334 21: 9334. https://doi.org/10.3390/IJMS21249334

Blitz D. M., and M. P. Nusbaum, 1999 Distinct Functions for Cotransmitters Mediating Motor
Pattern Selection. J. Neurosci. 19: 6774–6783. https://doi.org/10.1523/JNEUROSCI.19-16-
06774.1999

Boer S. F. de, 2018 Animal models of excessive aggression: implications for human aggression
and violence. Curr. Opin. Psychol. 19: 81–87.

Bogdanik L., R. Mohrmann, A. Ramaekers, J. Bockaert, Y. Grau, *et al.*, 2004 The Drosophila
metabotropic glutamate receptor DmGluRA regulates activity-dependent synaptic
facilitation and fine synaptic morphology. J. Neurosci. 24: 9105–9116.
https://doi.org/10.1523/JNEUROSCI.2724-04.2004

Brady A. E., and P. J. Conn, 2008 Metabotropic glutamate receptor ligands as novel therapeutic
agents, pp. 529–564 in *The Glutamate Receptors*, Humana Press.

Brauner-Osborne H., P. Wellendorph, and A. Jensen, 2006 Structure, Pharmacology and
Therapeutic Prospects of Family C G-Protein Coupled Receptors. Curr. Drug Targets 8:
169–184. https://doi.org/10.2174/138945007779315614

Breedlove S. M., and N. V Watson, 2013 *Biological psychology : an introduction to behavioral,
cognitive, and clinical neuroscience*. Sinauer Associates: An Imprint Of Oxford University
Press.

Brewer J. C., A. C. Olson, K. M. Collins, and M. R. Koelle, 2019 Serotonin and neuropeptides
are both released by the HSN command neuron to initiate Caenorhabditis elegans egg

laying, (A. C. Hart, Ed.). PLOS Genet. 15: e1007896.
https://doi.org/10.1371/journal.pgen.1007896

Brown C. M., J. C. McGrath, J. M. Midgley, A. G. B. Muir, J. W. O'Brien, *et al.*, 1988 Activities of octopamine and synephrine stereoisomers on α-adrenoceptors. Br. J. Pharmacol. 93: 417–429. https://doi.org/10.1111/J.1476-5381.1988.TB11449.X

Brownstein M. J., J. M. Saavedra, J. Axelrod, G. H. Zeman, and D. O. Carpenter, 1974 Coexistence of Several Putative Neurotransmitters in Single Identified Neurons of Aplysia. Proc. Natl. Acad. Sci. 71: 4662–4665. https://doi.org/10.1073/PNAS.71.12.4662

Bulgari D., A. Jha, D. L. Deitcher, and E. S. Levitan, 2018 Myopic (HD-PTP, PTPN23) selectively regulates synaptic neuropeptide release. Proc. Natl. Acad. Sci. 115: 1617–1622. https://doi.org/10.1073/PNAS.1716801115

Burnstock G., 1976 Do some nerve cells release more than one transmitter? Neuroscience 1: 239–248. https://doi.org/10.1016/0306-4522(76)90054-3

Burnstock G., 2004 Cotransmission. Curr. Opin. Pharmacol. 4: 47–52. https://doi.org/10.1016/j.coph.2003.08.001

Cai Y., B. E. Nielsen, E. E. Boxer, J. Aoto, and C. P. Ford, 2021 Loss of nigral excitation of cholinergic interneurons contributes to parkinsonian motor impairments. Neuron 109: 1137-1149.e5. https://doi.org/10.1016/J.NEURON.2021.01.028

Cassidy K. A., D. R. MacNulty, D. R. Stahler, D. W. Smith, and L. D. Mech, 2015 Group composition effects on aggressive interpack interactions of gray wolves in Yellowstone National Park. Behav. Ecol. 26: 1352–1360. https://doi.org/10.1093/beheco/arv081

Castillo P. E., R. C. Malenka, and R. A. Nicoll, 1997 Kainate receptors mediate a slow postsynaptic current in hippocampal CA3 neurons. Nat. 1997 3886638 388: 182–186. https://doi.org/10.1038/40645

Certel S. J., M. G. Savella, D. C. Schlegel, and E. A. Kravitz, 2007 Modulation of Drosophila male behavioral choice. Proc. Natl. Acad. Sci. U. S. A. 104: 4706–4711. https://doi.org/10.1073/pnas.0700328104

Certel S. J., A. K. Leung, C.-Y. Lin, P. Perez, A.-S. Chiang, *et al.*, 2010 Octopamine neuromodulatory effects on a social behavior decision-making network in Drosophila males, (W. S. Leal, Ed.). PLoS One 5: e13248. https://doi.org/10.1371/journal.pone.0013248

Certel S. J., and E. A. Kravitz, 2012 Scoring and analyzing aggression in Drosophila. Cold Spring Harb. Protoc. 2012: 319–325. https://doi.org/10.1101/pdb.prot068130

Choi C., G. Cao, A. K. Tanenhaus, E. v. McCarthy, M. Jung, *et al.*, 2012 Autoreceptor Control of Peptide/Neurotransmitter Corelease from PDF Neurons Determines Allocation of Circadian Activity in Drosophila. Cell Rep. 2: 332–344. https://doi.org/10.1016/J.CELREP.2012.06.021

Chorna T., and G. Hasan, 2012 The genetics of calcium signaling in Drosophila melanogaster. Biochim. Biophys. Acta - Gen. Subj. 1820: 1269–1282. https://doi.org/10.1016/J.BBAGEN.2011.11.002

Chowdhury B., Y.-B. Chan, and E. A. Kravitz, 2017 Putative transmembrane transporter modulates higher-level aggression in Drosophila. Proc. Natl. Acad. Sci. U. S. A. 114: 2373–2378. https://doi.org/10.1073/pnas.1618354114

Chowdhury B., M. Wang, J. P. Gnerer, and H. A. Dierick, 2021 The Divider Assay is a high-throughput pipeline for aggression analysis in Drosophila. Commun. Biol. 4: 1–12. https://doi.org/10.1038/s42003-020-01617-6

Chun-Jen Lin C., J. B. Summerville, E. Howlett, and M. Stern, 2011 The Metabotropic Glutamate Receptor Activates the Lipid Kinase PI3K in Drosophila Motor Neurons Through the Calcium/Calmodulin-Dependent Protein Kinase II and the Nonreceptor Tyrosine Protein Kinase DFak. Genetics 188: 601–613. https://doi.org/10.1534/GENETICS.111.128561

Chun L., W. Zhang, and J. Liu, 2012 Structure and ligand recognition of class C GPCRs. Acta Pharmacol. Sin. 2012 333 33: 312–323. https://doi.org/10.1038/aps.2011.186

Collins B., H. S. Kaplan, M. Cavey, K. R. Lelito, A. H. Bahle, *et al.*, 2014 Differentially Timed Extracellular Signals Synchronize Pacemaker Neuron Clocks. PLOS Biol. 12: e1001959. https://doi.org/10.1371/JOURNAL.PBIO.1001959

Conn P. J., C. W. Lindsley, and C. K. Jones, 2009 Activation of metabotropic glutamate receptors as a novel approach for the treatment of schizophrenia. Trends Pharmacol. Sci. 30: 25–31.

Cottrell G., 1976 Proceedings: Does the giant cerebral neurone of Helix release two transmitters: ACh and serotonin? - PubMed. J. Physiol. 259: 44–45.

Covington H. E., E. L. Newman, M. Z. Leonard, and K. A. Miczek, 2019 Translational models of adaptive and excessive fighting: An emerging role for neural circuits in pathological aggression. F1000Research 8: 963.

Crocker A., M. Shahidullah, I. B. Levitan, and A. Sehgal, 2010 Identification of a Neural Circuit that Underlies the Effects of Octopamine on Sleep:Wake Behavior. Neuron 65: 670–681. https://doi.org/10.1016/J.NEURON.2010.01.032

Croset V., R. Rytz, S. F. Cummins, A. Budd, D. Brawand, *et al.*, 2010 Ancient Protostome Origin of Chemosensory Ionotropic Glutamate Receptors and the Evolution of Insect Taste and Olfaction. PLOS Genet. 6: e1001064. https://doi.org/10.1371/JOURNAL.PGEN.1001064

Cully D. F., P. S. Paress, K. K. Liu, J. M. Schaeffer, and J. P. Arena, 1996 Identification of a Drosogaster melanogaster Glutamate-gated Chloride Channel Sensitive to the Antiparasitic Agent Avermectin *. J. Biol. Chem. 271: 20187–20191. https://doi.org/10.1074/JBC.271.33.20187

Dal Bo G., N. Bérubé-Carrière, J. A. Mendez, D. Leo, M. Riad, *et al.*, 2008 Enhanced glutamatergic phenotype of mesencephalic dopamine neurons after neonatal 6-hydroxydopamine lesion. Neuroscience 156: 59–70. https://doi.org/10.1016/J.NEUROSCIENCE.2008.07.032

Dale H., 1935 Pharmacology and Nerve-Endings: Proc. R. Soc. Med. 28: 319–332. https://doi.org/10.1177/003591573502800330

Daniels R. W., C. A. Collins, K. Chen, M. V Gelfand, D. E. Featherstone, *et al.*, 2006 A single vesicular glutamate transporter is sufficient to fill a synaptic vesicle. Neuron 49: 11–16. https://doi.org/10.1016/j.neuron.2005.11.032

Daniels R. W., M. V. Gelfand, C. A. Collins, and A. DiAntonio, 2008 Visualizing glutamatergic cell bodies and synapses in Drosophila larval and adult CNS. J. Comp. Neurol. 508: 131–152. https://doi.org/10.1002/CNE.21670

Danielson T. J., A. A. Boulton, and H. A. Robertson, 1977 m-Octopamine, p-octopamine and phenylethanolamine in rat brain: a sensitive, specific assay and the effects of some drugs. J. Neurochem. 29: 1131–1135. https://doi.org/10.1111/J.1471-4159.1977.TB06519.X

Dankert H., L. Wang, E. D. Hoopfer, D. J. Anderson, and P. Perona, 2009 Automated monitoring and analysis of social behavior in Drosophila. Nat. Methods 2009 64 6: 297–303. https://doi.org/10.1038/nmeth.1310

Darwin C., 1872 *The Expression of the Emotions in Man and Animals*. John Murray.

Davis S. M., A. L. Thomas, L. Liu, I. M. Campbell, and H. A. Dierick, 2018 Isolation of aggressive behavior mutants in Drosophila using a screen for wing damage. Genetics 208: 273–282. https://doi.org/10.1534/genetics.117.300292

Deng B., Q. Li, X. Liu, Y. Cao, B. Li, *et al.*, 2019 Chemoconnectomics: mapping chemical transmission in Drosophila. Neuron 101: 876-893.e4. https://doi.org/10.1016/J.NEURON.2019.01.045

DePuy S. D., R. L. Stornetta, G. Bochorishvili, K. Deisseroth, I. Witten, *et al.*, 2013 Glutamatergic Neurotransmission between the C1 Neurons and the Parasympathetic

Preganglionic Neurons of the Dorsal Motor Nucleus of the Vagus. J. Neurosci. 33: 1486–1497. https://doi.org/10.1523/JNEUROSCI.4269-12.2013

Devaud J. M., C. Clouet-Redt, J. Bockaert, Y. Grau, and M. L. Parmentier, 2008 Widespread brain distribution of the Drosophila metabotropic glutamate receptor. Neuroreport 19: 367–371. https://doi.org/10.1097/WNR.0B013E3282F524C7

Dingledine R., K. Borges, D. Bowie, and S. F. Traynelis, 1999 The Glutamate Receptor Ion Channels. Pharmacol. Rev. 51: 7–62.

Dugué G. P., A. Dumoulin, A. Triller, and S. Dieudonné, 2005 Target-Dependent Use of Coreleased Inhibitory Transmitters at Central Synapses. J. Neurosci. 25: 6490–6498. https://doi.org/10.1523/JNEUROSCI.1500-05.2005

Duistermars B. J., B. D. Pfeiffer, E. D. Hoopfer, and D. J. Anderson, 2018 A brain module for scalable control of complex, multi-motor threat displays. Neuron 100: 1474-1490.e4. https://doi.org/10.1016/j.neuron.2018.10.027

Eccles J. C., P. Fatt, and K. Koketsu, 1954 Cholinergic and inhibitory synapses in a pathway from motor-axon collaterals to motoneurones. J. Physiol. 126: 524–562. https://doi.org/10.1113/JPHYSIOL.1954.SP005226

Eccles J., 1976 From electrical to chemical transmission in the central nervous system: The closing address of the Sir Henry Dale Centennial Symposium Cambridge, 19 September 1975. Notes Rec. R. Soc. Lond. 30: 219–230. https://doi.org/10.1098/RSNR.1976.0015

Eroglu Ç., B. Brügger, F. Wieland, and I. Sinning, 2003 Glutamate-binding affinity of Drosophila metabotropic glutamate receptor is modulated by association with lipid rafts. Proc. Natl. Acad. Sci. U. S. A. 100: 10219–10224. https://doi.org/10.1073/pnas.1737042100

Evans P. D., and B. Maqueira, 2005 Insect octopamine receptors: a new classification scheme based on studies of cloned Drosophila G-protein coupled receptors. Invertebr. Neurosci. 2005 53 5: 111–118. https://doi.org/10.1007/S10158-005-0001-Z

Eyjolfsdottir E., S. Branson, X. P. Burgos-Artizzu, E. D. Hoopfer, J. Schor, *et al.*, 2014 Detecting Social Actions of Fruit Flies. Lect. Notes Comput. Sci. (including Subser. Lect. Notes Artif. Intell. Lect. Notes Bioinformatics) 8690 LNCS: 772–787. https://doi.org/10.1007/978-3-319-10605-2_50

Farooqui T., 2012 Review of octopamine in insect nervous systems. Open access insect physiol. 4: 1–17. https://doi.org/10.2147/OAIP.S20911

Fortin G. M., C. Ducrot, N. Giguère, W. M. Kouwenhoven, M.-J. Bourque, *et al.*, 2019 Segregation of dopamine and glutamate release sites in dopamine neuron axons: regulation by striatal target cells. FASEB J. 33: 400–417. https://doi.org/10.1096/fj.201800713RR

Furukawa H., S. K. Singh, R. Mancusso, and E. Gouaux, 2005 Subunit arrangement and function in NMDA receptors. Nat. 2005 4387065 438: 185–192. https://doi.org/10.1038/nature04089

Greger I. H., E. B. Ziff, and A. C. Penn, 2007 Molecular determinants of AMPA receptor subunit assembly. Trends Neurosci. 30: 407–416. https://doi.org/10.1016/J.TINS.2007.06.005

Grygoruk A., H. Fei, R. W. Daniels, B. R. Miller, A. DiAntonio, *et al.*, 2010 A tyrosine-based motif localizes a Drosophila vesicular transporter to synaptic vesicles in vivo. J. Biol. Chem. 285: 6867–6878. https://doi.org/10.1074/jbc.M109.073064

Guo F., J. Yu, H. J. Jung, K. C. Abruzzi, W. Luo, *et al.*, 2016 Circadian neuron feedback controls the Drosophila sleep–activity profile. Nat. 2016 5367616 536: 292–297. https://doi.org/10.1038/nature19097

Gupta T., H. R. Morgan, J. C. Andrews, E. R. Brewer, and S. J. Certel, 2017 Methyl-CpG binding domain proteins inhibit interspecies courtship and promote aggression in Drosophila. Sci. Rep. 7: 5420. https://doi.org/10.1038/s41598-017-05844-6

Hamasaka Y., D. Rieger, M.-L. Parmentier, Y. Grau, C. Helfrich-Förster, *et al.*, 2007 Glutamate and its metabotropic receptor in Drosophila clock neuron circuits. J. Comp. Neurol. 505: 32–45. https://doi.org/10.1002/CNE.21471

Han K.-A., N. S. Millar, and R. L. Davis, 1998 A Novel Octopamine Receptor with Preferential Expression inDrosophila Mushroom Bodies. J. Neurosci. 18: 3650–3658. https://doi.org/10.1523/JNEUROSCI.18-10-03650.1998

Han T. H., P. Dharkar, M. L. Mayer, and M. Serpe, 2015 Functional reconstitution of Drosophila melanogaster NMJ glutamate receptors. Proc. Natl. Acad. Sci. 112: 6182–6187. https://doi.org/10.1073/PNAS.1500458112

Harris-Warrick R., L. Coniglio, N. Barazangi, J. Guckenheimer, and S. Gueron, 1995 Dopamine modulation of transient potassium current evokes phase shifts in a central pattern generator network. J. Neurosci. 15: 342–358. https://doi.org/10.1523/JNEUROSCI.15-01-00342.1995

Hartenstein V., J. J. Omoto, K. T. Ngo, D. Wong, P. A. Kuert, *et al.*, 2018 Structure and development of the subesophageal zone of the Drosophila brain. I. Segmental architecture, compartmentalization, and lineage anatomy. J. Comp. Neurol. 526: 6–32. https://doi.org/10.1002/cne.24287

Hnasko T. S., N. Chuhma, H. Zhang, G. Y. Goh, D. Sulzer, *et al.*, 2010 Vesicular glutamate transport promotes dopamine storage and glutamate corelease in vivo. Neuron 65: 643–656. https://doi.org/10.1016/J.NEURON.2010.02.012

Hökfelt T., L. G. Elfvin, R. Elde, M. Schultzberg, M. Goldstein, *et al.*, 1977 Occurrence of somatostatin-like immunoreactivity in some peripheral sympathetic noradrenergic neurons. Proc. Natl. Acad. Sci. 74: 3587–3591. https://doi.org/10.1073/PNAS.74.8.3587

Hökfelt T., D. Blacker, C. Broberger, M. Herrera-Marschitz, G. Snyder, *et al.*, 2002 Some aspects on the anatomy and function of central cholecystokinin systems, pp. 382–386 in *Pharmacology and Toxicology*, John Wiley & Sons, Ltd.

Hökfelt T., T. Bartfai, and F. Bloom, 2003 Neuropeptides: opportunities for drug discovery. Lancet Neurol. 2: 463–472. https://doi.org/10.1016/S1474-4422(03)00482-4

Hollmann M., C. Maron, and S. Heinemann, 1994 N-glycosylation site tagging suggests a three transmembrane domain topology for the glutamate receptor GluR1. Neuron 13: 1331–1343. https://doi.org/10.1016/0896-6273(94)90419-7

Hoyer S. C., A. Eckart, A. Herrel, T. Zars, S. A. Fischer, *et al.*, 2008 Octopamine in male aggression of Drosophila. Curr. Biol. 18: 159–167. https://doi.org/10.1016/J.CUB.2007.12.052

Hu W., T. Wang, X. Wang, and J. Han, 2015 Ih Channels Control Feedback Regulation from Amacrine Cells to Photoreceptors. PLOS Biol. 13: e1002115. https://doi.org/10.1371/JOURNAL.PBIO.1002115

Huettner J. E., 2003 Kainate receptors and synaptic transmission. Prog. Neurobiol. 70: 387–407. https://doi.org/10.1016/S0301-0082(03)00122-9

Hutchison M. A., X. Gu, M. F. Adrover, M. R. Lee, T. S. Hnasko, *et al.*, 2018 Genetic inhibition of neurotransmission reveals role of glutamatergic input to dopamine neurons in high-effort behavior. Mol. Psychiatry 23: 1213–1225. https://doi.org/10.1038/mp.2017.7

Ibrahim K. E., M. W. Couch, C. M. Williams, M. J. Fregly, and J. M. Midgley, 1985 m-Octopamine: Normal Occurrence with p-Octopamine in Mammalian Sympathetic Nerves. J. Neurochem. 44: 1862–1867. https://doi.org/10.1111/J.1471-4159.1985.TB07180.X

Jaim-Etcheverry G., and L. Zieher, 1973 Proceedings: Coexistence of monoamines in adrenergic synaptic vesicles - PubMed. Acta Physiol. Lat. Am. 23: 616–618.

Ji-Quan Wang, and Anna-Liisa Brownell, 2007 Development of Metabotropic Glutamate Receptor Ligands for Neuroimaging. Curr. Med. Imaging Rev. 3: 186–205. https://doi.org/10.2174/157340507781387059

Kabra M., A. A. Robie, M. Rivera-Alba, S. Branson, and K. Branson, 2013 JAABA: interactive machine learning for automatic annotation of animal behavior. Nat. Methods 2012 101 10: 64–67. https://doi.org/10.1038/nmeth.2281

Kandel E. R., J. H. Schwartz, T. M. Jessell, S. A. Siegelbaum, and A. Hudspeth, 2012 *Principles of Neural Science*. McGraw-Hill Medical.

Kapoor V., A. C. Provost, P. Agarwal, and V. N. Murthy, 2016 Activation of raphe nuclei triggers rapid and distinct effects on parallel olfactory bulb output channels. Nat. Neurosci. 2016 192 19: 271–282. https://doi.org/10.1038/nn.4219

Karuppudurai T., T.-Y. Lin, C.-Y. Ting, R. Pursley, K. V. Melnattur, *et al.*, 2014 A Hard-Wired Glutamatergic Circuit Pools and Relays UV Signals to Mediate Spectral Preference in Drosophila. Neuron 81: 603–615. https://doi.org/10.1016/J.NEURON.2013.12.010

Katz P., and R. Harris-Warrick, 1990 Neuromodulation of the crab pyloric central pattern generator by serotonergic/cholinergic proprioceptive afferents. J. Neurosci. 10: 1495–1512. https://doi.org/10.1523/JNEUROSCI.10-05-01495.1990

Kennedy A., K. Asahina, E. D. Hoopfer, H. K. Inagaki, Y. Jung, *et al.*, 2014 Internal states and behavioral decision-making: toward an integration of emotion and cognition. Cold Spring Harb. Symp. Quant. Biol. 79: 199–210. https://doi.org/10.1101/sqb.2014.79.024984

Kim Y.-C., H.-G. Lee, J. Lim, and K.-A. Han, 2013 Appetitive learning requires the alpha1-like octopamine receptor OAMB in the Drosophila mushroom body neurons. J. Neurosci. 33: 1672–1677. https://doi.org/10.1523/JNEUROSCI.3042-12.2013

Kiyose K., M. Katsuki, Y. Suzaki, K. Okada, and Y. Okada, 2021 Octopaminergic system orchestrates combat and mating behaviors: A potential regulator of alternative male mating tactics in an armed beetle. J. Insect Physiol. 131: 104211. https://doi.org/10.1016/J.JINSPHYS.2021.104211

Koganezawa M., K. Kimura, and D. Yamamoto, 2016 The neural circuitry that functions as a switch for courtship versus aggression in Drosophila males. Curr. Biol. 26: 1395–1403. https://doi.org/10.1016/J.CUB.2016.04.017

Koon A. C., J. Ashley, R. Barria, S. DasGupta, R. Brain, *et al.*, 2010 Autoregulatory and paracrine control of synaptic and behavioral plasticity by octopaminergic signaling. Nat. Neurosci. 2010 142 14: 190–199. https://doi.org/10.1038/nn.2716

Koon A. C., and V. Budnik, 2012 Inhibitory control of synaptic and behavioral plasticity by octopaminergic signaling. J. Neurosci. 32: 6312–6322. https://doi.org/10.1523/JNEUROSCI.6517-11.2012

Kravitz E. A., and M. de la P. Fernández, 2015 Aggression in Drosophila. Behav. Neurosci. 129: 549–563.

Kumari R., C. Castillo, and A. Francesconi, 2013 Agonist-dependent signaling by group I metabotropic glutamate receptors is regulated by association with lipid domains. J. Biol. Chem. 288: 32004–32019. https://doi.org/10.1074/jbc.M113.475863

Kupfermann I., 1991 Functional studies of cotransmission. Physiol. Rev. 71: 683–732. https://doi.org/10.1152/PHYSREV.1991.71.3.683

Kvamme E., I. A. Torgner, and B. Roberg, 2001 Kinetics and localization of brain phosphate activated glutaminase. J. Neurosci. Res. 66: 951–958. https://doi.org/10.1002/JNR.10041

Lagerström M. C., K. Rogoz, B. Abrahamsen, A.-L. Lind, C. Ölund, *et al.*, 2011 A sensory subpopulation depends on vesicular glutamate transporter 2 for mechanical pain, and together with substance P, inflammatory pain. Proc. Natl. Acad. Sci. 108: 5789–5794. https://doi.org/10.1073/PNAS.1013602108

Langer S. Z., 2008 Presynaptic autoreceptors regulating transmitter release. Neurochem. Int. 52: 26–30. https://doi.org/10.1016/j.neuint.2007.04.031

Langer S. Z., 2015 α2-Adrenoceptors in the treatment of major neuropsychiatric disorders. Trends Pharmacol. Sci. 36: 196–202.

Lee J. Y., D. Bhatt, D. Bhatt, W. Y. Chung, and R. L. Cooper, 2009 Furthering pharmacological and physiological assessment of the glutamatergic receptors at the Drosophila neuromuscular junction. Comp. Biochem. Physiol. Part C Toxicol. Pharmacol. 150: 546–557. https://doi.org/10.1016/J.CBPC.2009.08.002

Levitz J., C. Habrian, S. Bharill, Z. Fu, R. Vafabakhsh, *et al.*, 2016 Mechanism of Assembly and Cooperativity of Homomeric and Heteromeric Metabotropic Glutamate Receptors. Neuron 92: 143–159. https://doi.org/10.1016/J.NEURON.2016.08.036

Li Y., P. Dharkar, T.-H. Han, M. Serpe, C.-H. Lee, *et al.*, 2016 Novel Functional Properties of Drosophila CNS Glutamate Receptors. Neuron 92: 1036–1048. https://doi.org/10.1016/J.NEURON.2016.10.058

Limapichat W., W. Y. Yu, E. Branigan, H. A. Lester, and D. A. Dougherty, 2012 Key Binding Interactions for Memantine in the NMDA Receptor. ACS Chem. Neurosci. 4: 255–260. https://doi.org/10.1021/CN300180A

Lin D., M. P. Boyle, P. Dollar, H. Lee, E. S. Lein, *et al.*, 2011 Functional identification of an aggression locus in the mouse hypothalamus. Nature 470: 221–227. https://doi.org/10.1038/nature09736

Lin C.-C., K. A. Prokop-Prigge, G. Preti, and C. J. Potter, 2015 Food odors trigger Drosophila males to deposit a pheromone that guides aggregation and female oviposition decisions. Elife 4. https://doi.org/10.7554/ELIFE.08688

Liu Y., O. A. Samad, L. Zhang, B. Duan, Q. Tong, *et al.*, 2010 VGLUT2-Dependent Glutamate Release from Nociceptors Is Required to Sense Pain and Suppress Itch. Neuron 68: 543–556. https://doi.org/10.1016/J.NEURON.2010.09.008

Livingstone M. S., and B. L. Tempel, 1983 Genetic dissection of monoamine neurotransmitter synthesis in Drosophila. Nat. 1983 3035912 303: 67–70. https://doi.org/10.1038/303067a0

Loftis J. M., and A. Janowsky, 2003 The N-methyl-d-aspartate receptor subunit NR2B: localization, functional properties, regulation, and clinical implications. Pharmacol. Ther. 97: 55–85. https://doi.org/10.1016/S0163-7258(02)00302-9

Lundberg J. M., 1996 Pharmacology of cotransmission in the autonomic nervous system: integrative aspects on amines, neuropeptides, adenosine triphosphate, amino acids and nitric oxide. Pharmacol. Rev. 48.

Ly S., E. Strus, and N. Naidoo, 2020 Genetic disruption of the putative binding site for Homer on DmGluRA reduces sleep in Drosophila. Sleep 43. https://doi.org/10.1093/SLEEP/ZSZ190

Malik A. R., and T. E. Willnow, 2019 Excitatory Amino Acid Transporters in Physiology and Disorders of the Central Nervous System. Int. J. Mol. Sci. 2019, Vol. 20, Page 5671 20: 5671. https://doi.org/10.3390/IJMS20225671

McKinney H., L. M. Sherer, J. L. Williams, S. J. Certel, and R. S. Stowers, 2020 Characterization of Drosophila octopamine receptor neuronal expression using MiMIC-converted Gal4 lines. J. Comp. Neurol. cne.24883. https://doi.org/10.1002/cne.24883

Meldrum B. S., 2000 Glutamate as a Neurotransmitter in the Brain: Review of Physiology and Pathology. J. Nutr. 130: 1007S-1015S. https://doi.org/10.1093/JN/130.4.1007S

Melone M., F. Quagliano, P. Barbaresi, H. Varoqui, J. D. Erickson, *et al.*, 2004 Localization of the Glutamine Transporter SNAT1 in Rat Cerebral Cortex and Neighboring Structures, With a Note on its Localization in Human Cortex. Cereb. Cortex 14: 562–574. https://doi.org/10.1093/CERCOR/BHH018

Mendez J. A., M.-J. Bourque, G. D. Bo, M. L. Bourdeau, M. Danik, *et al.*, 2008 Developmental and Target-Dependent Regulation of Vesicular Glutamate Transporter Expression by Dopamine Neurons. J. Neurosci. 28: 6309–6318. https://doi.org/10.1523/JNEUROSCI.1331-08.2008

Merino-Jiménez C., F. Miguel, J. A. Feria Pliego, M. E. Zetina Rosales, F. Cifuentes, *et al.*, 2018 Sympathetic hyperactivity and age affect segregation and expression of neurotransmitters. Front. Cell. Neurosci. 12: 411. https://doi.org/10.3389/fncel.2018.00411

Mestikawy S. El, Å. Wallén-Mackenzie, G. M. Fortin, L. Descarries, and L.-É. Trudeau, 2011 From glutamate co-release to vesicular synergy: vesicular glutamate transporters. Nat. Rev. Neurosci. 12: 204–216. https://doi.org/10.1038/nrn2969

Mingote S., N. Chuhma, A. Kalmbach, G. M. Thomsen, Y. Wang, *et al.*, 2017 Dopamine neuron dependent behaviors mediated by glutamate cotransmission. Elife 6: e27566. https://doi.org/10.7554/eLife.27566

Mingote S., A. Amsellem, A. Kempf, S. Rayport, and N. Chuhma, 2019 Dopamine-glutamate neuron projections to the nucleus accumbens medial shell and behavioral switching. Neurochem. Int. 129: 104482. https://doi.org/10.1016/j.neuint.2019.104482

Molina-Obando S., J. F. Vargas-Fique, M. Henning, B. Gür, T. M. Schlad, *et al.*, 2019 ON selectivity in the drosophila visual system is a multisynaptic process involving both glutamatergic and GABAergic inhibition. Elife 8. https://doi.org/10.7554/ELIFE.49373

Monastirioti M., C. E. Linn Jr, and K. White, 1996 Characterization of Drosophila Tyramine β-Hydroxylase Gene and Isolation of Mutant Flies Lacking Octopamine. J. Neurosci. 16: 3900–3911. https://doi.org/10.1523/JNEUROSCI.16-12-03900.1996

Mongia S., T. Yamaguchi, B. Liu, S. Zhang, H. Wang, *et al.*, 2019 The Ventral Tegmental Area has calbindin neurons with the capability to co-release glutamate and dopamine into the nucleus accumbens. Eur. J. Neurosci. ejn.14493. https://doi.org/10.1111/ejn.14493

Moustaine D. El, S. Granier, E. Doumazane, P. Scholler, R. Rahmeh, *et al.*, 2012 Distinct roles of metabotropic glutamate receptor dimerization in agonist activation and G-protein coupling. Proc. Natl. Acad. Sci. 109: 16342–16347. https://doi.org/10.1073/PNAS.1205838109

Münster-Wandowski A., J.-F. Zander, K. Richter, and G. Ahnert-Hilger, 2016 Co-existence of functionally different vesicular neurotransmitter transporters. Front. Synaptic Neurosci. 8: 4. https://doi.org/10.3389/fnsyn.2016.00004

Nässel D. R., 2018 Substrates for neuronal cotransmission with neuropeptides and small molecule neurotransmitters in Drosophila. Front. Cell. Neurosci. 12: 83. https://doi.org/10.3389/fncel.2018.00083

Nelson R. J., and B. C. Trainor, 2007 Neural mechanisms of aggression. Nat. Rev. Neurosci. 8: 536–546.

Niswender C. M., and P. J. Conn, 2010 Metabotropic glutamate receptors: physiology, pharmacology, and disease. Annu. Rev. Pharmacol. Toxicol. 50: 295–322. https://doi.org/10.1146/annurev.pharmtox.011008.145533

Noh J., R. P. Seal, J. A. Garver, R. H. Edwards, and K. Kandler, 2010 Glutamate co-release at GABA/glycinergic synapses is crucial for the refinement of an inhibitory map. Nat. Neurosci. 13: 232–238. https://doi.org/10.1038/nn.2478

Norenberg M. D., and A. Martinez-Hernandez, 1979 Fine structural localization of glutamine synthetase in astrocytes of rat brain. Brain Res. 161: 303–310. https://doi.org/10.1016/0006-8993(79)90071-4

Nusbaum M. P., D. M. Blitz, A. M. Swensen, D. Wood, and E. Marder, 2001 The roles of co-transmission in neural network modulation. Trends Neurosci. 24: 146–154. https://doi.org/10.1016/S0166-2236(00)01723-9

Okaty B. W., K. G. Commons, and S. M. Dymecki, 2019 Embracing diversity in the 5-HT neuronal system. Nat. Rev. Neurosci. 1. https://doi.org/10.1038/s41583-019-0151-3

Osborne N. N., 1983 Dale's Principle and Communication between Neurones : Based on a Colloquium of the Neurochemical Group of the Biochemical Society, Held at Oxford University, July 1982. 213.

Pagani M., G. W. Albisetti, N. Sivakumar, H. Wildner, M. Santello, *et al.*, 2019 How gastrin-releasing peptide opens the spinal gate for itch. Neuron 103: 102-117.e5. https://doi.org/10.1016/j.neuron.2019.04.022

Panneels V., C. Eroglu, P. Cronet, and I. Sinning, 2003 Pharmacological characterization and immunoaffinity purification of metabotropic glutamate receptor from Drosophila overexpressed in Sf9 cells. Protein Expr. Purif. 30: 275–282. https://doi.org/10.1016/S1046-5928(03)00100-1

Papathanou M., M. Creed, M. C. Dorst, Z. Bimpisidis, S. Dumas, *et al.*, 2018 Targeting VGLUT2 in mature dopamine neurons decreases mesoaccumbal glutamatergic transmission and identifies a role for glutamate co-release in synaptic plasticity by increasing baseline AMPA/NMDA ratio. Front. Neural Circuits 12: 64. https://doi.org/10.3389/fncir.2018.00064

Parmentier M.-L., J.-P. Pin, J. Bockaert, and Y. Grau, 1996 Cloning and Functional Expression of a DrosophilaMetabotropic Glutamate Receptor Expressed in the Embryonic CNS. J. Neurosci. 16: 6687–6694. https://doi.org/10.1523/JNEUROSCI.16-21-06687.1996

Penn J. K., M. F. Zito, and E. A. Kravitz, 2010 A single social defeat reduces aggression in a highly aggressive strain of Drosophila. Proc. Natl. Acad. Sci. U. S. A. 107: 12682–12686. https://doi.org/10.1073/pnas.1007016107

Platt S. R., 2007 The role of glutamate in central nervous system health and disease – A review. Vet. J. 173: 278–286. https://doi.org/10.1016/J.TVJL.2005.11.007

Qi Y., G. Xu, G. Gu, F. Mao, G. Ye, *et al.*, 2017 A new Drosophila octopamine receptor responds to serotonin. Insect Biochem. Mol. Biol. 90: 61–70. https://doi.org/10.1016/J.IBMB.2017.09.010

Qin G., T. Schwarz, R. J. Kittel, A. Schmid, T. M. Rasse, *et al.*, 2005 Four Different Subunits Are Essential for Expressing the Synaptic Glutamate Receptor at Neuromuscular Junctions of Drosophila. J. Neurosci. 25: 3209–3218. https://doi.org/10.1523/JNEUROSCI.4194-04.2005

Reiner A., and J. Levitz, 2018 Glutamatergic Signaling in the Central Nervous System: Ionotropic and Metabotropic Receptors in Concert. Neuron 98: 1080. https://doi.org/10.1016/J.NEURON.2018.05.018

Rillich J., and P. A. Stevenson, 2015 Releasing stimuli and aggression in crickets: octopamine promotes escalation and maintenance but not initiation. Front. Behav. Neurosci. 9: 95. https://doi.org/10.3389/fnbeh.2015.00095

Rillich J., and P. A. Stevenson, 2019 Fight or flee? Lessons from insects on aggression. Neuroforum 25: 3–13. https://doi.org/10.1515/nf-2017-0040

Robinson J. E., J. Paluch, D. K. Dickman, and W. J. Joiner, 2016 ADAR-mediated RNA editing suppresses sleep by acting as a brake on glutamatergic synaptic plasticity. Nat. Commun. 2015 71 7: 1–9. https://doi.org/10.1038/ncomms10512

Rubio-Aliaga I., and C. A. Wagner, 2016 Regulation and function of the SLC38A3/SNAT3 glutamine transporter. http://dx.doi.org/10.1080/19336950.2016.1207024 10: 440–452. https://doi.org/10.1080/19336950.2016.1207024

Sabandal J. M., P. R. Sabandal, Y.-C. Kim, and K.-A. Han, 2020 Concerted Actions of Octopamine and Dopamine Receptors Drive Olfactory Learning. J. Neurosci. JN-RM-1756-19. https://doi.org/10.1523/jneurosci.1756-19.2020

Salussolia C. L., M. L. Prodromou, P. Borker, and L. P. Wollmuth, 2011 Arrangement of Subunits in Functional NMDA Receptors. J. Neurosci. 31: 11295–11304. https://doi.org/10.1523/JNEUROSCI.5612-10.2011

Schoenfeld B. P., R. J. Choi, C. H. Choi, A. M. Terlizzi, P. Hinchey, *et al.*, 2013 The Drosophila DmGluRA is required for social interaction and memory. Front. Pharmacol. 4: 64. https://doi.org/10.3389/fphar.2013.00064

Sengupta A., M. Bocchio, D. M. Bannerman, T. Sharp, and M. Capogna, 2017 Control of amygdala circuits by 5-HT neurons via 5-HT and glutamate cotransmission. J. Neurosci. 37: 1785–1796. https://doi.org/10.1523/JNEUROSCI.2238-16.2016

Sherer L. M., E. Catudio Garrett, H. R. Morgan, E. D. Brewer, L. A. Sirrs, *et al.*, 2020 Octopamine neuron dependent aggression requires dVGLUT from dual-transmitting neurons, (G. Hasan, Ed.). PLOS Genet. 16: e1008609. https://doi.org/10.1371/journal.pgen.1008609

Shi S.-H., Y. Hayashi, R. S. Petralia, S. H. Zaman, R. J. Wenthold, *et al.*, 1999 Rapid Spine Delivery and Redistribution of AMPA Receptors After Synaptic NMDA Receptor Activation. Science (80-.). 284: 1811–1816. https://doi.org/10.1126/SCIENCE.284.5421.1811

Shigemoto R., A. Kinoshita, E. Wada, S. Nomura, H. Ohishi, *et al.*, 1997 Differential Presynaptic Localization of Metabotropic Glutamate Receptor Subtypes in the Rat Hippocampus. J. Neurosci. 17: 7503–7522. https://doi.org/10.1523/JNEUROSCI.17-19-07503.1997

Silm K., J. Yang, P. F. Marcott, C. S. Asensio, J. Eriksen, *et al.*, 2019 Synaptic vesicle recycling pathway determines neurotransmitter content and release properties. Neuron 102: 786-800.e5. https://doi.org/10.1016/J.NEURON.2019.03.031

Song I., and R. L. Huganir, 2002 Regulation of AMPA receptors during synaptic plasticity. Trends Neurosci. 25: 578–588. https://doi.org/10.1016/S0166-2236(02)02270-1

Starratt A. N., and R. P. Bodnaryk, 1981 Stereoisomeric identity of octopamine in the central nervous system of invertebrates. Insect Biochem. 11: 645–648. https://doi.org/10.1016/0020-1790(81)90053-6

Steinkellner T., V. Zell, Z. J. Farino, M. S. Sonders, M. Villeneuve, *et al.*, 2018 Role for VGLUT2 in selective vulnerability of midbrain dopamine neurons. J. Clin. Invest. 128: 774–788. https://doi.org/10.1172/JCI95795

Stornetta R. L., C. P. Sevigny, A. M. Schreihofer, D. L. Rosin, and P. G. Guyenet, 2002 Vesicular glutamate transporter DNPI/VGLUT2 is expressed by both C1 adrenergic and nonaminergic presympathetic vasomotor neurons of the rat medulla. J. Comp. Neurol. 444: 207–220. https://doi.org/10.1002/CNE.10142

Sturtevant A. H., 1915 Experiments on sex recognition and the problem of sexual selection in Drosoophilia. J. Anim. Behav. 5: 351–366. https://doi.org/10.1037/H0074109

Suga Y., 2006 Chinese cricket-fighting. Int. J. Asian Stud. 3: 77–93. https://doi.org/10.1017/S1479591405000239

Sujkowski A., A. Gretzinger, N. Soave, S. V. Todi, and R. Wessells, 2020 Alpha- and beta-adrenergic octopamine receptors in muscle and heart are required for Drosophila exercise adaptations, (H. Bai, Ed.). PLOS Genet. 16: e1008778. https://doi.org/10.1371/journal.pgen.1008778

Svensson E., J. Apergis-Schoute, G. Burnstock, M. P. Nusbaum, D. Parker, *et al.*, 2019 General principles of neuronal co-transmission: insights from multiple model systems. Front. Neural Circuits 12: 117. https://doi.org/10.3389/fncir.2018.00117

Swanson C. J., M. Bures, M. P. Johnson, A. M. Linden, J. A. Monn, *et al.*, 2005 Metabotropic glutamate receptors as novel targets for anxiety and stress disorders. Nat. Rev. Drug Discov. 4: 131–144.

Swensen A. M., and E. Marder, 2000 Multiple Peptides Converge to Activate the Same Voltage-Dependent Current in a Central Pattern-Generating Circuit. J. Neurosci. 20: 6752–6759. https://doi.org/10.1523/JNEUROSCI.20-18-06752.2000

Tao J., D. Bulgari, D. A. Berkhoudt, M. J. Calderon, S. C. Watkins, *et al.*, 2019 Drosophila Ptp4E regulates vesicular packaging for monoamine-neuropeptide co-transmission. J. Cell Sci. 132: jcs224568. https://doi.org/10.1242/jcs.224568

Traynelis S. F., L. P. Wollmuth, C. J. McBain, F. S. Menniti, K. M. Vance, *et al.*, 2010 Glutamate Receptor Ion Channels: Structure, Regulation, and Function. Pharmacol. Rev. 62: 405–496. https://doi.org/10.1124/PR.109.002451

Trudeau L.-É., 2004 Glutamate co-transmission as an emerging concept in monoamine neuron function. J. Psychiatry Neurosci. 29: 296–310.

Trudeau L.-É., and S. El Mestikawy, 2018 Glutamate cotransmission in cholinergic, GABAergic and monoamine systems: contrasts and commonalities. Front. Neural Circuits 12: 113. https://doi.org/10.3389/fncir.2018.00113

Ultsch A., C. M. Schuster, B. Laube, H. Betz, and B. Schmitt, 1993 Glutamate receptors of Drosophila melanogaster. FEBS Lett. 324: 171–177. https://doi.org/10.1016/0014-5793(93)81387-F

Vaaga C. E., M. Borisovska, and G. L. Westbrook, 2014 Dual-transmitter neurons: functional implications of co-release and co-transmission. Curr. Opin. Neurobiol. 29: 25–32. https://doi.org/10.1016/j.conb.2014.04.010

Vaaga C. E., J. T. Yorgason, J. T. Williams, and G. L. Westbrook, 2017 Presynaptic gain control by endogenous cotransmission of dopamine and GABA in the olfactory bulb. J. Neurophysiol. 117: 1163–1170. https://doi.org/10.1152/jn.00694.2016

Vega A., J. A. Luther, S. J. Birren, and M. A. Morales, 2010 Segregation of the classical transmitters norepinephrine and acetylcholine and the neuropeptide Y in sympathetic neurons: Modulation by ciliary neurotrophic factor or prolonged growth in culture. Dev. Neurobiol. 70: 913–928. https://doi.org/10.1002/DNEU.20834

Vega A., A. Cancino-Rodezno, P. Valle-Leija, B. M. Sánchez-Tafolla, D. Elinos, *et al.*, 2016 Neurotrophin-dependent plasticity of neurotransmitter segregation in the rat superior cervical ganglion in vivo. Dev. Neurobiol. 76: 832–846. https://doi.org/10.1002/DNEU.22362

Völkner M., B. Lenz-Böhme, H. Betz, and B. Schmitt, 2000 Novel CNS Glutamate Receptor Subunit Genes of Drosophila melanogaster. J. Neurochem. 75: 1791–1799. https://doi.org/10.1046/J.1471-4159.2000.0751791.X

Watanabe K., H. Chiu, B. D. Pfeiffer, A. M. Wong, E. D. Hoopfer, *et al.*, 2017 A circuit node that integrates convergent input from neuromodulatory and social behavior-promoting neurons to control aggression in Drosophila. Neuron 95: 1112–1128. https://doi.org/10.1016/j.neuron.2017.08.017

Willard S. S., and S. Koochekpour, 2013 Glutamate, glutamate receptors, and downstream signaling pathways. Int. J. Biol. Sci. 9: 948–959. https://doi.org/10.7150/IJBS.6426

Williams C. M., and M. W. Couch, 1978 Identification of ortho-octapamine and meta-octopamine in mammalian adrenal and salivary gland. Life Sci. 22: 2113–2120. https://doi.org/10.1016/0024-3205(78)90455-1

Wolf M. U., Y. Goldberg, and M. Freedman, 2018 Aggression and agitation in dementia. Continuum (N. Y). 24: 783–803. https://doi.org/10.1212/CON.0000000000000605

Wolstenholme A. J., 2012 Glutamate-gated Chloride Channels *. J. Biol. Chem. 287: 40232–40238. https://doi.org/10.1074/JBC.R112.406280

Wu S.-F., Y. Yao, J. Huang, and G.-Y. Ye, 2012 Characterization of a β-adrenergic-like octopamine receptor from the rice stem borer (Chilo suppressalis). J. Exp. Biol. 215: 2646–2652. https://doi.org/10.1242/JEB.068932

Wu S.-F., G. Xu, Y.-X. Qi, R.-Y. Xia, J. Huang, *et al.*, 2014 Two splicing variants of a novel family of octopamine receptors with different signaling properties. J. Neurochem. 129: 37–47. https://doi.org/10.1111/JNC.12526

Xia S., T. Miyashita, T.-F. Fu, W.-Y. Lin, C.-L. Wu, *et al.*, 2005 NMDA Receptors Mediate Olfactory Learning and Memory in Drosophila. Curr. Biol. 15: 603–615. https://doi.org/10.1016/J.CUB.2005.02.059

Xia S., and A.-S. Chiang, 2009 *NMDA Receptors in Drosophila*(A. M. Van Dongen, Ed.). CRC Press/Taylor & Francis, Boca Raton, FL.

Xie T., M. C. W. Ho, Q. Liu, W. Horiuchi, C.-C. Lin, *et al.*, 2018 A genetic toolkit for dissecting dopamine circuit function in Drosophila. Cell Rep. 23: 652–665. https://doi.org/10.1016/j.celrep.2018.03.068

Yellman C., H. Tao, B. He, and J. Hirsh, 1997 Conserved and sexually dimorphic behavioral responses to biogenic amines in decapitated Drosophila. Proc. Natl. Acad. Sci. U. S. A. 94: 4131–4136. https://doi.org/10.1073/pnas.94.8.4131

Youn H., C. Kirkhart, J. Chia, and K. Scott, 2018 A subset of octopaminergic neurons that promotes feeding initiation in Drosophila melanogaster, (F. Marion-Poll, Ed.). PLoS One 13: e0198362. https://doi.org/10.1371/journal.pone.0198362

Zelikowsky M., M. Hui, T. Karigo, A. Choe, B. Yang, *et al.*, 2018 The neuropeptide Tac2 controls a distributed brain state induced by chronic social isolation stress. Cell 173: 1265-1279.e19. https://doi.org/10.1016/J.CELL.2018.03.037

Zelikowsky M., K. Ding, and D. J. Anderson, 2019 Neuropeptidergic control of an internal brain state produced by prolonged social isolation stress. Cold Spring Harb. Symp. Quant. Biol. 83: 1–7. https://doi.org/10.1101/sqb.2018.83.038109

Zhang D., H. Kuromi, and Y. Kidokoro, 1999 Activation of metabotropic glutamate receptors enhances synaptic transmission at the Drosophila neuromuscular junction. Neuropharmacology 38: 645–657. https://doi.org/10.1016/S0028-3908(98)00232-9

Zhang S., J. Qi, X. Li, H.-L. Wang, J. P. Britt, *et al.*, 2015 Dopaminergic and glutamatergic microdomains in a subset of rodent mesoaccumbens axons. Nat. Neurosci. 18: 386–396. https://doi.org/10.1038/nn.3945

Zhang S. X., L. E. Miner, C. L. Boutros, D. Rogulja, and M. A. Crickmore, 2018 Motivation, perception, and chance converge to make a binary decision. Neuron 99: 376-388.e6. https://doi.org/10.1016/J.NEURON.2018.06.014

Zhang Q., B. Liu, Q. Wu, B. Liu, Y. Li, *et al.*, 2019 Differential co-release of two neurotransmitters from a vesicle fusion pore in mammalian adrenal chromaffin cells. Neuron 102: 173-183.e4. https://doi.org/10.1016/J.NEURON.2019.01.031

Zheng Z., J. S. Lauritzen, E. Perlman, C. G. Robinson, M. Nichols, *et al.*, 2018 A complete electron microscopy volume of the brain of adult Drosophila melanogaster. Cell 174: 730-743.e22. https://doi.org/10.1016/j.cell.2018.06.019

Octopamine neuron dependent aggression requires dVGLUT from dual-transmitting neurons

Lewis M. Sherer[1], Elizabeth Catudio Garrett[1], Hannah R. Morgan[4], Edmond D. Brewer[4], Lucy A. Sirrs[4], Harold K. Shearin[2], Jessica L. Williams[2], Brian D. McCabe[3], R. Steven Stowers[2], and Sarah J. Certel[1,4*]

[1]Cellular, Molecular and Microbial Biology Graduate Program, The University of Montana, Missoula, MT, United States.

[2]Cell Biology and Neuroscience Department, Montana State University, Bozeman, MT, United States.

[3]Brain Mind Institute, EPFL, 1015 Lausanne, Switzerland.

[4]Division of Biological Sciences, Center for Structural and Functional Neuroscience, The University of Montana, Missoula, MT, United States.

*Corresponding author: *sarah.certel@umontana.edu*

Abstract

Neuromodulators such as monoamines are often expressed in neurons that also release at least one fast-acting neurotransmitter. The release of a combination of transmitters provides both "classical" and "modulatory" signals that could produce diverse and/or complementary effects in associated circuits. Here, we establish that the majority of *Drosophila* octopamine (OA) neurons are also glutamatergic and identify the individual contributions of each neurotransmitter on sex-specific behaviors. Males without OA display low levels of aggression and high levels of inter-male courtship. Males deficient for dVGLUT solely in OA-glutamate neurons (OGNs) also exhibit a reduction in aggression, but without a concurrent increase in inter-male courtship. Within OGNs, a portion of VMAT and dVGLUT puncta differ in localization suggesting spatial differences in OA signaling. Our findings establish a previously undetermined role for dVGLUT in OA neurons and suggests that glutamate uncouples aggression from OA-dependent courtship-related behavior. These results indicate that dual neurotransmission can increase the efficacy of individual neurotransmitters while maintaining unique functions within a multi-functional social behavior neuronal network.

Author Summary

Neurons communicate with each other via electrical events and the release of chemical signals. An emerging challenge in understanding neuron communication is the realization that many neurons release more than one type of chemical signal or neurotransmitter. Here we ask how does the release of more than one neurotransmitter from a single neuron impact circuits that control behavior? We determined the monoamine octopamine and the classical transmitter glutamate are co-expressed in the *Drosophila* adult CNS. By manipulating the release of glutamate in OA-glutamate neurons, we demonstrated glutamate has both separable actions and complementary actions with OA on aggression and reproductive behaviors respectively. Aggression is a behavior that is highly conserved between organisms and present in many human disease states, including depression and Alzheimer's disease. Our results show that aggressive behavior requires the release of both neurotransmitters in dual-transmitting neurons and suggests within this set of neurons, glutamate may provide a new therapeutic target to modulate aggression in pathological conditions.

Introduction

The classical view of information transfer for many decades was that each neuron released a single neurotransmitter, leading to the 'one neuron, one transmitter' hypothesis [1], formalized by John Eccles as Dale's Principle [2]. Dale himself, however, recognized the possibility that neurons can release more than one molecule [3] and indeed, research from multiple systems and neuronal populations have established that many if not most, neurons release more than one neurotransmitter [4-7]. Dual neurotransmission has the potential to transform the way we consider the computation and transmission of information by neurons, circuits and networks. Presynaptically, the release of two neurotransmitters could impact information transfer by several mechanisms that are not mutually exclusive including; attenuating signals by modulating presynaptic autoreceptors, transmitting spatially distinct signals by segregating specific vesicle populations to different axon terminals, or conveying similar information through the release of both neurotransmitters from the same synaptic vesicle [8-11]. In addition, one vesicular neurotransmitter transporter can increase the packaging of the other neurotransmitter into the same synaptic vesicle (SV), a process called vesicular synergy [4, 12, 13]. At post-synaptic targets, the release of two transmitters can enhance the strength of the same signal and/or convey unique signals through spatially-restricted receptor expression and second messenger cascades [7, 14]. While recent studies have provided insight into these phenomena at the cellular level [11, 12, 15, 16], the behavioral relevance of co-transmission in normal as well as pathological conditions is an area of considerable complexity and interest.

The genetic tools of *Drosophila* provide the ability to genetically dissect the signaling properties of dual transmission on behavioral networks in general and upon the circuits that control aggression in particular. Aggression is an innate behavior that has evolved in the framework of defending or obtaining resources [17, 18]. Monoamines such as serotonin (5-HT), dopamine (DA), norepinephrine (NE) and octopamine (OA), the invertebrate homologue of NE, have powerful modulatory effects on aggression in systems ranging from insects and crustaceans to humans [19-23]. In humans, aggressive behavior can be expressed at extreme levels and out of context due to medical, neurologic and or psychiatric disorders including depression and schizophrenia [24-26]. Pharmacological agents that selectively manipulate monoamine signaling are used to treat anxiety and depression, yet these drugs are often ineffective, and in the case of serotonin/norepinephrine reuptake inhibitors (SNRIs) can induce side effects including increased aggression and impulsivity [25, 27-29].

At least two difficulties arise in targeting monoamines to achieve successful outcomes. First, monoamines can be released from synaptic vesicles (SVs) into the presynaptic cleft and by extrasynaptic release from large dense core vesicles (LDCVs) [30-33]. Thus, monoamines are recognized both as neurotransmitters and as neuromodulators that signal via diffusion [34, 35]. The second difficulty is that their effects are likely exerted through interactions with neuropeptides (neuropeptide Y and oxytocin are two examples) and with neurotransmitters including GABA and glutamate [5, 14, 36, 37]. Due in part to recent studies suggesting the expression of vesicular glutamate transporters (VGLUTs) can be altered by psychiatric medications [38-41] and the importance of dopamine neuron glutamate co-transmission on the schizophrenia resilience phenotype in mice [42], we generated new tools to identify and manipulate glutamate function in monoamine-expressing neurons.

We found that the majority of OA neurons within the *Drosophila* nervous system also express the vesicular neurotransmitter transporter for glutamate (dVGlut). Functionally, glutamate (GLU) co-expression could convey the same information by promoting the synaptic vesicle packing of OA or GLU may convey distinct information that is separate from the function of OA. In *Drosophila*, OA synthesis and release are essential for conserved social behaviors; males without OA display low levels of aggression and high levels of inter-male courtship [43-47]. We demonstrate that males deficient for dVGLUT solely in OA-glutamate neurons (OGNs) also exhibit a reduction in aggression, but without a concurrent increase in inter-male courtship. These results indicate both OA and dVGLUT are required in dual-transmitting neurons to promote aggression. However, only OA is required for the suppression of inter-male courtship and thus the function of dVGLUT in OGNs is not limited to vesicular synergy.

To ask if the separable effects of OA on courtship circuitry may be attributable to spatially distinct OA signals, we conditionally expressed a new epitope-tagged version of the *Drosophila* vesicular neurotransmitter transporter for monoamines (V5-tagged VMAT) in OGNs. While the majority of V5-VMAT and dVGLUT expression colocalize, VMAT is detected in distinct puncta without dVGLUT suggesting the possibility of separable signal transmission. Together, these results demonstrate the complex behavior of aggression requires both dVGLUT and OA in dual-transmitting neurons and

suggests within monoamine neurons, GLU may provide a therapeutic target to modulate aggression in pathological conditions.

Results

dVGLUT is co-expressed in OA neurons

The co-expression of vesicular neurotransmitter transporters has been primarily used to identify dual-transmitting neurons[48-52]. To examine glutamatergic transmitter expression, we generated a monoclonal dVGLUT antibody and validated its specificity using a new *dVGlut* allele, *dVGlut^{SS1}*. In homozygous *dVGlut^{SS1}* progeny, dVGLUT protein is not detectable (SFig 1, Methods), thus demonstrating the specificity of the dVGLUT antibody. As dVGLUT expression is widespread and mainly found in synaptic terminals (SFig 1), we used the Gal4-UAS system to identify monoamine neurons that express GLU. In this study, we focused specifically on OA neurons that co-express dVGLUT (OA-glutamate neurons (OGNs)).

Cell bodies of OGNs were visualized by a *UAS-dsRed.NLS* reporter under control of *dVGlut-gal4* (hereafter referred to as *dVGlut>dsRed*). OGNs were identified by antibodies to tyrosine decarboxylase 2 (TDC2) and tyramine □-hydroxylase (T□H) as OA is synthesized from the amino acid tyrosine via the action of Tdc and T□h in invertebrates [46]. OGNs from 10 *dVGlut>dsRed* Tdc2-labeled male brains were quantified by the multi-point ImageJ tool followed by manual verification of each optical section. Within the brain, OA neurons that co-express glutamate are found in the subesophageal zone (SEZ), the periesophageal neuropils (PENP), the anterior (ASMP) and posterior superior medial protocerebrum (PSMP), and the protocerebral bridge (Fig 1A-E). Co-expression occurs in each region of interest (Fig 1A-E). Tβh and *dVGlut>dsRed* co-localization (SFig 2) provides further support that glutamate is found in OA-expressing neurons.

In the adult ventral nervous system (VNS), the thoracic Tdc2+ neurons that innervate skeletal muscles express glutamate (SFig 3). In the abdominal ganglia, all but 2-3 Tdc2+ neurons express dVGlut (SFig 3) consistent with the previous finding of OA-glutamate co-expression in abdominal neurons [53]. After detecting no reporter expression from a *Tβh-gal4* driver, dVGLUT cell body expression in OGNs was detected in brains from *tdc2-gal4;UAS-dsRed* adults (SFig 4). In total,

this analysis reveals that of the ~100 OA neurons in the *Drosophila* adult nervous system, about 70% express dVGLUT.

dVGLUT is not required for OA neuron identity

To reduce glutamate function solely in OGNs, a UAS-driven inverted repeat transgene targeting *dVGlut* (*UAS-dVGlut-RNAi)* was expressed under control of the *tdc2-gal4* driver (hereafter *tdc2>dVGlut-RNAi*) (Fig 2A,B). The effectiveness of this *UAS-dVGlut-RNAi* line has been verified at the transcript level through RT-qPCR ([12]and SFig 5) and functionally as the frequency of miniature excitatory postsynaptic potentials (mEPSP) were reduced by this dVGlut RNAi in presynaptic glutamatergic larval motor neurons [12]. As the loss of VGLUT2 in vertebrate dopamine-glutamate dual transmitting neurons impairs survival and differentiation *in vitro* [49, 54], we examined OGNs in *tdc2>dsRed>dVGlut-RNAi* adults and did not observe obvious changes in OGN survival nor distribution (SFig 5). In addition, OGN neurotransmitter differentiation was retained as *tdc2>dVGlut-RNAi>dsRed* neurons express Tdc2 (SFig 5). Neurons labeled by this *tdc2-gal4* whether in the brain or VNS are all Tdc2+ (SFig 6A,B)

Reducing glutamate in OGNs decreases male aggression and inter-male courtship

We and others previously demonstrated OA is required for two distinct social male behaviors; the promotion of aggression, and the inhibition of intermale courtship [43, 46, 55, 56]. To address whether dVGLUT performs a related or separable role in these OA-dependent behaviors, we quantified changes in aggression and intermale courtship. Fights between pairs of *tdc2>dVGlut-RNAi* males, and transgenic controls were recorded and multiple agonistic parameters quantified including: latency to the first lunge, number of lunges, and number of agonistic wing threats (Fig 2A, [57, 58]). As behavioral patterns are scored for 30 minutes after the first lunge, each male pair has the same amount of time to exhibit aggressive events or inter-male courtship (Fig 2B).

Males with decreased dVGLUT in OGNs neurons exhibited a significant reduction in aggression as measured by lower numbers of lunges and wing threats, and an increase in the latency to initiate aggression (Fig 2D-F). These aggression deficits are the same as in males that lack OA [43, 46, 47]. Importantly, the locomotor activity of *tdc2>dVGlut-RNAi* adults during the aggression assay did not differ from *dVGlut-RNAi* controls (SFig 7A).

Interactions between control male pairings within a fight can include low levels of intermale courtship as measured by unilateral wing extensions (UWE, the courtship song motor pattern). Males without OA exhibit high levels of inter-male courtship [43, 55, 56] and previously, we determined the function of three OA-FruM+ neurons is required to suppress intermale courtship [55]. If dVGLUT is only needed to enhance monoamine vesicular packaging and thus modulate OA function, we would expect males with reduced *dVGlut* levels to display the same behavioral deficits, i.e. high levels of inter-male courtship. However, *tdc2>dVGlut-RNAi* males did not exhibit inter-male courtship (Fig 2G). These results suggest; 1) dVGLUT is required in OGNs to promote aggression, and 2) dVGLUT is not required to suppress inter-male courtship.

Aggression requires dVGLUT function in OA-GLU brain neurons
In the adult, motor neurons innervating leg and wing muscles express glutamate [59]. Therefore, the observed behavioral deficits in *tdc2>dVGlut-RNAi* males may reflect impairments at the neuromuscular junction. To address this possibility, we spatially restricted expression of the dVGlut-RNAi transgene to the brain using the *teashirt-lexA 8xlexAop2-IVS-Gal80* (hereafter *tsh>Gal80)* transgenic combination (Fig 2H). The *tsh>Gal80* transgenic combination was effective at blocking Gal4-mediated transcription in the entire VNS including in OGNs that innervate muscles required for courtship and wing threat behaviors (SFig 8).

With dVGlut function maintained in motor neurons, it was possible all aggressive behaviors would return to control levels. However, latency to initiate aggression remained longer in males with reduced dVGLUT in brain OGNs (*tdc2>tsh>Gal80>dVGlut-RNAi*) and lunge number remained lower when compared to controls (Fig 2I,J). Wing threat numbers were at levels lower than one control (Fig 2K) which likely reflects the incompleteness of dVGlut RNAi interference (see results in Fig 4G). In contrast, providing dVGLUT function in OGN VNS neurons restored intermale courtship to control levels (Fig 2L). Although total behavioral events by experimental males (lunges, wing threats, intermale courtship) per minute decreased, overall activity did not (SFig 7) nor did male-female courtship (Fig 3). These results indicating GLU transport in brain OGNs is required to initiate aggression may reflect deficits in the detection of male pheromones as we previously described for OA. Specifically, aggression requires pheromonal information from

Gr32a-expressing chemosensory neurons located in the mouth to OA SEZ neurons [43] and the suppression of intermale courtship requires the function of three OA-FruM+ neurons located in the brain [55].

Finally, males with reduced dVGLUT in brain OGNs (*tdc2>tsh>Gal80>dVGlut-RNAi*) performed all measured male-female courtship parameters including latency to court, courtship index, latency to copulation and copulation success at levels indistinguishable from controls (Fig 3). Together, these results indicate dVGlut in OGNs is required in males both for aggression and courtship toward a female and at the behavioral level, the functional requirement for dVGLUT in OGN motor neurons vs. central brain neurons is spatially separable.

Removal of glutamate in OGNs using the *B3RT-vGlut* conditional allele
The experiments above used two different approaches to reduce neurotransmitter levels, but not eliminate dVGLUT. To completely remove glutamate transporter function in OGNs, a conditional allele of *dVGlut*, *B3RT-dVGlut-LexA* (hereafter *B3RT-dVGlut*), was developed via genome editing. Genome edits to the *dVGlut* locus included flanking the dVGlut coding exons with B3 recombination target sites (B3RTs) [60] in the same orientation and inserting the coding sequences of the LexA transcription factor immediately downstream of the 3' B3RT (Fig 4A). With *B3RT-dVGlut,* glutamate function can be temporally and spatially controlled using Gal4 drivers of interest to express the B3 recombinase that in turn catalyzes the *in vivo* excision of DNA between the B3RTs (Fig 4B). Two outcomes result after B3 recombinase-mediated excision; 1) a *dVGlut* null allele is generated solely in the neurons of interest, and 2) a *dVGlut-LexA* driver is created that allows visualization of glutamatergic neurons when a LexAop reporter is present.

To assess the functionality of *dVGlut* within the *B3RT-dVGlut* chromosome pre- and post-excision, the *B3RT-dVGlut* chromosome was crossed with the null allele, *dVGlut^{SS1}* (SFig 1). In the absence of a Gal4 driver, *vGlut^{SS1}/B3RT-vGlut* progeny are fully viable and no LexAop-driven reporter gene expression is detected (Fig 4C). In contrast, when B3 recombinase (*UAS-B3)* is expressed in the nervous system by the pan-neuronal driver, *n-syb-Gal4,* dVGLUT expression is eliminated and *vGlut^{SS1}/B3RT-dVGlut;UAS-B3/n-syb-Gal4* progeny are inviable (data not shown). These results establish that the *B3RT-dVGlut* genome edits preserve dVGLUT function prior to excision, but

after excision, as expected with removal of the entire dVGLUT protein-coding sequence, a *dVGlut* null allele is generated.

To verify the functionality of the *B3RT-dVGlut* chromosome in Tdc2+ neurons, we crossed *tdc2-gal4* with *B3RT-dVGlut;UAS-B3*. Following B3-mediated excision in Tdc2+ neurons, the resulting *dVGlut-lexA* driver is active in OGNs demonstrating the *dVGlut* coding region was removed. The excision of dVGlut and substitution with LexA in the adult nervous system was confirmed by co-localization of nuclear markers (Fig 4D,D'). This result provides additional confirmation the majority of Tdc2+ neurons are glutamatergic. In addition, nuclear reporters were used to confirm the loss of dVGLUT does not obviously alter OGN differentiation (SFig 9).

To completely remove dVGLUT function, we used the *dVGlut*[SS1] null allele in combination with the *B3RT-dVGlut* conditional null allele. Due to the requirements for GLU in OA-GLU motor neurons, we crossed the *tsh>Gal80* transgenes onto the *B3RT-dVGlut* chromosome. Males with homozygous null *dVGlut* mutations in brain OGNs were generated by driving B3 recombinase with *tdc2-gal4* (*dVGlut*[SS1]/*B3RT-dVGlut tsh>Gal80;UAS-B3/tdc2-gal4*). As expected, the complete loss of GLU in brain OGNs reduced male aggression. Specifically, the latency to initiate aggression increased, and lunge numbers decreased (Fig 4E,F). Not unexpectedly, the complete elimination of dVGLUT function resulted in aggression deficits significantly worse when compared to the RNAi approach (Fig 4I) including now a reduction in wing threat number (Fig 4G) which demonstrates an advantage in using the conditional null *B3RT-dVGlut* allele. Finally, and significantly, the number of inter-male wing extensions did not differ from controls (Fig 4H) nor from males with a reduction of *dVGlut* in brain OGNs (Fig 2K). In summation, the *dVGlut*[SS1]/*B3RT-dVGlut* null combination elegantly and independently validates the aggression phenotypes based on *dVGlut* RNAi-based reduction, demonstrates the applicability of a powerful new conditional genetic tool, and confirms that dVGLUT function in OGNs is not required to regulate intermale courtship.

Reducing GLU by EAAT1 overexpression recapitulates the decrease in aggression
At this point, GLU function within OGNs has been altered by reducing glutamate transport into synaptic vesicles. Whether the aggression phenotypes of OGN dVGLUT mutant males are due to

deficits in the concentration of GLU into synaptic vesicles, the packaging of OA, or a reduction of released GLU is not clear. After release, glutamate is rapidly removed from synapses by excitatory amino acid transporters (EAATs) [61, 62]. Therefore, to reduce GLU signaling after release, we increased expression of the only high-affinity glutamate transporter in *Drosophila*, EAAT1 (Fig 5A) [63, 64].

EAAT1 is expressed in glia throughout the nervous system [64]. By examining 2-10 individual EAAT1-GFP clones in ~40 brains, we determined OGN neuronal cell bodies and arborizations are consistently enmeshed by EAAT1-expressing glia (Fig 5B-C). To reduce glutamate signaling after release, EAAT1 expression was increased via a transgene (*EAAT1-gal4;UAS-EAAT1*). While a loss of EAAT1 impairs larval movement [65], overexpression of EAAT1 has been used in adult long-term memory formation assays which requires locomotion [66]. Similar to the dVGLUT loss-of-function results above, the aggressive behavior of males with reduced GLU signaling by EAAT1 overexpression (*EAAT1-gal4;UAS-EAAT1*) was altered in two parameters: the latency to initiate lunging increased and lunge number decreased (Fig 5D,E). Locomotor activity during the aggression assay did not differ (Fig 5F). Although future experiments will be needed to determine if the promotion of aggression requires dVGLUT packaging of OA in synaptic vesicles and OGN glutamate signaling to downstream targets, results from this section support the hypothesis that OGN-mediated aggression requires GLU.

OA and Glu signal to a shared aggression-promoting circuit
If Glu and OA convey signals to separable aggression-promoting circuits, a loss of both neurotransmitters would reduce aggression greater than the loss of either alone (Fig 6A). If, however, Glu and OA signal to a shared circuit or circuits that converge, a loss of both transmitters would reduce aggression to the same levels as the loss of one alone. To address this question, we incorporated the previously described null allele $T\beta h^{nM18}$ [67] and generated $T\beta h^{nM18};tdc2>dVGlut-RNAi$ males. Additive deficits did not occur when males without OA and dVGLUT in OGNs were compared to males lacking only OA (Fig 6B-D) indicating that both signals, at least partially, converge onto a shared aggression-promoting pathway.

TβhnM18;tdc2>vGlut-RNAi males displayed levels of male-male courtship that are not significantly different from *TβhnM18* males (blue column, Fig 6E). This result further supports previously published data that OA is required to suppress intermale courtship [43, 55, 56]. Here, increased levels of inter-male courtship due to the absence of OA supersedes or relieves the lack of UWE due to a reduction in dVGlut function (Fig 2). At this point, it is possible the UWE phenotype occurs via OA-modulated circuitry that involves other neurotransmitters [56] or the actions of OA occur at spatially distinct locations.

Spatial segregation of VMAT and dVGLUT within OGNs

To compare localization of the two transporters within OGNs, we generated a conditionally expressible epitope-tagged version of VMAT, *RSRT>STOP>RSRT-6XV5-VMAT*, via genome editing. *RSRT>STOP>RSRT-6XV5-VMAT* has two insertions: 1) a STOP cassette between VMAT coding exons 5 and 6 and, 2) six in-frame tandem copies of a V5 epitope tag within exon 8 which is common to both VMAT-A and VMAT-B isoforms (Fig 7A). The effectiveness of the STOP cassette is confirmed by the lack of V5 expression prior to STOP cassette excision by Gal4-driven R recombinase (SFig 11) and the effectiveness of the epitope multimerization strategy has also been determined [68]. The conditionality of the *RSRT>STOP>RSRT-6XV5-VMAT* allele permits visualization of VMAT in subsets of neurons at expression levels driven by the endogenous promoter.

To focus on transporter distribution within OGNs, we expressed *RSRT>STOP>RSRT-6XV5-VMAT* under control of the split Gal4 combination of *tdc2-Gal4-AD* and *dVGlut-Gal4-DBD (tdc2-dVGlut-gal4)* which drives expression in OGNs (Fig 7B, SFig 6C-F). V5-VMAT was visualized in *tdc2-dVGlut-gal4; V5-VMAT UAS-R* by an antibody to V5 and dVGLUT using mAb dVGLUT (SFig 10). Figure 7C illustrates that as expected, a large fraction of the V5-VMAT puncta in the AL or SEZ (SFig 11) either co-localize with dVGLUT or are in close proximity (arrowheads). High resolution images in Fig 7D, H, however, reveal V5-VMAT puncta without dVGLUT (arrows). As OA can be found in SVs as well as LDCVs [69, 70], we incorporated a synaptic marker (*UAS-Synaptotagmin (Syt):HA*) and re-examined V5-VMAT and dVGLUT expression in the AL and SEZ (Fig 7F, SFig 11D). We found V5-VMAT puncta that either co-localize or are in close proximity to Syt:HA and dVGLUT (Fig 7F-J, SFig 11D-H). While the behavioral significance of potential OA

synaptic release on aggression circuitry remains to be determined, previous work has demonstrated amine-dependent behaviors can be altered by shifting the balance of OA release from SVs to LDCVs [70]. In addition, as mentioned above, we have previously shown that three OA-FruM^{+} neurons are required to suppress intermale courtship and recent work has identified a small subset of OA receptor OAMB-expressing neurons that when silenced, decrease aggression and increase intermale courtship [56]. The SEZ areas of V5-VMAT and dVGLUT puncta highlighted in Figs. 7 and 8 are consistent with projections made by OA-FruM^{+} neurons which are also OGNs (SFig 12) raising the possibility of distinct OA and GLU inputs to key downstream targets.

Due to the large number of *tdc2-dVGlut-gal4* neurons, we repeated the experiment using the OA-specific *MB113C-split-gal4* to drive V5-VMAT in ~2 OGNs (Fig 8A-B) [71]. Figure 8C illustrates that as expected, many V5-VMAT puncta in the SEZ either co-localize with dVGLUT or are in close proximity (arrowheads). High resolution images in Fig 8D, H, however, indicate small, but distinct regions that contain V5-VMAT puncta without dVGLUT (arrows). Within the areas of dVGLUT and V5-VMAT possible colocalization, this level of analysis does not indicate whether the two transporters segregate into adjacent but distinct puncta, nor are questions of transporter colocalization on the same vesicles addressed. Nevertheless, our results demonstrate that within OGNs, V5-VMAT and dVGLUT puncta can differ in localization suggesting the aggression vs. intermale courtship phenotype differences may be due to spatial differences in signaling by glutamate and octopamine.

DISCUSSION

Addressing the functional complexities of "one neuron, multiple transmitters" is critical to understanding how neuron communication, circuit computation, and behavior can be regulated by a single neuron. Over many decades, significant progress has been made elucidating the functional properties of neurons co-expressing neuropeptides and small molecule neurotransmitters, where the neuropeptide acts as a co-transmitter and modulates the action of the neurotransmitter [5, 6, 72]. Only recently have studies begun to examine the functional significance of co-transmission by a fast-acting neurotransmitter and a slow-acting monoamine.

In this study, we demonstrated that OA neurons express dVGLUT and utilized a new genetic tool to remove dVGLUT in OA-glutamate neurons. Quantifying changes in the complex social behaviors of aggression and courtship revealed that dVGLUT in brain OGNs is required to promote aggressive behavior and a specific behavioral pattern, the lunge. In contrast, males deficient for dVGLUT function do not exhibit an increase in inter-male courtship. These results establish a previously undetermined role for dVGLUT in OA neurons located in the adult brain and reveal glutamate uncouples aggression from inter-male courtship. It has been suggested that classical neurotransmitters and monoamines present in the same neuron modulate each other's packaging into synaptic vesicles or after release via autoreceptors [9, 49, 73-75]. For example, a reduction of dVGLUT in DA-glutamate neurons resulted in decreased AMPH-stimulated hyperlocomotion in *Drosophila* and mice suggesting a key function of dVGLUT is the mediation of vesicular DA content [12, 49, 76]. In this study, the independent behavioral changes suggests enhancing the packaging of OA into vesicles is not the sole function of dVGLUT co-expression and suggests differences in signaling by OA from OGNs on courtship-related circuitry.

Co-transmission can generate distinct circuit-level effects via multiple mechanisms. One mechanism includes spatial segregation; the release of two neurotransmitters or a neurotransmitter and monoamine from a single neuron occurring at different axon terminals or presynaptic zones. Recent studies examining this possible mechanism have described; (i) the release of GLU and DA from different synaptic vesicles in midbrain dopamine neurons[15, 77] and (ii) the presence of VMAT and VGLUT microdomains in a subset of rodent mesoaccumbens DA neurons[78]. In this study, we expressed a new conditionally expressed epitope-tagged version of VMAT in OGNs and visualized endogenous dVGLUT via antibody labeling. Within OGNs, the colocalization of VMAT and dVGLUT puncta was not complete suggesting the observed behavioral phenotype differences may be due to spatial differences in OA signaling.

A second mechanism by which co-transmission may generate unique functional properties relies on activating distinct postsynaptic receptors. In *Drosophila,* recent work has identified a small population of male-specific neurons that express the alpha-like adrenergic receptor, OAMB, as aggression-promoting circuit-level neuronal targets of OA modulation independent of any effect on arousal[56] and separately knockdown of the *Rdl* GABAa receptor in a specific *doublesex+*

population stimulated male aggression [79]. Future experiments identifying downstream targets that express both glutamate and octopamine receptors would be informative, as well as using additional split-Gal4 lines to determine if segregation of transporters is a hallmark of the majority of OGNs. Finally, a third possible mechanism is Glu may be co-released from OGNs and act on autoreceptors to regulate presynaptic OA release (reviewed in [75]).

Deciphering the signaling complexity that allows neural networks to integrate external stimuli with internal states to generate context-appropriate social behavior is a challenging endeavor. Neuromodulators including monoamines are released to signal changes in an animal's environment and positively or negatively reinforce network output. In invertebrates, a role for OA in responding to external chemosensory cues as well as promoting aggression has been well-established [43, 47, 56, 80-83]. In terms of identifying specific aggression circuit-components that utilize OA, previous results determined OA neurons directly receive male-specific pheromone information [43] and the aSP2 neurons serve as a hub through which OA can bias output from a multi-functional social behavior network towards aggression[56]. The ability of OA to bias behavioral decisions based on positive and negative reinforcement was also recently described for food odors [84]. In vertebrates, it has been proposed that DA-GLU cotransmission in the NAc medial shell might facilitate behavioral switching [85]. Our finding that the majority of OA neurons are glutamatergic, suggests that the complex social behavior of aggression may rely on small subsets of neurons that both signal the rapid temporal coding of critical external stimuli as well the frequency coding of such stimuli resulting in the enhancement of this behavioral network. One implication of our finding regarding the separable OA-dependent inhibition of inter-male courtship is the possibility of identifying specific synapses or axon terminals that when activated gate two different behavioral outcomes. A second implication is that aggressive behavior in other systems may be modified by targeting GLU function in monoamine neurons.

Finally, monoamine-expressing neurons play key roles in human behavior including aggression and illnesses that have an aggressive component such as depression, addiction, anxiety, and Alzheimer's [86, 87]. While progress is being made in addressing the functional complexities of dual transmission, the possible pathological implications of glutamate co-release by monoamine neurons remains virtually unknown. Analyzing the synaptic vesicle and release properties of

monoamine-glutamate neurons could offer new possibilities for therapeutic interventions aimed at controlling out-of-context aggression.

Author Contributions

R.S.S., S.J.C. and L.M.S. conceived the study and experiments within the study. L.M.S., E. C. G, H.R.M., and L.A.S. performed the experiments. L.M.S., E. C. G, H.R.M., L.A.S. and S.J.C carried out the analysis. H.K.S., J. L.W., R.S.S, and B.D.M. generated lines and provided reagents. L.M.S, R.S.S. and S.J.C. wrote the manuscript.

Competing interests

The authors declare no competing financial interests.

Methods

Drosophila Husbandry and Stocks: All flies were reared on standard cornmeal-based fly food. Unless noted otherwise, during developmental and post-eclosion, flies were raised at 25°C, ~50% humidity and a 12:12hr light-dark cycle (1400 ± 200 lx white fluorescent light) in humidity and temperature-controlled incubators. A list of stocks can be found in Supplementary Information.

Aggression Assays: Male pupae were isolated and aged individually in 16 x 100mm borosilicate glass tubes containing 1.5ml of standard food medium as previously described [88]. A dab of white or blue acrylic paint was applied to the thorax of two-day old males under CO_2 anesthesia for identification purposes. Flies were returned to their respective isolation tubes for a period of at least 24 hours to allow recovery. For aggression testing, pairs of 3-5 day old, socially naïve adult males were placed in

12-well polystyrene plates (VWR #82050-930) as described previously [43]. All assays were run at 25°C and ~45-50% humidity levels.

Scoring and Statistics: All aggression was assayed within first two hours of lights ON time (Zeitgeber hours 0-2) and scored manually using iMovie version 8.0.6. Total number of lunges, wing threats, and unilateral wing extensions were scored for a period of 30 minutes after the first lunge according to the criteria established previously [43, 88]. The time between the aspiration of the flies into the chamber and the first lunge was used for calculating the latency to lunge. Male-male courtship was the number of unilateral wing extensions (singing) followed by abdomen bends or repeated wing extensions. All graphs were generated with Graphpad Prism and Adobe Illustrator CS6. For data that did not meet parametric assumptions, Kruskal-Wallis Test with Dunn's multiple comparison was used unless otherwise specified. A standard unpaired t-test was performed in the case of only two comparisons and a modified chi-square test to compare copulation success.

Activity levels: Activity levels were measured by tracking the flies in each assay using the OpenCV module in the Python programming language to analyze the video and then output XY-coordinate and distance data. The distance traveled was calculated for each fly by determining the starting location followed by the second location after a 250-ms time interval and then taking the sum of the distance traveled in each interval. To calculate pixels moved per second, the distance data was divided by the total time spent tracking.

Immunohistochemistry: Adult male dissected brains were fixed in 4% paraformaldehyde (Electron Microscopy Sciences) for 25 minutes and labeled using a modification of protocols previously described [55]. The following primary antibodies were used: anti-bruchpilot (mAb nc82, 1:30, Developmental Studies Hybridoma Bank), monoclonal rabbit anti-GFP (1:200, Molecular Probes), rat anti-HA 3F10 (1:100, Roche), mAb dVGLUT (1:15), anti-T□H (1:400, [89]), rat anti-V5 (1:200, Biorbyt), and rabbit anti-TDC2 (1:100, Covalab). Secondary antibodies conjugated to Alexa 488, Alexa 594, or Alexa 647 (Molecular Probes) were used at a concentration of 1:200. Labeled brains were mounted in Vectashield (Vector Labs, #H1000). Images were collected on an Olympus Fluoview FV1000 laser scanning confocal mounted on an inverted IX81 microscope and processed using ImageJ (NIH) and Adobe Photoshop (Adobe, CA).

qPCR: Total RNA from ~40 heads using Direct-zol RNA Miniprep Pluskit (Zymo Research)and treated with DNase I per the manufacturer's protocol. RNA concentrations were measured with a ND-1000 nanodrop spectrometer. Reverse transcription was accomplished using iScript cDNA Synthesis kit (Bio-Rad Laboratories). RT-PCR was performed using 300 ng cDNA added to iTaq Universal SYBR Green Supermix (Bio-Rad Laboratories) and primers in a 20 µL reaction volume. All samples were run in triplicate using a Stratagene Mx3005P qPCR System(Agilent Technologies). Expression of *ribosomal protein 49* (*Rp49*) was used as the reference control to normalize expression between genotypes. Expression levels were determined using the ΔΔCT method and results from control (*UAS-dVGlut-RNAi/+*) and experimental (*nsyb-Gal4/UAS-dVGlut-RNAi*) groups were normalized relative to a transgenic control (*nsyb-Gal4/+*). The following primers were used: Rp49 Forward: 50-CATCCGCCCAGCATACAG-3' Rp49 Reverse: 5'-CCATTTGTGCGACAGCTTAG-3' dVGlut Forward: 5'-GCACGGTCATGTGGTGATTTG-3' dVGlut Reverse: 5'-CCAGAAACGCCAGATACCATGG-3'. Primer designs for all Rp49 and dVGlut primers used have been described previously [12].

Construction of *20XUAS-His2A-GFP*, *13XLexAop2-His2B-mCherry* and *20XUAS-R*: The *20XUAS-His2A-GFP*, *13XLexAop2-His2B-mCherry*, and *20XUAS-R* expression clones were assembled using Gateway MultiSite LR reactions as previously described[90] and as indicated in Supplementary Table 2. The *L1-20XUAS-DSCP-L4* and *L1-13XLexAop2-DSCP-L4* entry clones contain 20 copies of UAS and 13 copies of LexAop2 upstream of the *Drosophila* synthetic core promoter (DSCP) [91], respectively. The *R4-His2A-R3* and *R4-His2B-R3* entry clones were generated as previously described [90] using genomic DNA as templates. The *L3-GFP-L2* entry clone was generated from template *pJFRC165*[60] except the PEST sequence is omitted. The *L3-GFP-L2* and *L3-mCherry-HA-L2* entry clones were previously described [92]. The *L1-20XUAS-DSCP-R5* entry clone was previously described [90]. The *pDESTp10aw* destination vector was previously described[93]. Injections were performed by Bestgene, Inc.

Construction of *UAS-B3*: B3 recombinase derived from pJFRC157 [60] was PCR amplified using primers designed to add the syn21 translational enhancer sequence [94] and remove the PEST domain. The verified PCR product was cloned into pENTR (Invtrogen) and subsequently transferred to

pBID20xUAS, a derivative of the pBID vector [95] with 20 copies of the UAS binding sequence. Injection of *UAS-B3* was performed by Genetivision into landing site VK31.

Generation of *B3RT-vGlut*: The *B3RT-dVGlut-LexA* chromosome was generated via CRISPR/Cas9 genome editing. Both guide RNAs were incorporated into pCFD4 using previously described methods [96] to produce the double guide RNA plasmid *pCFD4-vGlut1*. The donor plasmid *B3RT-dVGlut-LexA* used the *pHSG298* backbone (Takara Bio) and was generated using NEBuilder HiFi (New England Biolabs). The complete annotated sequence of *B3RT-dVGlut-LexA* is shown in Supplementary Information. *pCFD4-vGlut1/B3RT-dVGlut-LexA* injections were performed by Bestgene, Inc.

To assess the functionality of *dVGlut* on the *B3RT-dVGlut* chromosome pre- and post-excision, the *B3RT-dVGlut* chromosome was crossed with the homozygous lethal *dVGlut* null allele, *dVGlut^{SS1}* in the presence and absence of the pan-neuronal driver *n-syb-Gal4*. In the absence of a Gal4 driver, *dVGlut^{SS1}/B3RT-dVGlut* progeny are fully viable and no LexAop-driven reporter gene expression is detected (Fig 2). When B3 recombinase (*UAS-B3)* is expressed in the nervous system by *n-syb-Gal4, dVGlut^{SS1}/B3RT-dVGlut;UAS-B3/n-syb-Gal4* progeny are inviable, therefore after excision, as expected with removal of the entire dVGlut protein-coding sequence, a *dVGlut* null allele results.

Generation of *dVGlut^{SS1}*: The *dVGlut^{SS1}* allele was generated by CRISPR/Cas9 genome editing with the same guide RNAs used to generate *B3RT-dVGlut LexA*. *dVGlut^{SS1}* was identified based on failed complementation with the existing *dVGlut^2* allele[97]. Sequencing of PCR products from this allele indicated a deletion of 2442bp that includes dVGlut amino acids 53-523. Genomic DNA sequence at the breakpoints of the *dVGlut^{SS1}* allele are indicated with the deleted region in bold: GGACCAGGCG**GCGGCCACGC**......**AACCTCCGGC**CGAGGAGCAA.

Generation of the *RSRT-STOP-RSRT-6XV5-vMAT* chromosome: *RSRT-STOP-RSRT-6XV5-vMAT* was generated via CRISPR/Cas9 genome editing. Both upstream guide RNAs were incorporated into pCFD4-vMAT1 and both downstream guide RNAs were incorporated into pCFD4-vMAT2 as previously described [96]. The *RSRT-STOP-RSRT-6XV5-vMAT* donor plasmid used the *pHSG298*

backbone (Takara Bio) and was generated using NEBuilder HiFi (New England Biolabs). The complete annotated sequence of *RSRT-STOP-RSRT-6XV5-vMAT* is shown in Supplementary Information. *pCFD4-vMAT1/pCFD4-vMAT2/RSRT-STOP-RSRT-6XV5-vMAT* injections into the *nos-Cas9* strain *TH_attP2*[98] were performed by Bestgene, Inc.

The R and B3 recombinases from yeast recognize sequence-specific recombination target sites, RSRTs and B3RTs, respectively [60]. These recombinases are highly efficient and highly specific as they exhibit virtually no cross-reactivity with each other's recombinase target sites. When pairs of recombinase target sites are in the same orientation, as is the case for both *B3RT-vGlut-LexA* and *RSRT-STOP-RSRT-6XV5-vMAT*, the recombinases catalyze excision of the intervening DNA and leave behind a single recombinase target site.

dVGlut Antibody: Drosophila anti-dVGLUT mouse monoclonal antibodies (10D6G) were generated (Life Technologies Europe) using the C-terminal peptide sequence TQGQMPSYDPQGYQQQ of dVGLUT coupled to KLH.

References

1.   Dale H. Pharmacology and Nerve-endings (Walter Ernest Dixon Memorial Lecture): (Section of Therapeutics and Pharmacology). Proc R Soc Med. 1935;28(3):319-32. Epub 1935/01/01. PubMed PMID: 19990108; PubMed Central PMCID: PMCPMC2205701.

2.   Eccles JC, Fatt P, Koketsu K. Cholinergic and inhibitory synapses in a pathway from motor-axon collaterals to motoneurones. J Physiol. 1954;126(3):524-62. Epub 1954/12/10. PubMed PMID: 13222354; PubMed Central PMCID: PMCPMC1365877.

3.   Strata P, Harvey R. Dale's principle. Brain Res Bull. 1999;50(5-6):349-50. Epub 2000/01/22. PubMed PMID: 10643431.

4.   Hnasko TS, Edwards RH. Neurotransmitter corelease: mechanism and physiological role. Annu Rev Physiol. 2012;74:225-43. Epub 2011/11/08. doi: 10.1146/annurev-physiol-020911-153315. PubMed PMID: 22054239; PubMed Central PMCID: PMC4090038.

5.   Nassel DR. Substrates for Neuronal Cotransmission With Neuropeptides and Small Molecule Neurotransmitters in Drosophila. Front Cell Neurosci. 2018;12:83. Epub 2018/04/14.

doi: 10.3389/fncel.2018.00083. PubMed PMID: 29651236; PubMed Central PMCID: PMCPMC5885757.

6.   Nusbaum MP, Blitz DM, Marder E. Functional consequences of neuropeptide and small-molecule co-transmission. Nat Rev Neurosci. 2017;18(7):389-403. Epub 2017/06/09. doi: 10.1038/nrn.2017.56. PubMed PMID: 28592905; PubMed Central PMCID: PMCPMC5547741.

7.   Vaaga CE, Borisovska M, Westbrook GL. Dual-transmitter neurons: functional implications of co-release and co-transmission. Curr Opin Neurobiol. 2014;29:25-32. Epub 2014/05/13. doi: 10.1016/j.conb.2014.04.010. PubMed PMID: 24816154; PubMed Central PMCID: PMCPMC4231002.

8.   El Mestikawy S, Wallen-Mackenzie A, Fortin GM, Descarries L, Trudeau LE. From glutamate co-release to vesicular synergy: vesicular glutamate transporters. Nat Rev Neurosci. 2011;12(4):204-16. Epub 2011/03/19. doi: 10.1038/nrn2969. PubMed PMID: 21415847.

9.   Gras C, Herzog E, Bellenchi GC, Bernard V, Ravassard P, Pohl M, et al. A third vesicular glutamate transporter expressed by cholinergic and serotoninergic neurons. J Neurosci. 2002;22(13):5442-51. Epub 2002/07/05. PubMed PMID: 12097496.

10.   Ottersen OP, Storm-Mathisen J. Glutamate- and GABA-containing neurons in the mouse and rat brain, as demonstrated with a new immunocytochemical technique. J Comp Neurol. 1984;229(3):374-92. Epub 1984/11/01. doi: 10.1002/cne.902290308. PubMed PMID: 6150049.

11.   Root DH, Zhang S, Barker DJ, Miranda-Barrientos J, Liu B, Wang HL, et al. Selective Brain Distribution and Distinctive Synaptic Architecture of Dual Glutamatergic-GABAergic Neurons. Cell Rep. 2018;23(12):3465-79. Epub 2018/06/21. doi: 10.1016/j.celrep.2018.05.063. PubMed PMID: 29924991.

12.   Aguilar JI, Dunn M, Mingote S, Karam CS, Farino ZJ, Sonders MS, et al. Neuronal Depolarization Drives Increased Dopamine Synaptic Vesicle Loading via VGLUT. Neuron. 2017;95(5):1074-88 e7. Epub 2017/08/22. doi: 10.1016/j.neuron.2017.07.038. PubMed PMID: 28823729; PubMed Central PMCID: PMCPMC5760215.

13.   Lohr KM, Bernstein AI, Stout KA, Dunn AR, Lazo CR, Alter SP, et al. Increased vesicular monoamine transporter enhances dopamine release and opposes Parkinson disease-related neurodegeneration in vivo. Proc Natl Acad Sci U S A. 2014;111(27):9977-82. Epub 2014/07/01. doi: 10.1073/pnas.1402134111. PubMed PMID: 24979780; PubMed Central PMCID: PMCPMC4103325.

14. Trudeau LE, El Mestikawy S. Glutamate Cotransmission in Cholinergic, GABAergic and Monoamine Systems: Contrasts and Commonalities. Front Neural Circuits. 2018;12:113. Epub 2019/01/09. doi: 10.3389/fncir.2018.00113. PubMed PMID: 30618649; PubMed Central PMCID: PMCPMC6305298.

15. Silm K, Yang J, Marcott PF, Asensio CS, Eriksen J, Guthrie DA, et al. Synaptic Vesicle Recycling Pathway Determines Neurotransmitter Content and Release Properties. Neuron. 2019;102(4):786-800 e5. Epub 2019/04/21. doi: 10.1016/j.neuron.2019.03.031. PubMed PMID: 31003725; PubMed Central PMCID: PMCPMC6541489.

16. Zhang Q, Liu B, Wu Q, Liu B, Li Y, Sun S, et al. Differential Co-release of Two Neurotransmitters from a Vesicle Fusion Pore in Mammalian Adrenal Chromaffin Cells. Neuron. 2019;102(1):173-83 e4. Epub 2019/02/19. doi: 10.1016/j.neuron.2019.01.031. PubMed PMID: 30773347.

17. Wrangham RW. Two types of aggression in human evolution. Proc Natl Acad Sci U S A. 2018;115(2):245-53. Epub 2017/12/28. doi: 10.1073/pnas.1713611115. PubMed PMID: 29279379; PubMed Central PMCID: PMCPMC5777045.

18. Thomas AL, Davis SM, Dierick HA. Of Fighting Flies, Mice, and Men: Are Some of the Molecular and Neuronal Mechanisms of Aggression Universal in the Animal Kingdom? PLoS Genet. 2015;11(8):e1005416. Epub 2015/08/28. doi: 10.1371/journal.pgen.1005416. PubMed PMID: 26312756; PubMed Central PMCID: PMCPMC4551476.

19. Craig IW, Halton KE. Genetics of human aggressive behaviour. Hum Genet. 2009;126(1):101-13. Epub 2009/06/10. doi: 10.1007/s00439-009-0695-9 [doi]. PubMed PMID: 19506905.

20. Hoopfer ED. Neural control of aggression in Drosophila. Curr Opin Neurobiol. 2016;38:109-18. Epub 2016/05/18. doi: 10.1016/j.conb.2016.04.007. PubMed PMID: 27179788.

21. Kravitz EA, Fernandez Mde L. Aggression in Drosophila. Behav Neurosci. 2015;129(5):549-63. doi: 10.1037/bne0000089. PubMed PMID: 26348714.

22. Nelson RJ, Trainor BC. Neural mechanisms of aggression. Nat Rev Neurosci. 2007;8(7):536-46. PubMed PMID: 17585306.

23. Rillich J, Rillich B, Stevenson PA. Differential modulation of courtship behavior and subsequent aggression by octopamine, dopamine and serotonin in male crickets. Horm Behav. 2019. Epub 2019/06/22. doi: 10.1016/j.yhbeh.2019.06.006. PubMed PMID: 31226329.

24.   Bruno V, Mancini D, Ghoche R, Arshinoff R, Miyasaki JM. High prevalence of physical and sexual aggression to caregivers in advanced Parkinson's disease. Experience in the Palliative Care Program. Parkinsonism Relat Disord. 2016;24:141-2. Epub 2016/01/21. doi: 10.1016/j.parkreldis.2016.01.010. PubMed PMID: 26786755.

25.   Liu CS, Ruthirakuhan M, Chau SA, Herrmann N, Carvalho AF, Lanctot KL. Pharmacological Management of Agitation and Aggression in Alzheimer's Disease: A Review of Current and Novel Treatments. Curr Alzheimer Res. 2016;13(10):1134-44. Epub 2016/05/04. PubMed PMID: 27137221.

26.   Stigler KA, McDougle CJ. Pharmacotherapy of irritability in pervasive developmental disorders. Child Adolesc Psychiatr Clin N Am. 2008;17(4):739-52, vii-viii. Epub 2008/09/09. doi: 10.1016/j.chc.2008.06.002. PubMed PMID: 18775367.

27.   Kim S, Boylan K. Effectiveness of Antidepressant Medications for Symptoms of Irritability and Disruptive Behaviors in Children and Adolescents. J Child Adolesc Psychopharmacol. 2016;26(8):694-704. Epub 2016/08/03. doi: 10.1089/cap.2015.0127. PubMed PMID: 27482998.

28.   Moret C, Briley M. The importance of norepinephrine in depression. Neuropsychiatr Dis Treat. 2011;7(Suppl 1):9-13. Epub 2011/07/14. doi: 10.2147/NDT.S19619. PubMed PMID: 21750623; PubMed Central PMCID: PMCPMC3131098.

29.   Sharma T, Guski LS, Freund N, Gotzsche PC. Suicidality and aggression during antidepressant treatment: systematic review and meta-analyses based on clinical study reports. BMJ. 2016;352:i65. Epub 2016/01/29. doi: 10.1136/bmj.i65. PubMed PMID: 26819231; PubMed Central PMCID: PMCPMC4729837.

30.   Agnati LF, Guidolin D, Guescini M, Genedani S, Fuxe K. Understanding wiring and volume transmission. Brain Res Rev. 2010;64(1):137-59. Epub 2010/03/30. doi: 10.1016/j.brainresrev.2010.03.003. PubMed PMID: 20347870.

31.   Beaudet A, Descarries L. The monoamine innervation of rat cerebral cortex: synaptic and nonsynaptic axon terminals. Neuroscience. 1978;3(10):851-60. Epub 1978/01/01. PubMed PMID: 215936.

32.   Descarries L, Berube-Carriere N, Riad M, Bo GD, Mendez JA, Trudeau LE. Glutamate in dopamine neurons: synaptic versus diffuse transmission. Brain Res Rev. 2008;58(2):290-302. Epub 2007/11/29. doi: 10.1016/j.brainresrev.2007.10.005. PubMed PMID: 18042492.

33.   Descarries L, Watkins KC, Lapierre Y. Noradrenergic axon terminals in the cerebral cortex of rat. III. Topometric ultrastructural analysis. Brain Res. 1977;133(2):197-222. Epub 1977/09/16. PubMed PMID: 902092.

34.   De-Miguel FF, Trueta C. Synaptic and extrasynaptic secretion of serotonin. Cell Mol Neurobiol. 2005;25(2):297-312. PubMed PMID: 16047543.

35.   Fuxe K, Agnati LF, Marcoli M, Borroto-Escuela DO. Volume Transmission in Central Dopamine and Noradrenaline Neurons and Its Astroglial Targets. Neurochem Res. 2015;40(12):2600-14. Epub 2015/04/22. doi: 10.1007/s11064-015-1574-5. PubMed PMID: 25894681.

36.   Marder E, Thirumalai V. Cellular, synaptic and network effects of neuromodulation. Neural Netw. 2002;15(4-6):479-93. PubMed PMID: 12371506.

37.   Takahashi A, Quadros IM, de Almeida RM, Miczek KA. Behavioral and pharmacogenetics of aggressive behavior. Curr Top Behav Neurosci. 2012;12:73-138. doi: 10.1007/7854_2011_191. PubMed PMID: 22297576; PubMed Central PMCID: PMCPMC3864145.

38.   Moutsimilli L, Farley S, El Khoury MA, Chamot C, Sibarita JB, Racine V, et al. Antipsychotics increase vesicular glutamate transporter 2 (VGLUT2) expression in thalamolimbic pathways. Neuropharmacology. 2008;54(3):497-508. Epub 2007/12/25. doi: 10.1016/j.neuropharm.2007.10.022. PubMed PMID: 18155072.

39.   Uezato A, Meador-Woodruff JH, McCullumsmith RE. Vesicular glutamate transporter mRNA expression in the medial temporal lobe in major depressive disorder, bipolar disorder, and schizophrenia. Bipolar Disord. 2009;11(7):711-25. Epub 2009/10/21. doi: 10.1111/j.1399-5618.2009.00752.x. PubMed PMID: 19839996.

40.   Tordera RM, Pei Q, Sharp T. Evidence for increased expression of the vesicular glutamate transporter, VGLUT1, by a course of antidepressant treatment. J Neurochem. 2005;94(4):875-83. Epub 2005/07/05. doi: 10.1111/j.1471-4159.2005.03192.x. PubMed PMID: 15992385.

41.   Shan D, Lucas EK, Drummond JB, Haroutunian V, Meador-Woodruff JH, McCullumsmith RE. Abnormal expression of glutamate transporters in temporal lobe areas in elderly patients with schizophrenia. Schizophr Res. 2013;144(1-3):1-8. Epub 2013/01/30. doi:

10.1016/j.schres.2012.12.019. PubMed PMID: 23356950; PubMed Central PMCID: PMCPMC3572263.

42.   Mingote S, Chuhma N, Kalmbach A, Thomsen GM, Wang Y, Mihali A, et al. Dopamine neuron dependent behaviors mediated by glutamate cotransmission. Elife. 2017;6. Epub 2017/07/14. doi: 10.7554/eLife.27566. PubMed PMID: 28703706; PubMed Central PMCID: PMCPMC5599237.

43.   Andrews JC, Fernandez MP, Yu Q, Leary GP, Leung AK, Kavanaugh MP, et al. Octopamine neuromodulation regulates Gr32a-linked aggression and courtship pathways in Drosophila males. PLoS Genet. 2014;10(5):e1004356. Epub 2014/05/24. doi: 10.1371/journal.pgen.1004356. PubMed PMID: 24852170; PubMed Central PMCID: PMC4031044.

44.   Baier A, Wittek B, Brembs B. Drosophila as a new model organism for the neurobiology of aggression? J Exp Biol. 2002;205(Pt 9):1233-40. PubMed PMID: 11948200.

45.   Certel SJ, Savella MG, Schlegel DC, Kravitz EA. Modulation of Drosophila male behavioral choice. Proc Natl Acad Sci U S A. 2007;104(11):4706-11. PubMed PMID: 17360588.

46.   Hoyer SC, Eckart A, Herrel A, Zars T, Fischer SA, Hardie SL, et al. Octopamine in male aggression of Drosophila. Curr Biol. 2008;18(3):159-67. PubMed PMID: 18249112.

47.   Zhou C, Rao Y, Rao Y. A subset of octopaminergic neurons are important for Drosophila aggression. Nat Neurosci. 2008;11(9):1059-67. doi: 10.1038/nn.2164. PubMed PMID: 19160504.

48.   Chaudhry FA, Reimer RJ, Bellocchio EE, Danbolt NC, Osen KK, Edwards RH, et al. The vesicular GABA transporter, VGAT, localizes to synaptic vesicles in sets of glycinergic as well as GABAergic neurons. J Neurosci. 1998;18(23):9733-50. Epub 1998/11/21. PubMed PMID: 9822734.

49.   Hnasko TS, Chuhma N, Zhang H, Goh GY, Sulzer D, Palmiter RD, et al. Vesicular glutamate transport promotes dopamine storage and glutamate corelease in vivo. Neuron. 2010;65(5):643-56. Epub 2010/03/13. doi: 10.1016/j.neuron.2010.02.012. PubMed PMID: 20223200; PubMed Central PMCID: PMCPMC2846457.

50.   Jonas P, Bischofberger J, Sandkuhler J. Corelease of two fast neurotransmitters at a central synapse. Science. 1998;281(5375):419-24. Epub 1998/07/17. doi: 10.1126/science.281.5375.419. PubMed PMID: 9665886.

51.   Ren J, Qin C, Hu F, Tan J, Qiu L, Zhao S, et al. Habenula "cholinergic" neurons co-release glutamate and acetylcholine and activate postsynaptic neurons via distinct transmission modes. Neuron. 2011;69(3):445-52. Epub 2011/02/15. doi: 10.1016/j.neuron.2010.12.038. PubMed PMID: 21315256.

52.   Tritsch NX, Ding JB, Sabatini BL. Dopaminergic neurons inhibit striatal output through non-canonical release of GABA. Nature. 2012;490(7419):262-6. Epub 2012/10/05. doi: 10.1038/nature11466. PubMed PMID: 23034651; PubMed Central PMCID: PMCPMC3944587.

53.   Rodriguez-Valentin R, Lopez-Gonzalez I, Jorquera R, Labarca P, Zurita M, Reynaud E. Oviduct contraction in Drosophila is modulated by a neural network that is both, octopaminergic and glutamatergic. J Cell Physiol. 2006;209(1):183-98. PubMed PMID: 16826564.

54.   Stuber GD, Hnasko TS, Britt JP, Edwards RH, Bonci A. Dopaminergic terminals in the nucleus accumbens but not the dorsal striatum corelease glutamate. J Neurosci. 2010;30(24):8229-33. Epub 2010/06/18. doi: 10.1523/JNEUROSCI.1754-10.2010. PubMed PMID: 20554874; PubMed Central PMCID: PMCPMC2918390.

55.   Certel SJ, Leung A, Lin CY, Perez P, Chiang AS, Kravitz EA. Octopamine neuromodulatory effects on a social behavior decision-making network in Drosophila males. PLoS One. 2010;5(10):e13248. Epub 2010/10/23. doi: 10.1371/journal.pone.0013248. PubMed PMID: 20967276; PubMed Central PMCID: PMCPMC2953509.

56.   Watanabe K, Chiu H, Pfeiffer BD, Wong AM, Hoopfer ED, Rubin GM, et al. A Circuit Node that Integrates Convergent Input from Neuromodulatory and Social Behavior-Promoting Neurons to Control Aggression in Drosophila. Neuron. 2017;95(5):1112-28 e7. Epub 2017/09/01. doi: 10.1016/j.neuron.2017.08.017. PubMed PMID: 28858617; PubMed Central PMCID: PMCPMC5588916.

57.   Chen S, Lee AY, Bowens NM, Huber R, Kravitz EA. Fighting fruit flies: a model system for the study of aggression. Proc Natl Acad Sci U S A. 2002;99(8):5664-8. PubMed PMID: 11960020.

58.   Dierick HA. A method for quantifying aggression in male Drosophila melanogaster. Nat Protoc. 2007;2(11):2712-8. PubMed PMID: 18007606.

59.   Baek M, Mann RS. Lineage and birth date specify motor neuron targeting and dendritic architecture in adult Drosophila. J Neurosci. 2009;29(21):6904-16. Epub 2009/05/29. doi: 10.1523/JNEUROSCI.1585-09.2009. PubMed PMID: 19474317.

60.   Nern A, Pfeiffer BD, Svoboda K, Rubin GM. Multiple new site-specific recombinases for use in manipulating animal genomes. Proc Natl Acad Sci U S A. 2011;108(34):14198-203. Epub 2011/08/13. doi: 10.1073/pnas.1111704108. PubMed PMID: 21831835; PubMed Central PMCID: PMCPMC3161616.

61.   Jensen AA, Fahlke C, Bjorn-Yoshimoto WE, Bunch L. Excitatory amino acid transporters: recent insights into molecular mechanisms, novel modes of modulation and new therapeutic possibilities. Curr Opin Pharmacol. 2015;20:116-23. Epub 2014/12/04. doi: 10.1016/j.coph.2014.10.008. PubMed PMID: 25466154.

62.   Martin CA, Krantz DE. Drosophila melanogaster as a genetic model system to study neurotransmitter transporters. Neurochem Int. 2014;73:71-88. Epub 2014/04/08. doi: 10.1016/j.neuint.2014.03.015. PubMed PMID: 24704795; PubMed Central PMCID: PMCPMC4264877.

63.   Seal RP, Daniels GM, Wolfgang WJ, Forte MA, Amara SG. Identification and characterization of a cDNA encoding a neuronal glutamate transporter from Drosophila melanogaster. Receptors Channels. 1998;6(1):51-64. Epub 1998/07/17. PubMed PMID: 9664622.

64.   Soustelle L, Besson MT, Rival T, Birman S. Terminal glial differentiation involves regulated expression of the excitatory amino acid transporters in the Drosophila embryonic CNS. Dev Biol. 2002;248(2):294-306. Epub 2002/08/09. PubMed PMID: 12167405.

65.   Stacey SM, Muraro NI, Peco E, Labbe A, Thomas GB, Baines RA, et al. Drosophila glial glutamate transporter Eaat1 is regulated by fringe-mediated notch signaling and is essential for larval locomotion. J Neurosci. 2010;30(43):14446-57. Epub 2010/10/29. doi: 10.1523/jneurosci.1021-10.2010. PubMed PMID: 20980602.

66.   Matsuno M, Horiuchi J, Ofusa K, Masuda T, Saitoe M. Inhibiting Glutamate Activity during Consolidation Suppresses Age-Related Long-Term Memory Impairment in Drosophila. iScience. 2019;15:55-65. Epub 2019/04/29. doi: 10.1016/j.isci.2019.04.014. PubMed PMID: 31030182; PubMed Central PMCID: PMCPMC6487374.

67.   Monastirioti M, Linn CE, Jr., White K. Characterization of Drosophila tyramine beta-hydroxylase gene and isolation of mutant flies lacking octopamine. J Neurosci. 1996;16(12):3900-11. PubMed PMID: 8656284.

68.   Tison KV, McKinney HM, Stowers RS. Demonstration of a Simple Epitope Tag Multimerization Strategy for Enhancing the Sensitivity of Protein Detection Using Drosophila vAChT. G3 (Bethesda). 2019. Epub 2019/11/27. doi: 10.1534/g3.119.400750. PubMed PMID: 31767639.

69.   Atwood HL, Govind CK, Wu CF. Differential ultrastructure of synaptic terminals on ventral longitudinal abdominal muscles in Drosophila larvae. J Neurobiol. 1993;24(8):1008-24. Epub 1993/08/01. doi: 10.1002/neu.480240803. PubMed PMID: 8409966.

70.   Grygoruk A, Chen A, Martin CA, Lawal HO, Fei H, Gutierrez G, et al. The redistribution of Drosophila vesicular monoamine transporter mutants from synaptic vesicles to large dense-core vesicles impairs amine-dependent behaviors. J Neurosci. 2014;34(20):6924-37. Epub 2014/05/16. doi: 10.1523/JNEUROSCI.0694-14.2014. PubMed PMID: 24828646; PubMed Central PMCID: PMCPMC4019805.

71.   Sujkowski A, Ramesh D, Brockmann A, Wessells R. Octopamine Drives Endurance Exercise Adaptations in Drosophila. Cell Rep. 2017;21(7):1809-23. Epub 2017/11/16. doi: 10.1016/j.celrep.2017.10.065. PubMed PMID: 29141215; PubMed Central PMCID: PMCPMC5693351.

72.   Brewer JC, Olson AC, Collins KM, Koelle MR. Serotonin and neuropeptides are both released by the HSN command neuron to initiate Caenorhabditis elegans egg laying. PLoS Genet. 2019;15(1):e1007896. Epub 2019/01/25. doi: 10.1371/journal.pgen.1007896. PubMed PMID: 30677018; PubMed Central PMCID: PMCPMC6363226.

73.   Amilhon B, Lepicard E, Renoir T, Mongeau R, Popa D, Poirel O, et al. VGLUT3 (vesicular glutamate transporter type 3) contribution to the regulation of serotonergic transmission and anxiety. J Neurosci. 2010;30(6):2198-210. Epub 2010/02/12. doi: 10.1523/JNEUROSCI.5196-09.2010. PubMed PMID: 20147547.

74.   Ciranna L. Serotonin as a modulator of glutamate- and GABA-mediated neurotransmission: implications in physiological functions and in pathology. Curr Neuropharmacol. 2006;4(2):101-14. Epub 2008/07/11. PubMed PMID: 18615128; PubMed Central PMCID: PMCPMC2430669.

75.   Pittaluga A. Presynaptic Release-Regulating mGlu1 Receptors in Central Nervous System. Front Pharmacol. 2016;7:295. Epub 2016/09/16. doi: 10.3389/fphar.2016.00295. PubMed PMID: 27630571; PubMed Central PMCID: PMCPMC5006178.

76.   Birgner C, Nordenankar K, Lundblad M, Mendez JA, Smith C, le Greves M, et al. VGLUT2 in dopamine neurons is required for psychostimulant-induced behavioral activation. Proc Natl Acad Sci U S A. 2010;107(1):389-94. Epub 2009/12/19. doi: 10.1073/pnas.0910986107. PubMed PMID: 20018672; PubMed Central PMCID: PMCPMC2806710.

77.   Fortin GM, Ducrot C, Giguere N, Kouwenhoven WM, Bourque MJ, Pacelli C, et al. Segregation of dopamine and glutamate release sites in dopamine neuron axons: regulation by striatal target cells. FASEB J. 2019;33(1):400-17. Epub 2018/07/17. doi: 10.1096/fj.201800713RR. PubMed PMID: 30011230.

78.   Zhang S, Qi J, Li X, Wang HL, Britt JP, Hoffman AF, et al. Dopaminergic and glutamatergic microdomains in a subset of rodent mesoaccumbens axons. Nat Neurosci. 2015;18(3):386-92. Epub 2015/02/11. doi: 10.1038/nn.3945. PubMed PMID: 25664911; PubMed Central PMCID: PMCPMC4340758.

79.   Koganezawa M, Kimura K, Yamamoto D. The Neural Circuitry that Functions as a Switch for Courtship versus Aggression in Drosophila Males. Curr Biol. 2016;26(11):1395-403. Epub 2016/05/18. doi: 10.1016/j.cub.2016.04.017. PubMed PMID: 27185554.

80.   Crocker A, Sehgal A. Octopamine regulates sleep in Drosophila through protein kinase A-dependent mechanisms. J Neurosci. 2008;28(38):9377-85. PubMed PMID: 18799671.

81.   Scheiner R, Steinbach A, Classen G, Strudthoff N, Scholz H. Octopamine indirectly affects proboscis extension response habituation in Drosophila melanogaster by controlling sucrose responsiveness. J Insect Physiol. 2014;69:107-17. Epub 2014/05/14. doi: 10.1016/j.jinsphys.2014.03.011. PubMed PMID: 24819202.

82.   Stevenson PA, Dyakonova V, Rillich J, Schildberger K. Octopamine and experience-dependent modulation of aggression in crickets. J Neurosci. 2005;25(6):1431-41. PubMed PMID: 15703397.

83.   Youn H, Kirkhart C, Chia J, Scott K. A subset of octopaminergic neurons that promotes feeding initiation in Drosophila melanogaster. PLoS One. 2018;13(6):e0198362. Epub 2018/06/28. doi: 10.1371/journal.pone.0198362. PubMed PMID: 29949586; PubMed Central PMCID: PMCPMC6021039.

84.   Classen G, Scholz H. Octopamine Shifts the Behavioral Response From Indecision to Approach or Aversion in Drosophila melanogaster. Front Behav Neurosci. 2018;12:131. Epub

2018/07/19. doi: 10.3389/fnbeh.2018.00131. PubMed PMID: 30018540; PubMed Central PMCID: PMCPMC6037846.

85.   Mingote S, Amsellem A, Kempf A, Rayport S, Chuhma N. Dopamine-glutamate neuron projections to the nucleus accumbens medial shell and behavioral switching. Neurochem Int. 2019;129:104482. Epub 2019/06/07. doi: 10.1016/j.neuint.2019.104482. PubMed PMID: 31170424.

86.   Manchia M, Carpiniello B, Valtorta F, Comai S. Serotonin Dysfunction, Aggressive Behavior, and Mental Illness: Exploring the Link Using a Dimensional Approach. ACS Chem Neurosci. 2017;8(5):961-72. Epub 2017/04/06. doi: 10.1021/acschemneuro.6b00427. PubMed PMID: 28378993.

87.   Vermeiren Y, Van Dam D, Aerts T, Engelborghs S, De Deyn PP. Monoaminergic neurotransmitter alterations in postmortem brain regions of depressed and aggressive patients with Alzheimer's disease. Neurobiol Aging. 2014;35(12):2691-700. Epub 2014/07/07. doi: 10.1016/j.neurobiolaging.2014.05.031. PubMed PMID: 24997673.

88.   Certel SJ, Kravitz EA. Scoring and analyzing aggression in Drosophila. Cold Spring Harb Protoc. 2012;2012(3):319-25. Epub 2012/03/03. doi: 10.1101/pdb.prot068130. PubMed PMID: 22383642.

89.   Koon AC, Ashley J, Barria R, DasGupta S, Brain R, Waddell S, et al. Autoregulatory and paracrine control of synaptic and behavioral plasticity by octopaminergic signaling. Nat Neurosci. 2011;14(2):190-9. Epub 2010/12/28. doi: nn.2716 [pii] 10.1038/nn.2716 [doi]. PubMed PMID: 21186359.

90.   Petersen LK, Stowers RS. A Gateway MultiSite recombination cloning toolkit. PLoS One. 2011;6(9):e24531. Epub 2011/09/21. doi: 10.1371/journal.pone.0024531. PubMed PMID: 21931740; PubMed Central PMCID: PMCPMC3170369.

91.   Pfeiffer BD, Jenett A, Hammonds AS, Ngo TT, Misra S, Murphy C, et al. Tools for neuroanatomy and neurogenetics in Drosophila. Proc Natl Acad Sci U S A. 2008;105(28):9715-20. PubMed PMID: 18621688.

92.   Williams JL, Shearin HK, Stowers RS. Conditional Synaptic Vesicle Markers for Drosophila. G3 (Bethesda). 2019. Epub 2019/01/13. doi: 10.1534/g3.118.200975. PubMed PMID: 30635441.

93.   Shearin HK, Dvarishkis AR, Kozeluh CD, Stowers RS. Expansion of the gateway multisite recombination cloning toolkit. PLoS One. 2013;8(10):e77724. Epub 2013/11/10. doi: 10.1371/journal.pone.0077724. PubMed PMID: 24204935; PubMed Central PMCID: PMCPMC3799639.

94.   Pfeiffer BD, Truman JW, Rubin GM. Using translational enhancers to increase transgene expression in Drosophila. Proc Natl Acad Sci U S A. 2012;109(17):6626-31. Epub 2012/04/12. doi: 10.1073/pnas.1204520109. PubMed PMID: 22493255; PubMed Central PMCID: PMCPMC3340069.

95.   Wang JW, Beck ES, McCabe BD. A modular toolset for recombination transgenesis and neurogenetic analysis of Drosophila. PLoS One. 2012;7(7):e42102. Epub 2012/08/01. doi: 10.1371/journal.pone.0042102. PubMed PMID: 22848718; PubMed Central PMCID: PMCPMC3405054.

96.   Port F, Chen HM, Lee T, Bullock SL. Optimized CRISPR/Cas tools for efficient germline and somatic genome engineering in Drosophila. Proc Natl Acad Sci U S A. 2014;111(29):E2967-76. Epub 2014/07/09. doi: 10.1073/pnas.1405500111. PubMed PMID: 25002478; PubMed Central PMCID: PMCPMC4115528.

97.   Daniels RW, Collins CA, Chen K, Gelfand MV, Featherstone DE, DiAntonio A. A single vesicular glutamate transporter is sufficient to fill a synaptic vesicle. Neuron. 2006;49(1):11-6. Epub 2006/01/03. doi: 10.1016/j.neuron.2005.11.032. PubMed PMID: 16387635; PubMed Central PMCID: PMCPMC2248602.

98.   Ren X, Sun J, Housden BE, Hu Y, Roesel C, Lin S, et al. Optimized gene editing technology for Drosophila melanogaster using germ line-specific Cas9. Proc Natl Acad Sci U S A. 2013;110(47):19012-7. Epub 2013/11/06. doi: 10.1073/pnas.1318481110. PubMed PMID: 24191015; PubMed Central PMCID: PMCPMC3839733.
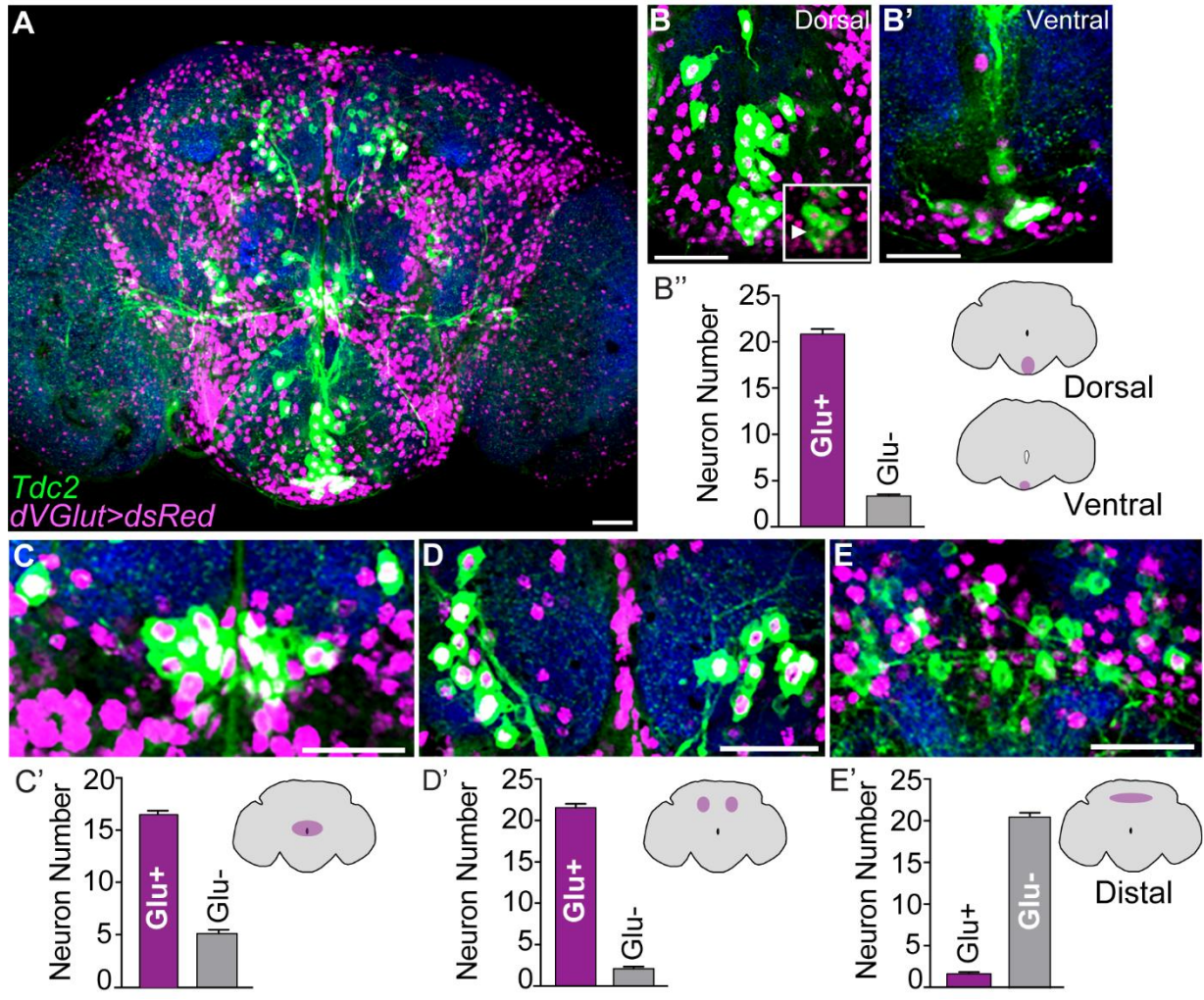
Figures

Fig 1. OA neurons co-express glutamate.

(A) OA-glutamate co-expression in a *dVGlut>dsRed* male brain labeled with anti-Tdc2 (green). Anti-brp (nc82, blue) labels the neuropil. Scale bar = 10 µm. **(B-B')** Dorsal (B) and ventral (B') confocal sections of neurons co-expressing OA and dVGlut in the SEZ. Non-dVGlut positive neurons are indicated (B inset, arrowhead). **(B")** Quantification of OGN SEZ co-expression. **(C-C')** OGNs in the PENP and quantification. **(D-D')** *dVGlut>dsRed* neurons expressing Tdc2 in the ASMP and quantification. **(E-E')** Neurons co-expressing OA and glutamate in the PSMP and quantification. Scale bar = 20 µm for panels B-E.
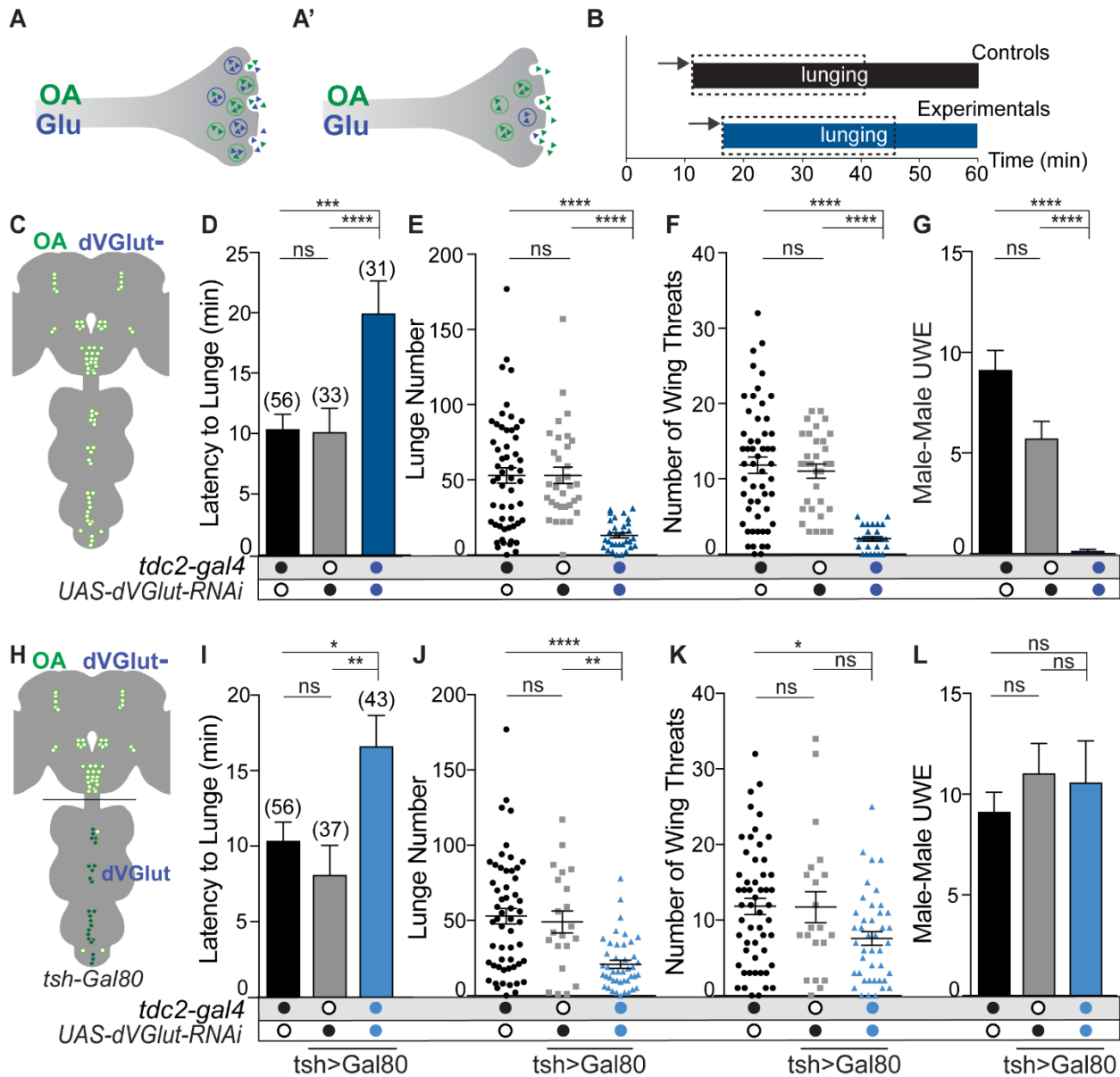
Fig 2. Male aggression requires dVGLUT function in OGNs.

(A) dVGLUT reduction in OGNs through RNAi. **(B)** Behaviors for control and experimental male pairs were scored for thirty minutes beginning with the first lunge. **(C)** Schematic illustrating the brain and VNS OGNs**.** **(D)** Latency to lunge increased in *tdc2>dVGlut-RNAi* males (all statistical tests are Kruskal-Wallis with Dunn's multiple comparisons test, (*p<0.05, **p<0.01, ***p<0.001, ****p<0.0001). **(E)** *tdc2>dVGlut-RNAi* males displayed a decrease in the average number of lunges. **(F)** Wing threats were reduced in *tdc2-dVGlut-RNAi* males. **(G)** *tdc2-dVGlut-RNAi* males did not exhibit inter-male courtship (unilateral wing extensions = UWE). **(H)** Schematic illustrating the addition of *tsh>Gal80* limits dVGLUT reduction to brain OGNs. **(I)** Latency to

lunge by *tdc2-gal4/tsh>Gal80;UAS-dVGlut-RNAi* males is significantly longer than controls. **(J)** Lunge number by *tdc2-gal4/tsh>Gal80;UAS-dVGlut-RNAi* males decreases as compared to controls. **(K)** Wing threat number was rescued to *UAS-dVGlut-RNAi* control levels. **(L)** Male-male UWE was rescued to control levels. N values for each genotype, panels D, I. Error bars denote s.e.m.
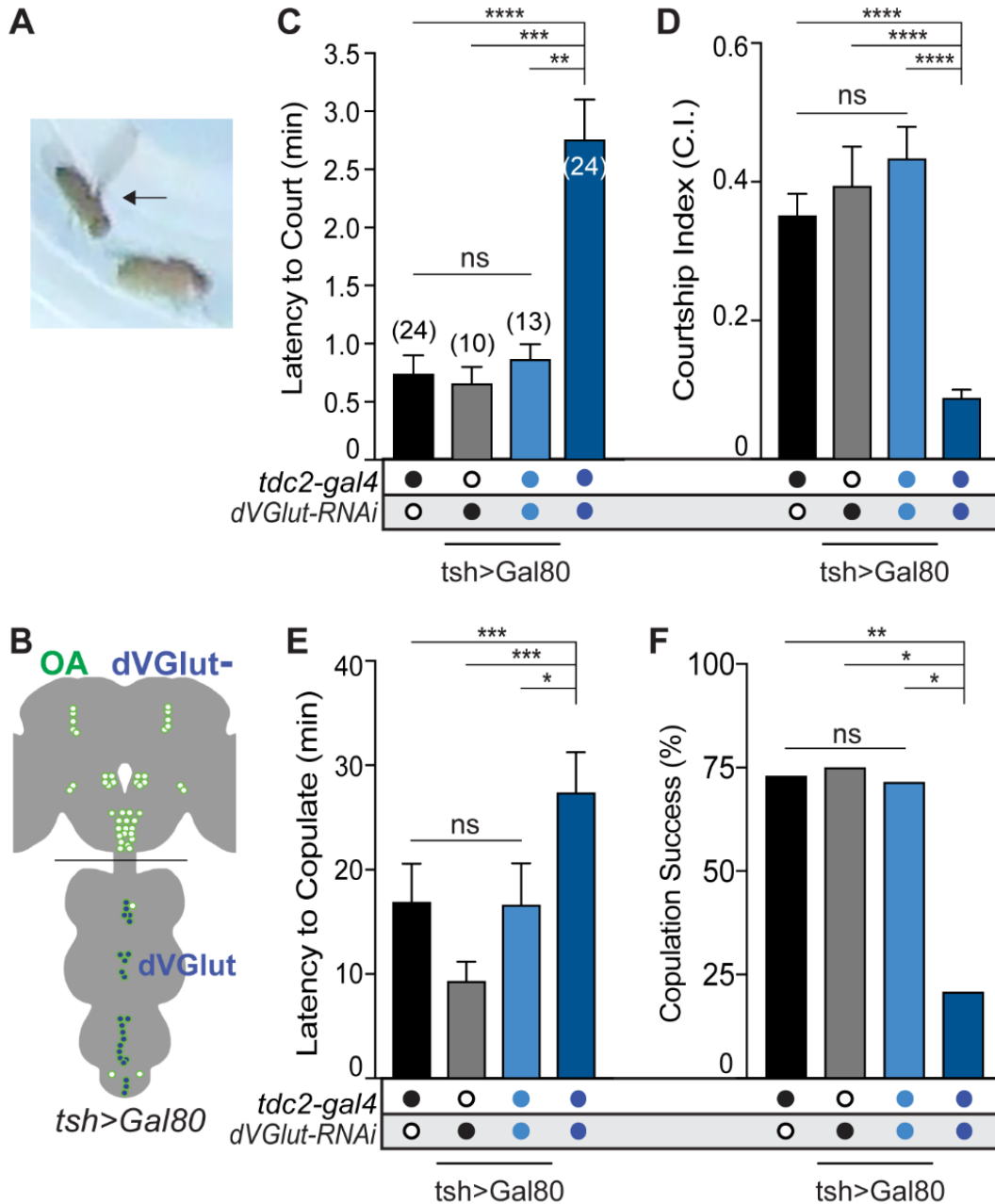

Fig 3. dVGLUT function is required in VNS OGNs for male-female courtship.

(A) Male (arrow) to female courtship. **(B)** Schematic illustrating the addition of *tsh>Gal80* limits dVGLUT reduction to brain OGNs. **(C-F)** All parameters of male to female courtship were rescued by restoring glutamate function to OGNs within the VNC. **(C)** The latency to initiate courtship towards a female returned to control levels in males with reduced dVGLUT in brain OGNs. **(D)** The courtship index was restored to control levels in *tdc2-gal4/tsh>Gal80;dVGlut-RNAi* males. **(E)** *tdc2-gal4/tsh>Gal80;dVGlut-RNAi* males exhibited the same latency to copulation as controls. **(F)** The copulation success of males with a dVGLUT reduction in brain OGNs was not significantly different from controls. N values for each genotype located on panel A. All statistical tests are Kruskal-Wallis with Dunn's multiple comparisons test, (*p<0.05, **p<0.01, ***p<0.001, ****p<0.0001.

A Before excision: dVGlut wildtype function, *no LexA expression*

B After excision:
dVGlut LOF
dVGlut-LexA

+ B3 recombinase

C *B3RT-dVGlut/UAS-B3*
Control

D *B3RT-dVGlut-LexA/tdc2-gal4;UAS-B3*

D'

I

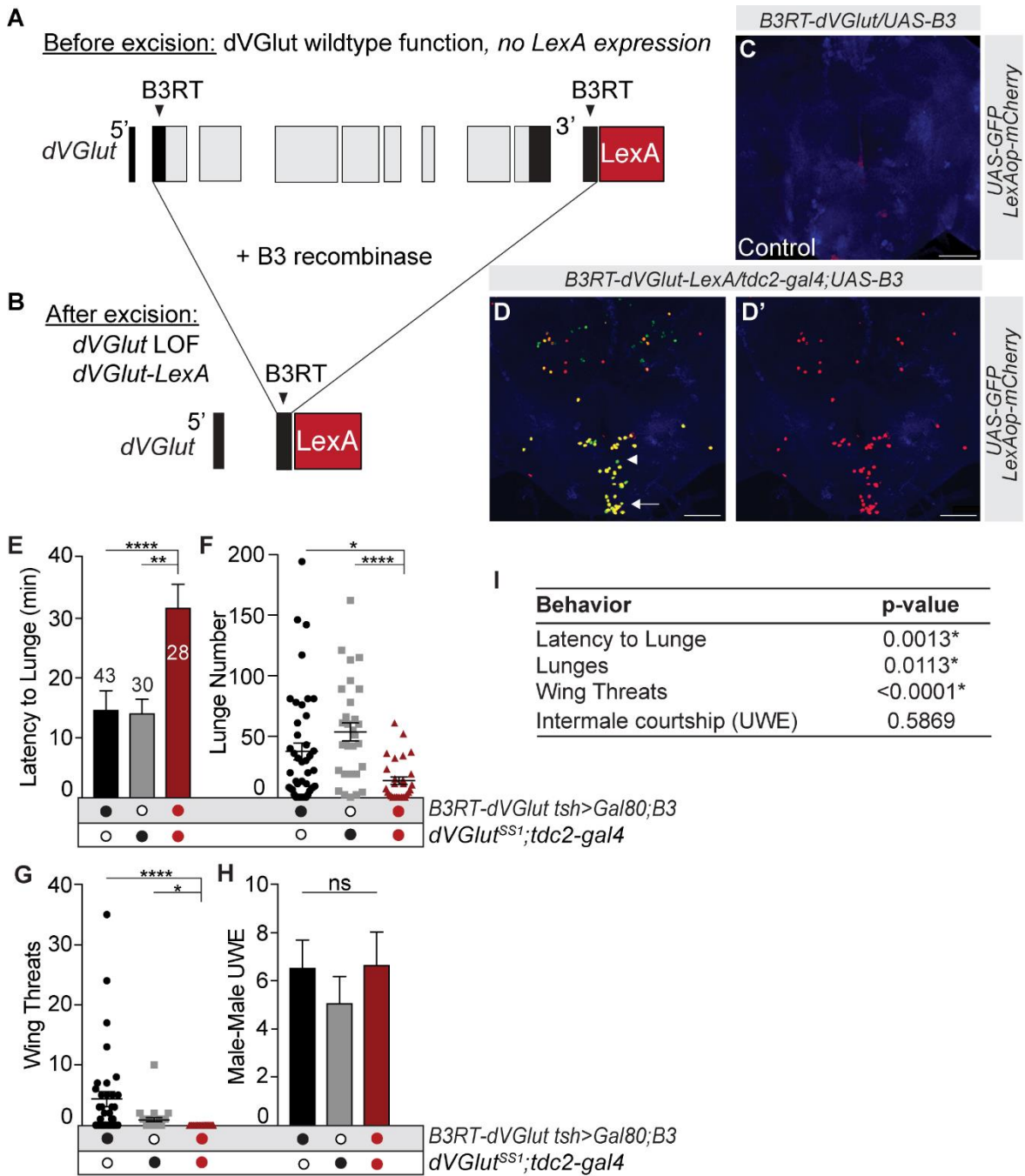| Behavior	p-value
Latency to Lunge	0.0013*
Lunges	0.0113*
Wing Threats	<0.0001*
Intermale courtship (UWE)	0.5869

Fig 4. B3-mediated elimination of dVGLUT in OGNs reduces male aggression.

(A,B) Schematic of the *B3RT-dVGlut-LexA* conditional allele. B3RTs flank dVGlut coding exons **(A)** and excise the entire dVGlut coding sequence in a specific subset of neurons upon expression of the B3 recombinase **(B)**. After excision, a *dVGlut* null loss-of-function allele and *dVGlut-LexA* driver is created **(B)**. **(C)** Control brain demonstrating without a source of Gal4-driven B3 recombinase, excision and therefore LexA expression does not occur. **(D-D')** *tdc2-gal4* driven B3

recombinase-mediated excision effectively removes *dVGlut* resulting in *B3RT-LexA*-driven mCherry expression is in the majority of OA neurons (yellow). As expected, a few Tdc2+ neurons do not express dVGLUT (arrowhead, green). LexAop reporter expression that does not also show UAS expression may be observed as a result of excisions that occurred during development in former Tdc2+ neurons. **(E)** Latency to lunge increased in males lacking dVGLUT function (*B3RT-dVGlut tsh>Gal80/dVGlut^{SS1};UAS-B3*) in OGNs. **(F)** Males without dVGLUT function lunged significantly less when compared to controls. **(G)** Wing threat number decreased in experimental males. **(H)** No significant differences in male-male courtship. **(I)** Aggression is significantly reduced by the complete loss of dVGLUT in OGNs as compared to the RNAi-based dVGLUT reduction. All statistical tests are Kruskal-Wallis with Dunn's multiple comparisons test, (*$p<0.05$, **$p<0.01$, ***$p<0.001$, ****$p<0.0001$. Error bars denote s.e.m. N values for each genotype, panel E.
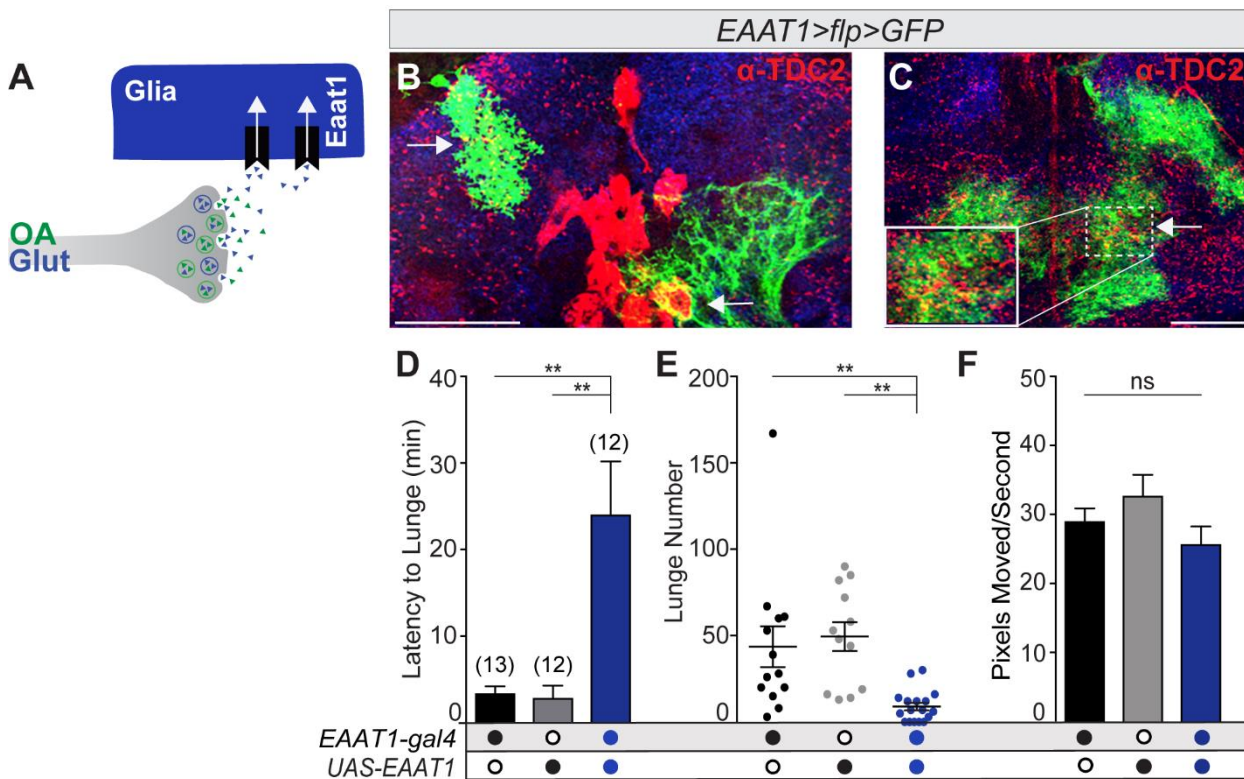
Fig 5

Fig 5. Reducing glutamate function through EAAT1 overexpression decreases male aggression **(A)** Glutamate function was reduced by increasing EAAT1 expression in EAAT1-expressing glia.

(B, C) GFP-expressing EAAT1 glia (*hs-flp; EAAT1-gal4/UAS>stop>CD8:GFP*) enwrap Tdc2+ neuron cell bodies (arrowhead) and endings (arrow). Higher magnification of dashed box in C. Scale bar = 30 um. **(D)** The latency to lunge by *EAAT1>Eaat1* males was increased as compared to controls. **(E)** A decrease in lunge number was exhibited by *EAAT1>Eaat1* males as compared to controls. **(F)** Locomotor activity during the aggression assay did not differ. All statistical tests are Kruskal-Wallis with Dunn's multiple comparisons tests. N values for each genotype are in panel D.
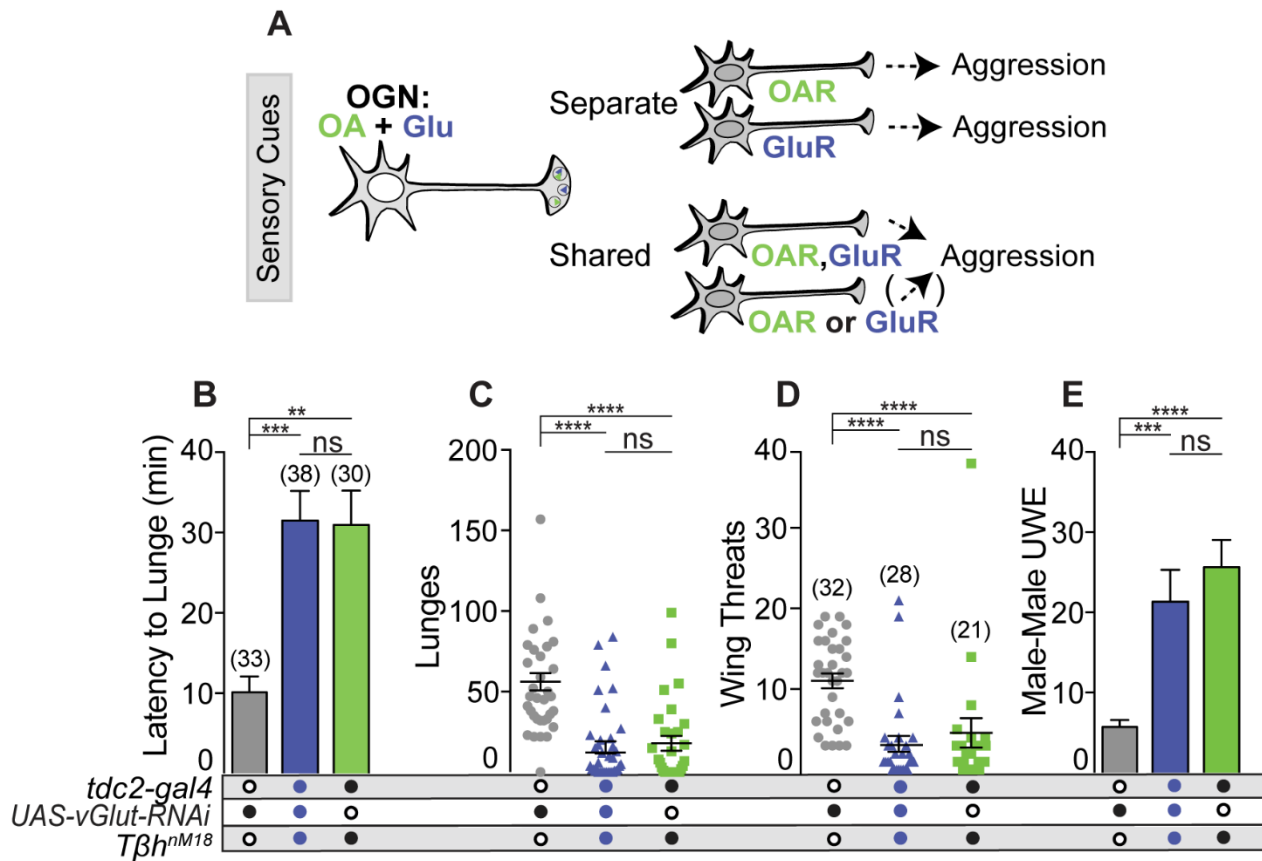

Fig 6. OA and Glu signal to a shared aggression-promoting circuit

(A) OGNs could signal to separate aggression-promoting circuits (resulting in aggression deficits greater than the single mutant) or to a shared or converged circuit. **(B-E)** dVGlut was reduced in OGNs of *TβhM18* males (*TβhM18;tdc2>dVGlut-RNAi*). **(C)** Latency to lunge increased in *TβhM18;tdc2>dVGlut-RNAi* males compared to the transgenic control but not *TβhM18* males. **(D)** Lunge number by males with reduced dVGLUT and lacking OA was not significantly different than *TβhM18* males. **(E)** *TβhM18;tdc2>dVGlut-RNAi* males displayed lower wing threat numbers compared to the transgenic control but not *TβhM18* males. **(F)** Males with reduced dVGLUT and

lacking OA (blue column) displayed an increase in inter-male courtship at levels higher than the control but not significantly different from *TβhM18* mutants (green column). All statistical tests are Kruskal-Wallis with Dunn's multiple comparisons test, (*p<0.05, **p<0.01, ***p<0.001, ****p<0.0001. Error bars denote s.e.m.
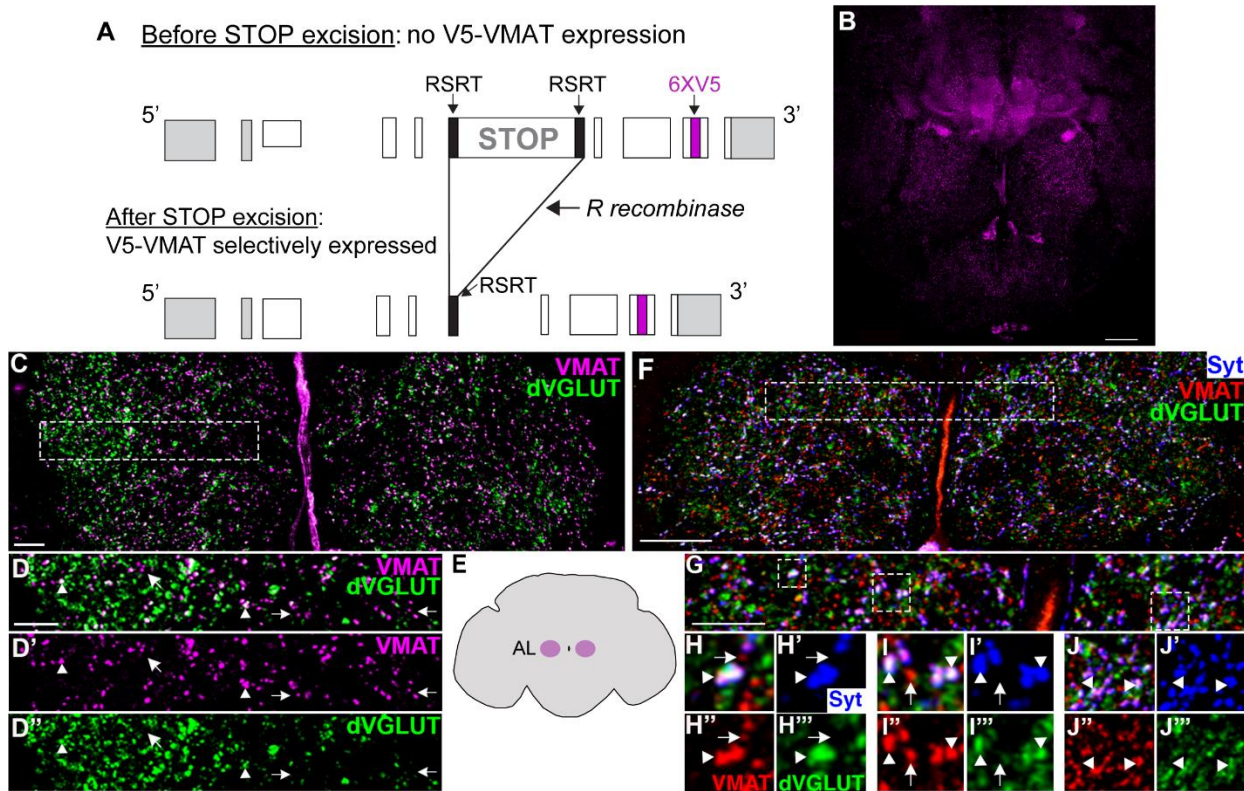

Fig 7. Spatial segregation of VMAT and dVGLUT within OGNs

(A) Schematic of the *RSRT>STOP>RSRT-6XV5-VMAT* conditional allele. RSRTs flank a STOP cassette inserted between VMAT coding exon 5 and 6. Upon Gal4-driven expression of the R recombinase enzyme, the STOP cassette is excised and V5-tagged VMAT expression under control of the endogenous promoter is expressed. **(B)** Representative brain showing V5-VMAT expression in OGNs after excision by *tdc2-dVGlut-gal4* driven R recombinase. The brain is labeled with anti-V5 (magenta) and mAb dVGLUT (green in panels C,D). Scale bar is 30 µm. **(C)** Higher magnification of the antennal lobe region showing dVGLUT expression (green) with V5-VMAT (magenta). Scale bar is 10 µm. **(D)** The region in the dashed box in C showing puncta with dVGLUT and V5-VMAT colocalization (arrowheads) and puncta with only V5-VMAT (arrows). **(E)** Schematic showing the regions of the brain that are depicted in C and F. **(F)** Antennal lobe

region of a representative brain with a synaptic marker incorporated (*UAS-synaptotagmin;HA, tdc2-dVGlut split gal4/UAS-R RSRT-STOP-RSRT-6XV5-vMAT*). The brain is labeled with anti-HA (blue), anti-V5 (magenta), and mAb dVGLUT (green). Scale bar is 20 µm. **(G-J''')** Higher magnification of the SEZ region of the AL in F showing dVGLUT expression (green), V5-VMAT (red), and Syt:HA (blue). Arrowheads indicate puncta with dVGLUT, V5-VMAT and Syt:HA and arrows indicate puncta with only V5-VMAT and Syt:HA. The stack for panels C and D contains two optical sections at 0.45 µm. Stacks for panels G-J contain 7 optical sections at 0.5 µm.
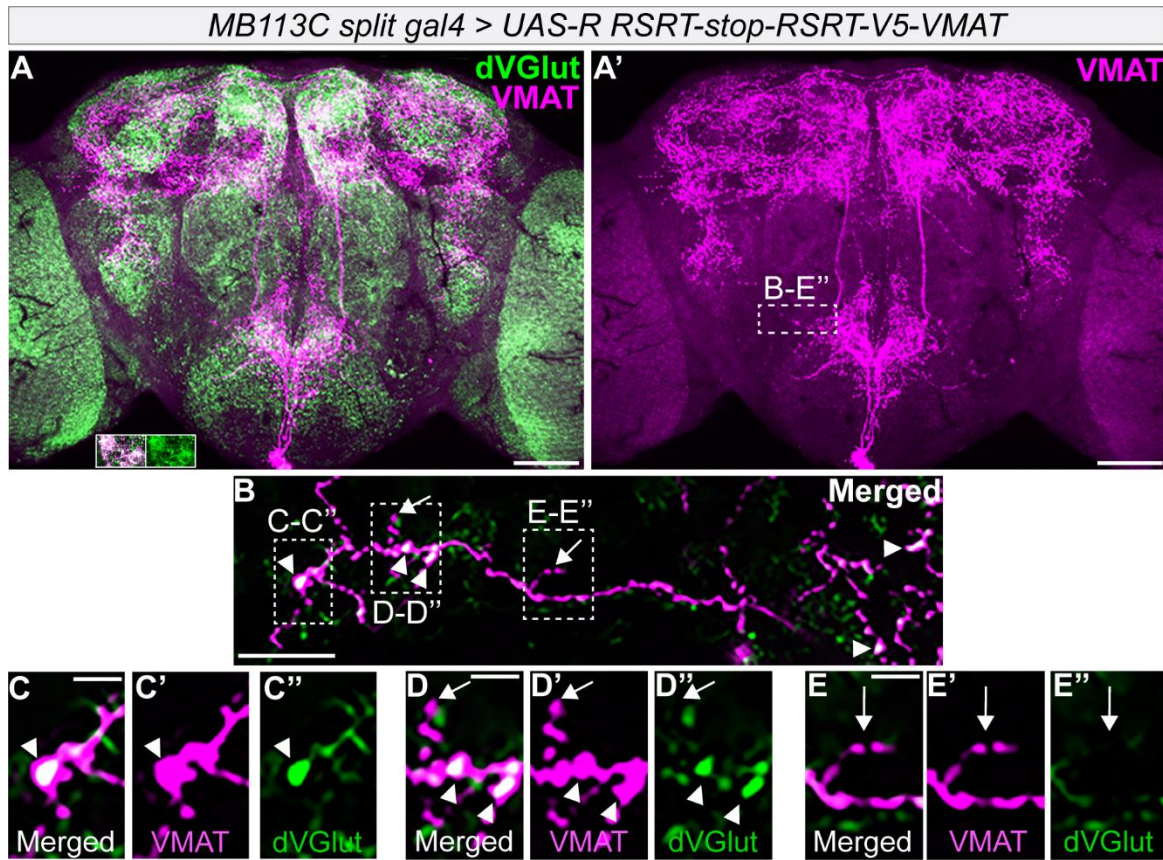

Fig 8. Spatial segregation of VMAT and dVGLUT within two OGNs

(A-A') Representative brain showing V5-VMAT expression in two OGNs after excision by *MB113C-split-gal4* driven R recombinase. The brain is labeled with anti-V5 (magenta) and mAb dVGLUT (green). Scale bar is 50 µm. The inlet in A which is from a separate brain demonstrates this OA neuron driver also expresses dVGLUT (green). **(B-E)** Higher magnification of the SEZ boxed region in A'. Arrowheads point to puncta with V5-VMAT and dVGLUT, arrows indicate V5-VMAT only puncta. Scale bar is 10 µm. **(C-E)** The regions in the dashed boxes in B showing puncta with dVGLUT and V5-VMAT colocalization (arrowheads) and puncta with only V5-VMAT

(arrows). Panels B-E contain stacks of four optical sections at 0.45 µm. Scale bar for panels C-E is 5 µm.

Supporting Information

Supplementary Fig 1.

Verification of mAb dVGLUT specificity using the null *dVGlut^SS1* allele. **(A)** dVGLUT expression detected by mAb dVGLUT in a heterozygous *yw, dVGlut^SS1/+* late stage embryo. **(B)** dVGLUT expression is not detectable by mAb dVGLUT in a homozygous *yw, dVGlut^SS1/ dVGlut^SS1* late stage embryo.
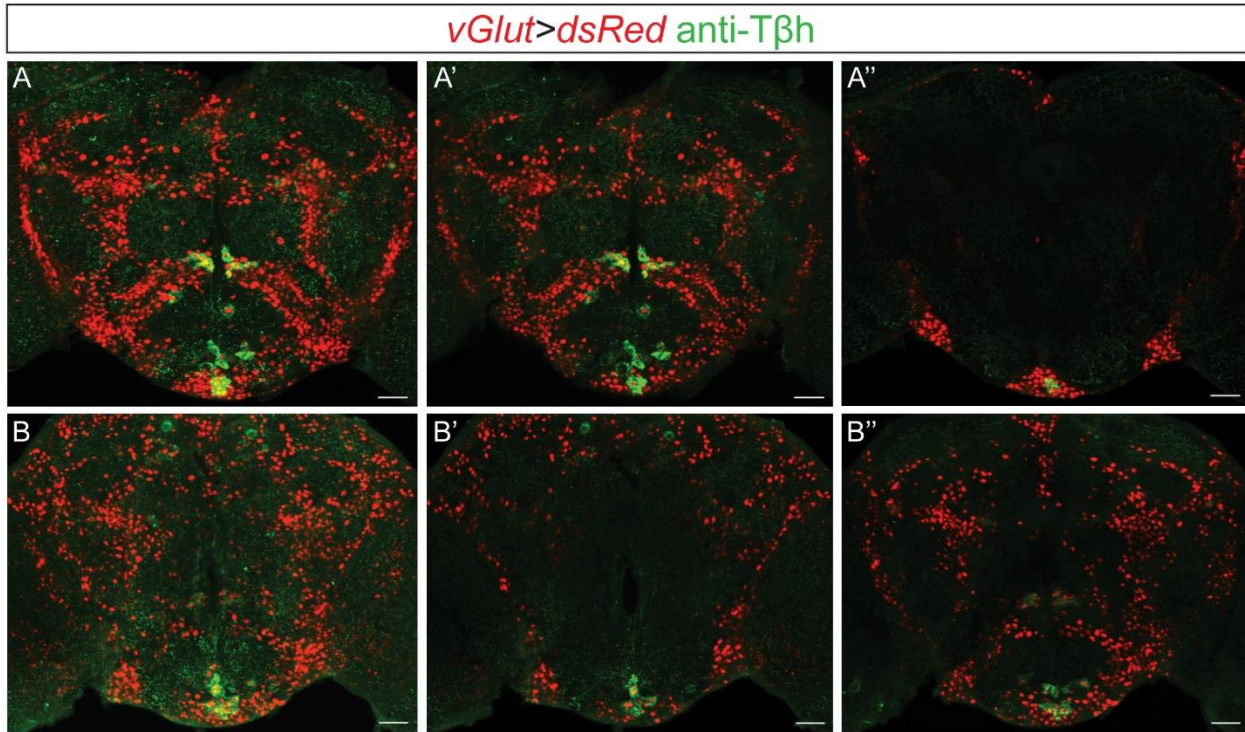
Supplementary Fig 2.

Multiple optical sections from *dVGlut>dsRed* male brains labeled with anti-Tβh. **(A-B)** Although the Tβh shows weaker immunoreactivity than the anti-Tdc2 antibody, Tβh is mainly detected in *dVGlut>dsRed* neurons at dorsal and ventral positions (A', A", B' and B"). Scale bar = 20 µm.
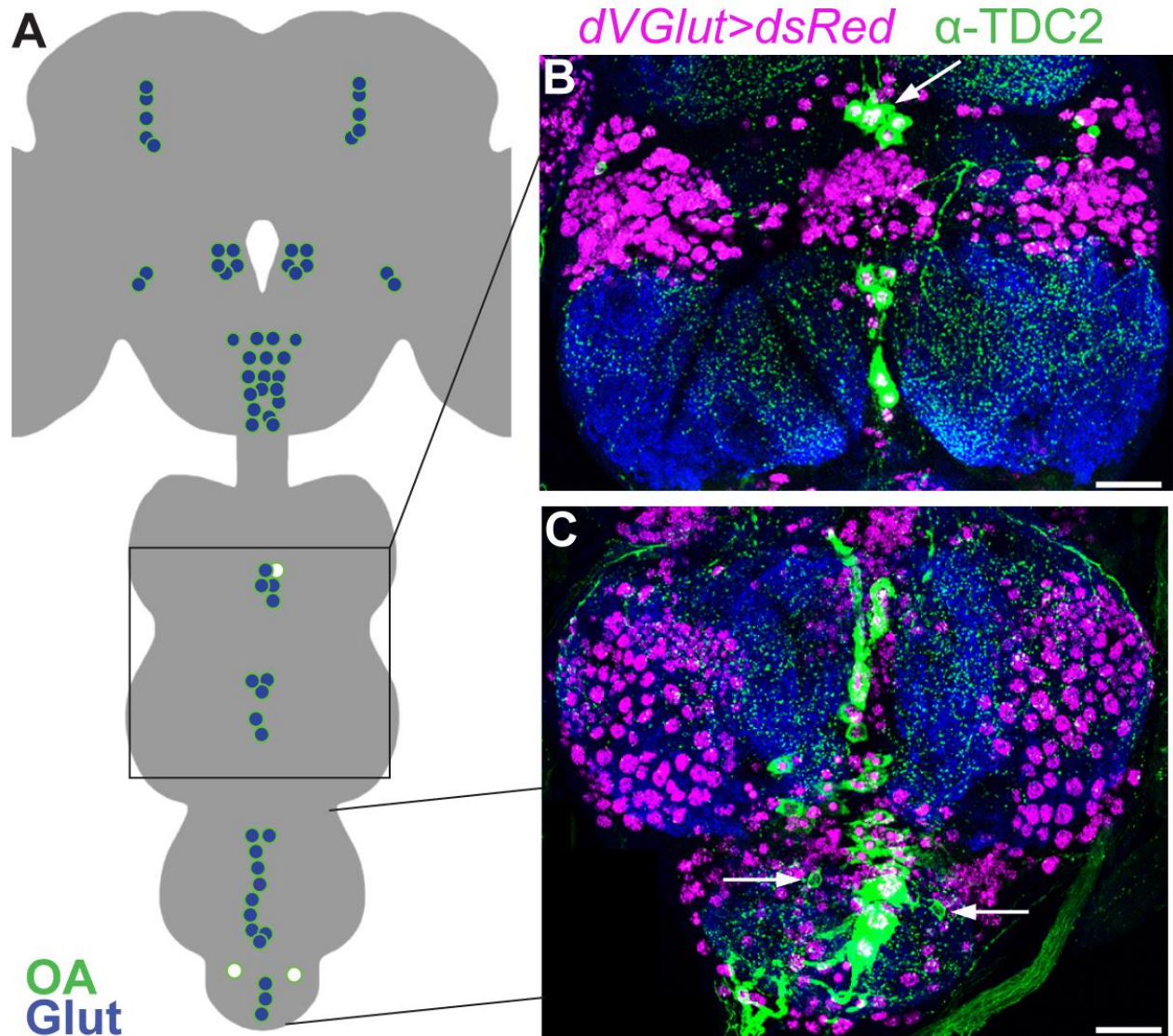
Supplementary Fig 3.

(A-A') Schematic showing the regions (boxes) of the VNS imaged in panels B and C. **(D-E)** A male *dVGlut>dsRed* adult VNS labeled with anti-Tdc2. The majority of dVGLUT+ neurons within the thoracic VNS **(D)** and abdominal VNS **(E)** express Tdc2 with a few exceptions (arrows). Scale bar = 10 µm.
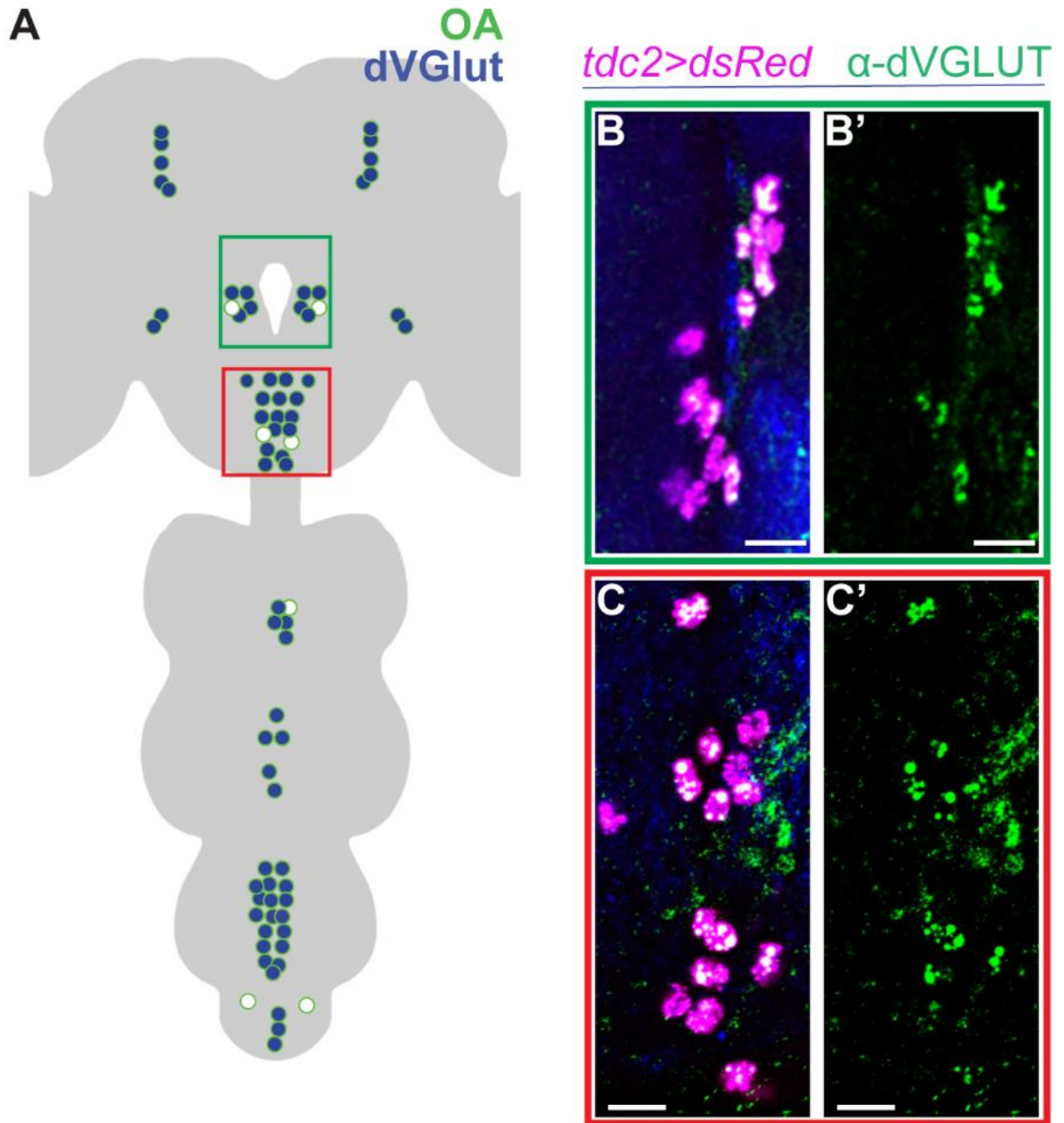
Supplementary Fig 4.

(A) Schematic showing the regions imaged in panels B and C (colored boxes). **(B-C)** The majority of OA neurons within the PENP **(B)** and SEZ **(C)** regions co-express dVGLUT as visualized in a male *tdc2>dsRed* adult brain labeled with anti-dVGLUT. Scale bar = 10 µm.

SFig. 6

A

B

Ventral

C

anti-TDC2
dsRed

tdc2-gal4/UAS-dVGlut-RNAi;UAS-dsRed

D

Dorsal

E

anti-TDC2
dsRed
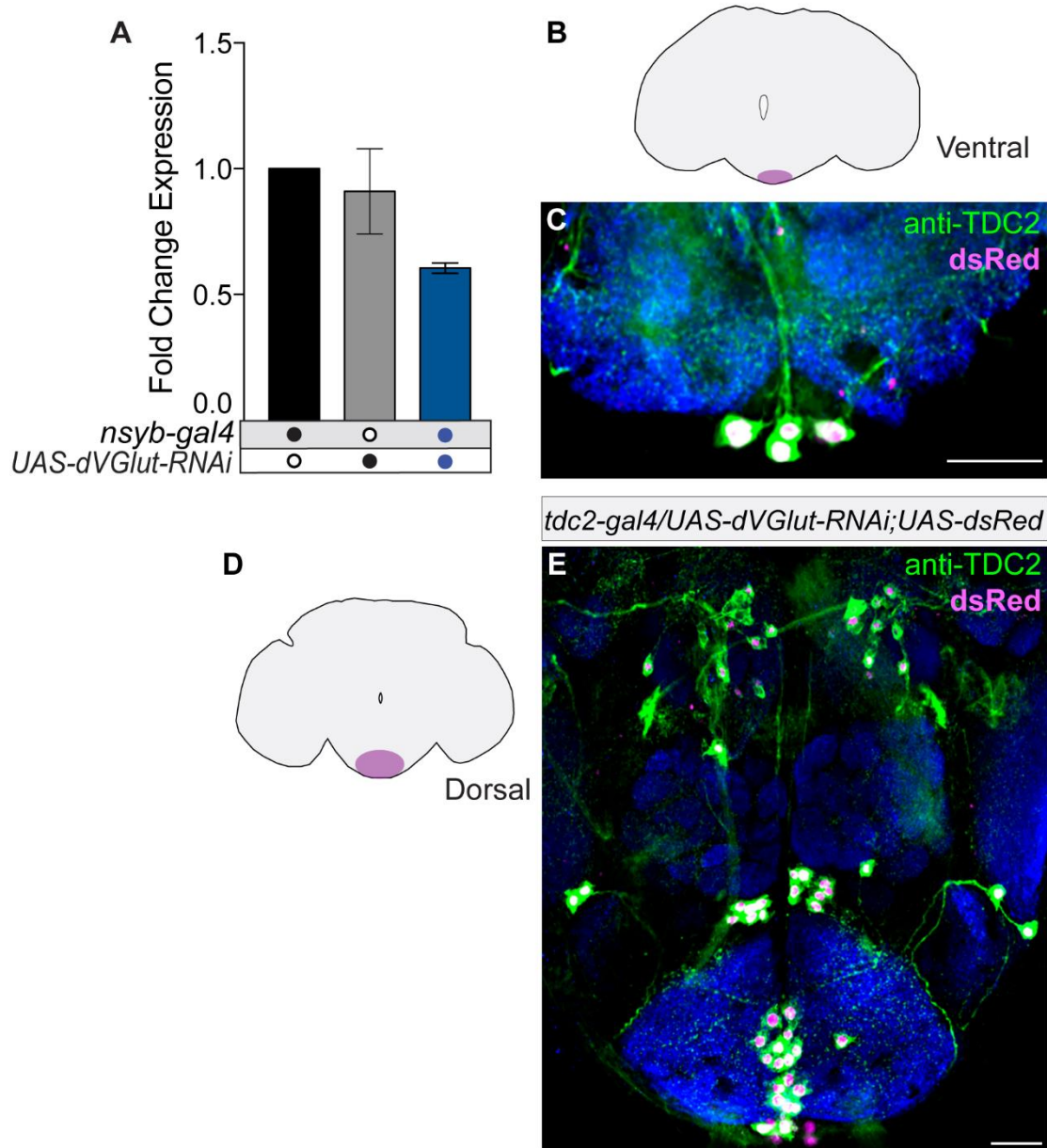
Supplementary Fig 5.

(**A**) *dVGlut* transcript levels were decreased in *n-syb-gal4>dVGLUT-RNAi* males as compared to the *n-syb-gal4* control (n=3; p<0.01). (**B-C**) Representative images of ventral sections of the SEZ from a *tdc2-gal4>dVGLUT-RNAi;UAS-dsRed* male brain labeled with anti-Tdc2. OGN differentiation as measured by Tdc2 expression is not altered by a reduction of dVGLUT. Scale bar = 10 µm. (**D-E**) Dorsal sections of the SEZ, PENP and protocerebral bridge region from the same

brain as in B. There are no obvious changes in ventral OGN survival and differentiation as measured by Tdc2 expression. Scale bar = 20 µm.
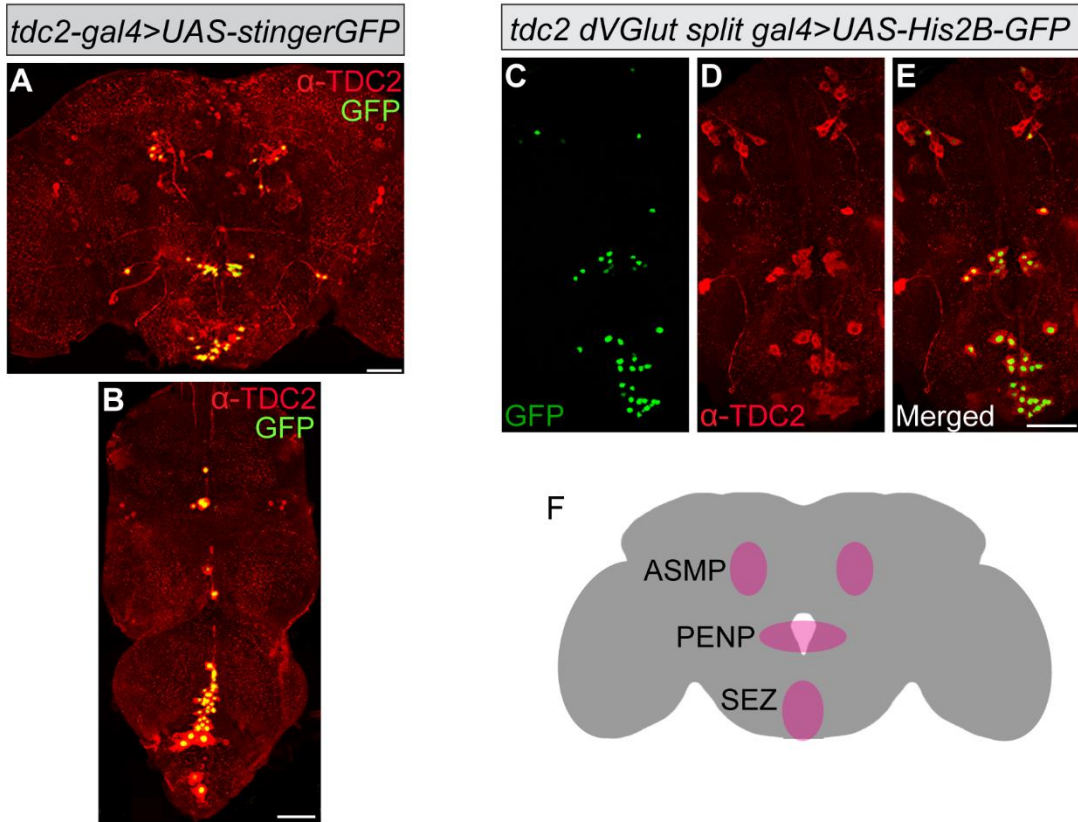
Supplementary Fig 6.

(**A**) Verification that each *tdc2>GFP* neuron in the brain and VNS is Tdc2+. The stack for panel A contains 30 optical sections at 1.0 µm. Scale bar = 20 µm. (**B**) The stack for panel B contains 34 optical sections at 1.0 µm. Scale bar = 20 µm. (**C**) Verification that each *tdc2-dVGlut-split>GFP* neuron is Tdc2+. The stack for panels C-E contains 56 optical sections at 0.5 µm. Scale bar = 20 µm.
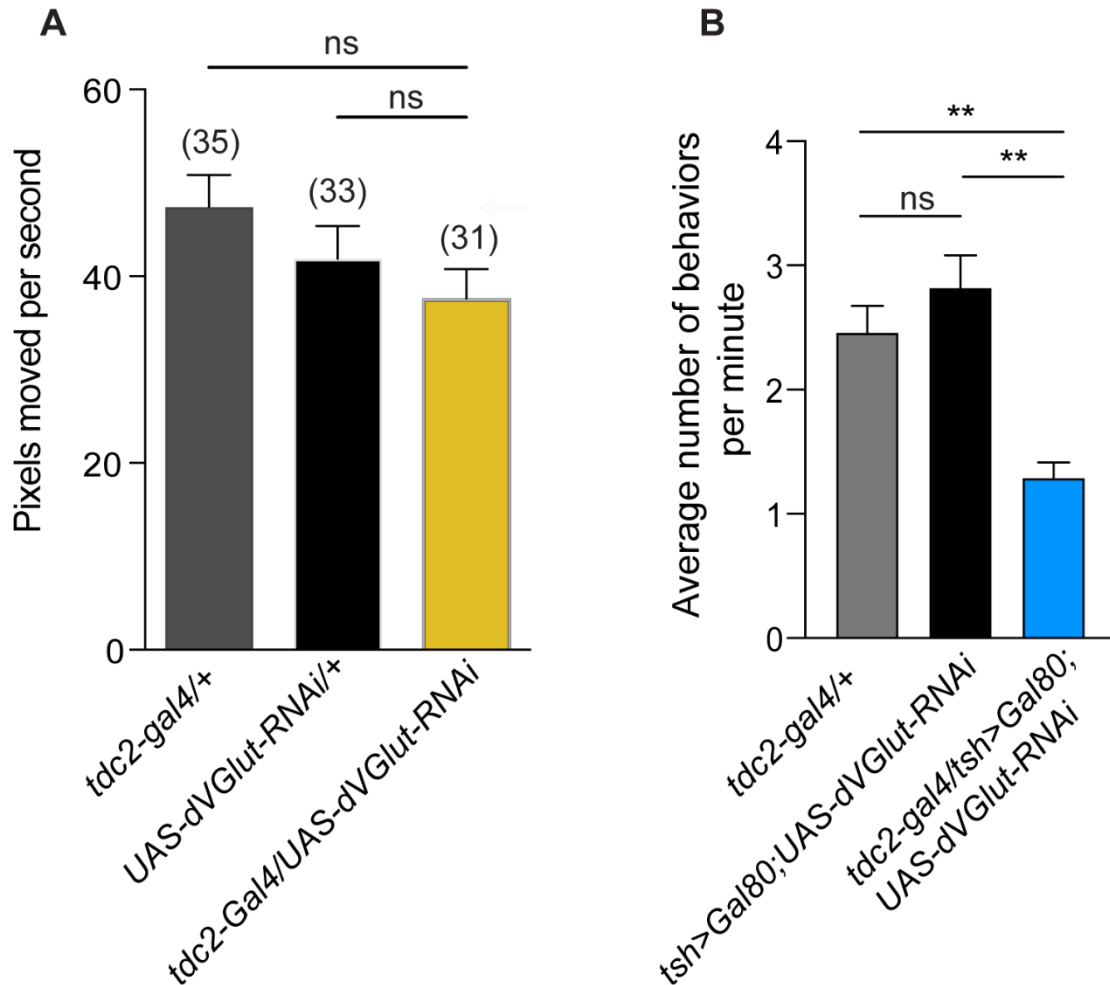
Supplementary Fig 7.

(A) The activity levels of controls and *tdc2>dVGlut-RNAi* males did not differ during the aggression assay as measured by pixels moved/second. **(B)** Total behavioral events (lunges, wing threats, inter-male courtship) per minute was calculated. The average number of behavioral events per minute exhibited by experimental males (*tdc2>tsh>Gal80>dVGlut-RNAi*) was lower than controls (**p<0.01)
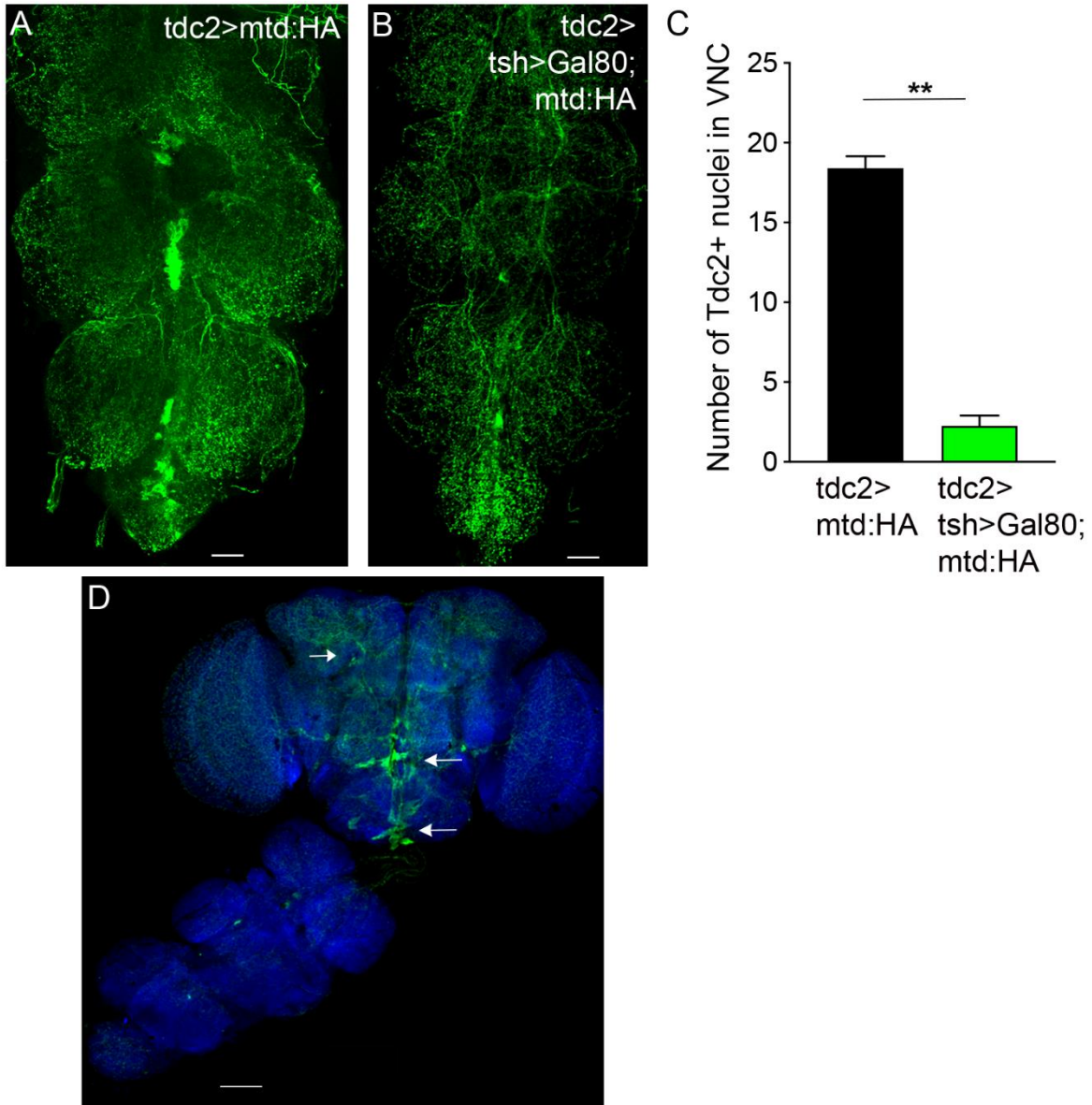
Supplementary Fig 8.

(A) The VNS of a *tdc2>mtd:HA* male, note the Tdc2+ cell bodies. **(B)** The addition of *tsh>Gal80* blocked the Gal4-mediated expression of mtd:HA in the majority of Tdc2+ VNS neurons (*tdc2/tsh>Gal80;dsRed)*. Axonal projections from brain Tdc2+ neurons are visualized in the VNS. **(C)** Significantly less Tdc2+ VNS neurons are detected in *tdc2/tsh>Gal80;dsRed* vs. *tdc2>dsRed* males. (Mann Whitney, P=0.001). **(D)** The addition of *tsh>Gal80* does not alter brain *tdc2-gal4* reporter driven expression.
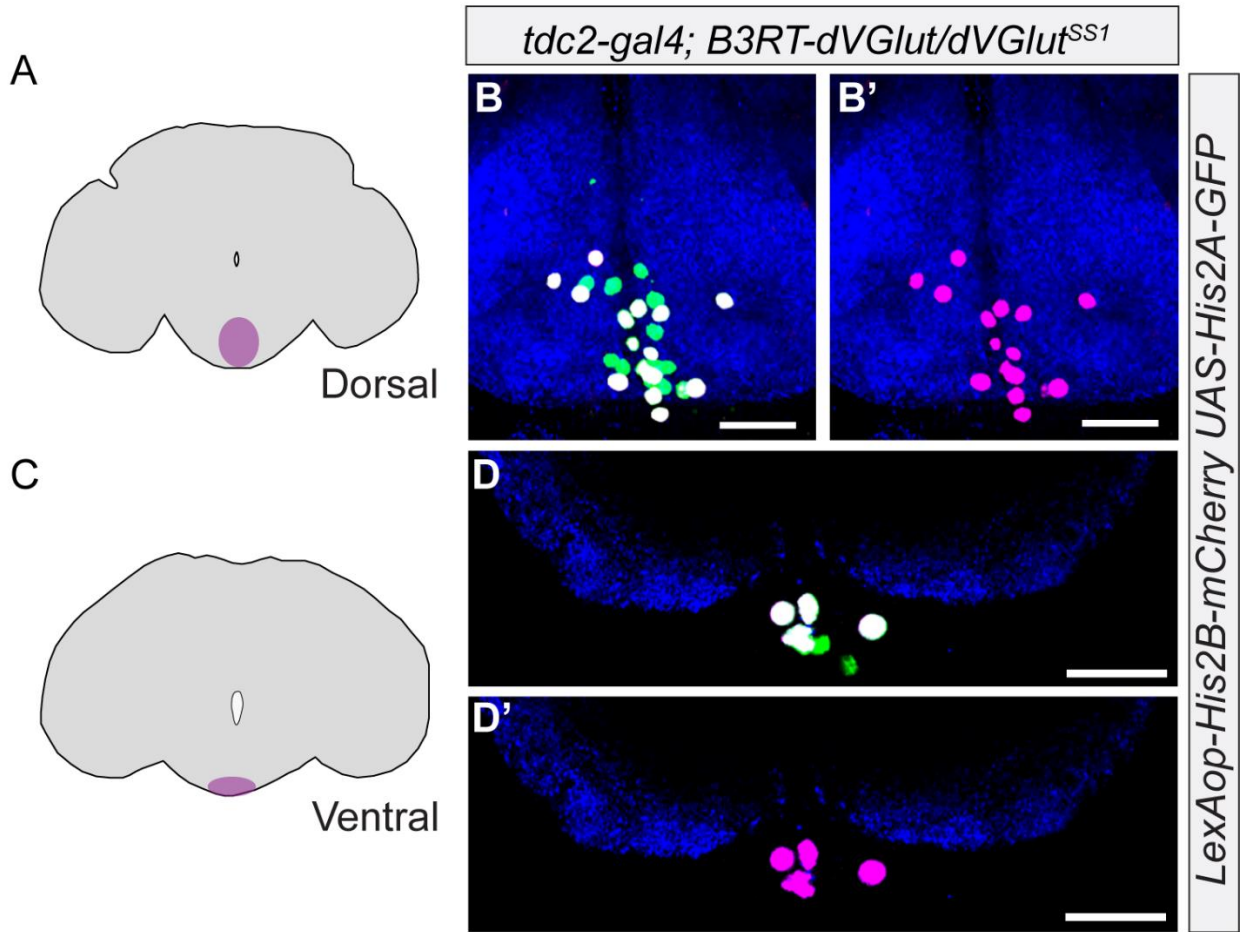
Supplementary Fig 9.

Neuron survival or distribution is not altered by the complete loss of dVGLUT in OGNs **(A-B)**

Representative images of dorsal and ventral optical sections of the SEZ region from *tdc2-gal4;B3RT-dVGlut/dVGLUT^{SS1};UAS-B3 lexAop-His2B-mCherry UAS-His2A-GFP* males. OGNs are visualized by the mCherry reporter and white co-colocalization in the merged channel. Scale bar = 20 µm.

tdc2-Gal4-AD dVGLUT-Gal4-DBD;
UAS-R RSRT>stop>RSRT-6XV5-VMAT

A dVGLUT V5-VMAT

A' V5-VMAT

+; UAS-R RSRT>stop>RSRT-6XV5-VMAT

B dVGLUT V5-VMAT
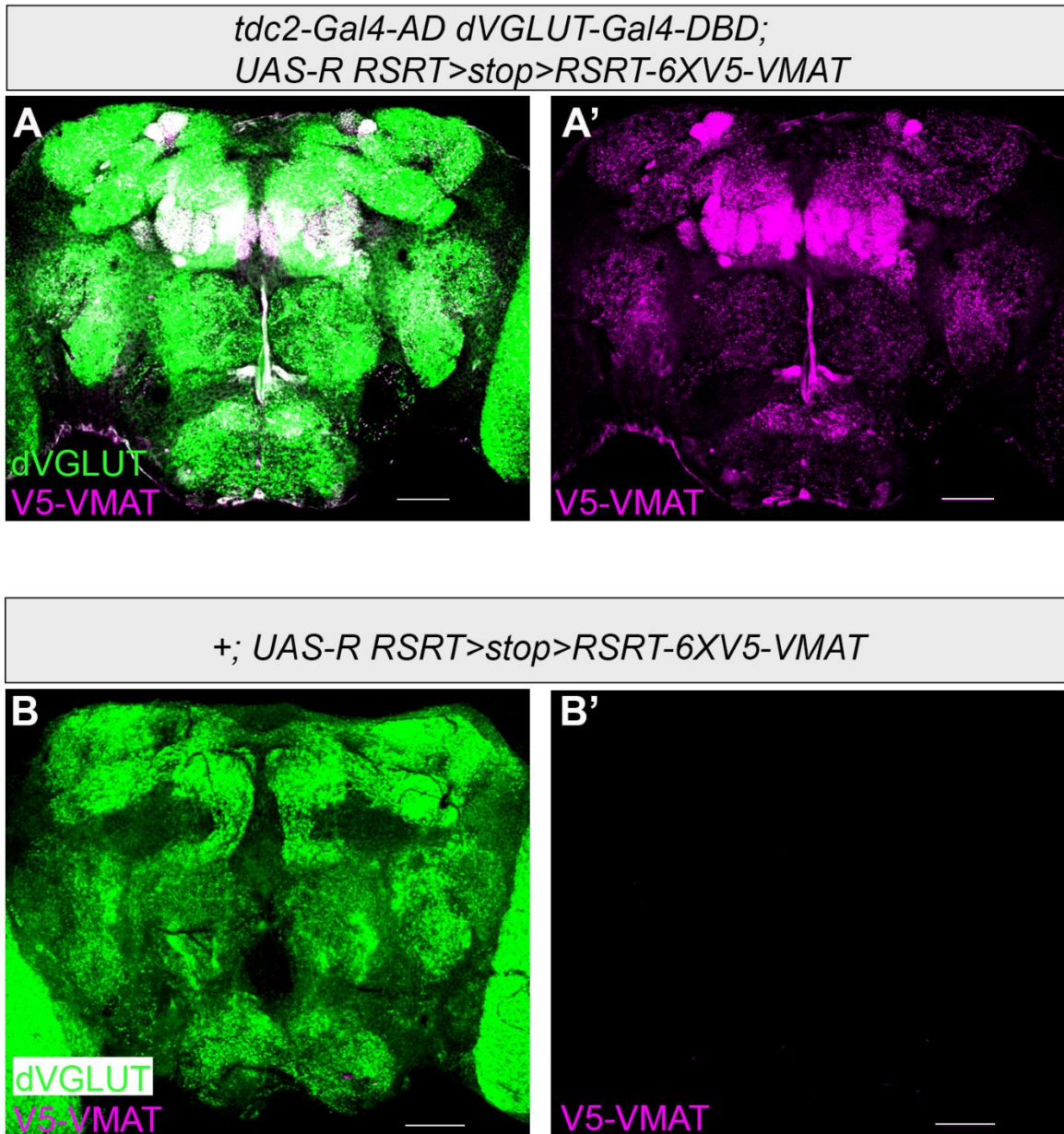
B' V5-VMAT

Supplementary Fig 10.

RSRT>stop>6xV5-VMAT is not expressed without Gal4-mediated excision of the stop cassette.

(A-A') In the presence of a Gal4 driver (*tdc2-Gal4-AD dVGlut-Gal4-DBD*) to drive R recombinase (*UAS-R*) expression, the stop cassette of RSRT>stop>6XV5-VMAT is excised and V5-VMAT (magenta) is expressed and visualized by anti-V5. dVGLUT (green) is visualized by mAb dVGLUT. **(B-B')** Without the presence of a Gal4 driver, dVGLUT expression is apparent while expression from RSRT>stop>6XV5-VMAT is not detected by anti-V5. Scale bar = 30 μm.
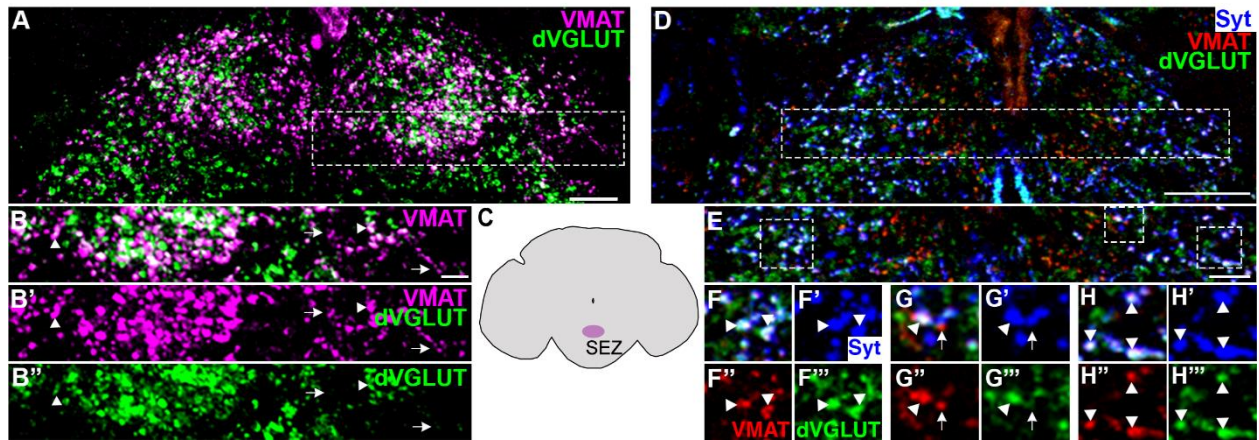
Supplementary Fig 11.

(A) Higher magnification of the SEZ region showing V5-VMAT expression in OGNs after excision by *tdc2-dVGlut-gal4* driven R recombinase. The brain is labeled with anti-V5 (magenta) and mAb dVGLUT (green). Scale bar = 15 μm. **(B-B")** Higher magnification of the SEZ region of the region in the dashed box in panel B. Arrowheads indicate puncta with dVGLUT and V5-VMAT colocalization. Arrows indicate puncta with only V5-VMAT (arrows). **(C)** Schematic indicating the location of the SEZ region. **(D)** SEZ region of a representative brain with a synaptic marker incorporated (*UAS-synaptotagmin;HA, tdc2-dVGlut-gal4/UAS-R RSRT-STOP-RSRT-6XV5-vMAT)*. The brain is labeled with anti-HA (blue), anti-V5 (magenta), and mAb dVGLUT (green). Scale bar = 20 μm. **(E)** Higher magnification of the SEZ region in D. Scale bar = 10 μm. **(F-H)** Regions of interest from E showing puncta with dVGLUT, V5-VMAT and Syt:HA. The stack for panel B contains two optical sections at 0.45 µm. Six optical sections at 0.45 µm were stacked in panels E-H.
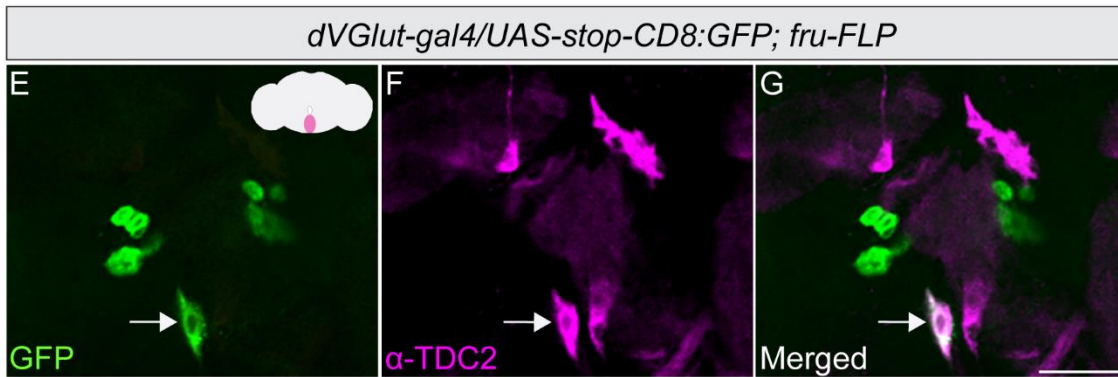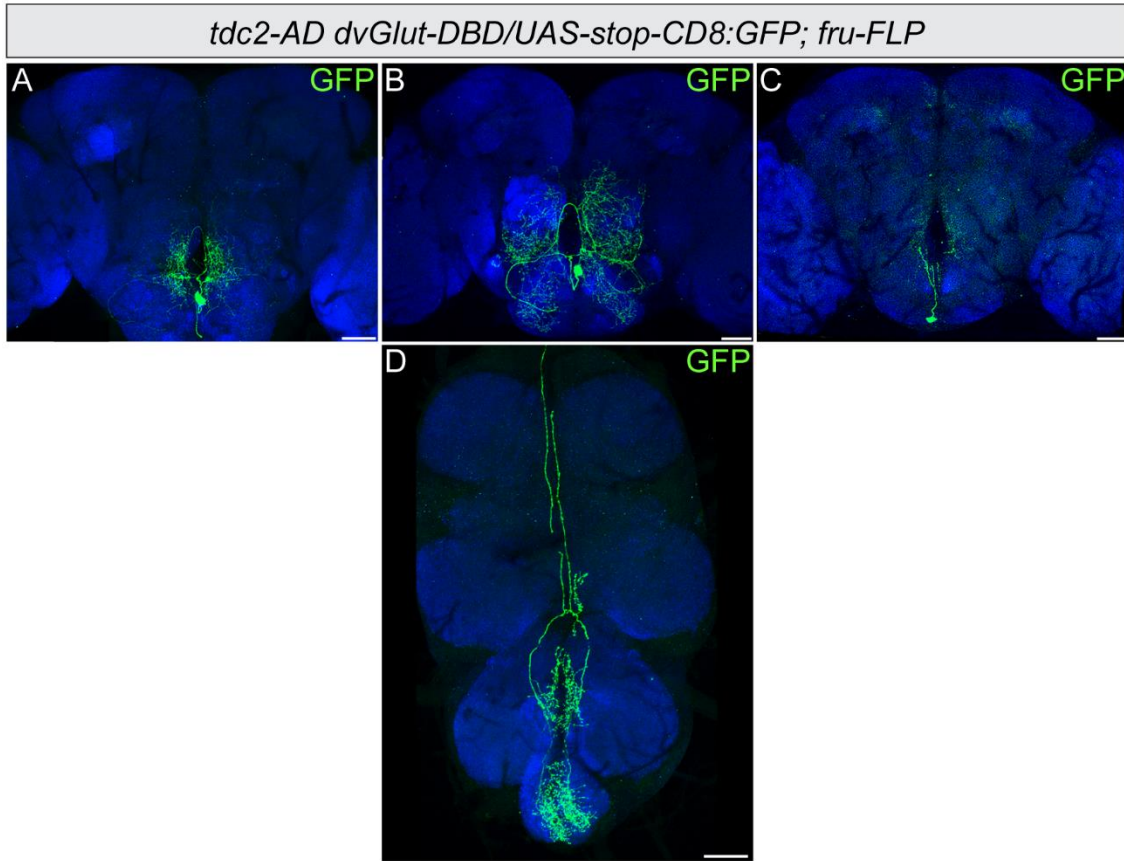
Supplementary Figure 12.

OGNs include the three OA-FruM$^+$ neurons. **(A-C)** Brains from *tdc2-dVGlut-split-gal4/UAS>stop>CD8:GFP;fru-flp* males demonstrate OA-FruM$^+$ neurons are also dVGlut+. **(D)** No OGNs in the VNS are FruM$^+$ although as expected the OGN-FruM$^+$ neurons project into the

VNS. Scale bar = 20 µm. **(E-G)** OGN-FruM+ neurons (arrow) were also identified in *dVGlut-gal4/UAS>stop>CD8:GFP;fru-flp* male brains labeled with anti-Tdc2 (magenta). Scale bar = 20 µm.

Supplementary Table 1. Identified OGNs based on OA neuron nomenclature.

S1 Table. Identified OGNs based on OA neuron nomenclature

Subesophageal Zone (SEZ)	Antennal Lobe (AL)
VM	AL2
VMmd	**Ventrolateral Protocerebrum (VLPR)**
VMmx	VL
VMlb	
VPM1 (fru+)	
VPM4 (fru+)	

Anterior Superior Medial Protocerebrum (ASMPR)
ASM

Supplementary Table 2. Cloning components used for the construction of the 20XUAS-His2A-GFP and 13XLexAop2-His2B-mCherry lines.

Supplementary Table 2

Component Entry Clones for

Expression clone	Gateway MultiSite LR reactions			Destination vector	Landing sites
20XUAS-His2A-GFP	L1-2XUAS-DSCP-L4	R4-His2A-R3	L3-GFP-L2	pDEST10aw	VK5
13XLexAop2-His2B-mCherry-HA	L1-13X-LexAop2-DSCP-L4	R4-His2B-R3	L3-mCherry-HA-L2	pDEST10aw	JK66B
20XUAS-R	L1-20XUAS-DSCP-R5	L5-R-L2			JK22C

Resources Table

REAGENT, RESOURCE, or PRODUCT	SOURCE	IDENTIFIER
Antibodies		
mAb bruchpilot (nc82)	Developmental Studies Hybridoma Bank (DSHB)	Cat# nc82; RRID: AB_2314866
mAb dVGLUT	Brian McCabe	Methods
Rabbit anti-GFP	Thermo Fisher Scientific	Cat# G10362, RRID:AB_2536526
Rat anti-HA	Roche	Cat# 11867423001; RRID:AB_10094468
Rabbit anti-TDC2	Covalab	Cat# pab0822-P
Rat anti-V5	Biorbyt	Cat# orb256445
Anti-Tβh	Vivian Budnik	Koon et al., 2011
Donkey anti-mouse Alexa 647	Thermo Fisher Scientific	Cat# A-31571, RRID:AB_162542
Goat anti-rabbit Alexa 488	Thermo Fisher Scientific	Cat# R37116, RRID:AB_2556544
Goat anti-rat Alexa 594	Thermo Fisher Scientific	Cat# A-11007, RRID:AB_10561522
Goat anti-mouse Alexa 594	Thermo Fisher Scientific	Cat# A-21125, RRID:AB_2535767
Donkey anti-rabbit Alexa 647	Thermo Fisher Scientific	Cat# A-31573, RRID:AB_2536183
Rabbit anti-V5	Novus Biologicals	Cat# NBP2-52653,
***Drosophila* lines**		
EAAT1-Gal4	BDSC	RRID: BDSC_8849
Canton-S	BDSC	RRID: BDSC_64349
UAS-CD8:GFP	BDSC	RRID: BDSC_5130
20xUAS-IVS-mCD8:GFP	BDSC	RRID: BDSC_32194
hs-FLP;;10xUAS(FRT.stop)myr::smGdP-HA 10xUAS(FRT.stop)myr::smGdP-V5	BDSC	RRID: BDSC_64085
UAS-dVGlut RNAi	BDSC	RRID: BDSC_40927
UAS-dVGlut RNAi	BDSC	RRID: BDSC_40845
dVGlut-Gal4	BDSC	RRID: BDSC_60312
UAS-dsRed	BDSC	RRID: BDSC_6282
tdc2-Gal4	Jay Hirsh	RRID: BDSC_9313
tsh-lexA 8xlexAop2-IVS-Gal80	Julie Simpson	
UAS-EAAT1	BDSC	RRID: BDSC_8202
B3RT-vGlut-B3RT	Steve Stowers	see Methods
UAS-B3	Steve Stowers	see Methods
20XUAS-His2A-GFP 13XLexAop2-His2B-mCherry	Steve Stowers	see Methods
tdc2-Gal4	Steve Stowers	RRID: BDSC_52243
dVGlut SS1	Steve Stowers	see Methods
Tβh-Gal4	BDSC	RRID: BDSC_77665
TβhnM18	Maria Monastirioti	Monastirioti et al., 1996
vGlut-Gal4-DBD	Diao et al., 2015	RRID: BDSC_2015
tdc2-Gal4-AD	BDSC	RRID: BDSC_70862

In collaboration with the Stowers lab, we determined that the majority of OA neurons co-express glutamate and that both OA and glutamate release from OGNs is required for aggressive behavior. The dual transmission of OA and glutamate suggests several potential pre- and postsynaptic mechanisms through which responses to transmitter release from OGNs could be controlled. In our continued collaboration, I worked with Dr. Hannah McKinney to characterize the expression pattern of OA and Glu Gal4 lines generated by the Stowers lab, resulting in a publication in the Journal of Comparative Neurology. In this study, we examined the expression of 5 OA receptors and 1 glutamate receptor and determined both that OA receptors are widely expressed within OA neurons and that OA and glutamate receptors can be co-expressed. These results suggest that dual transmitting neurons are able to promote or inhibit transmitter release through autoreceptor activity. They also suggest that downstream synaptic partners can selectively receive signals from dual transmitting neurons via postsynaptic receptor expression.

RESEARCH ARTICLE

JCN RESEARCH IN SYSTEMS NEUROSCIENCE / THE JOURNAL OF COMPARATIVE NEUROLOGY · WILEY

Characterization of Drosophila octopamine receptor neuronal expression using MiMIC-converted Gal4 lines

Hannah M. McKinney[1] ⓘ | Lewis M. Sherer[2] ⓘ | Jessica L. Williams[1,3] |
Sarah J. Certel[2,4] | R. Steven Stowers[1]

[1]Department of Cell Biology and Neuroscience, Montana State University, Bozeman, Montana

[2]Cellular, Molecular and Microbial Biology Graduate Program, The University of Montana, Missoula, Montana

[3]Department of Plant Sciences, Montana State University, Bozeman, Montana

[4]Division of Biological Sciences, Center for Structural and Functional Neuroscience, The University of Montana, Missoula, Montana

Correspondence
R. Steven Stowers, Department of Cell Biology and Neuroscience, Montana State University, Bozeman, MT.
Email: sstowers@montana.edu

Funding information
NIH Center for Scientific Review, Grant/Award Number: R01 GM115510

Peer Review
The peer review history for this article is available at https://publons.com/publon/10.1002/cne.24883.

Abstract

Octopamine, the invertebrate analog of norepinephrine, is known to modulate a large variety of behaviors in Drosophila including feeding initiation, locomotion, aggression, and courtship, among many others. Significantly less is known about the identity of the neurons that receive octopamine input and how they mediate octopamine-regulated behaviors. Here, we characterize adult neuronal expression of MiMIC-converted Trojan-Gal4 lines for each of the five Drosophila octopamine receptors. Broad neuronal expression was observed for all five octopamine receptors, yet distinct differences among them were also apparent. Use of immunostaining for the octopamine neurotransmitter synthesis enzyme Tdc2, along with a novel genome-edited conditional Tdc2-LexA driver, revealed all five octopamine receptors express in Tdc2/octopamine neurons to varying degrees. This suggests autoreception may be an important circuit mechanism by which octopamine modulates behavior.

KEYWORDS
autoreception, Drosophila, octopamine, octopamine receptor, RRID:AB_221568, RRID:AB_2340686, RRID:AB_2340850, RRID:AB_2536611, RRID:AB_2633280, RRID:AB_2814891, RRID:BDSC_27392, RRID:BDSC_42119, RRID:BDSC_43050, RRID:BDSC_57940, RRID:BDSC_59133, RRID:BDSC_60312, RRID:BDSC_60313, RRID:BDSC_67636, RRID:BDSC_68264

1 | INTRODUCTION

The vertebrate adrenergic system is integral to countless behavioral and physiological processes, including stress response (Snyder & Silberman, 2019), metabolic maintenance (Ciccarelli, Sorriento, Coscioni, Iaccarino, & Santulli, 2016), and neuropsychiatric diseases (Langer, 2015; Sallee, Connor, & Newcorn, 2013). Adrenergic signaling occurs via the release of adrenaline (epinephrine) and noradrenaline (norepinephrine). Both adrenaline and noradrenaline exert their various effects by binding to G-protein coupled receptors (GPCRs). These receptors are classified as either α-adrenergic or β-adrenergic and trigger numerous downstream signaling events, including the activation of protein kinases and increased gene transcription, through the second messengers cyclic AMP (cAMP) and calcium (Ca^{2+}) (Ciccarelli et al., 2016; Cole & Sood, 2012; Santulli & Iaccarino, 2013; Vaniotis et al., 2011). In addition to the complexity of downstream signaling, the location of adrenergic receptors is multifaceted with receptors located presynaptically as well as postsynaptically (Langer & Angel, 1991). While many studies in recent decades have examined the role of postsynaptic adrenergic receptors, the impact of presynaptic receptors, or autoreceptors, on circuits that regulate behavior and as targets for drug discovery remains poorly examined.

Drosophila melanogaster offers several advantages to investigating adrenergic receptor localization and function including a sophisticated genetic toolbox, a simpler nervous system, and a reduced number of neurotransmitter receptors as compared to vertebrates. In Drosophila,

octopamine (Oct), the structural analogue of norepinephrine, is synthesized from the amino acid tyrosine via the action of tyrosine decarboxylase (Tdc) and tyramine-ß-hydroxylase (Roeder, 1999). Oct exerts its effects by binding to Oct receptors (OctRs), including five adrenergic-like receptors in *Drosophila*: two α-adrenergic-like GPCRs (OAMB and Octα2R) and three β-adrenergic-like GPCRs (Octβ1R, Octβ2R, and Octβ3R) (Balfanz, Strunker, Frings, & Baumann, 2005; El-Kholy et al., 2015; Evans & Maqueira, 2005; Han, Millar, & Davis, 1998; Maqueira, Chatwin, & Evans, 2005; Qi et al., 2017).

Presynaptic autoreceptors provide a retrograde transfer of information mediated by the released transmitter of the presynaptic neuron and can perform autoregulatory functions in neurotransmission. For example, at the *Drosophila* neuromuscular junction (NMJ), activation of Octβ2R autoreceptors is required for the growth of Oct arbors during development and in response to starvation, while the inhibition of this synaptic growth depends on the autoreceptor function of Octβ1R (Koon et al., 2011; Koon & Budnik, 2012). Autoreception may also provide a critical component in regulating the activity of neurons that release more than one neurotransmitter, neuropeptide or neuromodulator, such as neurons expressing dopamine and the vesicular glutamate transporter (Aguilar et al., 2017). Most recently, it has been shown that the majority of octopaminergic neurons also express glutamate (Sherer et al., in press). As dual neurotransmitter usage is now recognized to occur throughout the nervous system of invertebrates and vertebrates (Hoopfer, 2016; Nassel, 2018; Seal & Edwards, 2006; Vaaga, Borisovska, & Westbrook, 2014), elucidating the role of the corresponding neurotransmitter receptors, including as autoreceptors, is important for understanding of the functionality of dual transmitter neurons.

As a precursor to addressing the functional impact of OctR presynaptic and postsynaptic signaling on Oct transmission, we first sought to determine the neuronal expression patterns of Drosophila OctRs. Our approach was to generate Trojan-Gal4 lines for *OAMB*, *Octβ1R*, *Octβ2R*, and *Octβ3R* through MiMIC conversion (Diao et al., 2015). MiMIC converted Gal4 drivers faithfully recapitulate the cellular expression of their corresponding genes (Diao et al., 2015) as they are located at the endogenous chromosomal locus of their respective genes and thus the complete regulatory region of each gene directs their expression. Here, we characterized the adult central nervous system expression patterns of each new *OctR-Gal4* line along with the *Octα2R* Trojan-Gal4 from the Gene Disruption Project (Li-Kroeger et al., 2018), and examined *OctR* autoreception expression in Tdc2 neurons. To further refine our autoreceptor analysis, we generated new intersectional genetic tools for *Tdc2* and the *Drosophila* non-NMDA ionotropic glutamate receptor *DmGluR1A* (Ultsch et al., 1992) to provide a genetic means of identifying co-expression with OctRs. Each OctR exhibited unique autoreceptor expression patterns using both antibody staining and genetic approaches. We also identified a number of neurons co-expressing *OctRs* and *GluRIA*, thus indicating the potential convergence of dual Oct-glutamate signals to the same downstream target neurons. Our new tools provide novel intersectional methods to use in further identifying and understanding the complexities of adrenergic receptor signaling and localization.

2 | MATERIALS AND METHODS

Plasmid construction

The *pCFD4-Tdc2* and *pCFD4-GluRIA* double guide RNA plasmids were generated as previously described (Port, Chen, Lee, & Bullock, 2014). Targeting sequences included in *pCFD4-Tdc2* guide RNAs are CATAATAAAGCTCACCGT and AAATCTTTTATAGGACGA. Targeting sequences included in *pCFD4-GluRIA* guide RNAs are GGCGAGCC CAGGCGAATT and GCCATGGCTCGTTGGGGA. Donor plasmids were constructed with NEBuilder HiFi (New England Biolabs) in the vector *pHSG298* (Takara Biosciences). The complete sequences of all donor plasmids are shown in Supplemental Information.

The *20XUAS-DSCP-KD*, *20XUAS-B3*, *10XQUAS-DSCP-His2B-mCherry*, and *10XQUAS-DSCP-His2A-GFP* expression clones were assembled using Gateway MultiSite cloning as previously described (Petersen & Stowers, 2011). The *L1-10XQUAS-DSCP-L5* entry clone was generated using the *L1-10XQUAS-L4* entry clone (Petersen & Stowers, 2011) as template such that the *hsp70* minimal promoter was replaced with the Drosophila synthetic core promoter (DSCP) (Pfeiffer et al., 2008). The table below includes fly lines created for publication in this article.

Genome-edited Fly Strains	
B3RT-Tdc2-LexA	
KDRT-GluRIA-QF2	
Transgenic Fly Strains	**Landing Site**
LexAop2-6XmCherry	JMK66B
UAS-His2A-GFP	VK18 (53B), VK5 (75A)
LexAop2-His2B-mCherry	JMK66B
UAS-KD	VK18 (53B)
UAS-B3	VK31 (62E)
QUAS-His2B-mCherry	VK2 (28E)

Genome editing

The *pCFD4-Tdc2* guide RNA plasmid was co-injected with the *B3RT-TDC2-LexA* donor plasmid into embryos of strain *nos-Cas9 TH_attP2* (Ren et al., 2013) by Bestgene, Inc. The surviving adults that were injected as embryos were crossed to *yw; UAS-B3; n-syb-GAL4, LexAop2-6XmCherry* and genome-edited *B3RT-TDC2-LexA* chromosomes were identified by fluorescence. The observation that the *B3RT-Tdc2* female is homozygous sterile suggests the function of the *Tdc2* gene is likely disrupted prior to excision as this is the phenotype of the octopamine null mutant (Monastirioti, 2003). Nevertheless, *B3RT-Tdc2* remains a reliable and valid tool for identifying Tdc2 neurons. The *pCFD4-GluRIA* guide RNA plasmid was co-injected with the *KDRT-GluRIA-QF2* donor plasmid into embryos of strain *nos-Cas9 TH_attP40* (Ren et al., 2013) by Bestgene, Inc. The surviving adults that were injected as embryos were crossed to *yw; N-syb-GAL4;*
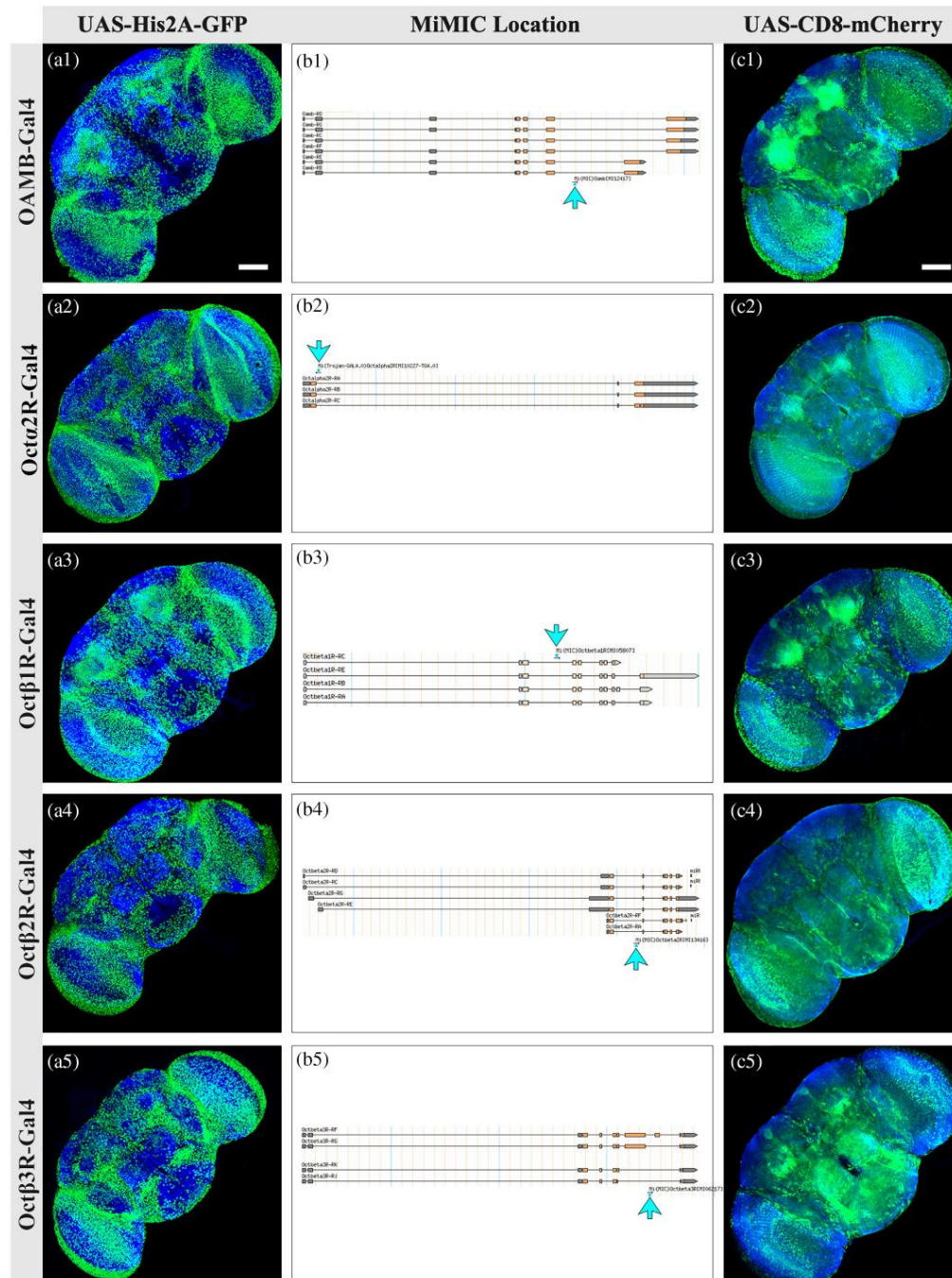
FIGURE 1 Legend on next page.

UAS-B3, LexAop2-6XmCherry and genome-edited KDRT-GluRIA-QF2 chromosomes were identified by fluorescence.

Germline excisions and inversions

Germline excisions were generated by crossing B3RT-Tdc2-LexA to yw; nos-GAL4; UAS-DSCP-B3 and KDRT-GluRIA-QF2 to yw; nos-GAL4; 20XUAS-DSCP-KD. Progeny males of the appropriate genotype were crossed to a second chromosome balancer stock to generate individual flies with potential germline excisions. Germline excisions were identified by taking individual males from the first balancer cross and crossing them to a 13XLexAop2-6XmCherry-HA or 10XQUAS-6XmCherry-HA fluorescent reporter and screening directly for fluorescence. Balanced fly stocks containing the desired germline excised or inverted chromosomes were established from progeny of positive single male crosses.

Fly strains/MiMIC lines

A table of original fly lines used in this paper can be found in the Supplemental Information. Flies were raised on standard cornmeal, yeast and agar food at 25°C and occasionally kept at 18°C after sorting and prior to dissection. MiMIC lines OAMB (BDSC #57940); Octβ1R (BDSC #42119); Octβ2R (BDSC #59133); Octβ3R BDSC #43050) were converted to Trojan-Gal4 lines following recombinase-mediated cassette exchange as described in Diao et al. (2015). Octα2R-Gal4 (BDSC #67636), vGlut-Gal4 (BDSC #60312) Tdc2-Gal4-AD (BDSC #68264) and vGlut-Gal4-DBD (BDSC # 60313), and UAS-CD8-mCherry (F. Schnorrer, BDSC# 27392) were obtained from the Bloomington Drosophila Stock Center.

2.1 | Immunostaining

Immunostaining was performed as previously described (Certel & Thor, 2004). Primary antibodies and dilution factors: The SYN (3C11) mAb 1:50 developed by Buchner (Klagges et al., 1996), anti-bruchpilot (nc82) mAb 1:30 developed by Buchner were obtained from the Developmental Studies Hybridoma Bank, created by the NICHD of the NIH and maintained at The University of Iowa, Department of Biology, Iowa City, IA 52242; rabbit Abfinity anti-GFP (Thermo-Fisher) 1:400, mouse anti-GFP 3E6 (Thermo-Fisher) 1:200, rat anti-mCherry 16D7 (Thermo-Fisher) 1:400, rabbit anti-mCherry (Abcam ab213511) 1:500, mouse anti-mCherry 1:400 (Biorbyt orb256058); rat anti-GFP 8H12 (Kerafast)

1:200; rabbit anti-Tdc2 (pab0822-P, Covalab) 1:400 and 1:200). Secondary antibodies and dilution factors: donkey anti-mouse Alexa 488 (Jackson Immunoresearch 715-546-151) 1:400; goat anti-rabbit Alexa 488 (Thermo-Fisher A32731) 1:400; donkey anti-rat Alexa 488 (Jackson 712-546-153) 1:400; goat anti-rabbit JF549 (Novus NBP1-72732JF549) 1:200; donkey anti-mouse JF549 (Novus NBP1-75119JF549) 1:200; goat anti-rat JF549 (Novus NBP1-75398JF549) 1:200; goat anti-rabbit JF646 (NBP1-72732JF646) 1:200; donkey anti-mouse JF646 (Novus NBP1-75119JF646) 1:200, and goat anti-rat JF646 (Novus NBP1-75398JF646) 1:200.

3 | RESULTS

Earlier generation OctR-Gal4 drivers utilized only one to three kilobases of OctR promoter regions (El-Kholy et al., 2015), even though each of the OctR genes span tens of kilobases in the Drosophila genome. As such, the respective regulatory regions are likely more extensive, making it probable that existing OctR-Gal4 lines provide incomplete OctR expression patterns. Additionally, as with all transgenes, the existing OctR-Gal4 lines are potentially subject to position effects associated with transgenic insertion sites. To more accurately recapitulate the complete neuronal expression pattern of Drosophila OctRs as a precursor to functional studies, we generated Trojan-Gal4 lines for OAMB, Octβ1R, Octβ2R, and Octβ3R using the previously described cross scheme (Diao et al., 2015) and examined their expression patterns using both nuclear (UAS-His2A-GFP; Figure 1a1–a5) and plasma membrane (UAS-CD-mCherry; Figure 1c1–c5) markers. These drivers likely are complete and accurate reporters of the transcriptional expression of their respective OctR genes since the Trojan-GAL4 lines are located at the endogenous genomic location of each OctR gene within coding introns common to all isoforms (Figure 1b1–b5). As such, they represent the "gold standard" for reporting on the complete expression pattern of a gene (Diao et al., 2015). It is worth noting, however, that translational regulation of OctR protein expression cannot be ruled out and thus could differ from the patterns reported here using fluorescent reporters. Additional advantages of these lines include the absence of position effects and the detection of OctR gene expression with higher sensitivity and higher fidelity.

3.1 | Tdc2 and OctR co-expression

To assess the possibility of OctR autoreception in the central brain, we mapped OctR expression in octopaminergic neurons using two

FIGURE 1 Expression patterns of MiMIC OctR-Gal4 lines. Nuclear expression patterns in male adult brains for (a1) OAMB > His2A-GFP, (a2) Octα2R > His2A-GFP, (a3) Octβ1R > His2A-GFP, (a4) Octβ2R > His2A-GFP, (a5) Octβ3R > His2A-GFP; genomic locations of MiMIC insertions retrieved from flybase.org for (b1) OAMB-Gal4, (b2) Octα2R, (b3) Octβ1R, (b4) Octβ2R, (b5) Octβ3R; expression patterns using a plasma membrane reporter (c1) OAMB > CD8-mCherry, (c2) Octα2R > CD8-mCherry, (c3) Octβ1R > CD8-mCherry, (c4) Octβ2R > CD8-mCherry, (c5) Octβ3R > CD8-mCherry. Scale bar = 75 μm. Antibodies used: anti-mCherry (green) and anti-SYN (blue)

approaches. First, we expressed a UAS-driven nuclear GFP reporter via the individual *OctR-Gal4* lines and analyzed Oct/tyramine co-expression with an antibody against Tdc2. As Oct is synthesized from

the amino acid tyrosine via the action of Tdc2 and Tβh in inverte-brates (Cole et al., 2005), the Tdc2 antibody (Meiselman, Kingan, & Adams, 2018; Pauls, Blechschmidt, Frantzmann, El Jundi, & Selcho,
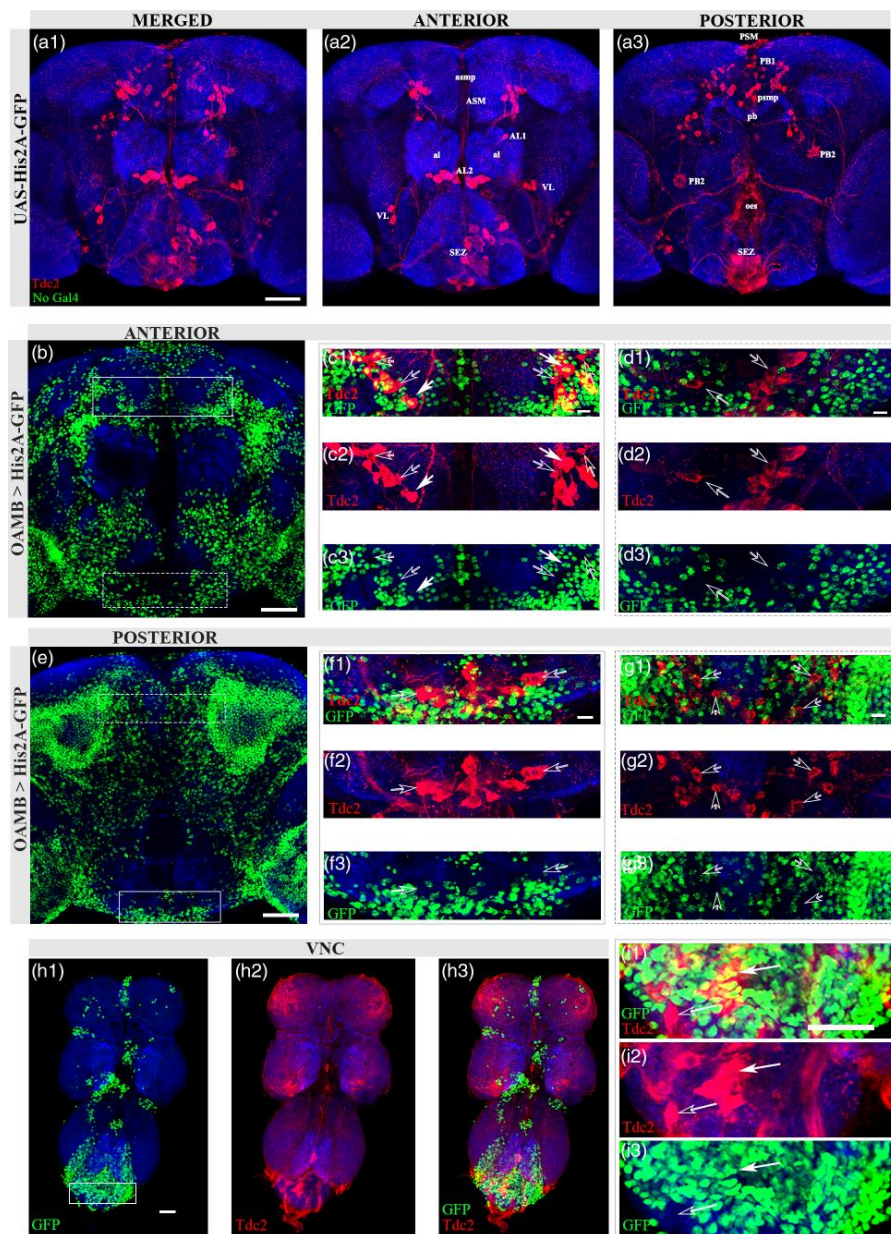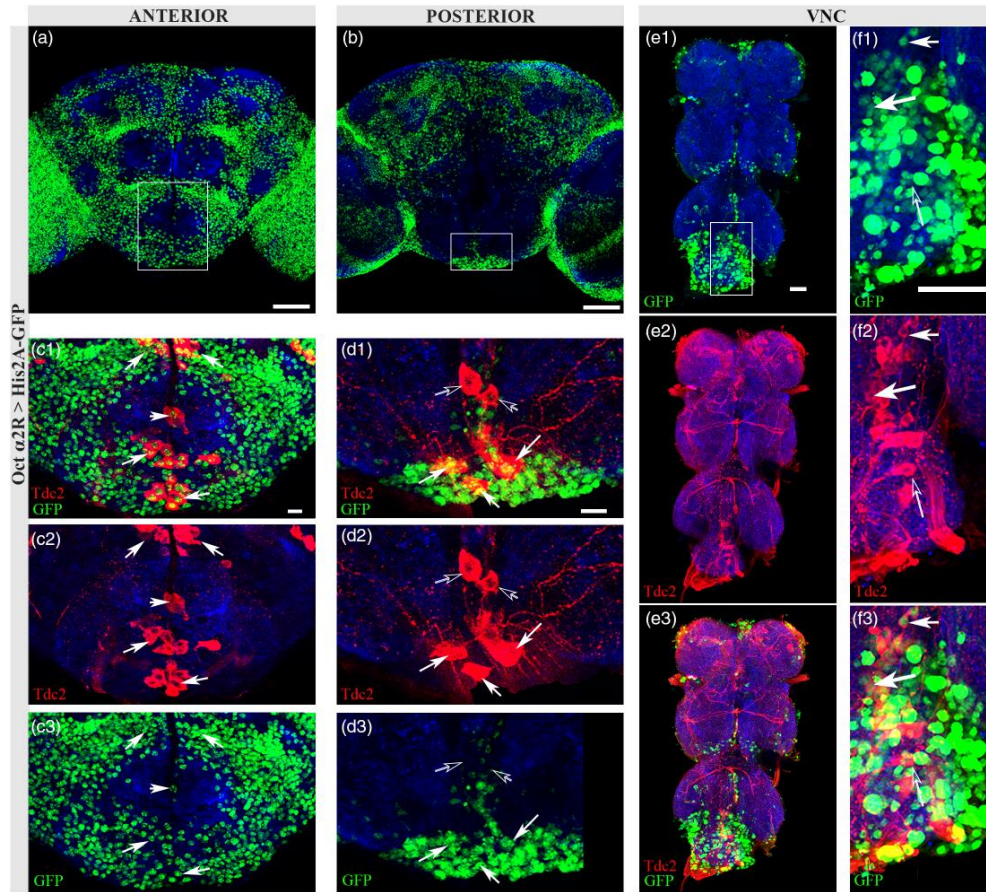

FIGURE 2 Legend on next page.

FIGURE 3 *Octα2R* is expressed in a subset of Oct neurons. (a) Anterior optical sections (58–79) of *Octα2R > His2A-GFP*. Scale bar = 50 μm. (b) Posterior sections (3–37) of *Octα2R > His2A-GFP*. Scale bar = 50 μm. (c1–c3) Solid white rectangle from (a) showing co-expression of nuclear GFP (green) in Tdc2-stained somata (red) of the SEZ (closed arrows). Scale bar = 10 μm. (d1–d3) Solid white rectangle from (b) showing co-expression (closed arrows) of Tdc2 and nuclear GFP in posterior SEZ neurons. Open arrows indicate a single pair of SEZ neurons with no co-expression. Scale bar = 10 μm. Antibodies used: anti-GFP (green), anti-SYN (blue), anti-Tdc2 (red). (e1–e3) Nuclear GFP (e1, green) expression pattern in adult VNC with Tdc2 (e2, red) co-expression (e3, closed white arrows). Scale bar = 30 μm. (f1–f3) Solid rectangle from (e1) showing co-expression (closed white arrows) and at least one neuron with no co-expression (open arrow) in the VNC. Scale bar = 30 μm. Antibodies used (e1–f3): anti-brp (blue), anti-GFP (green), and anti-Tdc2 (red)

FIGURE 2 *OAMB* is expressed in a subset of Oct neurons. (a1) Tdc2 expression (red) in a control *UAS-His2A-GFP/+* brain. Scale bar = 50 μm (a2) Anterior optical sections of (a1) outlining Tdc2+ neuronal clusters (uppercase): ASM cluster in the ASMP (anterior superior medial protocerebrum), AL (antennal lobe) clusters AL1 and AL2, VL (ventrolateral), SEZ (subesophageal ganglion) (a3) Posterior sections of (a1): PSM and PB1 clusters in posterior superior medial protocerebrum (PSMP), PB2 cluster in pb (protocerebral bridge), oes (esophagus), SEZ (b) Anterior sections (46–76) of *OAMB > His2A-GFP*. Scale bar = 50 μm. (c1–c3) Solid white rectangle from b showing co-expression of Tdc2 (red) and *OAMB* (green) in the ASM cluster of Tdc2 neurons (closed arrows) and neurons with no co-expression (open arrows). Scale bar = 10 μm. (d1–d3) Dashed rectangle from (b) showing no co-expressing neurons in the SEZ (open arrows) Scale bar = 10 μm. (e) Posterior sections (1–37) of *OAMB > His2A-GFP*. Scale bar = 50 μm. (f1–f3) Solid white rectangle from (e) showing no discernible co-expression in the SEZ (open arrows). (g) Dashed rectangle from (e) showing no co-expression seen in the PSMP region of the brain (open arrows). Scale bar = 10 μm. Antibodies used: anti-Tdc2 (red), anti-GFP (green), and anti-SYN (blue). (h1–h3) Nuclear GFP (h1, green) expression pattern in adult VNC with Tdc2 (h2, red) co-expression (h3, closed white arrow). Scale bar =30 μm. (i1–i3) Solid rectangle from (h1) showing neurons co-expressing with Tdc2 (closed white arrow) and neurons without Tdc2 co-expression (open white arrow) in the VNC. Scale bar = 30 μm. Antibodies used (i1–i3): anti-brp (blue), anti-GFP (green), anti-Tdc2 (red)

2018; Pech, Pooryasin, Birman, & Fiala, 2013) recognizes neurons that express Oct and/or tyramine (hereafter "Tdc2+ neurons" for simplicity).

Second, we utilized a novel intersectional genetic method to label Tdc2-expressing neurons and determine co-expression with each *OctR-Gal4* driven reporter. For each *OctR-Gal4*, at least
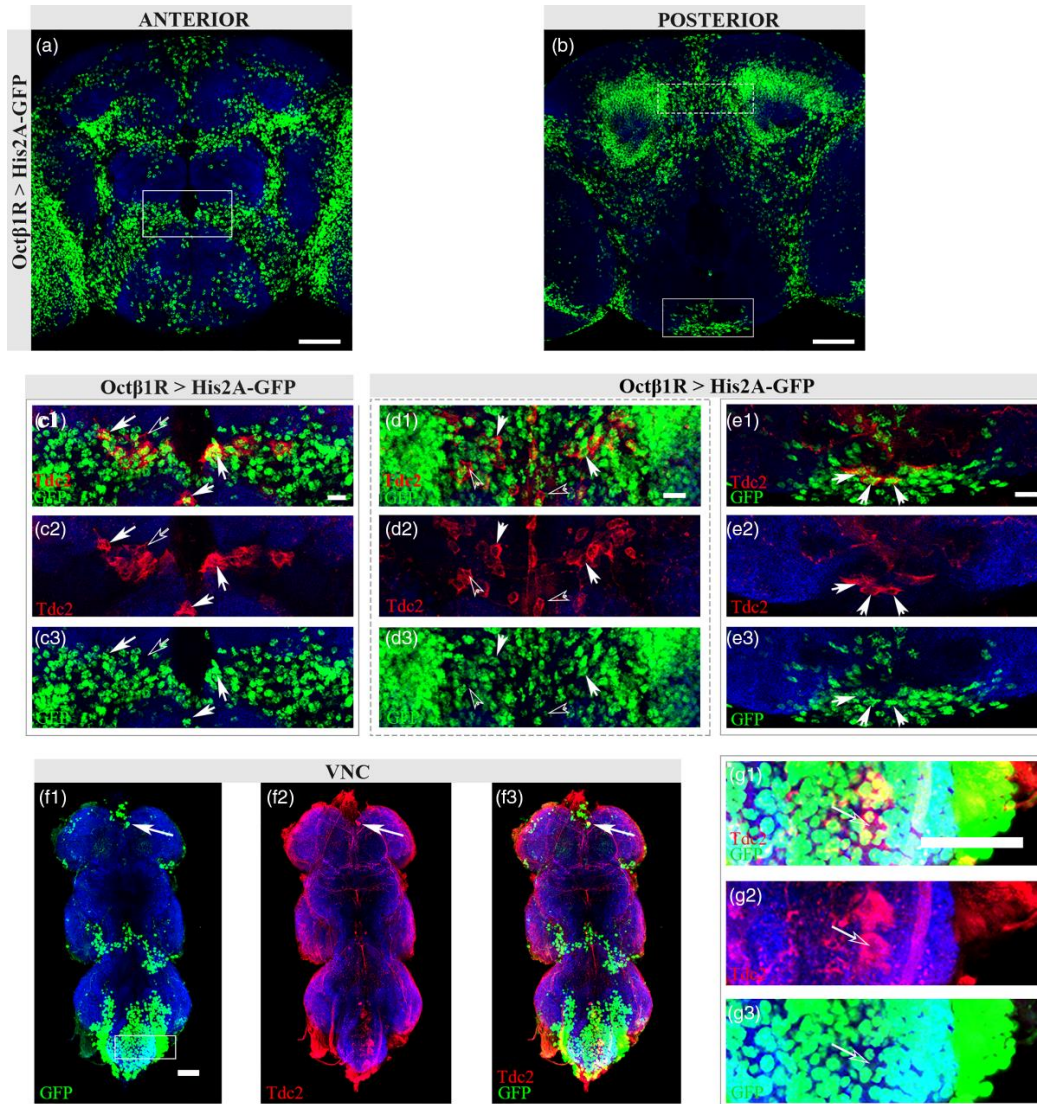
FIGURE 4 Octβ1R is expressed in a subset of Oct neurons. (a) Anterior sections (26–33) of *Octβ1R > His2A-GFP* showing broad GFP expression. Scale bar = 50 μm. (b) Posterior sections (6–14) of *Octβ1R > His2A-GFP*. Scale bar = 50 μm. (c–c2) Solid white rectangle from (a) showing co-expression of *Octβ1R > His2A-GFP* (green) in the AL2 cluster Tdc2+ neurons (red). Scale bar = 10 μm. (d–d2) Dashed rectangle from (b) showing *Octβ1R* co-expression in the Tdc2+ (red) PB1 cluster (closed arrows). Neurons negative for co-expression are illustrated with open arrows. Scale bar = 10 μm. (e1–e3) Solid white rectangle from (b) showing co-expression of *Octβ1R > His2A-GFP* (green) in Tdc2+ neurons (red) in posterior SEZ (closed arrows). Scale bar = 10 μm. Antibodies used: anti-GFP (green), anti-Tdc2 (red), anti-SYN (blue). (f1–f3) Nuclear GFP (f1, green) expression pattern in adult VNC with Tdc2 (f2, red) co-expression (f3, closed white arrow). Scale bar = 30 μm. (g1–g3) Solid rectangle from (f1) showing a neuron without co-expression with Tdc2 (open arrow). Scale bar =30 μm. Antibodies used (f1–g3): anti-brp (blue), anti-GFP (green), anti-Tdc2 (red)
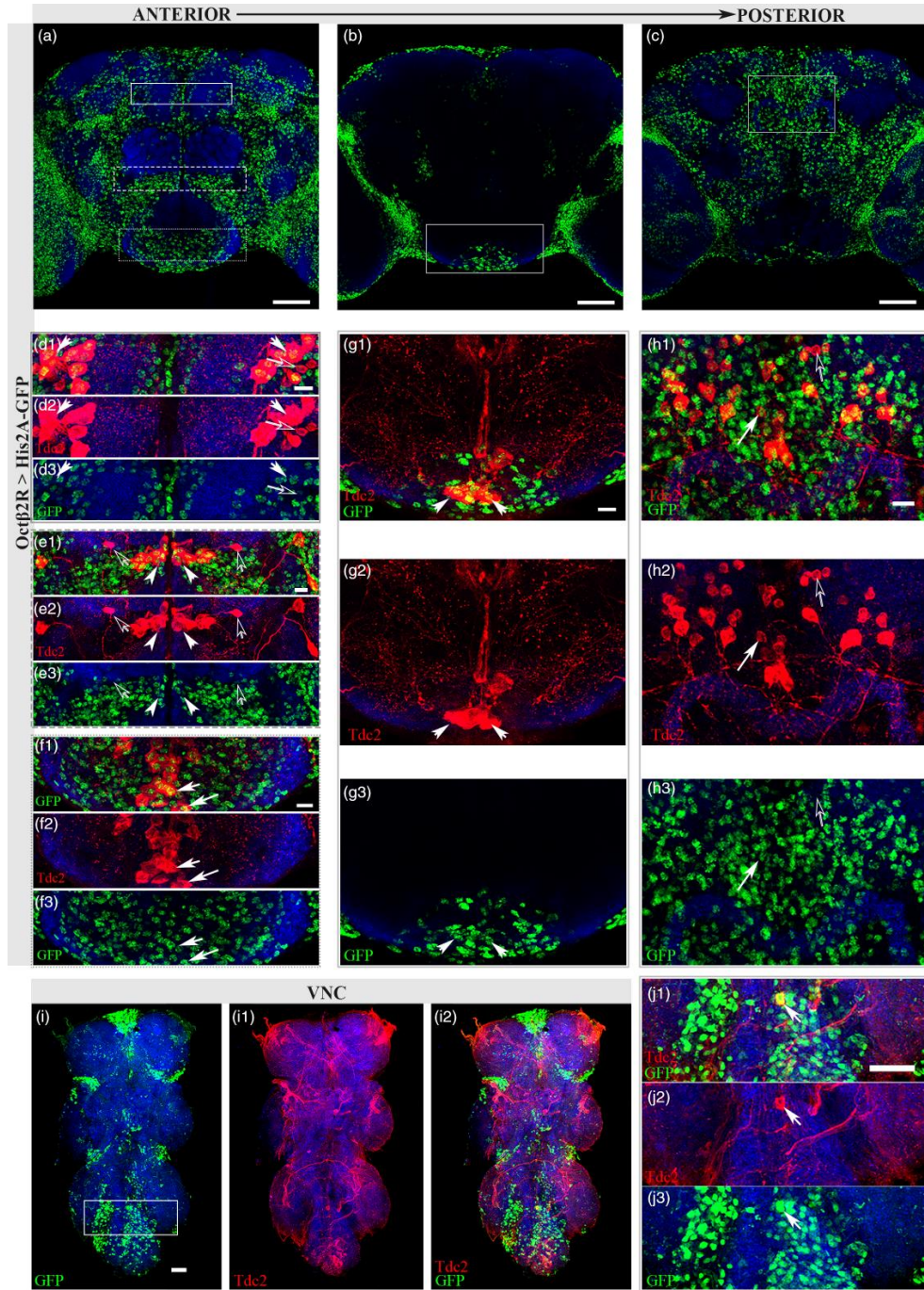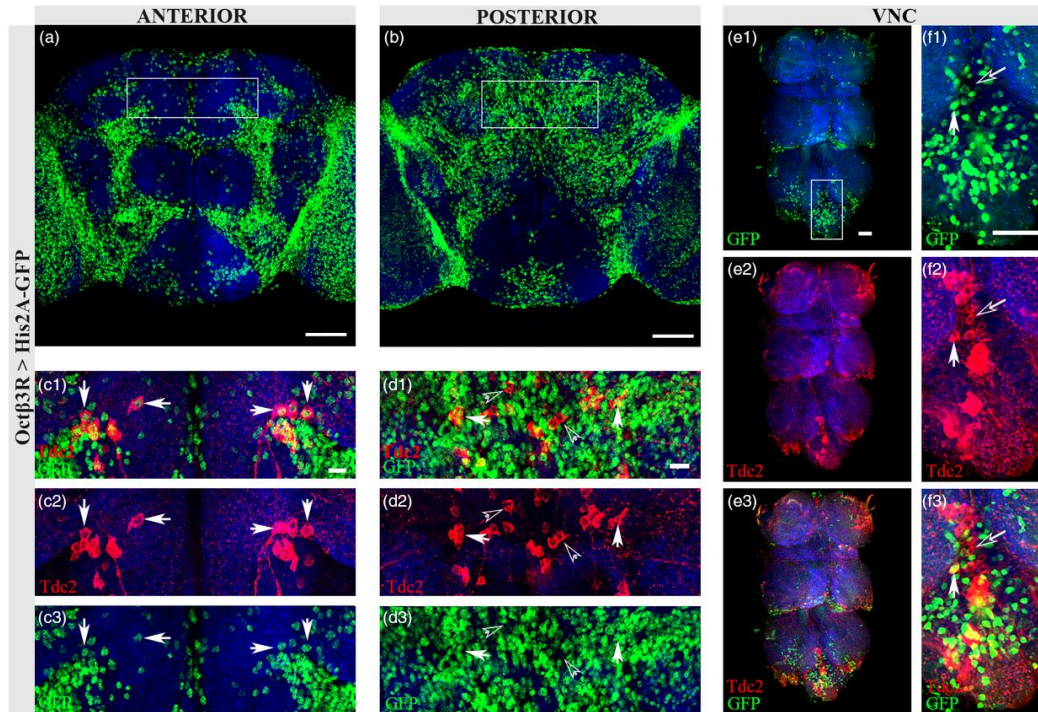
FIGURE 5 Legend on next page.

FIGURE 6 *Octβ3R* is expressed in a subset of Oct neurons. (a) Anterior sections (32–42) of *Octβ3R > His2A-GFP*. Scale bar = 50 μm. (b) Posterior sections (0–26) of *Octβ3R > His2A-GFP*. Scale bar = 50 μm. (c1-c3) White rectangle from (a) showing co-expression in the ASM cluster of Tdc2 neurons (closed arrows). Scale bar = 10 μm. (d1–d3) White rectangle from (b) showing some co-expression in PSMP cluster of Tdc2 neurons (closed arrows) and some neurons negative for co-expression (open arrows). Scale bar 10 μm. Antibodies used: anti-Tdc2 (red), anti-GFP (green) and anti-SYN (blue). (e1–e3) Nuclear GFP (e1, green) expression pattern in adult VNC with Tdc2 (e2, red) co-expression (e3). Scale bar = 30 μm. (f1–f3) Solid rectangle from (e1) showing co-expression with Tdc2 (closed white arrow) and neurons showing no co-expression (open arrow). Scale bar = 30 μm. Antibodies used: anti-brp (blue), anti-GFP (green), anti-Tdc2 (red)

25 adult brains were examined per genotype and the representative nuclear expression pattern in anterior and posterior sections is shown. Results from both methods revealed significant co-expression of Tdc2 and *OctR*'s, suggesting putative locations for autoreception.

3.2 | Oct α-adrenergic receptors: OAMB and Octα2R

Oct neurons in the adult *Drosophila* brain are located in discernible clusters (Busch et al., 2009) throughout anterior and posterior sections

FIGURE 5 *Octβ2R* expresses in a subset of Oct neurons. (a) Anterior sections (70–93) of *Octβ2R > His2A-GFP*. Scale bar = 50 μm. (b) Middle sections (36–65) of *Octβ2R > His2A-GFP*. Scale bar = 50 μm. (c) Posterior sections (15–31) of *Octβ2R > His2A-GFP*. Scale bar 50 μm. (d1–d3) Solid white rectangle from (a) showing co-expression of Tdc2 (red) and *Octβ2R > His2A-GFP*(green) in the ASM cluster (closed arrows) with at least one pair of Tdc2 neurons showing no co-expression (open arrows). Scale bar = 10 μm (e1–e3) Dashed rectangle from (a) indicating co-expression of Tdc2 (red) and *Octβ2R > His2A-GFP* (green) in AL2 cluster (closed white arrows). A pair of AL1 neurons (open white arrows) did not exhibit co-expression. Scale bar = 10 μm. (f1–f3) Dotted rectangle from (a) showing co-expression in the anterior section of the SEZ (closed arrows). Scale bar = 10 μm (g1–g3) Solid white rectangle from (b) showing co-expression in the SEZ. Scale bar = 10 μm. (h1–h3) Some co-expression of Tdc2 and *Octβ2R > His2A-GFP* (closed arrows) and neurons not showing co-expression (open arrows) in the PB1 cluster of the PSMP region. Scale bar = 10 μm. Antibodies used: anti-Tdc2 (red), anti-GFP (green) and anti-SYN (blue). (i1–i3) Nuclear GFP (i1, green) expression pattern in adult VNC with Tdc2 (i2, red) co-expression in one neuron (i3). Scale bar = 30 μm. (j1–j3) Solid rectangle from (i1) with only one neuron showing co-expression with Tdc2 (closed white arrow). Scale bar = 30 μm. Antibodies used (f1–g3): anti-brp (blue), anti-GFP (green), anti-Tdc2 (red)
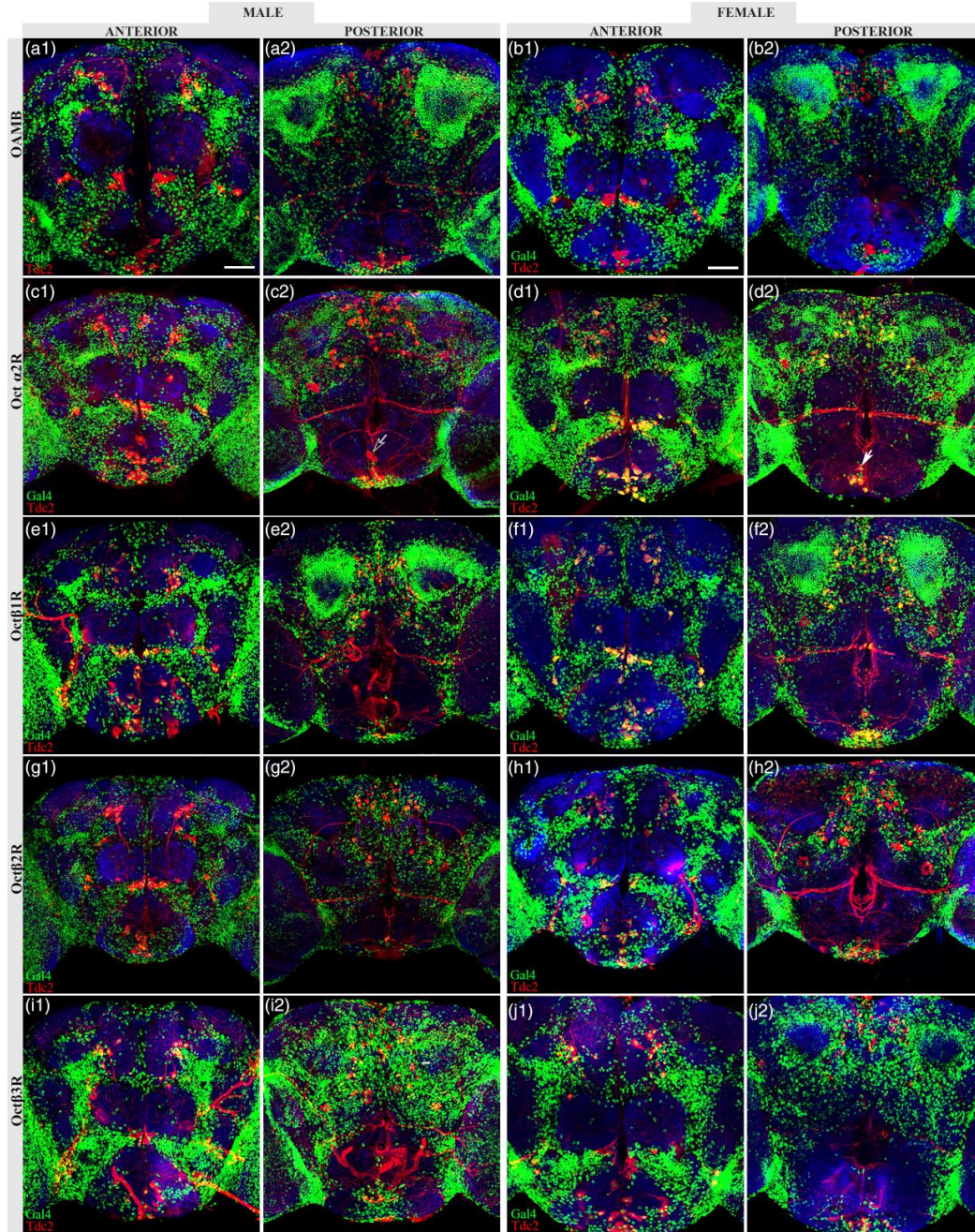
FIGURE 7 Examination of sex differences among *OctR-Gal4* lines. Full z-stacks of anterior and posterior sections of male and female brains with overlapping Tdc2 stain. (a1–b2) *OAMB-Gal4 > His2A-GFP*, (c1–d2) *Octα2R-Gal4 > His2A-GFP*, (e1–f2) *Octβ1R-Gal4 > His2A-GFP*, (g1–h2) *Octβ2R-Gal4 > His2A-GFP*, and (i1–j2) *Octβ3R-Gal4 > His2A-GFP*. Scale bars = 50 μm. Antibodies used: anti-SYN (blue), anti-GFP (green), anti-Tdc2 (red)

FIGURE 8 Legend on next page.

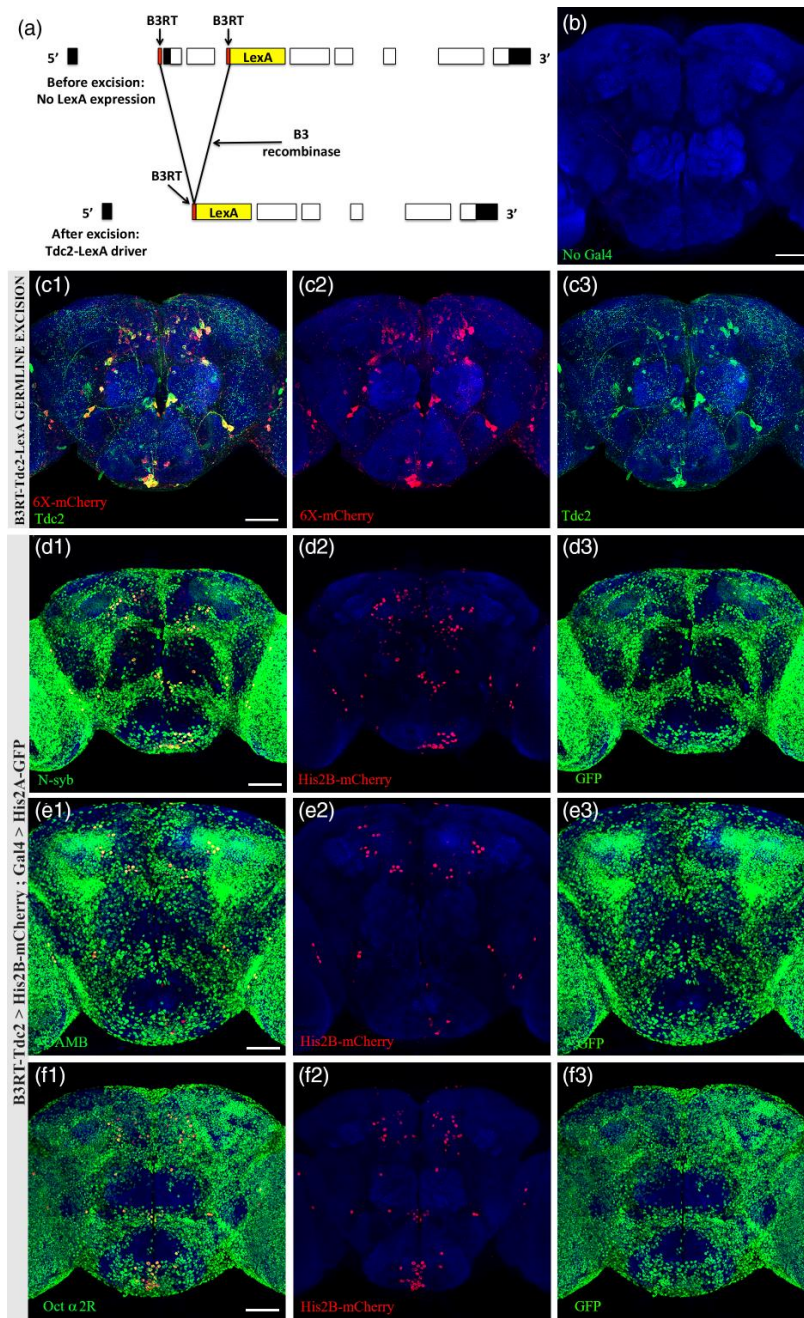(Figure 2a1–a3). Our newly generated *OAMB-Gal4* line drives nuclear GFP expression as expected in the mushroom body Kenyon cells (El-Kholy et al., 2015; Han et al., 1998) as well as broadly throughout the rest of the brain (see Figure 2b–g3) and VNC (Figure 2h1–i3). In anterior sections of the brain, Tdc2 and His2A-GFP nuclear expression driven by *OAMB-Gal4* (henceforth *OAMB > His2A-GFP*) are co-expressed within the ASM cluster of Tdc2+ neurons (Figure 2c1–c3, closed arrows), which is located superior to the antennal lobes (AL) (Figure 2a2). Within this cluster, *OAMB > His2A-GFP* was not found in two pairs of Tdc2+ neurons (Figure 2c1–c3, open arrows). Tdc2 and *OAMB > His2A-GFP* were co-expressed in the VL neurons, located between the AL and the ventrolateral protocerebrum (Figure 2a2, see Figure 7). Co-expression was not detected in the anterior or posterior subesophageal ganglion (SEZ; Figure 2d1–d3, f1–f3, open arrows) or in the PB1 cluster of Tdc2+ neurons in the posterior superior medial protocerebrum (PSMP; Figure 2g1–g3, open arrows).

Similar to *OAMB*, we found *Octα2R-Gal4* driven His2A-GFP (*Octα2R > His2A-GFP*) expression widespread throughout the brain (Figure 3a,b) and VNC (Figure 3e1–f3). *Octα2R > His2A-GFP*/Tdc2 co-expression was seen within the majority of ASM Tdc2+ neurons, and in the SEZ and AL2 neurons (Figure 3c1–c3, closed white arrows). Examination of single confocal sections of the VNC revealed a number of neurons showing co-expression with Tdc2 (Figure 3f1–f3, closed white arrows) and a number of Tdc2+ neurons lacking His2A-GFP expression (Figure 3f1–f3, closed white arrow). In contrast to the absence of *OAMB*/Tdc2 co-expression in the SEZ, *Octα2R > His2A-GFP* is co-expressed in the majority of Tdc2+ neurons in the SEZ (Figure 3c1–d3, closed arrows) with the exception of one pair in the posterior SEZ (Figure 3d1–d3, open arrows). Co-expression was also detected in the PSM and VL clusters (see Figure 7). The identification of distinct clusters of alpha-adrenergic autoreceptor expression indicates potential key areas of functional differences.

3.3 | Oct β-adrenergic receptors: Octβ1R, Octβ2R, and Octβ3R

His2A-GFP expression driven by *Octβ1R-Gal4* (*Octβ1R > His2A-GFP*) was widespread throughout the central brain, including the Kenyon cells (Figure 4a,b), and the VNC (Figure 4f1–g3). In contrast to *OAMB*, Tdc2 and *Octβ1R > His2A-GFP* were co-expressed in the AL1, PB1 and VM clusters of Tdc2+ neurons (Figure 4c1–d3). Within the AL clusters, there were a number of co-expressing neurons (Figure 4c1–c3, closed arrows) and at least one neuron with no co-expression (Figure 4c–c2, open arrow). In the posterior and anterior sections of the SEZ, *Octβ1R > His2A-GFP* exhibited co-expression with Tdc2 (Figure 4e–e2). At least one neuron in the VNC of *Octβ1R > His2A-GFP* co-expressed with Tdc2 (Figure 4f1–f3, closed white arrow) while the majority of neurons in the VNC did not co-express with Tdc2 (Figure 4g1–g3, open white arrow).

Octβ2R-Gal4 driven His2A-GFP expression (*Octβ2R > His2A-GFP*; Figure 5a–c) was detected with Tdc2 in all Tdc2+ neuron clusters in the adult brain (Figure 5d–h2) and only one neuron in the VNC (Figure 5i1–j3, closed white arrow). Several pairs of Tdc2+ neurons in the ASM cluster co-expressed Tdc2 and *Octβ2R > His2A-GFP*, with at least one pair negative for co-expression (Figure 5d1–d3). A significant amount of co-expression was observed in the AL2 cluster of the AL (Figure 5e1–e3, closed white arrows), however *Octβ2R > His2A-GFP* was not detected in AL1 neurons (Figure 5e1–e3, open arrows). At least two VM neurons in the SEZ co-expressed *Octβ2R > His2A-GFP* and Tdc2 (Figure 5g1–g3), with co-expression also seen in PB1 cluster of the PSMP region (Figure 5h1–h3, closed white arrow).

Figure 6 illustrates the widespread neuronal expression of His2A-GFP driven by the *Octβ3R-Gal4* (*Octβ3R > His2A-GFP*; Figure 6a,b). *Octβ3R > His2A-GFP* co-expression with Tdc2 was detected in several Tdc2+ neuronal clusters, including both the anterior and PSMP of adult brains (Figure 6c1–d3, closed white arrows) and in at least one neuron in the VNC (Figure 6f1–f3, closed white arrow). Lack of co-expression was also seen in the PSMP (Figure 6d1–d3, open white arrows) and in the VNC (Figure 6f1–f3, open white arrows).

3.4 | Sex differences in *OctR-Gal4* expression

Levels of Octα2R mRNA in particular have been reported to be higher in males than females (Qi et al., 2017). This difference could reflect a greater number of Octα2R-expressing neurons in males or sex-specific differences in gene expression. We thus decided to examine

FIGURE 8 *B3RT-Tdc2* expression in α-adrenergic-like receptors. (a) Schematic of *B3RT-Tdc2-LexA*. CRISPR/Cas9 genome editing was used to insert same orientation B3 recombinase target sites (*B3RTs*) into the 5′ untranslated region (UTR) of the *Tdc2* gene and into the intron between the first two *Tdc2* coding exons. The coding sequence of the LexA transcription factor was also inserted immediately adjacent to the downstream *B3RT*. The B3 recombinase mediates excision between the B3RT's in all neurons that express the B3 recombinase using a Gal4 driver and *UAS-B3*. After the excision, a *Tdc2-LexA* driver is created and is expressed only in the subset of Gal4-expressing neurons that also express *Tdc2* and not in Gal4-expressing neurons that do not express *Tdc2*. Black rectangles are untranslated exons, white rectangles are coding exons, red rectangles are B3RTs, and yellow rectangles are coding LexA sequence. (b) Control *B3RT-Tdc2* with no Gal4 driver, anti-mCherry (red), anti-SYN (blue), anti-GFP (green). (c) Germline excision of *B3RT-Tdc2* (see Section 2), where *Tdc2-LexA* is expressed in all *Tdc2* neurons, anti-syn (blue), anti-mCherry (red), anti-Tdc2 (green). (d1–d3) Nuclear expression of *n-syb-Gal4* (d3, anti-GFP, green) and subset of *nsyb-Gal4* neurons that express *Tdc2* (d2, anti-mCherry, red), anti-SYN (blue) *yw; B3RT-Tdc2, nsyb-Gal4; LexAop2-His2B-mCherry, UAS-His2A-GFP.* (e1–e3) *OAMB > His2A-GFP* (e3, anti-GFP, green) and the subset of *OAMB-Gal4* neurons which express *Tdc2* (e2, anti-mCherry, red), anti-SYN (blue): *yw; B3RT-Tdc2; LexAop2-His2B-mCherry, UAS-His2A-GFP/OAMB-Gal4.* (f1–f3) *Octα2R > His2A-GFP* (f3, anti-GFP, green) and subset of *Octα2-Gal4* neurons which express *Tdc2* (f2, anti-mCherry, red), anti-SYN (blue): *yw; B3RT-Tdc2; LexAop2-His2B-mCherry, UAS-His2A-GFP/ Oct2R-Gal4.* All scale bars 50 μm
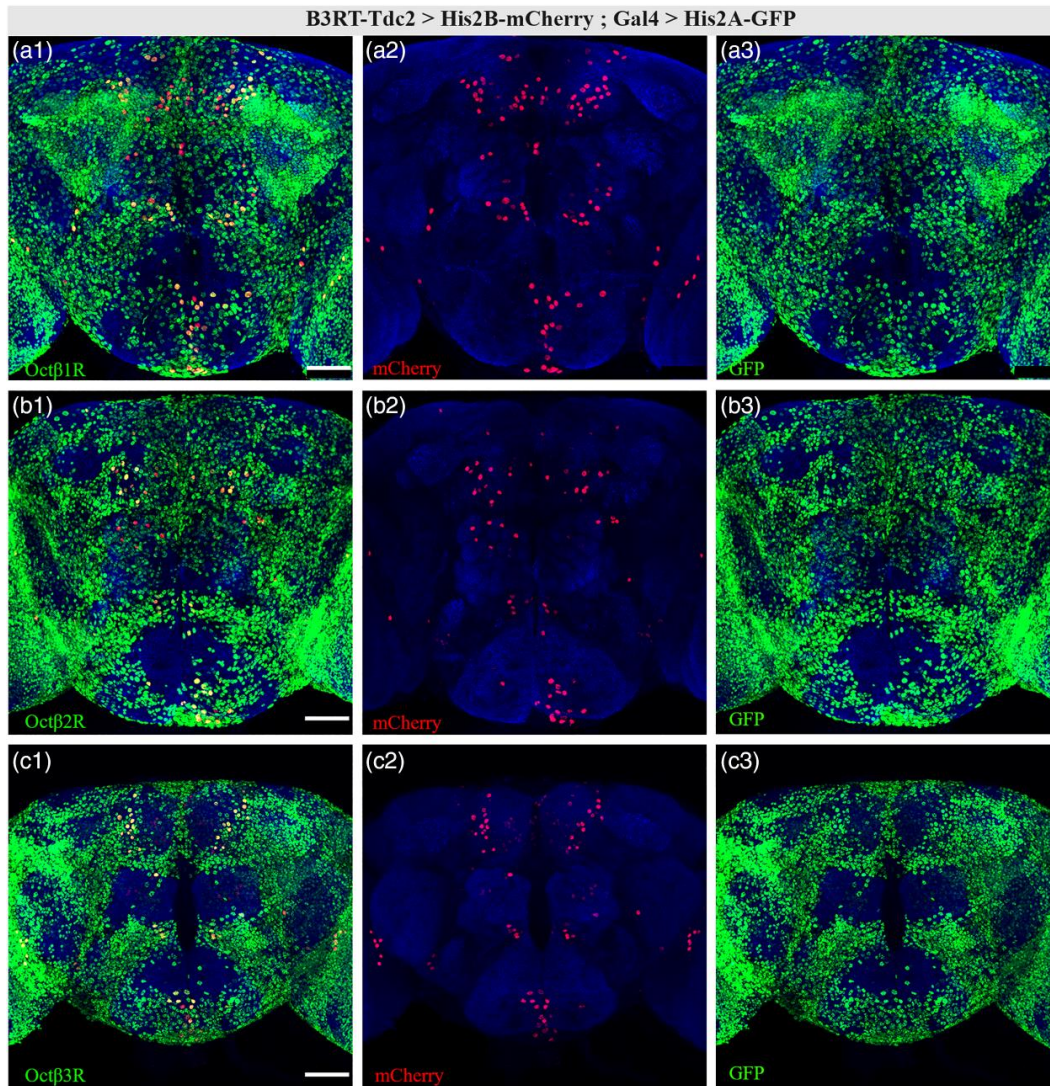
B3RT-Tdc2 > His2B-mCherry ; Gal4 > His2A-GFP

FIGURE 9 *B3RT-Tdc2* expression in *OctβR-Gal4*s. (a1–a3) *yw; B3RT-Tdc2; LexAop2-His2B-mCherry, UAS-His2A-GFP/ Octβ1R-Gal4* showing subset of *Octβ1R-Gal4* neurons which also express *Tdc2* (a2, red), only the Gal4 pattern (a3, green) and merged (a1). (b1–b3) *yw; B3RT-Tdc2; LexAop2-His2B-mCherry, UAS-His2A-GFP/ Octβ2R-Gal4* showing subset of *Octβ2R-Gal4* neurons that also express *Tdc2* (b2, red), only the Gal4 pattern (b3, green) and merged (b1). (c1–c3) *yw; B3RT-Tdc2; LexAop2-His2B-mCherry, UAS-His2A-GFP/ Octβ3R-Gal4* showing subset of *Octβ3R-Gal4* neurons that also express *Tdc2* (c2, red), only the Gal4 pattern (c3, green) and merged (c1). Antibodies used: anti-GFP (green), anti-mCherry (red), and anti-SYN (blue). Scale bar = 50 μm

differences between males and females in every *OctR-Gal4* line and also observe any differences in their co-expression with the Tdc2 antibody (Figure 7). While neuron count was not quantified, no gross differences in *Gal4 > His2A-GFP* expression patterns were seen between males and females (Figure 7a1–j2). However, we did determine *Octα2R > His2A-GFP* expression in females co-localized with

Tdc2 in the posterior SEZ (Figure 7d2, closed white arrow) while in males *Octα2R > His2A-GFP* expression was not detectable in this pair of Tdc2+ VM neurons (Figure 7c2, open white arrow). These results indicate potential sex-specific differences in α-adrenergic autoreceptor expression and suggest an area for further study. In summary, we have generated new *OctR-Gal4* lines and determined
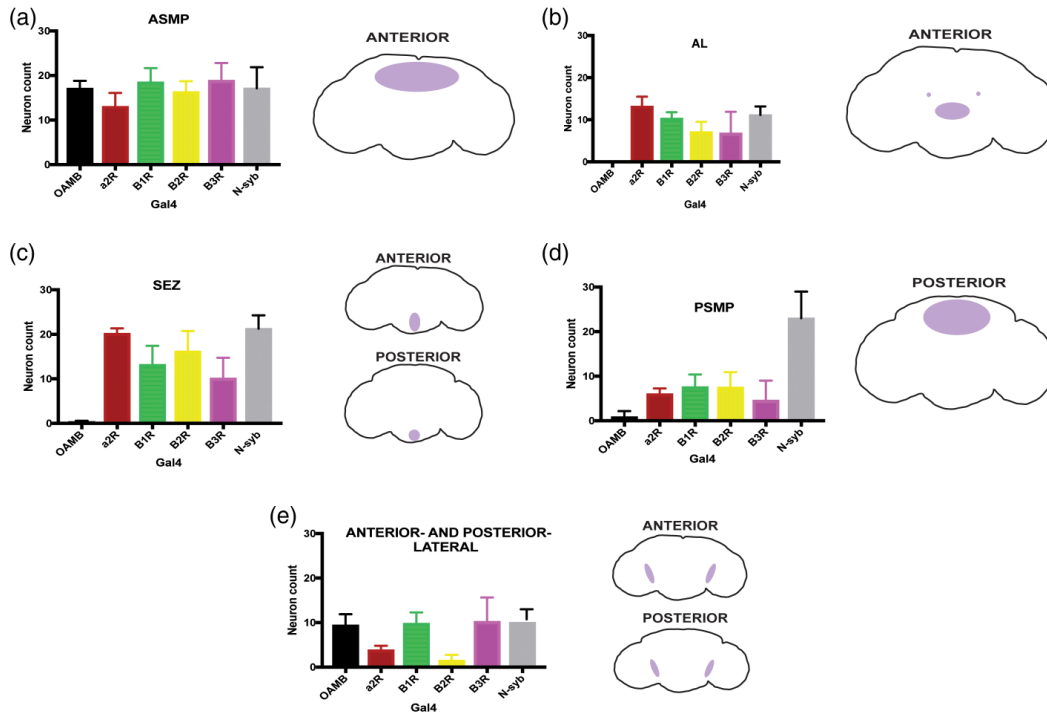
FIGURE 10 Average number of co-expressing *OctR-Gal4/B3RT-Tdc2* neurons. Co-expressing *Gal4 > His2A-GFP/Tdc2-LexA > His2B-mCherry* neurons were manually counted in brain regions (a) anterior superior medial protocerebrum (ASMP), (b) antennal lobe (AL), (c) suboesophageal ganglion (SEZ), (d) posterior superior medial protocerebrum (PSMP), and (e) anterior- and posterior-lateral regions. *OAMB-Gal4* (*n* = 12), *Octα2R-*Gal4 (*n* = 6), *Octβ1R*-Gal4 (*n* = 10), *Octβ2R-Gal4* (*n* = 10), *Octβ3R-Gal4* (*n* = 9), *N-syb-Gal4* (*n* = 8) [Color figure can be viewed at wileyonlinelibrary.com]

each OctR has the potential to serve an autoregulatory function due to co-expression within distinct Tdc2+ clusters.

3.5 | *B3RT-Tdc2-LexA* intersectional genetics confirms potential autoreceptor locations

As shown above with the MiMIC *OctR-Gal4*s, distinct presynaptic receptor expression was observed for each OctR. To independently assess the overlap of *OctR* expression with Tdc2+ neurons, a variant of *Tdc2*, *B3RT-Tdc2-LexA* (hereafter *B3RT-Tdc2*), was developed via CRISPR/Cas9 genome editing (see Section 2). *B3RT-Tdc2* incorporates one B3 recombinase target site, *B3RT*, (Nern, Pfeiffer, Svoboda, & Rubin, 2011) into the 5′ untranslated region (UTR) of the *Tdc2* genomic locus, and a second *B3RT* adjacent to the coding sequence of the LexA transcription factor in an intron between the first two coding exons (Figure 8a). Prior to excision of the DNA between the *B3RT*s, LexA is not expressed, but after excision, a *Tdc2-LexA* driver results. Thus, intersectional expression between any Gal4 driver and *Tdc2* neurons can be revealed using *B3RT-Tdc2* in combination with a

UAS-B3 recombinase transgene and a *LexAop* reporter. Since *B3RT* excisions are effectively permanent, any neurons experiencing excisions during development will retain those excisions in the adult, even if Gal4 expression is not maintained. *LexAop* reporter expression that does not also show *UAS* expression may thus be observed with some Gal4 drivers as a result of excisions that occurred during development. No *LexAop2* reporter expression was detected in the absence of a Gal4 driver (Figure 8b), thus indicating neither the *UAS-B3* recombinase nor *LexAop2-6XmCherry* reporter exhibits leaky expression.

To assess whether the *B3RT-Tdc2* recapitulates endogenous expression of *Tdc2*, a germline excision of *B3RT-Tdc2* was generated and the resulting *LexAop2-6XmCherry* reporter expression was compared to endogenous Tdc2 protein expression. Neuronal expression of the 6XmCherry reporter recapitulates Tdc2 expression (Figure 8c1–c3), as expected for genome editing at the endogenous chromosomal locus of *Tdc2* with its complete regulatory region. A similar *Tdc2* neuronal expression pattern was also observed upon pan-neuronal excision using the *n-syb-Gal4* driver and the *LexAop2-His2B-mCherry* reporter (Figure 8d1–d3), thus indicating B3 recombinase-mediated excision occurs with a high level of efficiency.
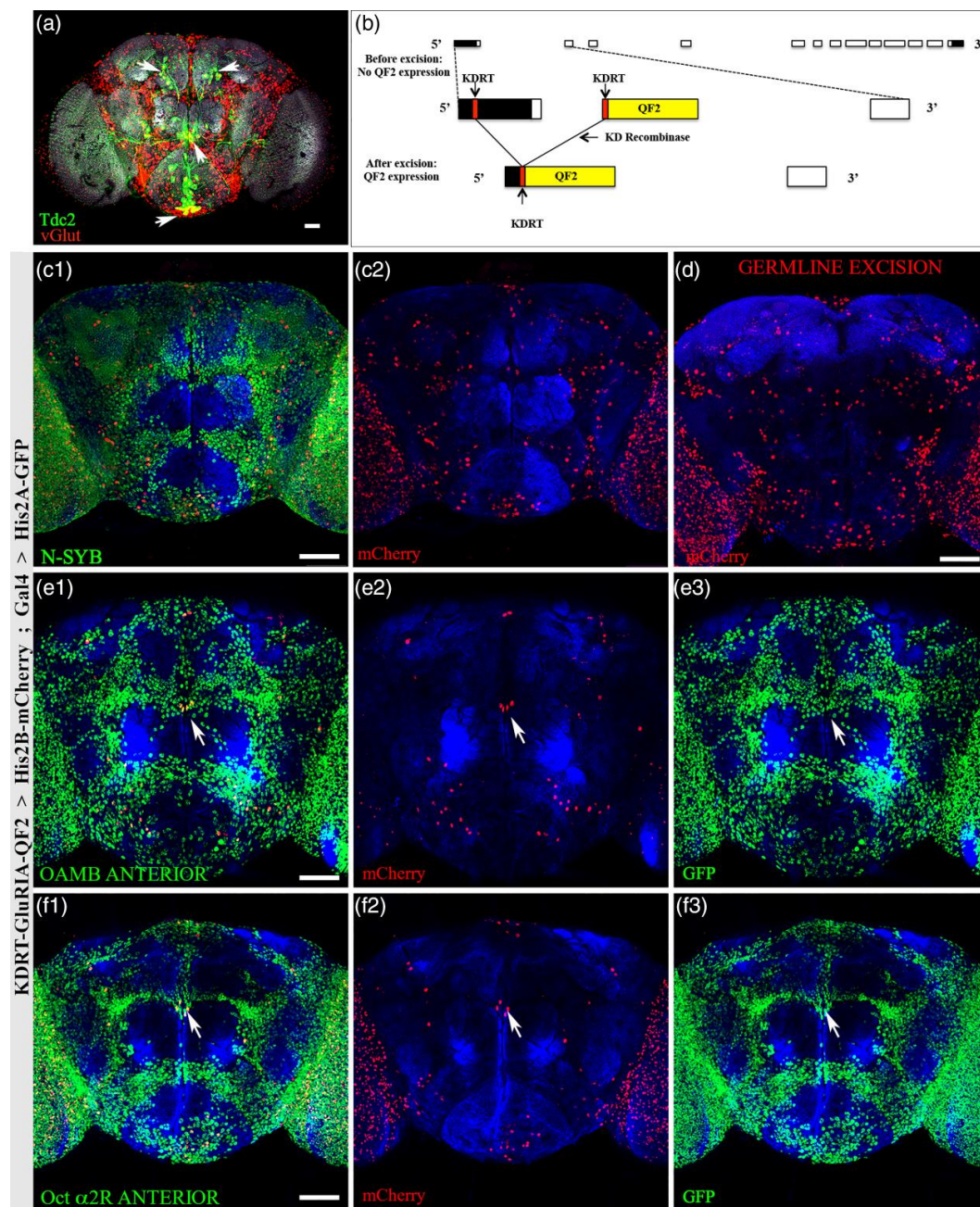
FIGURE 11 Legend on next page.

After verifying that both the germline excision and pan-neuronal excision of *B3RT-Tdc2* closely recapitulated endogenous Tdc2 expression, we utilized this method to further assess overlapping expression of Tdc2 and OctRs. To visualize *Tdc2* and *OctR* co-expression, we utilized the same *UAS-His2A-GFP* nuclear reporter for all *OctR-Gal4s* and the *LexAop2-His2BCherry* nuclear reporter to reveal conditional *B3RT-Tdc2* expression (Figure 6e1–f3, Figure 7). *B3RT-Tdc2 > His2B-mCherry* labeled a similar pattern of neurons in the intersection of the *OAMB-Gal4* and *B3RT-Tdc2* as was seen with the Tdc2 antibody (Figure 8e1–e3, compare to Figure 2b–g3), including the VL neurons and those within the ASM cluster. Likewise, driving B3 recombinase with *Octα2R-Gal4* resulted in co-expression of His2B-mCherry and His2A-GFP in both pairs of VL neurons, as well as neurons within the AL, the ASMP and PSMP clusters, and the SEZ (Figure 8f1–f3).

B3RT-Tdc2 also corroborated the overlapping expression of Tdc2 with each *OctβR-Gal4* (Figure 9a1–c3), demonstrating co-expression in the PSMP, ASMP, AL (with *Octβ3R* exhibiting the least on average, of the *OctβR-Gal4s*; see Figure 9b), and VM clusters of Tdc2+ neurons, closely recapitulating results seen with the Tdc2 antibody and *OctR* co-expression in Figures 4–7. Using the nuclear reporters with the *B3RT-Tdc2* method also allowed us to manually count co-expressing *OctR-Tdc2* neurons with greater ease than with antibody staining (Figure 10). In the ASMP, *Octα2R-Gal4* had the lowest average of co-expressing neurons (Figure 10a), though *Octα2R-Gal4* showed the highest average of co-expression in the antennal lobe, followed by *Octβ1R-Gal4* (Figure 10b). In the SEZ, *OAMB-Gal4* had the lowest average of co-expressing neurons with *B3RT-Tdc2*, with *Octα2R-Gal4* again having the highest average, followed by *Octβ2R-Gal4*. All *OctR-Gal4s* co-expressed neurons in low numbers in the PSMP, with *OAMB-Gal4* co-expressing the least on average (Figure 10d). However, within the lateral clusters of the Tdc2+ neurons, *Octβ2R-Gal4* co-expressed the least (Figure 10e). In summary, *B3RT-Tdc2* independently confirms the co-expression observed using the Tdc2 immunostaining approach and also demonstrates its utility for identifying *Tdc2* neurons whose expression overlaps that of a Gal4 driver of interest.

3.6 | Intersectional genetics reveals co-expression of two types of receptors

We recently demonstrated that Oct neurons in the adult brain co-express the *Drosophila* vesicular glutamate transporter (dVGlut) (Sherer et al., in press) (Figure 11a). In addition, single-cell transcriptomics data demonstrate a high percentage of mid-brain Oct-expressing neurons also express markers for dVGlut (Croset, Treiber, & Waddell, 2018). The functional capabilities of such dual neurotransmission neurons are complex. For example, the postsynaptic response to Oct and glutamate may be determined by neurons expressing receptors for one or both neurotransmitters. In an initial attempt to determine whether glutamate and octopamine receptors are expressed in the same neurons, co-expression between OctRs and the *Drosophila* non-NMDA ionotropic glutamate receptor, GluRIA (Ultsch et al., 1992) was investigated.

As the intersectional genetic approach provides a powerful means to assess co-expression, we used CRISPR/Cas9 genome editing to generate a conditional *GluRIA* allele, *KDRT-GluR1A-QF2* (hereafter *KDRT-GluR1A*) at the endogenous *GluR1A* chromosomal locus. *KDRT-GluR1A* is analogous to *B3RT-Tdc2* described above except it uses KD recombinase target sites (*KDRTs*) (Nern et al., 2011) and the QF2 transcription factor (Riabinina & Potter, 2016). *KDRT-GluR1A* contains one *KDRT* in the 5′ UTR and a second *KDRT* with adjacent QF2 coding sequences in the intron between the first two coding exons of *GluR1A*. Prior to excision, the QF2 driver is not expressed (Figure 11b). However, after pan-neuronal KD recombinase-mediated excision using the *n-syb-Gal4*, a *GluR1A-QF2* driver is created that expresses broadly in the optic lobes and sparsely in the central brain (Figure 11c1,c2). This pattern is highly similar to the pattern observed in a *KDRT-GluR1A* germline excision (Figure 11d), indicating KD recombinase-mediated excisions occur with high efficiency. *KDRT-GluRIA* can thus be used to reveal intersectional expression of any Gal4 driver with GluRIA neurons. Additionally, *KDRT-GluR1A* can be used to remove GluR1A receptor function in individual neurons.

Images demonstrating the intersection of the expression of *OctR > His2A-GFP* and *KDRT-GluRIA > His2B-mCherry* in anterior sections of the brains are shown in Figures 11 and 12. The *OAMB* receptor and *KDRT-GluRIA* are co-expressed in neurons surrounding the

FIGURE 11 *KDRT-GluRIA* expression in α-adrenergic-like receptors. (a) *vGlut-Gal4; UAS-dsRed* (red) and anti-Tdc2 (green) showing distinct co-localization, indicative of dual transmitting neurons (white arrows). Scale bar 30 μm. (b) Schematic of *KDRT-GluRIA-QF2* construct. The first KD recombination target site (*KDRT*) was CRISPR'd upstream of the endogenous locus of the *GluRIA* translation start site within the 5′ untranslated region (UTR) while the second *KDRT* was placed in an intron downstream of the translation start site, directly preceding a QF2 driver sequence. Prior to the excision of the DNA the two *KDRTs* flank, no QF2 expression occurs. After the excision mediated by the KD recombinase, a null mutation in the *GluRIA* gene is formed, along with a *GluRIA-QF2* driver, which can drive the expression of our *QUAS* reporter of interest. (c1–c3) Pan-neuronal Gal4 driving expression of the KD recombinase in the subset of *n-syb-Gal4* neurons that express *GluRIA* (c2, red). *yw;n-syb-Gal4; KDRT-GluRIA, UAS-KD, UAS-His2A-GFP, QUAS-His2B-mCherry*. (d) Germline excision of *KDRT-GluRIA* driving expression of *QUAS-His2B-mCherry* in all *GluRIA*-expressing neurons (red). (e1–e3) *OAMB-His2A-GFP* pattern (e3, green), subset of *OAMB-Gal4* neurons expressing *GluRIA* (e2, red), and merged channels (e1) *yw; UAS-KD, UAS-His2A-GFP, QUAS-His2B-mCherry; KDRT-GluRIA, OAMB-Gal4*. Closed white arrow indicating four PENP neurons co-expressing *OAMB* and *GluRIA*. (f1–f3) *Octα2R > His2A-GFP* pattern (f3, green) and subset of *Octα2R-Gal4* neurons expressing *GluRIA* (f2, red), with broad expression seen in optic lobes. Merged channels (f1) *yw; UAS-KD, UAS-His2A-GFP, QUAS-His2B-mCherry; KDRT-GluRIA, Octα2R-Gal4*. Closed white arrow indicating four PENP neurons co-expressing *Octα2R* and *GluRIA*. Antibodies used: anti-GFP (green), anti-mCherry (red), and anti-SYN (blue). All scale bars = 50 μm unless otherwise specified
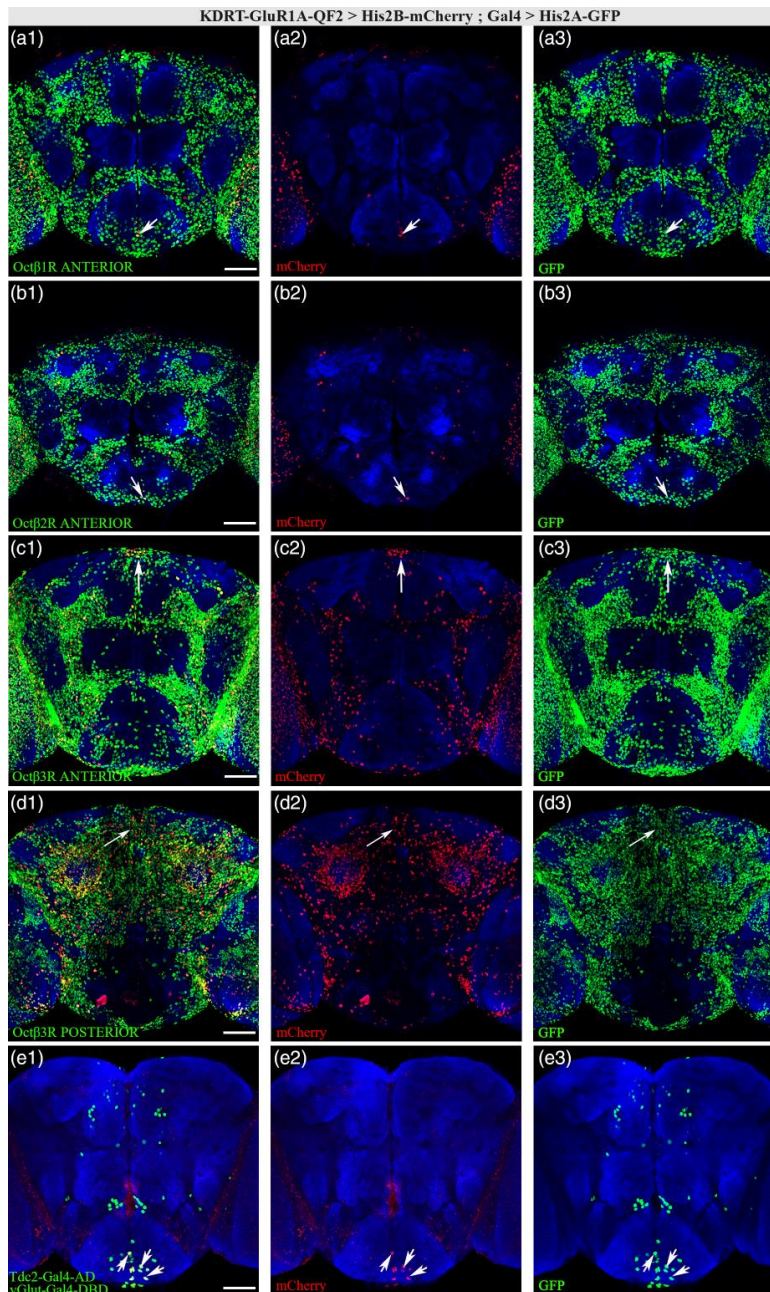
KDRT-GluR1A-QF2 > His2B-mCherry ; Gal4 > His2A-GFP

FIGURE 12 *KDRT-GluRIA* expression in *OctβR-Gal4s*. (a1–a3) *yw; UAS-His2A-GFP, QUAS-His2B-mCherry; KDRT-GluRIA, UAS-KD/Octβ1R-Gal4* showing subset of *Octβ1R-Gal4* neurons in the anterior sections (a3, green) that also express *GluRIA* (a2, red), and merged channels (a1) with closed white arrow indicating at least one neuron co-expressing *Octβ1R and GluRIA in the anterior SEZ*. Very little co-expression was seen in the central brain, with the majority seen in the optic lobes. (b1–b3) *yw; UAS-His2A-GFP, QUAS-His2B-mCherry; KDRT-GluRIA, UAS-KD/Octβ2R-Gal4* labeling the subset of *Octβ2R-Gal4* neurons in the anterior sections (b3, green) also expressing *GluRIA* (b2, red), and merged channels (b1) with closed white arrow indicating at least one neuron co-expressing *Octβ2R and GluRIA in the anterior SEZ*. (c1–d3) *yw; UAS-His2A-GFP, QUAS-His2B-mCherry; KDRT-GluRIA, UAS-KD/Octβ3R* anterior (c) and posterior (d) sections showing the subset of *Octβ3R-Gal4* neurons (c3, d3, green) also expressing *GluRIA* (c2, d2, red) and merged channels (c1,d1). Closed white arrows indicate co-expressing neurons in anterior and posterior superior medial protocerebrum. (e1–e3) *yw; UAS-His2A-GFP, QUAS-His2B-mCherry/ Tdc2-Gal4-AD, vGlut-Gal4-DBD; KDRT-GluRIA, UAS-KD* labeling *GluRIA*-expressing neurons (e2) within the subset of neurons labeled by the *Tdc2/vGlut* split Gal4 (e3) and merged channels (e1). Closed white arrows indicate co-expressing neurons in the SEZ. Stained with anti-GFP (green), anti-mCherry (red), and anti-SYN (blue). Scale bars = 50 μm

SEZ, a region that contains many Oct neurons and receives chemosensory information, as well as two neurons in the superior medial protocerebrum (SMP) and four neurons within the peri-esophageal neuropils (PENP) (Figure 11e1–e3, closed white arrow).

Octα2R > His2A-GFP neurons that co-express *KDRT-GluRIA > His2B-mCherry* are also found in the central brain within the medial area of the SEZ as well as SMP and PENP neurons (Figure 11f1–f3, closed white arrow).
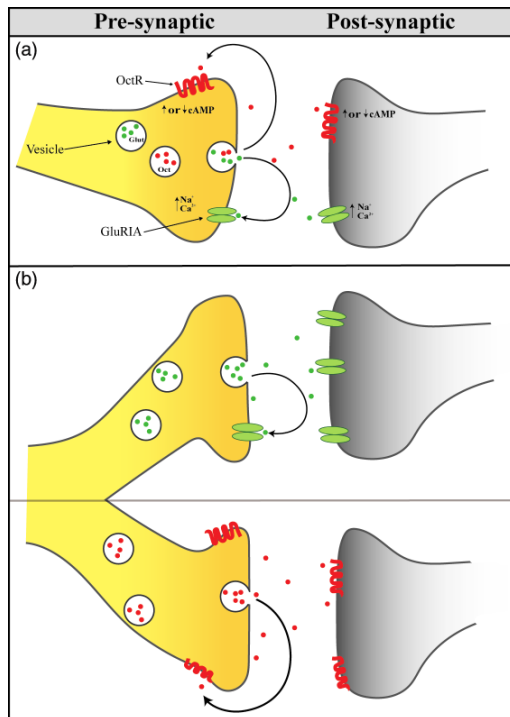
FIGURE 13 Dual transmission and postsynaptic receptor scenarios. In dual transmitting neurons, neurotransmitters are either packaged in synaptic vesicles together (a, presynaptic) or separately (b,c, presynaptic) and may be released at the same synapse (a, presynaptic) or separate ones (b,c, postsynaptic). From our experiments here, we show OctR expression in Tdc2+ neurons, which are indicate autoreception properties as shown in (a) and (c). Additional data indicates potential GluRIA autoreception as seen in (a) and (b). Postsynaptically, receptors may be expressed together (a, postsynaptic) or on different neurons (b,c, postsynaptic). Our data indicate a number of neurons express *OctR* and a *GluRIA*, as in (a) [Color figure can be viewed at wileyonlinelibrary.com]

The co-expression of *OctβR*'s and *KDRT-GluRIA* ranges from a small number of neurons to widespread co-expression (e.g., *Octβ3R-Gal4*), suggesting the possibility of key differences in neurons that have the potential to respond to both octopamine and glutamate signaling (Figure 9). *KDRT-GluRIA* and *Octβ1R* or *KDRT-GluRIA* and *Octβ2R* were co-expressed in neurons located in the SEZ and ventromedial to the AL (Figure 12a1–b3, closed white arrows). *Octβ3R* and *KDRT-GluRIA* are broadly co-expressed in the central brain and optic lobes (Figure 12c1–d3, closed white arrows). Co-expression was observed in the SMP, the superior lateral protocerebrum, the PENP, and posterior lateral protocerebrum (Figure 12d1–d3). The *Octβ3R-Gal4* was the only OctR that showed substantial co-expression with *KDRT-GluRIA* in the posterior sections of the brain (Figure 12d–d2).

These results indicate widespread differences in the co-expression of *OctR*s and *GluRIA*.

As these results indicate substantial evidence for Oct autoreceptor usage, we decided to also investigate GluRIA potential autoreception within Oct-Glut dual transmitting neurons seen in Figure 11a. Although less common, glutamate receptors have also been known to function as autoreceptors (Pittaluga, 2016). A *Tdc2−/vGlut-* split *Gal4* line, which labels all neurons expressing both *Tdc2* and *vGlut* (Figure 9e3), crossed to our *KDRT-GluRIA* labeled an average of 11.5 dual transmitting neurons in the SEZ that also express *GluRIA* (Figure 12e1–e3, closed white arrows, *n* = 6). This result indicates these dual transmission SEZ neurons may use presynaptic glutamate receptors as autoreceptors. The schematic in Figure 10 offers plausible scenarios for both pre- and postsynaptic signaling from dual transmission neurons. On the presynaptic side (Figure 13a–c), synaptic vesicles of dual transmitting neurons may release neurotransmitters from the same (Figure 13a) or separate (Figure 13b,c) synaptic vesicles and this release may also be spatially segregated (Hnasko & Edwards, 2012). Our results demonstrate Oct presynaptic receptor localization, which is likely utilized for autoreceptor presynaptic signal regulation as seen in Figure 13a,c. Our data also suggest the possibility of a presynaptic glutamate autoreceptor (Figure 13a). Downstream from dual Oct-Glut neurons, postsynaptic neurons may express receptors for Oct or Glut (Figure 13b,c) or as our results also indicate, downstream neurons can express both an OctR and a GluR, (Figure 13a). Using the new intersectional genetic tools described here, further studies will be able to address the function of presynaptic and postsynaptic receptor localization on octopamine signaling.

4 | DISCUSSION

In this study, we used MiMIC Trojan-Gal4 lines for each of the five OctRs to characterize *OctR* expression in Drosophila. Broad expression of each *OctR* receptor was observed throughout the adult brain and VNC, including in Tdc2/Oct neurons. These results were independently substantiated using the conditional *Tdc2-LexA* driver *B3RT-Tdc2* that allows assessment of intersectional expression between any Gal4 driver and *Tdc2* neurons. While it is possible that OctR distribution in Oct neurons is not presynaptic, results from vertebrates suggest autoreceptor modulation is likely (Cragg & Greenfield, 1997; Starke, 2001; Trendelenburg et al., 2003), even in dual neurotransmitter neurons (Takacs et al., 2018).

In the case of autoreception, the released neurotransmitter may activate the autoreceptor to regulate secretion of that same transmitter by either inhibiting or facilitating its release. Thus, autoreception brings a key regulatory aspect to neurotransmitter signaling that significantly impacts synaptic transmission, circuit output, and behavior (Choi et al., 2012; Koon et al., 2011; Koon & Budnik, 2012; Langer, 2015). In *Drosophila*, receptors for the neuropeptide peptide dispersing factor (PDF) are expressed in and required by PDF-expressing lateral ventral pacemaker neurons (LNv's) to shift the balance of activity from evening to morning (Choi et al., 2012). Serotonin regulates

neurite outgrowth in an autocrine manner in Helisoma (Diefenbach, Sloley, & Goldberg, 1995) and in the ventral nerve cord of *Drosophila* larvae (Sykes & Condron, 2005). At the *Drosophila* NMJ, the growth of Oct arbors during development and in response to starvation requires the activation of Octβ2R autoreceptors, while the inhibition of synaptic growth depends on Octβ1R on presynaptic motorneurons (Koon et al., 2011; Koon & Budnik, 2012).

As Oct functions in such diverse capacities in invertebrates, the capability of an Oct neuron to presynaptically modulate its own release could have significant impacts on downstream circuit targets. For example, Tdc2+ neurons are required to promote aggression (Zhou, Rao, & Rao, 2008) and inhibit inter-male courtship (Andrews et al., 2014; Certel et al., 2010). Oct autoreceptors on these neurons may function to provide negative feedback to inhibit either aggression or courtship, depending on the social situation. While we investigated *OctR* expression in Oct neurons, the presence of other neurotransmitter receptors on Tdc2+ neurons may additionally affect computational output from these neurons, affecting a variety of systems in the fly. Our novel *B3RT-Tdc2* intersectional genetic tool allows future studies of other neurotransmitters or neurotransmitter receptors inputs in Tdc2+ neurons as it can be used in conjunction with any available Gal4 driver.

In such an investigation of Tdc2 expression with other neurotransmitters, we recently identified a subset of Tdc2+ neurons that also utilize glutamate (Sherer et al., in press). Glutamate is the major excitatory neurotransmitter at the *Drosophila* NMJ and glutamatergic neurons are found in all regions of the adult central brain (Daniels, Gelfand, Collins, & DiAntonio, 2008; Jan & Jan, 1976). In vertebrates, glutamate is co-released with dopamine, serotonin, acetylcholine, and GABA (Danik et al., 2005; Fattorini, Antonucci, Menna, Matteoli, & Conti, 2015; Ottem, Godwin, Krishnan, & Petersen, 2004; Wang et al., 2019). In *Drosophila*, glutamate enhances the efficiency of dopamine loading into synaptic vesicles (Aguilar et al., 2017).

Given recent results demonstrating Oct-glut co-expression (Sherer et al., in press), we investigated potential Oct and Glut postsynaptic receptor expression using the new Trojan-Gal4's. Similar to the conditional *Tdc2* driver created here, a conditional glutamate receptor driver, *KDRT-GluRIA*, was developed and used to reveal that *GluRIA* is co-expressed to a different degree with each *OctR-Gal4*. These results indicate these co-expressing neurons as putative postsynaptic targets of upstream dual Oct-Glut transmitting neurons (see Figure 13). While we investigated *GluRIA* and *Tdc2* co-expression with *OctR*s, other neurotransmitters and neurotransmitter receptors are likely also co-expressed with Tdc2 (Croset et al., 2018), and future studies utilizing these new conditionally expressible genetic tools can expand our knowledge of octopaminergic dual transmitting signaling mechanisms.

ORCID

Hannah M. McKinney https://orcid.org/0000-0003-4774-4317
Lewis M. Sherer https://orcid.org/0000-0001-5875-1737

REFERENCES

Aguilar, J. I., Dunn, M., Mingote, S., Karam, C. S., Farino, Z. J., Sonders, M. S., ... Freyberg, Z. (2017). Neuronal depolarization drives increased dopamine synaptic vesicle loading via VGLUT. *Neuron*, *95*(5), 1074–1088 e1077. https://doi.org/10.1016/j.neuron.2017.07.038

Andrews, J. C., Fernandez, M. P., Yu, Q., Leary, G. P., Leung, A. K., Kavanaugh, M. P., ... Certel, S. J. (2014). Octopamine neuromodulation regulates Gr32a-linked aggression and courtship pathways in drosophila males. *PLoS Genetics*, *10*(5), e1004356. https://doi.org/10.1371/journal.pgen.1004356

Balfanz, S., Strunker, T., Frings, S., & Baumann, A. (2005). A family of octopamine [corrected] receptors that specifically induce cyclic AMP production or Ca2+ release in Drosophila melanogaster. *Journal of Neurochemistry*, *93*(2), 440–451. https://doi.org/10.1111/j.1471-4159.2005.03034.x

Busch, S., Selcho, M., Ito, K., & Tanimoto, H. (2009). A map of octopaminergic neurons in the Drosophila brain. *The Journal of Comparative Neurology*, *513*(6), 643–667. https://doi.org/10.1002/cne.21966

Certel, S. J., Leung, A., Lin, C. Y., Perez, P., Chiang, A. S., & Kravitz, E. A. (2010). Octopamine neuromodulatory effects on a social behavior decision-making network in drosophila males. *PLoS One*, *5*(10), e13248. https://doi.org/10.1371/journal.pone.0013248

Certel, S. J., & Thor, S. (2004). Specification of drosophila motoneuron identity by the combinatorial action of POU and LIM-HD factors. *Development*, *131*(21), 5429–5439. https://doi.org/10.1242/dev.01418

Choi, C., Cao, G., Tanenhaus, A. K., McCarthy, E. V., Jung, M., Schleyer, W., ... Nitabach, M. N. (2012). Autoreceptor control of peptide/neurotransmitter corelease from PDF neurons determines allocation of circadian activity in drosophila. *Cell Reports*, *2*(2), 332–344. https://doi.org/10.1016/j.celrep.2012.06.021

Ciccarelli, M., Sorriento, D., Coscioni, E., Iaccarino, G., & Santulli, G. (2016). Adrenergic receptors. In *Endocrinology of the heart in health and disease* (pp. 285–315). Elsevier.

Cole, S. H., Carney, G. E., McClung, C. A., Willard, S. S., Taylor, B. J., & Hirsh, J. (2005). Two functional but noncomplementing drosophila tyrosine decarboxylase genes: Distinct roles for neural tyramine and octopamine in female fertility. *The Journal of Biological Chemistry*, *280*(15), 14948–14955. https://doi.org/10.1074/jbc.M414197200

Cole, S. W., & Sood, A. K. (2012). Molecular pathways: Beta-adrenergic signaling in cancer. *Clinical Cancer Research*, *18*(5), 1201–1206. https://doi.org/10.1158/1078-0432.CCR-11-0641

Cragg, S. J., & Greenfield, S. A. (1997). Differential autoreceptor control of somatodendritic and axon terminal dopamine release in substantia nigra, ventral tegmental area, and striatum. *Journal of Neuroscience*, *17*(15), 5738–5746 Retrieved from https://www.ncbi.nlm.nih.gov/pubmed/9221772

Croset, V., Treiber, C. D., & Waddell, S. (2018). Cellular diversity in the drosophila midbrain revealed by single-cell transcriptomics. *Elife*, *7*, e34550. https://doi.org/10.7554/eLife.34550

Daniels, R. W., Gelfand, M. V., Collins, C. A., & DiAntonio, A. (2008). Visualizing glutamatergic cell bodies and synapses in drosophila larval and adult CNS. *The Journal of Comparative Neurology*, *508*(1), 131–152. https://doi.org/10.1002/cne.21670

Danik, M., Cassoly, E., Manseau, F., Sotty, F., Mouginot, D., & Williams, S. (2005). Frequent coexpression of the vesicular glutamate transporter 1 and 2 genes, as well as coexpression with genes for choline acetyltransferase or glutamic acid decarboxylase in neurons of rat brain. *Journal of Neuroscience Research*, *81*(4), 506–521. https://doi.org/10.1002/jnr.20500

Diao, F., Ironfield, H., Luan, H., Diao, F., Shropshire, W. C., Ewer, J., ... White, B. H. (2015). Plug-and-play genetic access to drosophila cell types using exchangeable exon cassettes. *Cell Reports*, *10*(8), 1410–1421. https://doi.org/10.1016/j.celrep.2015.01.059

Diefenbach, T. J., Sloley, B. D., & Goldberg, J. I. (1995). Neurite branch development of an identified serotonergic neuron from embryonic Helisoma: Evidence for autoregulation by serotonin. *Developmental Biology*, *167*(1), 282–293. https://doi.org/10.1006/dbio.1995.1023

El-Kholy, S., Stephano, F., Li, Y., Bhandari, A., Fink, C., & Roeder, T. (2015). Expression analysis of octopamine and tyramine receptors in drosophila. *Cell and Tissue Research*, *361*(3), 669–684. https://doi.org/10.1007/s00441-015-2137-4

Evans, P. D., & Maqueira, B. (2005). Insect octopamine receptors: A new classification scheme based on studies of cloned drosophila G-protein coupled receptors. *Invertebrate Neuroscience*, *5*(3–4), 111–118. https://doi.org/10.1007/s10158-005-0001-z

Fattorini, G., Antonucci, F., Menna, E., Matteoli, M., & Conti, F. (2015). Co-expression of VGLUT1 and VGAT sustains glutamate and GABA co-release and is regulated by activity in cortical neurons. *Journal of Cell Science*, *128*(9), 1669–1673. https://doi.org/10.1242/jcs.164210

Han, K. A., Millar, N. S., & Davis, R. L. (1998). A novel octopamine receptor with preferential expression in drosophila mushroom bodies. *Journal of Neuroscience*, *18*(10), 3650–3658 Retrieved from https://www.ncbi.nlm.nih.gov/pubmed/9570796

Hnasko, T. S., & Edwards, R. H. (2012). Neurotransmitter corelease: Mechanism and physiological role. *Annual Review of Physiology*, *74*, 225–243. https://doi.org/10.1146/annurev-physiol-020911-153315

Hoopfer, E. D. (2016). Neural control of aggression in drosophila. *Current Opinion in Neurobiology*, *38*, 109–118. https://doi.org/10.1016/j.conb.2016.04.007

Jan, L. Y., & Jan, Y. N. (1976). L-glutamate as an excitatory transmitter at the drosophila larval neuromuscular junction. *The Journal of Physiology*, *262*(1), 215–236. https://doi.org/10.1113/jphysiol.1976.sp011593

Klagges, B. R., Heimbeck, G., Godenschwege, T. A., Hofbauer, A., Pflugfelder, G. O., Reifegerste, R., ... Buchner, E. (1996). Invertebrate synapsins: A single gene codes for several isoforms in drosophila. *Journal of Neuroscience*, *16*(10), 3154–3165 Retrieved from https://www.ncbi.nlm.nih.gov/pubmed/8627354

Koon, A. C., Ashley, J., Barria, R., DasGupta, S., Brain, R., Waddell, S., ... Budnik, V. (2011). Autoregulatory and paracrine control of synaptic and behavioral plasticity by octopaminergic signaling. *Nature Neuroscience*, *14*(2), 190–199. https://doi.org/10.1038/nn.2716

Koon, A. C., & Budnik, V. (2012). Inhibitory control of synaptic and behavioral plasticity by octopaminergic signaling. *The Journal of Neuroscience*, *32*(18), 6312–6322. https://doi.org/10.1523/JNEUROSCI.6517-11.2012

Langer, S. Z. (2015). alpha2-Adrenoceptors in the treatment of major neuropsychiatric disorders. *Trends in Pharmacological Sciences*, *36*(4), 196–202. https://doi.org/10.1016/j.tips.2015.02.006

Langer, S. Z., & Angel, I. (1991). Pre- and postsynaptic alpha-2 adrenoceptors as target for drug discovery. *Journal of Neural Transmission. Supplementum*, *34*, 171–177. https://doi.org/10.1007/978-3-7091-9175-0_22

Li-Kroeger, D., Kanca, O., Lee, P. T., Cowan, S., Lee, M. T., Jaiswal, M., ... Bellen, H. J. (2018). An expanded toolkit for gene tagging based on MiMIC and scarless CRISPR tagging in drosophila. *Elife*, *7*, e38709. https://doi.org/10.7554/eLife.38709

Maqueira, B., Chatwin, H., & Evans, P. D. (2005). Identification and characterization of a novel family of Drosophila beta-adrenergic-like octopamine G-protein coupled receptors. *Journal of Neurochemistry*, *94*(2), 547–560. https://doi.org/10.1111/j.1471-4159.2005.03251.x

Meiselman, M. R., Kingan, T. G., & Adams, M. E. (2018). Stress-induced reproductive arrest in drosophila occurs through ETH deficiency-mediated suppression of oogenesis and ovulation. *BMC Biology*, *16*(1), 18. https://doi.org/10.1186/s12915-018-0484-9

Monastirioti, M. (2003). Distinct octopamine cell population residing in the CNS abdominal ganglion controls ovulation in *Drosophila melanogaster*. *Developmental Biology*, *264*(1), 38–49. https://doi.org/10.1016/j.ydbio.2003.07.019

Nassel, D. R. (2018). Substrates for neuronal Cotransmission with neuropeptides and small molecule neurotransmitters in drosophila. *Frontiers in Cellular Neuroscience*, *12*, 83. https://doi.org/10.3389/fncel.2018.00083

Nern, A., Pfeiffer, B. D., Svoboda, K., & Rubin, G. M. (2011). Multiple new site-specific recombinases for use in manipulating animal genomes. *Proceedings of the National Academy of Sciences of the United States of America*, *108*(34), 14198–14203. https://doi.org/10.1073/pnas.1111704108

Ottem, E. N., Godwin, J. G., Krishnan, S., & Petersen, S. L. (2004). Dual-phenotype GABA/glutamate neurons in adult preoptic area: Sexual dimorphism and function. *The Journal of Neuroscience*, *24*(37), 8097–8105. https://doi.org/10.1523/JNEUROSCI.2267-04.2004

Pauls, D., Blechschmidt, C., Frantzmann, F., El Jundi, B., & Selcho, M. (2018). A comprehensive anatomical map of the peripheral octopaminergic/tyraminergic system of *Drosophila melanogaster*. *Scientific Reports*, *8*(1), 15314. https://doi.org/10.1038/s41598-018-33686-3

Pech, U., Pooryasin, A., Birman, S., & Fiala, A. (2013). Localization of the contacts between Kenyon cells and aminergic neurons in the *Drosophila melanogaster* brain using SplitGFP reconstitution. *The Journal of Comparative Neurology*, *521*(17), 3992–4026. https://doi.org/10.1002/cne.23388

Petersen, L. K., & Stowers, R. S. (2011). A gateway MultiSite recombination cloning toolkit. *PLoS One*, *6*(9), e24531. https://doi.org/10.1371/journal.pone.0024531

Pfeiffer, B. D., Jenett, A., Hammonds, A. S., Ngo, T. T., Misra, S., Murphy, C., ... Rubin, G. M. (2008). Tools for neuroanatomy and neurogenetics in drosophila. *Proceedings of the National Academy of Sciences of the United States of America*, *105*(28), 9715–9720. https://doi.org/10.1073/pnas.0803697105

Pittaluga, A. (2016). Presynaptic release-regulating mGlu1 receptors in central nervous system. *Frontiers in Pharmacology*, *7*, 295. https://doi.org/10.3389/fphar.2016.00295

Port, F., Chen, H. M., Lee, T., & Bullock, S. L. (2014). Optimized CRISPR/Cas tools for efficient germline and somatic genome engineering in drosophila. *Proceedings of the National Academy of Sciences of the United States of America*, *111*(29), E2967–E2976. https://doi.org/10.1073/pnas.1405500111

Qi, Y. X., Xu, G., Gu, G. X., Mao, F., Ye, G. Y., Liu, W., & Huang, J. (2017). A new drosophila octopamine receptor responds to serotonin. *Insect Biochemistry and Molecular Biology*, *90*, 61–70. https://doi.org/10.1016/j.ibmb.2017.09.010

Ren, X., Sun, J., Housden, B. E., Hu, Y., Roesel, C., Lin, S., ... Ni, J. Q. (2013). Optimized gene editing technology for *Drosophila melanogaster* using germ line-specific Cas9. *Proceedings of the National Academy of Sciences of the United States of America*, *110*(47), 19012–19017. https://doi.org/10.1073/pnas.1318481110

Riabinina, O., & Potter, C. J. (2016). The Q-system: A versatile expression system for drosophila. *Methods in Molecular Biology*, *1478*, 53–78. https://doi.org/10.1007/978-1-4939-6371-3_3

Roeder, T. (1999). Octopamine in invertebrates. *Progress in Neurobiology*, *59*(5), 533–561 Retrieved from https://www.ncbi.nlm.nih.gov/pubmed/10515667

Sallee, F., Connor, D. F., & Newcorn, J. H. (2013). A review of the rationale and clinical utilization of alpha2-adrenoceptor agonists for the treatment of attention-deficit/hyperactivity and related disorders. *Journal of Child and Adolescent Psychopharmacology*, *23*(5), 308–319. https://doi.org/10.1089/cap.2013.0028

Santulli, G., & Iaccarino, G. (2013). Pinpointing beta adrenergic receptor in ageing pathophysiology: Victim or executioner? Evidence from crime scenes. *Immunity & Ageing*, *10*(1), 10. https://doi.org/10.1186/1742-4933-10-10

Seal, R. P., & Edwards, R. H. (2006). Functional implications of neurotransmitter co-release: Glutamate and GABA share the load. *Current Opinion in Pharmacology*, *6*(1), 114–119. https://doi.org/10.1016/j.coph.2005.12.001

Sherer, L. M., Catudio-Garrett, E., Morgan, H. R., Sirrs, L. A., Shearin, H. K., Williams, J. L., ... Certel, S. J. (2020). Octopamine-dependent aggression requires dVGLUT from dual-transmitting neurons. *PLoS Genetics*, [Epub ahead of print]

Snyder, A., & Silberman, Y. (2019). Stress engages novel beta-adrenergic receptor and CRF1 receptor mediated glutamatergic signaling in the ventral bed nucleus of the stria terminalis. *The FASEB Journal*, *33* (1_Suppl), 850.816. https://doi.org/10.1096/fasebj.2019.33.1_supplement.850.16

Starke, K. (2001). Presynaptic autoreceptors in the third decade: Focus on alpha2-adrenoceptors. *Journal of Neurochemistry*, *78*(4), 685–693. https://doi.org/10.1046/j.1471-4159.2001.00484.x

Sykes, P. A., & Condron, B. G. (2005). Development and sensitivity to serotonin of drosophila serotonergic varicosities in the central nervous system. *Developmental Biology*, *286*(1), 207–216. https://doi.org/10.1016/j.ydbio.2005.07.025

Takacs, V. T., Cserep, C., Schlingloff, D., Posfai, B., Szonyi, A., Sos, K. E., ... Nyiri, G. (2018). Co-transmission of acetylcholine and GABA regulates hippocampal states. *Nature Communications*, *9*(1), 2848. https://doi.org/10.1038/s41467-018-05136-1

Trendelenburg, A. U., Philipp, M., Meyer, A., Klebroff, W., Hein, L., & Starke, K. (2003). All three alpha2-adrenoceptor types serve as autoreceptors in postganglionic sympathetic neurons. *Naunyn-Schmiedeberg's Archives of Pharmacology*, *368*(6), 504–512. https://doi.org/10.1007/s00210-003-0829-x

Ultsch, A., Schuster, C. M., Laube, B., Schloss, P., Schmitt, B., & Betz, H. (1992). Glutamate receptors of *Drosophila melanogaster*: Cloning of a kainate-selective subunit expressed in the central nervous system. *Proceedings of the National Academy of Sciences of the United States of America*, *89*(21), 10484–10488. https://doi.org/10.1073/pnas.89.21.10484

Vaaga, C. E., Borisovska, M., & Westbrook, G. L. (2014). Dual-transmitter neurons: Functional implications of co-release and co-transmission. *Current Opinion in Neurobiology*, *29*, 25–32. https://doi.org/10.1016/j.conb.2014.04.010

Vaniotis, G., Del Duca, D., Trieu, P., Rohlicek, C. V., Hebert, T. E., & Allen, B. G. (2011). Nuclear beta-adrenergic receptors modulate gene expression in adult rat heart. *Cellular Signalling*, *23*(1), 89–98. https://doi.org/10.1016/j.cellsig.2010.08.007

Wang, H. L., Zhang, S., Qi, J., Wang, H., Cachope, R., Mejias-Aponte, C. A., ... Morales, M. (2019). Dorsal raphe dual serotonin-glutamate neurons drive reward by establishing excitatory synapses on VTA mesoaccumbens dopamine neurons. *Cell Reports*, *26*(5), 1128–1142 e1127. https://doi.org/10.1016/j.celrep.2019.01.014

Zhou, C., Rao, Y., & Rao, Y. (2008). A subset of octopaminergic neurons are important for drosophila aggression. *Nature Neuroscience*, *11*(9), 1059–1067. https://doi.org/10.1038/nn.2164

SUPPORTING INFORMATION

Additional supporting information may be found online in the Supporting Information section at the end of this article.

Aim 3: Is the regulation of neurotransmitter release by presynaptic mechanisms critical to constraining aggression?

Introduction

Aggression is an innate and evolutionarily-conserved behavior that animals use to gain access to food, mates, territory, and other resources. Aggressive behaviors expressed in ethological contexts are considered adaptive, as they increase an organism's chances of survival (Cassidy *et al.* 2015; de Boer 2018; Covington *et al.* 2019; Rillich *et al.* 2019; Kiyose *et al.* 2021). However, aggressive behaviors that are exaggerated, persistent, and/or expressed out of context can decrease an organism's chances of survival and reduce overall fitness (Nelson and Trainor 2007; Blair 2016; de Boer 2018; Wolf *et al.* 2018). Mechanisms that constrain aggression-promoting signals are thus a requirement for any organism, and the nervous system must provide such constraints. One such mechanism is to control the release of neurotransmitters, neuromodulators or neuropeptides from the individual presynapse (Swanson *et al.* 2005; Brady and Conn 2008; Niswender and Conn 2010; Holm and Markham 2012; Langer 2015). Such regulation either attenuates or enhances the amount or duration of each signaling molecule (Niswender and Conn 2010). To accomplish release regulation, neurons express autoreceptors.

An autoreceptor is a presynaptic receptor that responds to a neurotransmitter released from the same nerve cell in which it is expressed (Meltzer 1980; Hedqvist and Gustafsson 1981; Langer 2008, 2015). Autoreceptors regulate the presynaptic concentration of neurotransmitters by inhibiting transmitter release and synthesis, thereby reducing synaptic transmission (Langer 2008; Albert 2012). Although the responses of autoreceptors to different agonists and antagonists have been studied for decades, how presynaptic autoreceptors function to regulate neuron activity that drive behavior, the ultimate readout of circuit activity, is still poorly understood. Here, we examine the effects of increasing neurotransmitter release on aggression circuitry by reducing adrenergic and glutamatergic autoreceptor expression in a single OAergic neuron (VPM4). Our results demonstrate that control of neurotransmitter release by autoreception is critical for the regulation of high-intensity aggression.

One of the most well-studied classes of autoreceptors is the α2-adrenergic receptors (Starke 2001; Votava *et al.* 2008; Holm and Markham 2012; Rinne *et al.* 2013; Langer 2015; Qi *et al.* 2017; Devoto *et al.* 2019). In vertebrates, α2-adrenergic receptors are divided into three homologous classes: α_{2A}-, α_{2B}-, and α_{2C}-adrenergic receptors (Bylund *et al.* 1994; Saunders and Limbird 1999). α2-adrenergic receptors are members of the G_i-coupled inhibitory class of G-protein coupled receptors (GPCRs), are expressed in different regions of the vertebrate CNS, and expressed pre- and post-synaptically (Saunders and Limbird 1999; Haller and Kruk 2006). When localized to the presynapse, α2-adrenergic receptors release G_i protein upon their activation, which inhibits adenylyl cyclase activity (Saunders and Limbird 1999). This inhibition of the cAMP-dependent pathway serves as a negative feedback mechanism to inhibit further release of noradrenaline (NA) (Drouin *et al.* 2017). α2-adrenergic receptor function has been implicated in neurological disorders, with agonists being used to treat attention deficit hyperactivity disorder (Kamisaki *et al.* 1992; Connor and Rubin 2010) and antagonists being used to treat major depressive disorder (Watanabe *et al.* 2012), schizophrenia (Frånberg *et al.* 2012), bipolar disorder (Frye *et al.* 1998), and dementia (Rinne *et al.* 2013). However, it remains unclear (and at times contradictory) how α2-adrenergic receptor activity relates to pathological behavior (Gregg and Siegel 2001; Votava *et al.* 2008) due to the difficulty of separating the effects of presynaptic and postsynaptic α2-adrenergic receptor activation via pharmacological agents (Nelson and Trainor 2007). This research limitation can be overcome *in vivo* with the comprehensive genetic toolkit available in *Drosophila*.

Octopamine (OA), the invertebrate analog of NA, activates functionally conserved adrenergic receptors (Yellman *et al.* 1997; Evans and Maqueira 2005; Farooqui 2012; Qi *et al.* 2017). An ortholog of vertebrate α2-adrenergic receptors (OAα2R) was recently described and shown to function in the inhibition of cAMP via inhibiting adenylyl cyclase (Qi *et al.* 2017), a novel role for OA. In conjunction with our collaborators, we recently determined OAα2R to be widely expressed in OAergic neurons in the *Drosophila* CNS (McKinney *et al.* 2020), suggesting that autoreception is an important presynaptic regulatory mechanism in OAergic neurons. The α2-like-adrenergic family was unknown in invertebrates (Evans and Maqueira 2005; Farooqui 2012; Bayliss *et al.* 2013) until the first α2 family member was isolated from *Chilo suppressalis* (Wu *et al.* 2014)*,* and the *Drosophila* OAα2R was the second α2 member to be characterized (Qi *et al.*

2017; Blenau *et al.* 2020). Thus, these experiments present an exciting opportunity to examine the functional effects of α2 autoreceptor activity at single-neuron resolution *in vivo.*

Glutamatergic autoreception occurs through the activation of metabotropic glutamate receptors (mGluRs) (Shigemoto *et al.* 1997; Swanson *et al.* 2005). mGluRs are glutamate-activated GPCRs that form through the dimerization of mGluR subunit proteins (Niswender and Conn 2010; Moustaine *et al.* 2012; Levitz *et al.* 2016). Vertebrate mGluRs are subdivided into three groups based on sequence similarity, second-messenger pathway, and pharmacological profile (Ji-Quan Wang and Anna-Liisa Brownell 2007). Group I mGluRs (consisting of mGluR1 and mGluR5) are excitatory G_q-coupled that localize to the postsynapse (Swanson *et al.* 2005; Conn *et al.* 2009; Kumari *et al.* 2013). Group II (consisting of mGluR2 and mGluR3) and Group III mGluRs (consisting of mGluR4, mGluR6, mGluR7, and mGluR8) function as negative feedback autoreceptors that inhibit the cAMP-dependent pathway via the release of $G_{i/o}$ protein that negatively regulates adenylyl cyclase activity (Shigemoto *et al.* 1997; Brady and Conn 2008; Niswender and Conn 2010). This inhibition reduces neuron excitability and thus further release of glutamate. In vertebrates, mGluRs have been implicated in neurological disorders such as general anxiety disorder (Swanson *et al.* 2005), Alzheimer's (Niswender and Conn 2010), and schizophrenia (Conn *et al.* 2009). Despite their apparent clinical importance, the challenge of synthesizing and administering receptor-specific pharmacological agents to differentially activate a highly-conserved glutamate-binding domain has made determining the roles of specific mGluRs in disease difficult (Conn *et al.* 2009).

The single *Drosophila* mGluR (mGluR) is an ortholog of group II mGluRs (Eroglu *et al.* 2003; Bogdanik *et al.* 2004; Devaud *et al.* 2008). Due to the prominent role for glutamate as an excitatory neurotransmitter in both the invertebrate CNS and peripheral nervous system (PNS), mGluR is widely expressed in many types of neurons. (Devaud *et al.* 2008; Schoenfeld *et al.* 2013) mGluR is found in the periactive zone of the larval NMJ, where it modulates frequency-dependent glutamate release (Bogdanik *et al.* 2004). In the adult brain, mGluR is expressed and required in Kenyon cells for olfactory learning (Andlauer *et al.* 2014) and in the CNS generally for social behaviors, such as courtship (Schoenfeld *et al.* 2013). Despite its widespread expression throughout the *Drosophila* brain, mGluR is expressed in <10 octopamine-glutamate

dual-transmitting neurons (OGNs) (Kuchenbrod, Sherer, and Certel, unpublished data). This sparse expression suggests an important role for mGluR in regulating glutamate release within individual OGNs.

The VPM4 neuron in the adult *Drosophila* brain provides an excellent model with which to examine the functional effects of mGluR- and α2-mediated autoreception. VPM4 was originally described as a cluster of ~5 OAergic neurons (Busch *et al.* 2009), but subsequent studies have identified it as a single neuron (Burke *et al.* 2012; Hoopfer 2016; Youn *et al.* 2018; Sayin *et al.* 2019). VPM4 is located in the subesophageal zone (SEZ) of the adult *Drosophila* brain, a region which plays a role in processing sensory information (Andrews *et al.* 2014; Hartenstein *et al.* 2018). VPM4 has previously been shown to promote feeding behavior by switching behavior from tracking to feeding via mushroom body output neuron inhibition and extending the proboscis in response to sugar (Youn *et al.* 2018; Sayin *et al.* 2019). More recent work has characterized VPM4 as expressing vesicular transporters for both monoamines and glutamate, with both transporters localized together in the majority of synaptic endings (Sherer *et al.* 2020). The major role that VPM4 plays in processing and relaying information to critical behavioral circuits via multiple transmitters suggests the existence of presynaptic mechanisms that serve to carefully control transmitter release. Indeed, uncommon for OA neurons, VPM4 expresses autoreceptors for OA and glutamate, namely both the α2 adrenergic-like receptor (OAα2R) and the single *Drosophila* metabotropic glutamate receptor (mGluR).

In this study, we test the hypothesis that negative-feedback autoreceptors constrain aggression-promoting signals from OGNs using a single OGN, VPM4, which we have previously identified as an OGN regulator in the transmission of aggression-promoting information (Sherer *et al.* 2020). We demonstrate expression of OAα2R and mGluR in VPM4 and examine the role of these autoreceptors in constraining mid-intensity and high-intensity aggressive behaviors. RNAi-mediated knockdown of either OAα2R or mGluR in males results in a significant increase in the number of boxing and holding bouts (high-intensity aggressive behavior) without changing the number of lunges (medium-intensity aggressive behavior) performed. Moreover, RNAi reduction of either the rate-limiting enzyme in OA synthesis TβH (i.e., decreasing OA release) or OAα2R (i.e., increasing OA release) demonstrate a secondary role for OA release from VPM4 in

inhibiting inter-male courtship and suggest the involvement of VPM4 within multiple decision-making circuits. Taken together, these experiments determine that mGluR- and OAα2R-mediated autoreception is a presynaptic mechanism in VPM4 that constrains the transmission of aggression-promoting signals and offers Group II mGluRs and α2 adrenergic autoreceptors as potential targets in the treatment of high-intensity aggression.

Results

VPM4 expresses both octopamine and glutamate

Autoreceptors that are able to attenuate or enhance transmitter release as a result of neuron activity have been proposed as a presynaptic mechanism that would expand the functionality of individual dual-transmitting neurons by allowing them greater control over neurotransmitter release (Figure 1A) (Burnstock 2004; De-Miguel *et al.* 2015; Shin *et al.* 2018; Nässel 2018; Trudeau and El Mestikawy 2018; Svensson *et al.* 2019; Nässel and Zandawala 2019). To test the hypothesis that presynaptic mechanisms in OGNs play a role in constraining aggression, we characterized a ventral paired median OA neuron, VPM4, as an autoreceptor-expressing OGN. Previous studies have identified VPM4 as an OAergic neuron that extends arborizations to higher brain regions that mediate gustatory behaviors such as the subesophagheal ganglion, the periesophageal neuropil, and the γ-lobe of the mushroom body (Busch *et al.* 2009; Burke *et al.* 2012; Youn *et al.* 2018; Sayin *et al.* 2019). We used the Janelia split-Gal4 driver MB113C (hereafter *VPM4-gal4*) to identify and manipulate the VPM4 neuron. Here we report that VPM4 is also glutamatergic and expresses the OA autoreceptor OAα2R and the glutamate autoreceptor mGluR.
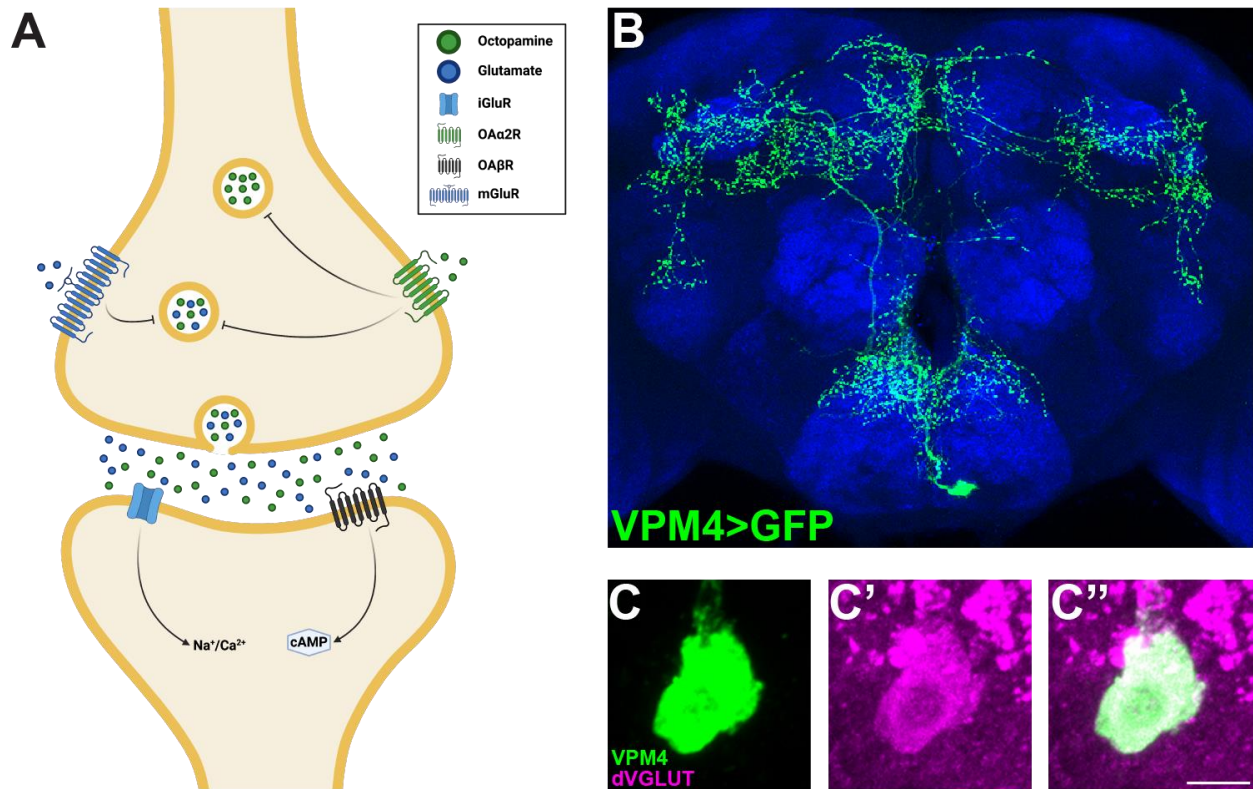
Figure 2 Description and Characterization of a Single OGN (**A**) Individual OGNs can use several mechanisms to expand their signaling capabilities, including segregating OA and glutamate in different vesicles within the same terminal (green and blue circles) and inhibiting transmitter release through OA (green) or glutamate (blue) autoreceptors. Signaling can be further refined downstream through expression of OA receptors (black) and/or glutamate-gated ion channels (blue) at the postsynapse. (**B**) Fluorescent labeling of VPM4, a single OA neuron, using *VPM4-gal4*. The cell body of VPM4 is localized to the SEZ and the neuron extends arborizations throughout the *Drosophila* brain. (**C-C"**) VPM4 consistently co-expresses dVGLUT, confirming its status as an OGN. Scale bar represents 5 µm. (Note: the image shown in Figure 1B is also shown in Figures 2A, 3A, and 4A).

Expression of a vesicular glutamate transporter (VGLUT) has been used to demonstrate glutamate expression within dual-transmitting neurons (Zhang *et al.* 2015; Aguilar *et al.* 2017; Pagani *et al.* 2019; Okaty *et al.* 2019; Mingote *et al.* 2019). To examine glutamate expression in VPM4, we used a dVGlut monoclonal antibody that has been previously characterized (Banerjee *et al.* 2021). VPM4 was visualized by a *UAS-6xGFP* reporter (*VPM4>GFP*) (Figure 1B). We identified colocalization between dGVLUT and *VPM4>GFP* (Figure 1C-C"), consistent with our previous finding that a majority of OA neurons in the SEZ co-express glutamate.

Reducing mGluR in VPM4 increases high-intensity aggression

Within neuronal subsets, small numbers of neurons exist that are required to modulate specific behaviors (Hoopfer *et al.* 2015; Duistermars *et al.* 2018; Palavicino-Maggio *et al.* 2019). Even within the ~100 neuron OAergic system, small neuronal subsets have been shown to be required for crucial behaviors (Certel *et al.* 2007; Zhou *et al.* 2008; Machado *et al.* 2017; Youn *et al.* 2018; Claßen and Scholz 2018; Masuzzo *et al.* 2019). The *Drosophila* mGluR is an ortholog to vertebrate group II mGluRs, which localize to glutamatergic synapses and constrain glutamate release (Panneels *et al.* 2003; Eroglu *et al.* 2003; Bogdanik *et al.* 2004). Within OGNs, mGluR expression is limited to <10 neurons, suggesting an important role for a mechanism to constrain glutamatergic transmission within mGluR-expressing OGNs. We reasoned that, due to this sparseness of expression, glutamatergic output from mGluR-expressing OGNs would be critical to their function and examined VPM4 for mGluR expression using *VPM4>GFP* and a monoclonal antibody specific to the *Drosophila* mGluR (Figure 2A) that has been previously characterized (Panneels *et al.* 2003). We identified colocalization between *VPM4>GFP* and mGluR (Figure 2B-B''), indicating expression of a glutamate autoreceptor in VPM4.

Figure 3 Expression of mGluR in VPM4 is required to constrain high-intensity aggression
(**A**) Fluorescent labeling of VPM4 using *VPM-gal4*. (**B-B"**) VPM4 expresses the *Drosophila* glutamate autoreceptor mGluR. Scale bar represents 5 μm. (**C**) The number of lunges performed by *VPM4-mGluR^RNAi* males does not differ significantly from controls (all significance tests are Kruskal-Wallis with Dunn's multiple comparison test except where noted, ns = no significance). (**D**) The number of boxing bouts performed by *VPM4-mGluR^RNAi* males is significantly higher compared to controls (***p < 0.001, ****p < 0.0001). (**E**) The number of holding bouts performed by *VPM4-mGluR^RNAi* males is significantly higher compared to controls (*p < 0.05, **p < 0.01). (**F**) A significantly higher percentage of *VPM4-mGluR^RNAi* pairs (85%) exhibit high-intensity aggression compared to control pairs (46%, 39%) (*p < 0.05)

122

Our lab recently demonstrated that glutamatergic release is required for aggressive behavior (Sherer *et al.* 2020). Determining if mGluR-mediated inhibition of glutamate release alters the transmission of aggression-promoting signals would further indicate the importance of glutamate release from OGNs to promote aggression. We reduced expression of mGluR in VPM4 using *VPM4-gal4*-driven UAS inverted repeat transgene targeting *mGluR* (*VPM4>UAS-mGluR^{RNAi}*). *VPM4>mGluR^{RNAi}* males and transgenic controls were recorded and multiple agonistic parameters quantified including the number of lunges, the number of holding bouts, and the number of boxing bouts. As behavioral patterns are scored only after the first lunge occurs, each male pair has the same amount of time to exhibit aggressive behavior. Certel lab undergraduate researchers Samantha Chong and Raegan Hauschildt were instrumental in quantifying boxing, holding, and courtship data for this study. *VPM4>mGluR^{RNAi}* male pairs exhibited no change in the number of lunges performed compared to transgenic controls (Figure 2C). However, *VPM4-mGluR^{RNAi}* males displayed a significant increase in the number of holding bouts (Figure 2D) and boxing bouts (Figure 2E) as compared to controls. Furthermore, nearly 100% of fights between *VPM4-mGluR^{RNAi}* males included two or more bouts of holding or boxing as compared to control pairs, which exhibited $\leq$ 50% (Figure 2F). These results indicate mGluR is required within VPM4 neurons to inhibit glutamate release and constrain high-intensity aggression.

Reducing OAα2R in VPM4 increases high-intensity aggression

The recently-identified *Drosophila* OAα2R is an ortholog to vertebrate α2-adrenergic receptors, which localize to NA synapses and constrain NA release (Drouin *et al.* 2017; Devoto *et al.* 2019). Both α2-adrenergic receptors and OAα2R attenuate neurotransmitter release by inhibiting cAMP synthesis (Saunders and Limbird 1999; Qi *et al.* 2017), thus acting as inhibitory autoreceptors. Along with our collaborators, we determined that OAα2R is widely expressed throughout OA neurons, suggesting that OAα2R activation attenuates octopamine signaling from OGNs (McKinney *et al.* 2020). We examined VPM4 for OAα2R expression using *VPM4>GFP* and a *UAS-nucRFP* reporter under control of *OAα2R-lexA* (*OAα2R>nucRFP*) (Figure 3A). Colocalization between the soma of *VPM4>GFP* and the nuclei of *OAα2R>nucRFP* occurs, indicating OAα2R expression in VPM4 (Figure 3B-B'').
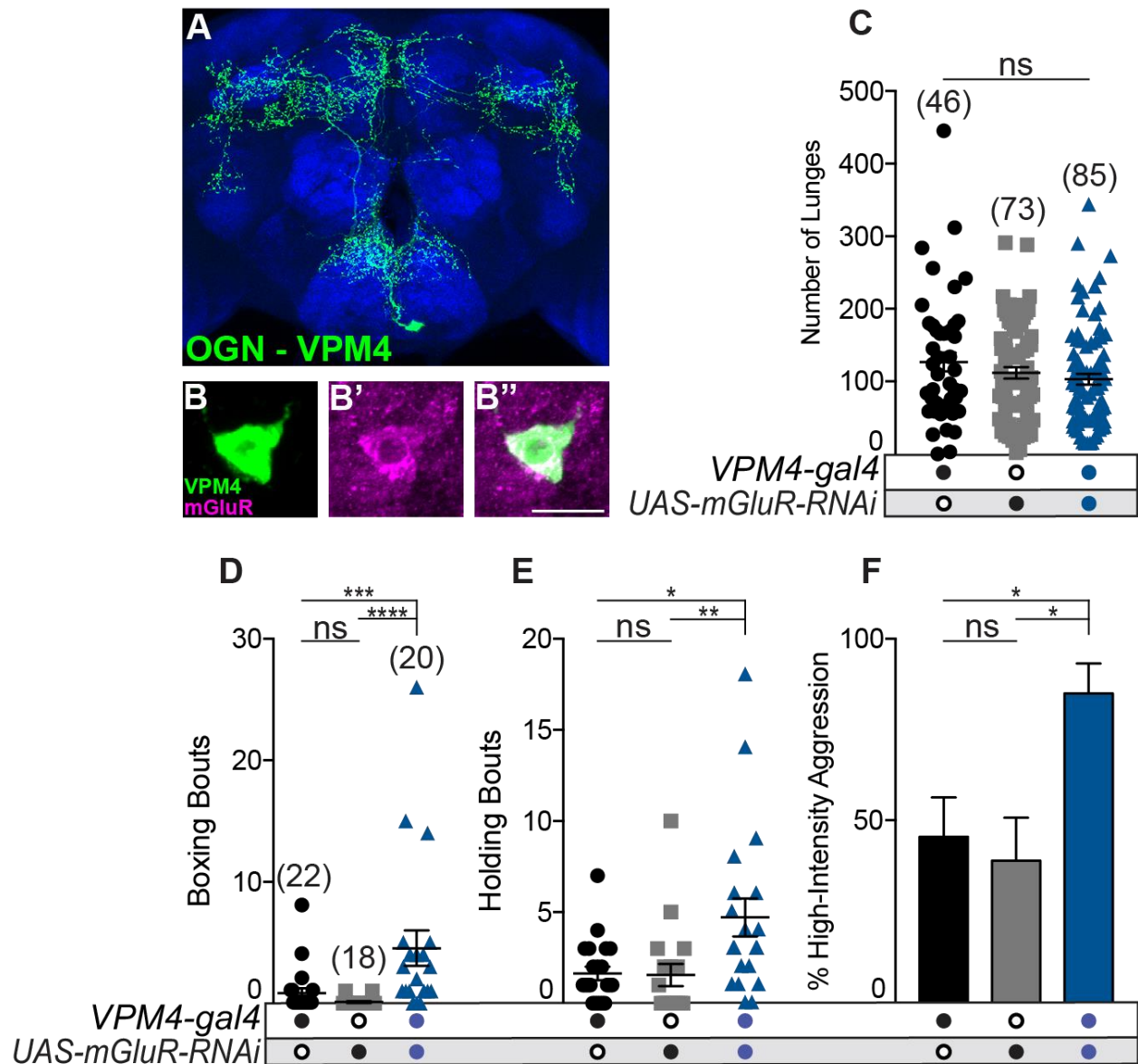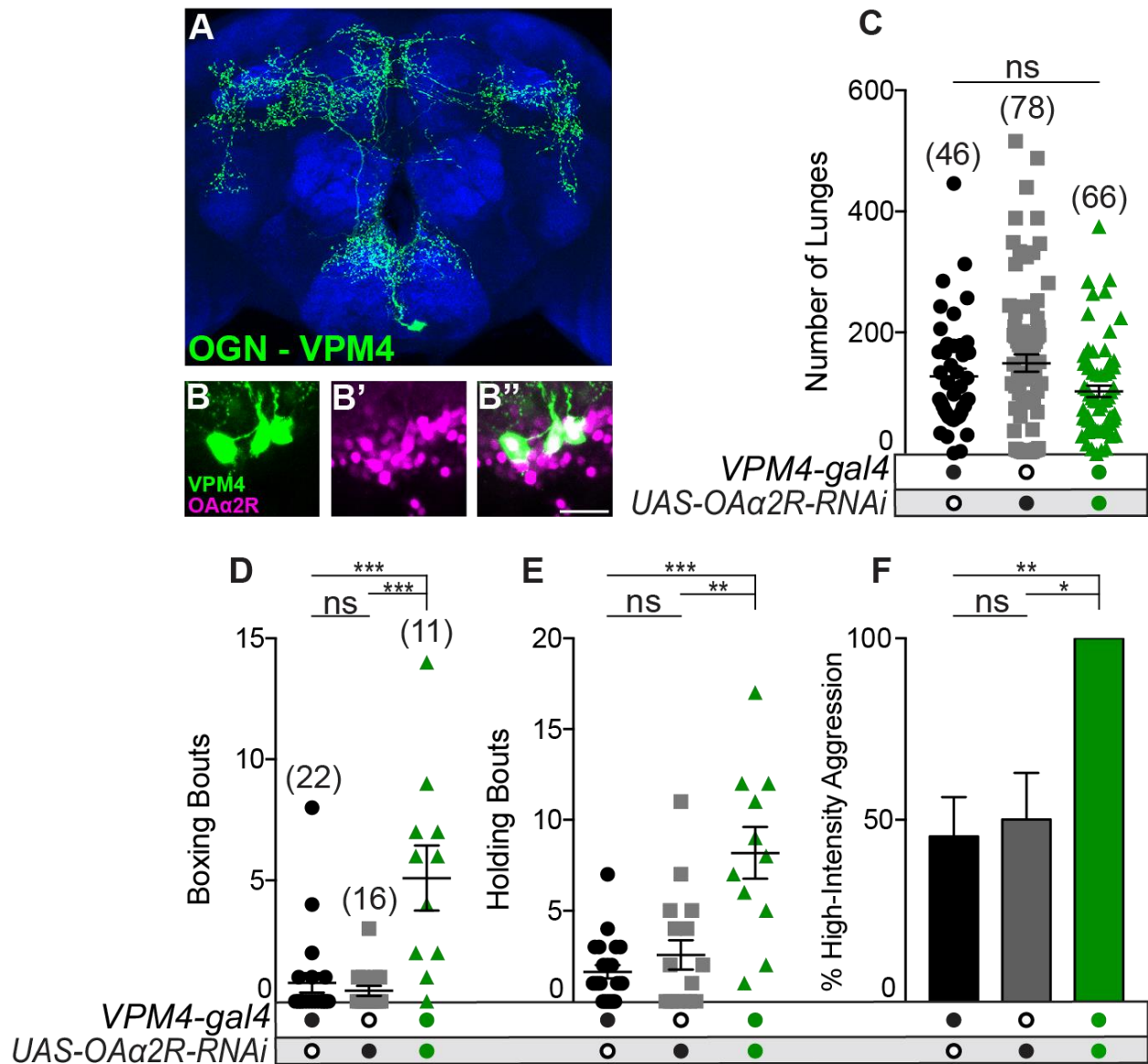
Figure 4 Expression of OAα2R in VPM4 is required to constrain high-intensity aggression
(**A**) Fluorescent labeling of VPM4 using *VPM-gal4*. (**B-B”**) VPM4 expresses the *Drosophila* OA autoreceptor OAα2R. Scale bar represents 20 μm. (**C**) The number of lunges performed by *VPM4>OAα2R^{RNAi}* males does not differ significantly from controls (ns = no significance). (**D**) The number of boxing bouts performed by *VPM4>OAα2R^{RNAi}* males is significantly higher compared to controls (***$p < 0.001$). (**E**) The number of holding bouts performed by *VPM4>OAα2R^{RNAi}* males is significantly higher compared to controls (**$p < 0.01$, ***$p < 0.001$). (**F**) A significantly higher percentage of *VPM4>OAα2R^{RNAi}* pairs (100%) exhibit high-intensity aggression compared to control pairs (46%, 50%) (*$p < 0.05$, **$p < 0.01$).

Our lab and others have determined OA release is required to promote male aggression and inhibit inter-male courtship. We hypothesized that like mGluR, OAα2R-mediated inhibition of

OA release from VPM4 would provide a presynaptic mechanism for regulating aggression and courtship and would serve to constrain aggressive behavior. We reduced expression of OAα2R in VPM4 using a *VPM4-gal4*-driven inverted repeat transgene targeting *OAα2R* (*VPM4>OAα2R^RNAi*) and quantified agonistic behavior. As in *VPM4>mGluR^RNAi* flies, male *VPM4>OAα2R^RNAi* pairs exhibited no change in the numbers of lunges performed (Figure 3C) but exhibited a significant increase in the number of holding bouts (Figure 3D) and boxing bouts (Figure 3E). We also observed a significant increase in the percentage of highly-aggressive *VPM4>OAα2R^RNAi* male pairs compared to controls (Figure 3F). These results indicate a role for OAα2R activity within VPM4 in constraining high-intensity aggression by inhibiting the release of OA.
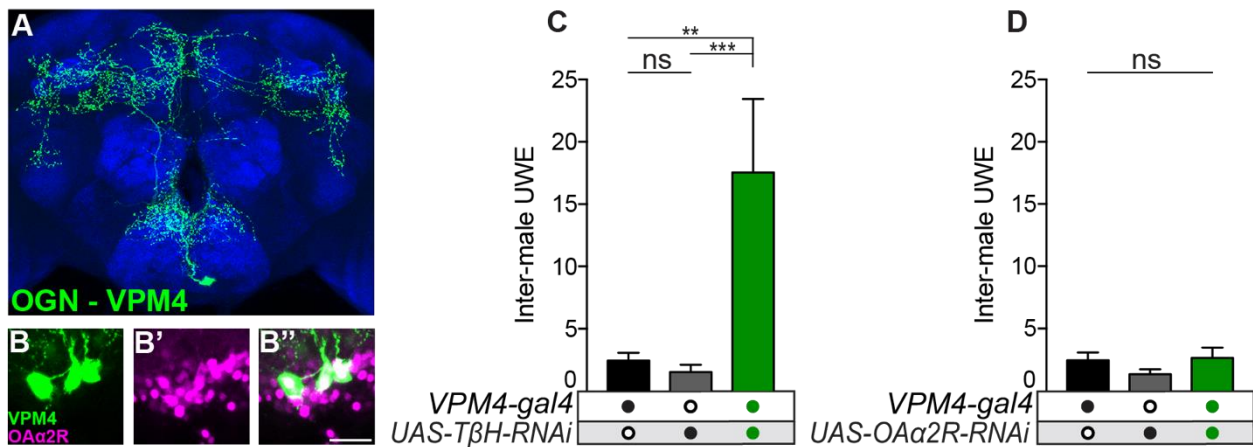

Figure 5 OA signaling is required from VPM4 to inhibit inter-male courtship (**A**) Fluorescent labeling of VPM4 using *VPM-gal4*. (**B-B"**) VPM4 expresses the *Drosophila* OA autoreceptor OAα2R. Scale bar represents 20 μm. (**C**) The number of inter-male courtship behaviors performed by *VPM4>TβH^RNAi* males is significantly higher compared to controls (****p < 0.01, ***p < 0.001). (**D**) The number of inter-male courtship behaviors performed by *VPM4>OAα2R^RNAi* males does not differ significantly from controls (ns = no significance).

Based on studies using classical mutants to eliminate OA, it is known that OA is required to inhibit inter-male courtship within an aggression assay (Certel *et al.* 2007, 2010; Andrews *et al.* 2014). To verify that OA is required from the VPM4 neuron itself to inhibit inter-male courtship, we reduced OA function by expressing the rate-limiting enzyme for OA, tyramine β-hydroxylase (TβH) using a *VPM4*-driven inverted repeat transgene targeting *TβH* (*VPM4>TβH^RNAi*) and quantified inter-male courtship behaviors as unilateral wing extensions (UWE, or "singing")

followed by additional courtship behaviors (licking, abdomen bends, repeated wing extensions, etc.). Inter-male courtship is usually observed among wild-type male pairs (albeit at low levels) at the beginning of fights, presumably while males are identifying the sex of the second fly in the chamber (Gupta et al. 2017). As expected, we observed a significant increase in inter-male courtship between *VPM4>TβH^RNAi* males relative to transgenic controls (Figure 4C). This result indicates a role for OA signaling from VPM4 in attenuating courtship circuits. Since decreasing OA signaling resulted in an increase in courtship, we reasoned that increasing OA release by reducing *OAα2R*-mediated negative feedback would lead to a decrease in courtship (i.e. that reducing *OAα2R* expression in VPM4 would have the opposite effect of reducing *TβH* expression). When we quantified inter-male courtship in the *VPM4>OAα2R^RNAi* males described previously, we observed a recapitulation of the wild-type inter-male courtship phenotype (Figure 4D), indicating that OAα2R-mediated inhibition of OA release from VPM4 is important for constraining courtship behaviors.

VPM4 synaptically connects to MBON11 and receives OA input

VPM4 extends arborizations to higher brain regions such as the subesophagheal ganglion, the periesophageal neuropil, and the γ-lobe of the mushroom body (Busch *et al.* 2009; Burke *et al.* 2012; Youn *et al.* 2018; Sayin *et al.* 2019). Using a recently-published EM connectome of a partial female adult *Drosophila* brain (Zheng *et al.* 2018), we examined VPM4 innervation to identify potential downstream neurons that might be part of an aggression circuit. We identified a mushroom body output neuron, MBON11, as a potential downstream partner due to the relatively high number of synaptic contacts formed (MBON11 is the neuron with the fourth-highest number of post-synapses with VPM4) (Sayin *et al.* 2019) and its location in the γ-lobe of the mushroom body, a region which has previously been shown to modulate arousal threshold, olfactory learning, and salience-based decision making (McGuire *et al.* 2001; Zhang *et al.* 2007; Aso *et al.* 2014; Vogt *et al.* 2014; Awata *et al.* 2019).
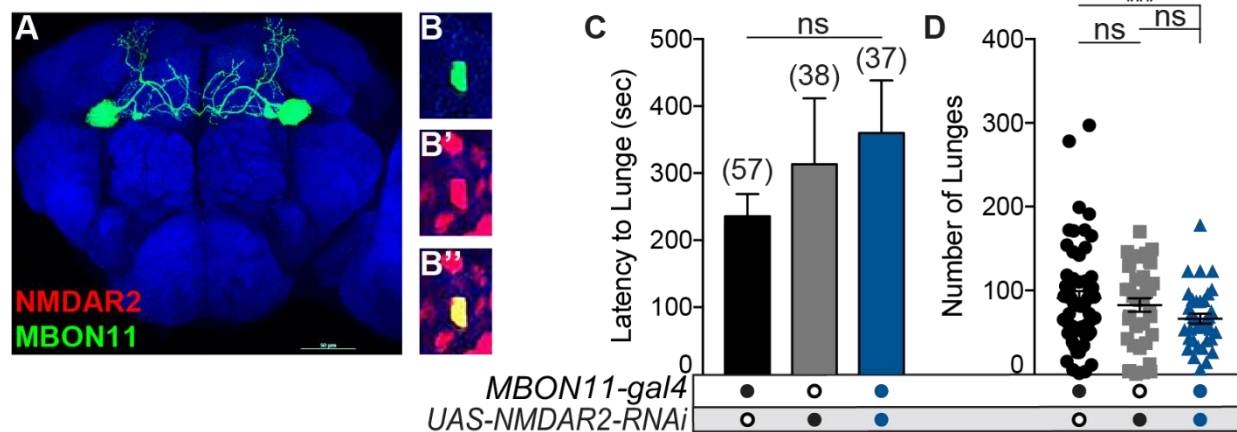
Figure 6 MBON11 expresses the glutamate-gated ion channel subunit NMDAR2 (**A**) Fluorescent labeling of MBON11, a neuron directly downstream of VPM4, using *MBON11-gal4*. (**B-B"**) MBON11 expresses the *Drosophila* NMDA receptor subunit NMDAR2. Scale bar represents 50 μm. (**C**) The latency to lunge does not differ significantly between *MBON11>NMDAR2^{RNAi}* males and controls (ns = no significance). (**D**) The number of lunges performed by *MBON11>NMDAR2^{RNAi}* males is significantly lower than *MBON11-gal4* controls but not *UAS-NMDAR2^{RNAi}* controls (***$p < 0.001$, ns = no significance).

Based on our previous results indicating the importance of OA and glutamate release from VPM4, we reasoned that neurons downstream to VPM4 would express OA and/or glutamate receptors to receive this signal. Our collaborators performed a screen for glutamate receptors using the Janelia split-Gal4 driver MB112C (hereafter *MBON11-gal4*), to identify and manipulate MBON11, and lexA lines for glutamate receptor subunits (*GluR-lexA*). *MBON11-gal4* and *GluR-lexA*-driven nuclear reporters were used to visualize expression patterns (Figure 5A). We identified expression of the NMDA receptor subunit NMDAR2 in MBON11 (Figure 5B-B"), suggesting that expression of NMDA receptors is a postsynaptic mechanism by which MBON11 receives glutamatergic signals. To determine the role of MBON11 NMDARs in aggression, we reduced expression of NMDAR2 in MBON11 using an *MBON11-gal4*-driven inverted repeat transgene targeting NMDAR2 (*MBON11>NMDAR2^{RNAi}*) and quantified the latency to lunge (the amount of time it takes for a pair to initiate aggressive behavior) (Figure 5C) and the number of lunges performed by *MBON11>NMDAR2^{RNAi}* male pairs and transgenic control male pairs (Figure 5D). While these experiments are still ongoing, existing statistical significance between *MBON11>NMDAR2^{RNAi}* the and the transgenic *MBON11-gal4* control suggests that NMDAR2 expression in MBON11 is required for aggressive behavior.
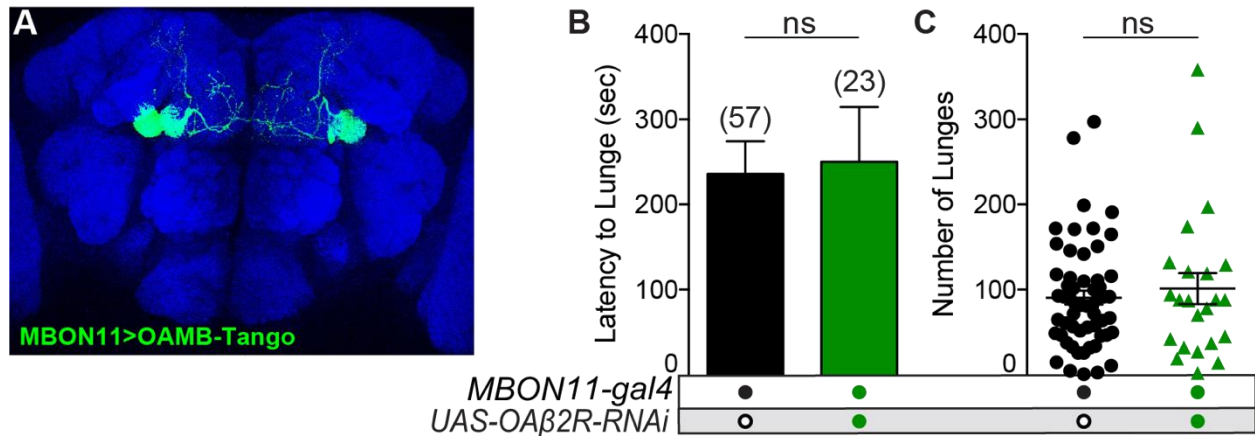
Figure 7 MBON11 responds to OA signaling (**A**) OAMB-Tango expressed using *MBON11-gal4*. GFP expression is mediated through OA binding to the OAMB-Tango construct, indicating a response to an OA signal. (**B**) The latency to lunge does not differ significantly between *MBON11>OAβ2R^{RNAi}* males and controls (Mann-Whitney test, ns = no significance). (**C**) The number of lunges performed by *MBON11>OAβ2R^{RNAi}* males does not differ significantly from *MBON11-gal4* controls (Mann-Whitney test, ns = no significance).

To determine whether MBON11 receives OAergic input, we expressed a *UAS*-driven transgene encoding an OA-responsive variant of the Tango assay (Barnea *et al.* 2008) under control of *MBON11-gal4* (*MBON11>OAMB-Tango*). Briefly, OAMB-Tango is expressed in neuron(s) of interest under control of a *GAL4* and subsequently drives *lexA*-mediated expression of a *lexAop*-controlled reporter upon OA binding (Inagaki *et al.* 2012). We detected expression of our *MBON11>OAMB-Tango*-mediated GFP reporter (Figure 6A), indicating that MBON11 receives OA input. An RNAi-mediated screen for OA receptors in MBON11 is currently ongoing to identify which receptor(s) are expressed by MBON11 to receive this OA input and their contributions to aggression (Figure 6B-C).

Discussion

The functional outcome of dual transmission adds a layer of complexity to neuron communication, expanding a neuron's signaling capabilities by enabling it to modulate the spatial and temporal aspects of neurotransmitter release, enhance packaging of transmitters in synaptic vesicles to modulate signal strength, and even regulate its own activity via negative feedback (Starke 2001; Burnstock 2004; El Mestikawy et al. 2011; Vaaga et al. 2014; Trudeau and El Mestikawy 2018; Svensson et al. 2019). However, little is known about how neurons

themselves manage this additional complexity, and investigating the mechanisms within neurons that control transmitter release provides an opportunity to both better understand how neurons transmit signals and provides new targets for regulating behavior. In this study, we identified autoreception as a critical presynaptic mechanism to constrain aggression by inhibiting transmitter release from a dual transmitting neuron. We determined that the OAergic neuron VPM4 also expresses glutamate, identified expression of the glutamate autoreceptor mGluR in VPM4, and describe a functional role for glutamate release by determining that mGluR is required for constraining holding and boxing but not lunging. Furthermore, we determined that the OA autoreceptor OAα2R is also required in VPM4 to constrain holding and boxing and show that OA release from VPM4 is required to inhibit courtship. Lastly, we determine that a neuron directly downstream of VPM4, MBON11, expresses both OA and glutamate receptors, suggesting a postsynaptic mechanism to control signaling.

Our data show the same effects on holding and boxing when either mGluR is reduced (leading to increased glutamate release) or OAα2R is reduced (leading to increased OA release) in VPM4, and that decreased OA release from VPM4 results in increased courtship. Two important findings emerge from these results. First, they provide an additional functional role for dual transmission in the nervous system by identifying behaviors constrained by autoreceptor-mediated inhibition of two transmitters released from a single neuron. Secondly, these results indicate that high-intensity aggressive behaviors can be separated from both mid-intensity aggressive behaviors (lunges) and mutually-exclusive sexually dimorphic behaviors (courtship) by modifying neurotransmitter release from a single neuron, suggesting the existence of neuronal circuits that control different behaviors.

The fact that a holding/boxing phenotype is observed when either mGluR or OAα2R is reduced suggests that OA and glutamate release from VPM4 act in a synergistic manner. How would two neurotransmitters work to constrain a single behavior? One possibility is that the release of one transmitter might enhance the release of the other. If OA and glutamate release from VPM4 functions in this way, we would expect to see the same increase in holding/boxing if either mGluR or OAα2R was reduced (i.e. if the negative feedback mechanism for either transmitter was disrupted). Such a role would fit in the Glutamate Amplifies Noradrenergic Effects (GANE)

model (Mather *et al.* 2016). In this model, increased glutamate release that spills over into depolarized noradrenergic terminals evokes increased noradrenaline release. Typically, noradrenaline is released constantly at low-to-moderate levels (Berridge *et al.* 2012; Sara and Bouret 2012). This continuous low level is sufficient to activate high-affinity α2 receptors, which inhibit release of higher levels of noradrenaline (Mather *et al.* 2016). Glutamate spillover onto noradrenergic terminals causes high levels of norepinephrine release that are able to overcome the inhibitory effects of α2 receptors. In this way, glutamatergic neurons can increase local NA release from separate NA terminals. However, there is no reason GANE couldn't also occur in individual NA/glutamate terminals. If both transmitters were released from the same neuron, GANE would lead to multiple excitotoxic positive feedback loops, and thus we would expect the release of both transmitters in that neuron to be tightly controlled. Glutamate release from noradrenergic neurons might thus be a mechanism used by OGNs to locally enhance OA release, and expression of autoreceptors for both glutamate and OA would be a mechanism for OGNs to inhibit unrestrained positive feedback loops. This tight control over transmitter release would ultimately allow OGNs to mediate between their fast-excitatory and neuromodulatory effects in response to weak and strong stimuli, respectively. Another possibility that cannot be ruled out is that OAα2R and mGluR act independently within VPM4 to constrain high-intensity aggression. In this case, the holding/boxing pheonotype resulting from reducing expression of both autoreceptors simultaneously would be greater than the phenotype from reducing either autoreceptor alone. Future experiments in which expression of both mGluR and OAα2R are simultaneously reduced will distinguish between these possibilities.

Recent work has focused on identifying modules of just a few neurons that mediate specific behaviors (Youn *et al.* 2018; Carreira-Rosario *et al.* 2018; Duistermars *et al.* 2018; Awata *et al.* 2019; Masuzzo *et al.* 2019; Sayin *et al.* 2019). Our results demonstrate a role for VPM4 in regulating both courtship and high-intensity aggression. How might a single neuron mediate a switch between such mutually exclusive behaviors? Koganezawa *et al* proposed a multilayered inhibitory network that mediates a switch from courtship behavior to aggression. In this model, courtship behavior is the result of inhibitory circuits that suppress aggression centers, while aggressive behavior is initiated by activation of aggression centers as a result of the inactivation of these inhibitory circuits in response to male conspecifics (Koganezawa *et al.* 2016). Our data

supports a similar decision-making principle, in which OA release from VPM4 functions as a behavioral switch between mutually-exclusive sex-specific behaviors. Our lab and others have demonstrated that OA release is required to promote aggression and to inhibit courtship. Our results show that decreased OA release from VPM4 as a result of decreased OA synthesis and inhibitory OAα2R activity results in increased courtship, while increased OA release in response to decreased OAα2R activity mediates a switch from courtship to aggression. In this way, OA release levels allow downstream circuitry to distinguish between mutually exclusive OA-dependent behaviors in response to OA signal strength.

While this study is focused on the presynaptic mechanisms that constrain neurotransmitter release, it also has broader implications for the evolution of these mechanisms in organisms. Why would a neuron involved in feeding also regulate both aggression and courtship? OA signaling and aminergic signaling broadly is a requirement for appetitive learning (in which reward signaling is imbued with motivational salience) (Burke *et al.* 2012; Wu *et al.* 2013; Benelli *et al.* 2015; Sayin *et al.* 2019), although VPM4 alone is not sufficient for reward conditioning (Burke *et al.* 2012). While a single neuron is unsurprisingly not the only factor involved in reward memory formation, VPM4 is responsible for controlling significant behaviors relating to motivational state. Transmitter release from VPM4 is sufficient to inhibit odor seeking and promote feeding behavior by enhancing the responses of sensory neurons (Youn *et al.* 2018; Sayin *et al.* 2019). The coupling of food source evaluation to increased motivation for aggression via a single neuronal signal would provide an advantage in making any quick fight-or-flight decision. It might also provide advantages in mating decisions. Andrews *et al* show that gustatory neurons form synaptic connections to OA neurons in the SEZ (such as VPM4) and define an aggression-promoting circuit in which the male-specific hormone (*z*)-7-tricosene is detected by gustatory neurons and relayed to OA neurons (Andrews *et al.* 2014). While these pheromones are generally found on the cuticle of adult flies and detected via close proximity (Fan *et al.* 2013; Kravitz and Fernández 2015; Kim *et al.* 2017), it has also been shown that male flies place (*z*)-7-tricosene on valuable food sources both to stake a territorial claim and to encourage female oviposition (Lin *et al.* 2015). Activation of a gustatory neuron that can both allow an organism to determine the value of a resource and detect a threat to resource access which would jeopardize both its prolonged survival and its ability to pass on its genes would be

expected to generate intense aggressive motivation. Our results advance an understanding of how the controlled release of neuromodulatory substances from neurons can allow organisms to respond appropriately to stimuli from a dynamic social environment.

Materials and Methods

Drosophila Husbandry and Stocks

The following strains were used in this study: Canton-S (BDSC 64349), *MB113C* (BDSC 68264), *MB112C* (BDSC 68263) *OAα2R-lexA* (BDSC 52743), *20x-UAS-6xGFP* (Steve Stowers), *13xlexAop2-CD8::GFP* (BDSC 32205), *lexAop-nucRFP* (Steve Stowers), *UAS-OAMB-Tango* (BDSC 68235), *UAS-mGluR^{IR}* (BDSC 34872), *UAS-OAα2R^{IR}* (BDSC 50678), *UAS-TβH^{IR}* (BDSC 27667), *UAS-NMDAR2^{IR}* (BDSC 40846). All flies were reared on standard cornmeal-based fly food (Toivonen *et al.* 2007). Unless noted otherwise, during development and post-eclosion, flies were raised at 25°C, ~50% humidity and a 12:12hr light-dark cycle (1400±200 lx white fluorescent light) in humidity- and temperature-controlled incubators.

Aggression Assays

Male pupae were isolated and aged individually in 16x100mm borosilicate glass tubes containing ~1.5 mL of standard food medium as previously described (Certel and Kravitz 2012). For aggression assays, pairs of 3–7 day old, socially naïve adult males were aspirated into divided behavior chambers and left for a period of at least 24 hours to allow for recovery from anesthetization as described previously (Chowdhury *et al.* 2021). All assays were run at 25 ± 1 °C and $\geq 45\%$ humidity.

Scoring and Statistics

All aggression was assayed within the first thirty minutes of lights ON time (Zeitgeber hours 0–0.5) and scored in MATLAB (MathWorks). Video data were collected using HMX-F80 camcorders (Samsung). Behavior chambers assembled on clear agarose with a yeast/sucrose-based food top were placed on top of an LED light pad (AGPtek). Fly movements were tracked using CalTech FlyTracker 1.0.5 (Eyrún Eyjólfsdóttir & Pietro Perona, Caltech, available for download at http://www.vision.caltech.edu/Tools/FlyTracker/) and lunges were subsequently quantified using the Janelia Automatic Animal Behavior Annotator (JAABA) (Kabra *et al.* 2013).

The lunge classifier (Certel_lungeClassifier.jab) was designed in JAABA (referencing human-scored data) and used to detect lunges from individual flies. Annotated frames were postprocessed in JAABA with the internal post-processing filter set at 0.06, a value that provided the best signal-to-noise ratio *a posteriori* for lunge classification. An additional post-processing filter was applied in MATLAB using JAABA postprocessed files in combination with tracking data to eliminate misclassified lunges detected at a distance of two or more fly body lengths. Total number of lunges, wing threats, and unilateral wing extensions were scored for a period of 30 minutes after the first lunge using a custom MATLAB script (analysis.m). The time between the beginning of the video recording and the first lunge was used for calculating the latency to lunge. Inter-male courtship was defined as the number of unilateral wing extensions (singing) followed by additional courtship behaviors (licking, abdomen bends, repeated wing extensions, etc.) (Yamamoto and Koganezawa 2013). Holding and boxing were scored for a period of 10 minutes after the first lunge as described previously (Penn *et al.* 2010; Davis *et al.* 2018). All graphs were generated with Prism (GraphPad Software) and Adobe Illustrator CS6 (Adobe). For data that did not meet parametric assumptions, a Kruskal-Wallis test with Dunn's multiple comparison was used unless otherwise specified. A Mann-Whitney test was performed in the case of only two comparisons.

Immunohistochemistry

Adult male brains were dissected and fixed in 4% paraformaldehyde (Electron Microscopy Sciences) for 30 minutes and labeled using a modification of protocols previously described (Certel and Johnson 1996). After repeated PBT washes (1X phosphate-buffered saline, 1% Triton X-100) at room temperature, blocking solution (1X phosphate-buffered saline, 2% normal goat serum, 2%w/v bovine serum albumin, 1% Triton X-100) was applied and primary antibodies were left to incubate overnight. Secondary antibodies were applied the next day after repeated washes in blocking solution. The following primary and secondary antibodies were used: anti-bruchpilot (mAb nc82, 1:40, Developmental Studies Hybridoma Bank developed under the auspices of the NICHD and maintained by the Department of Biology, University of Iowa (Iowa City, IA).), monoclonal rabbit anti-GFP (1:350, Molecular Probes), mAb dVGLUT (1:10) (Sherer *et al.* 2020), and mAB mGluR (1:400) (Eroglu *et al.* 2003). Secondary antibodies conjugated to Alexa 488, Alexa 594, or Alexa 647 (Molecular Probes) were used at a

concentration of 1:200. Labeled brains were mounted in Vectashield (Vector Labs, #H1000). Images were collected on a Zeiss LSM780 laser scanning confocal mounted on an inverted Axio Observer microscope and processed using ImageJ (NIH) and Adobe Photoshop (Adobe).

References

Aguilar J. I., M. Dunn, S. Mingote, C. S. Karam, Z. J. Farino, *et al.*, 2017 Neuronal depolarization drives increased dopamine synaptic vesicle loading via VGLUT. Neuron 95: 1074-1088.e7. https://doi.org/10.1016/J.NEURON.2017.07.038

Albert P. R., 2012 Transcriptional regulation of the 5-HT1A receptor: implications for mental illness. Philos Trans R Soc B Biol Sci 367: 2402–2415. https://doi.org/10.1098/RSTB.2011.0376

Andlauer T. F. M., S. Scholz-Kornehl, R. Tian, M. Kirchner, H. A. Babikir, *et al.*, 2014 Drep-2 is a novel synaptic protein important for learning and memory. Elife 3: 1–24. https://doi.org/10.7554/ELIFE.03895

Andrews J. C., M. de la P. Fernández, Q. Yu, G. P. Leary, A. K. Leung, *et al.*, 2014 Octopamine neuromodulation regulates Gr32a-linked aggression and courtship pathways in Drosophila males, (T. Clandinin, Ed.). PLOS Genet 10: e1004356. https://doi.org/10.1371/journal.pgen.1004356

Aso Y., D. Sitaraman, T. Ichinose, K. R. Kaun, K. Vogt, *et al.*, 2014 Mushroom body output neurons encode valence and guide memory-based action selection in Drosophila. Elife 3: e04580. https://doi.org/10.7554/eLife.04580

Awata H., M. Takakura, Y. Kimura, I. Iwata, T. Masuda, *et al.*, 2019 The neural circuit linking mushroom body parallel circuits induces memory consolidation in Drosophila. Proc Natl Acad Sci U S A 116: 16080–16085. https://doi.org/10.1073/pnas.1901292116

Banerjee S., S. Vernon, W. Jiao, B. J. Choi, E. Ruchti, *et al.*, 2021 Miniature neurotransmission is required to maintain Drosophila synaptic structures during ageing. Nat Commun 2021 121 12: 1–12. https://doi.org/10.1038/s41467-021-24490-1

Barnea G., W. Strapps, G. Herrada, Y. Berman, J. Ong, *et al.*, 2008 The genetic design of signaling cascades to record receptor activation. Proc Natl Acad Sci 105: 64–69. https://doi.org/10.1073/PNAS.0710487105

Bayliss A., G. Roselli, and P. D. Evans, 2013 A comparison of the signalling properties of two

tyramine receptors from Drosophila. J Neurochem 125: 37–48.
https://doi.org/10.1111/JNC.12158

Benelli G., N. Desneux, D. Romano, G. Conte, R. H. Messing, *et al.*, 2015 Contest experience
enhances aggressive behaviour in a fly: when losers learn to win. Sci Rep 5: 9347.
https://doi.org/10.1038/srep09347

Berridge C. W., B. E. Schmeichel, and R. A. España, 2012 Noradrenergic modulation of
wakefulness/arousal. Sleep Med Rev 16: 187–197.
https://doi.org/10.1016/J.SMRV.2011.12.003

Blair R. J. R., 2016 The Neurobiology of Impulsive Aggression. J Child Adolesc
Psychopharmacol 26: 4–9.

Blenau W., J. A. Wilms, S. Balfanz, and A. Baumann, 2020 AmOctα2R: Functional
Characterization of a Honeybee Octopamine Receptor Inhibiting Adenylyl Cyclase Activity.
Int J Mol Sci 2020, Vol 21, Page 9334 21: 9334. https://doi.org/10.3390/IJMS21249334

Boer S. F. de, 2018 Animal models of excessive aggression: implications for human aggression
and violence. Curr Opin Psychol 19: 81–87.

Bogdanik L., R. Mohrmann, A. Ramaekers, J. Bockaert, Y. Grau, *et al.*, 2004 The Drosophila
metabotropic glutamate receptor DmGluRA regulates activity-dependent synaptic
facilitation and fine synaptic morphology. J Neurosci 24: 9105–9116.
https://doi.org/10.1523/JNEUROSCI.2724-04.2004

Brady A. E., and P. J. Conn, 2008 Metabotropic glutamate receptor ligands as novel therapeutic
agents, pp. 529–564 in *The Glutamate Receptors*, Humana Press.

Burke C. J., W. Huetteroth, D. Owald, E. Perisse, M. J. Krashes, *et al.*, 2012 Layered reward
signalling through octopamine and dopamine in Drosophila. Nature 492: 433–437.
https://doi.org/10.1038/nature11614

Burnstock G., 2004 Cotransmission. Curr Opin Pharmacol 4: 47–52.
https://doi.org/10.1016/j.coph.2003.08.001

Busch S., M. Selcho, K. Ito, and H. Tanimoto, 2009 A map of octopaminergic neurons in the
Drosophila brain. J Comp Neurol 513: 643–667. https://doi.org/10.1002/cne.21966

Bylund D. B., D. C. Eikenberg, J. P. Hieble, S. Z. Langer, R. J. Lefkowitz, *et al.*, 1994
International Union of Pharmacology Nomenclature of Adrenoceptors. Pharmacol Rev 46:
121–136.

Cassidy K. A., D. R. MacNulty, D. R. Stahler, D. W. Smith, and L. D. Mech, 2015 Group
composition effects on aggressive interpack interactions of gray wolves in Yellowstone
National Park. Behav Ecol 26: 1352–1360. https://doi.org/10.1093/beheco/arv081

Certel S. J., and W. A. Johnson, 1996 Disruption of Mesectodermal Lineages by Temporal
Misexpression of the Drosophila POU-Domain Transcription Factor, Drifter. Dev Genet 18:
279–288. https://doi.org/10.1002/(SICI)1520-6408(1996)18:4

Certel S. J., M. G. Savella, D. C. Schlegel, and E. A. Kravitz, 2007 Modulation of Drosophila
male behavioral choice. Proc Natl Acad Sci U S A 104: 4706–4711.
https://doi.org/10.1073/pnas.0700328104

Certel S. J., A. K. Leung, C.-Y. Lin, P. Perez, A.-S. Chiang, *et al.*, 2010 Octopamine
neuromodulatory effects on a social behavior decision-making network in Drosophila
males, (W. S. Leal, Ed.). PLoS One 5: e13248.
https://doi.org/10.1371/journal.pone.0013248

Certel S. J., and E. A. Kravitz, 2012 Scoring and analyzing aggression in Drosophila. Cold
Spring Harb Protoc 2012: 319–325. https://doi.org/10.1101/pdb.prot068130

Chowdhury B., M. Wang, J. P. Gnerer, and H. A. Dierick, 2021 The Divider Assay is a high-
throughput pipeline for aggression analysis in Drosophila. Commun Biol 4: 1–12.
https://doi.org/10.1038/s42003-020-01617-6

Claßen G., and H. Scholz, 2018 Octopamine shifts the behavioral response from indecision to
approach or aversion in Drosophila melanogaster. Front Behav Neurosci 12: 131.
https://doi.org/10.3389/fnbeh.2018.00131

Conn P. J., C. W. Lindsley, and C. K. Jones, 2009 Activation of metabotropic glutamate receptors
as a novel approach for the treatment of schizophrenia. Trends Pharmacol Sci 30: 25–31.

Connor D., and J. Rubin, 2010 Guanfacine extended release in the treatment of attention deficit
hyperactivity disorder in children and adolescents. Drugs Today (Barc) 46: 299–314.
https://doi.org/10.1358/DOT.2010.46.5.1450095

Covington H. E., E. L. Newman, M. Z. Leonard, and K. A. Miczek, 2019 Translational models of
adaptive and excessive fighting: An emerging role for neural circuits in pathological
aggression. F1000Research 8: 963.

Davis S. M., A. L. Thomas, L. Liu, I. M. Campbell, and H. A. Dierick, 2018 Isolation of
aggressive behavior mutants in Drosophila using a screen for wing damage. Genetics 208:

273–282. https://doi.org/10.1534/genetics.117.300292

De-Miguel F. F., C. Leon-Pinzon, P. Noguez, and B. Mendez, 2015 Serotonin release from the neuronal cell body and its long-lasting effects on the nervous system. Philos Trans R Soc B Biol Sci 370: 20140196. https://doi.org/10.1098/rstb.2014.0196

Devaud J. M., C. Clouet-Redt, J. Bockaert, Y. Grau, and M. L. Parmentier, 2008 Widespread brain distribution of the Drosophila metabotropic glutamate receptor. Neuroreport 19: 367–371. https://doi.org/10.1097/WNR.0B013E3282F524C7

Devoto P., G. Flore, P. Saba, S. Scheggi, G. Mulas, *et al.*, 2019 Noradrenergic terminals are the primary source of α2-adrenoceptor mediated dopamine release in the medial prefrontal cortex. Prog Neuro-Psychopharmacology Biol Psychiatry 90: 97–103. https://doi.org/10.1016/j.pnpbp.2018.11.015

Drouin C., A. C. Bobadilla, and J. P. Tassin, 2017 Norepinephrine. Curated Ref Collect Neurosci Biobehav Psychol 625–646. https://doi.org/10.1016/B978-0-12-809324-5.03130-8

Duistermars B. J., B. D. Pfeiffer, E. D. Hoopfer, and D. J. Anderson, 2018 A brain module for scalable control of complex, multi-motor threat displays. Neuron 100: 1474-1490.e4. https://doi.org/10.1016/j.neuron.2018.10.027

Eroglu Ç., B. Brügger, F. Wieland, and I. Sinning, 2003 Glutamate-binding affinity of Drosophila metabotropic glutamate receptor is modulated by association with lipid rafts. Proc Natl Acad Sci U S A 100: 10219–10224. https://doi.org/10.1073/pnas.1737042100

Evans P. D., and B. Maqueira, 2005 Insect octopamine receptors: a new classification scheme based on studies of cloned Drosophila G-protein coupled receptors. Invertebr Neurosci 2005 53 5: 111–118. https://doi.org/10.1007/S10158-005-0001-Z

Fan P., D. S. Manoli, O. M. Ahmed, Y. Chen, N. Agarwal, *et al.*, 2013 Genetic and neural mechanisms that inhibit drosophila from mating with other species. Cell 154: 89–102. https://doi.org/10.1016/j.cell.2013.06.008

Farooqui T., 2012 Review of octopamine in insect nervous systems. Open access insect physiol 4: 1–17. https://doi.org/10.2147/OAIP.S20911

Frånberg O., M. M. Marcus, and T. H. Svensson, 2012 Involvement of 5-HT2A receptor and α2-adrenoceptor blockade in the asenapine-induced elevation of prefrontal cortical monoamine outflow. Synapse 66: 650–660. https://doi.org/10.1002/SYN.21551

Frye M. A., T. A. Ketter, L. L. Altshuler, K. Denicoff, R. T. Dunn, *et al.*, 1998 Clozapine in

bipolar disorder: treatment implications for other atypical antipsychotics. J Affect Disord 48: 91–104. https://doi.org/10.1016/S0165-0327(97)00160-2

Gregg T. R., and A. Siegel, 2001 Brain structures and neurotransmitters regulating aggression in cats: Implications for human aggression. Prog Neuro-Psychopharmacology Biol Psychiatry 25: 91–140. https://doi.org/10.1016/S0278-5846(00)00150-0

Gupta T., H. R. Morgan, J. C. Andrews, E. R. Brewer, and S. J. Certel, 2017 Methyl-CpG binding domain proteins inhibit interspecies courtship and promote aggression in Drosophila. Sci Rep 7: 5420. https://doi.org/10.1038/s41598-017-05844-6

Haller J., and M. R. Kruk, 2006 Normal and abnormal aggression: human disorders and novel laboratory models. Neurosci Biobehav Rev 30: 292–303. https://doi.org/10.1016/J.NEUBIOREV.2005.01.005

Hartenstein V., J. J. Omoto, K. T. Ngo, D. Wong, P. A. Kuert, *et al.*, 2018 Structure and development of the subesophageal zone of the Drosophila brain. I. Segmental architecture, compartmentalization, and lineage anatomy. J Comp Neurol 526: 6–32. https://doi.org/10.1002/cne.24287

Hedqvist P., and L. Gustafsson, 1981 Transsynaptic control of the release of noradrenaline and acetylcholine by prostaglandin E2 and adenosine. Physiol Excit Membr 259–265. https://doi.org/10.1016/B978-0-08-026816-3.50037-7

Holm K. J., and A. Markham, 2012 Mirtazapine. Drugs 1999 574 57: 607–631. https://doi.org/10.2165/00003495-199957040-00010

Hoopfer E. D., Y. Jung, H. K. Inagaki, G. M. Rubin, and D. J. Anderson, 2015 P1 interneurons promote a persistent internal state that enhances inter-male aggression in Drosophila. Elife 4: e11346. https://doi.org/10.7554/eLife.11346

Hoopfer E. D., 2016 Neural control of aggression in Drosophila. Curr Opin Neurobiol 38: 109–118. https://doi.org/10.1016/J.CONB.2016.04.007

Inagaki H. K., S. Ben-Tabou de-Leon, A. M. Wong, S. Jagadish, H. Ishimoto, *et al.*, 2012 Visualizing neuromodulation in vivo: TANGO-mapping of dopamine signaling reveals appetite control of sugar sensing. Cell 148: 583–595. https://doi.org/10.1016/j.cell.2011.12.022

Ji-Quan Wang, and Anna-Liisa Brownell, 2007 Development of Metabotropic Glutamate Receptor Ligands for Neuroimaging. Curr Med Imaging Rev 3: 186–205.

https://doi.org/10.2174/157340507781387059

Kabra M., A. A. Robie, M. Rivera-Alba, S. Branson, and K. Branson, 2013 JAABA: interactive machine learning for automatic annotation of animal behavior. Nat Methods 2012 101 10: 64–67. https://doi.org/10.1038/nmeth.2281

Kamisaki Y., T. Hamahashi, T. Hamada, K. Maeda, and T. Itoh, 1992 Presynaptic inhibition by clonidine of neurotransmitter amino acid release in various brain regions. Eur J Pharmacol 217: 57–63. https://doi.org/10.1016/0014-2999(92)90511-2

Kim S. M., C.-Y. Su, and J. W. Wang, 2017 Neuromodulation of innate behaviors in Drosophila. Annu Rev Neurosci 40: 327–348. https://doi.org/10.1146/annurev-neuro-072116-031558

Kiyose K., M. Katsuki, Y. Suzaki, K. Okada, and Y. Okada, 2021 Octopaminergic system orchestrates combat and mating behaviors: A potential regulator of alternative male mating tactics in an armed beetle. J Insect Physiol 131: 104211. https://doi.org/10.1016/J.JINSPHYS.2021.104211

Kravitz E. A., and M. de la P. Fernández, 2015 Aggression in Drosophila. Behav Neurosci 129: 549–563.

Kumari R., C. Castillo, and A. Francesconi, 2013 Agonist-dependent signaling by group I metabotropic glutamate receptors is regulated by association with lipid domains. J Biol Chem 288: 32004–32019. https://doi.org/10.1074/jbc.M113.475863

Langer S. Z., 2008 Presynaptic autoreceptors regulating transmitter release. Neurochem Int 52: 26–30. https://doi.org/10.1016/j.neuint.2007.04.031

Langer S. Z., 2015 α2-Adrenoceptors in the treatment of major neuropsychiatric disorders. Trends Pharmacol Sci 36: 196–202.

Levitz J., C. Habrian, S. Bharill, Z. Fu, R. Vafabakhsh, *et al.*, 2016 Mechanism of Assembly and Cooperativity of Homomeric and Heteromeric Metabotropic Glutamate Receptors. Neuron 92: 143–159. https://doi.org/10.1016/J.NEURON.2016.08.036

Machado D. R., D. J. Afonso, A. R. Kenny, A. Öztürk-Çolak, E. H. Moscato, *et al.*, 2017 Identification of octopaminergic neurons that modulate sleep suppression by male sex drive. Elife 6: e23130. https://doi.org/10.7554/eLife.23130

Masuzzo A., G. Manière, A. Viallat-Lieutaud, É. Avazeri, O. Zugasti, *et al.*, 2019 Peptidoglycan-dependent NF-κB activation in a small subset of brain octopaminergic neurons controls female oviposition. Elife 8: e50559. https://doi.org/10.7554/eLife.50559

Mather M., D. Clewett, M. Sakaki, and C. W. Harley, 2016 Norepinephrine ignites local hotspots of neuronal excitation: How arousal amplifies selectivity in perception and memory. Behav Brain Sci 39: e200. https://doi.org/10.1017/S0140525X15000667

McGuire S. E., P. T. Le, and R. L. Davis, 2001 The Role of Drosophila Mushroom Body Signaling in Olfactory Memory. Science (80-) 293: 1330–1333. https://doi.org/10.1126/SCIENCE.1062622

McKinney H., L. M. Sherer, J. L. Williams, S. J. Certel, and R. S. Stowers, 2020 Characterization of Drosophila octopamine receptor neuronal expression using MiMIC-converted Gal4 lines. J Comp Neurol cne.24883. https://doi.org/10.1002/cne.24883

Meltzer H. Y., 1980 Relevance of Dopamine Autoreceptors for Psychiatry: Preclinical and Clinical Studies. Schizophr Bull 6: 456–475. https://doi.org/10.1093/SCHBUL/6.3.456

Mestikawy S. El, Å. Wallén-Mackenzie, G. M. Fortin, L. Descarries, and L.-É. Trudeau, 2011 From glutamate co-release to vesicular synergy: vesicular glutamate transporters. Nat Rev Neurosci 12: 204–216. https://doi.org/10.1038/nrn2969

Mingote S., A. Amsellem, A. Kempf, S. Rayport, and N. Chuhma, 2019 Dopamine-glutamate neuron projections to the nucleus accumbens medial shell and behavioral switching. Neurochem Int 129: 104482. https://doi.org/10.1016/j.neuint.2019.104482

Moustaine D. El, S. Granier, E. Doumazane, P. Scholler, R. Rahmeh, *et al.*, 2012 Distinct roles of metabotropic glutamate receptor dimerization in agonist activation and G-protein coupling. Proc Natl Acad Sci 109: 16342–16347. https://doi.org/10.1073/PNAS.1205838109

Nässel D. R., 2018 Substrates for neuronal cotransmission with neuropeptides and small molecule neurotransmitters in Drosophila. Front Cell Neurosci 12: 83. https://doi.org/10.3389/fncel.2018.00083

Nässel D. R., and M. Zandawala, 2019 Recent advances in neuropeptide signaling in Drosophila, from genes to physiology and behavior. Prog Neurobiol 179: 101607. https://doi.org/10.1016/J.PNEUROBIO.2019.02.003

Nelson R. J., and B. C. Trainor, 2007 Neural mechanisms of aggression. Nat Rev Neurosci 8: 536–546.

Niswender C. M., and P. J. Conn, 2010 Metabotropic glutamate receptors: physiology, pharmacology, and disease. Annu Rev Pharmacol Toxicol 50: 295–322. https://doi.org/10.1146/annurev.pharmtox.011008.145533

Okaty B. W., K. G. Commons, and S. M. Dymecki, 2019 Embracing diversity in the 5-HT neuronal system. Nat Rev Neurosci 1. https://doi.org/10.1038/s41583-019-0151-3

Pagani M., G. W. Albisetti, N. Sivakumar, H. Wildner, M. Santello, *et al.*, 2019 How gastrin-releasing peptide opens the spinal gate for itch. Neuron 103: 102-117.e5. https://doi.org/10.1016/j.neuron.2019.04.022

Palavicino-Maggio C. B., Y.-B. Chan, C. McKellar, and E. A. Kravitz, 2019 A small number of cholinergic neurons mediate hyperaggression in female Drosophila. Proc Natl Acad Sci U S A 116: 17029–17038. https://doi.org/10.1073/pnas.1907042116

Panneels V., C. Eroglu, P. Cronet, and I. Sinning, 2003 Pharmacological characterization and immunoaffinity purification of metabotropic glutamate receptor from Drosophila overexpressed in Sf9 cells. Protein Expr Purif 30: 275–282. https://doi.org/10.1016/S1046-5928(03)00100-1

Penn J. K., M. F. Zito, and E. A. Kravitz, 2010 A single social defeat reduces aggression in a highly aggressive strain of Drosophila. Proc Natl Acad Sci U S A 107: 12682–12686. https://doi.org/10.1073/pnas.1007016107

Qi Y., G. Xu, G. Gu, F. Mao, G. Ye, *et al.*, 2017 A new Drosophila octopamine receptor responds to serotonin. Insect Biochem Mol Biol 90: 61–70. https://doi.org/10.1016/J.IBMB.2017.09.010

Rillich J., B. Rillich, and P. A. Stevenson, 2019 Differential modulation of courtship behavior and subsequent aggression by octopamine, dopamine and serotonin in male crickets. Horm Behav 114: 104542. https://doi.org/10.1016/J.YHBEH.2019.06.006

Rinne J. O., K. Wesnes, J. Hänninen, M. Murphy, H. Riordan, *et al.*, 2013 Safety and efficacy of ORM-12741 on cognitive and behavioral symptoms in patients with Alzheimer's disease: A randomized, double-blind, proof-of-concept study. J Neurol Sci 333: e322. https://doi.org/10.1016/J.JNS.2013.07.1199

Sara S. J., and S. Bouret, 2012 Orienting and Reorienting: The Locus Coeruleus Mediates Cognition through Arousal. Neuron 76: 130–141. https://doi.org/10.1016/J.NEURON.2012.09.011

Saunders C., and L. E. Limbird, 1999 Localization and trafficking of α2-adrenergic receptor subtypes in cells and tissues. Pharmacol Ther 84: 193–205. https://doi.org/10.1016/S0163-7258(99)00032-7

Sayin S., J. F. De Backer, K. Siju, M. E. Wosniack, L. P. Lewis, *et al.*, 2019 A neural circuit arbitrates between persistence and withdrawal in hungry Drosophila. Neuron 104: 544-558.e6. https://doi.org/10.1016/j.neuron.2019.07.028

Schoenfeld B. P., R. J. Choi, C. H. Choi, A. M. Terlizzi, P. Hinchey, *et al.*, 2013 The Drosophila DmGluRA is required for social interaction and memory. Front Pharmacol 4: 64. https://doi.org/10.3389/fphar.2013.00064

Sherer L. M., E. Catudio Garrett, H. R. Morgan, E. D. Brewer, L. A. Sirrs, *et al.*, 2020 Octopamine neuron dependent aggression requires dVGLUT from dual-transmitting neurons, (G. Hasan, Ed.). PLOS Genet 16: e1008609. https://doi.org/10.1371/journal.pgen.1008609

Shigemoto R., A. Kinoshita, E. Wada, S. Nomura, H. Ohishi, *et al.*, 1997 Differential Presynaptic Localization of Metabotropic Glutamate Receptor Subtypes in the Rat Hippocampus. J Neurosci 17: 7503–7522. https://doi.org/10.1523/JNEUROSCI.17-19-07503.1997

Shin M., J. M. Copeland, and B. J. Venton, 2018 Drosophila as a model system for neurotransmitter measurements. ACS Chem Neurosci acschemneuro.7b00456. https://doi.org/10.1021/acschemneuro.7b00456

Starke K., 2001 Presynaptic autoreceptors in the third decade: focus on α2-adrenoceptors. J Neurochem 78: 685–693. https://doi.org/10.1046/J.1471-4159.2001.00484.X

Svensson E., J. Apergis-Schoute, G. Burnstock, M. P. Nusbaum, D. Parker, *et al.*, 2019 General principles of neuronal co-transmission: insights from multiple model systems. Front Neural Circuits 12: 117. https://doi.org/10.3389/fncir.2018.00117

Swanson C. J., M. Bures, M. P. Johnson, A. M. Linden, J. A. Monn, *et al.*, 2005 Metabotropic glutamate receptors as novel targets for anxiety and stress disorders. Nat Rev Drug Discov 4: 131–144.

Toivonen J. M., G. A. Walker, P. Martinez-Diaz, I. Bjedov, Y. Driege, *et al.*, 2007 No Influence of Indy on Lifespan in Drosophila after Correction for Genetic and Cytoplasmic Background Effects. PLOS Genet 3: e95. https://doi.org/10.1371/JOURNAL.PGEN.0030095

Trudeau L.-É., and S. El Mestikawy, 2018 Glutamate cotransmission in cholinergic, GABAergic and monoamine systems: contrasts and commonalities. Front Neural Circuits 12: 113. https://doi.org/10.3389/fncir.2018.00113

Vaaga C. E., M. Borisovska, and G. L. Westbrook, 2014 Dual-transmitter neurons: functional implications of co-release and co-transmission. Curr Opin Neurobiol 29: 25–32. https://doi.org/10.1016/j.conb.2014.04.010

Vogt K., C. Schnaitmann, K. V. Dylla, S. Knapek, Y. Aso, *et al.*, 2014 Shared mushroom body circuits underlie visual and olfactory memories in Drosophila. Elife 3: e02395. https://doi.org/10.7554/ELIFE.02395

Votava M., L. Hess, and M. Kršiak, 2008 Selective antiaggressive effect of an alpha-2 adrenoceptor agonist naphthylmedetomidine in mice. Aggress Behav 34: 394–403. https://doi.org/10.1002/ab.20253

Watanabe N., I. M. Omori, A. Nakagawa, A. Cipriani, C. Barbui, *et al.*, 2012 Safety Reporting and Adverse-Event Profile of Mirtazapine Described in Randomized Controlled Trials in Comparison with Other Classes of Antidepressants in the Acute-Phase Treatment of Adults with Depression. CNS Drugs 2010 241 24: 35–53. https://doi.org/10.2165/11319480-000000000-00000

Wolf M. U., Y. Goldberg, and M. Freedman, 2018 Aggression and agitation in dementia. Continuum (N Y) 24: 783–803. https://doi.org/10.1212/CON.0000000000000605

Wu C.-L., M.-F. M. Shih, P.-T. Lee, and A.-S. Chiang, 2013 An octopamine-mushroom body circuit modulates the formation of anesthesia-resistant memory in Drosophila. Curr Biol 23: 2346–2354. https://doi.org/10.1016/j.cub.2013.09.056

Wu S.-F., G. Xu, Y.-X. Qi, R.-Y. Xia, J. Huang, *et al.*, 2014 Two splicing variants of a novel family of octopamine receptors with different signaling properties. J Neurochem 129: 37–47. https://doi.org/10.1111/JNC.12526

Yamamoto D., and M. Koganezawa, 2013 Genes and circuits of courtship behaviour in Drosophila males. Nat Rev Neurosci 2013 1410 14: 681–692. https://doi.org/10.1038/nrn3567

Yellman C., H. Tao, B. He, and J. Hirsh, 1997 Conserved and sexually dimorphic behavioral responses to biogenic amines in decapitated Drosophila. Proc Natl Acad Sci U S A 94: 4131–4136. https://doi.org/10.1073/pnas.94.8.4131

Youn H., C. Kirkhart, J. Chia, and K. Scott, 2018 A subset of octopaminergic neurons that promotes feeding initiation in Drosophila melanogaster, (F. Marion-Poll, Ed.). PLoS One 13: e0198362. https://doi.org/10.1371/journal.pone.0198362

Zhang K., J. Z. Guo, Y. Peng, W. Xi, and A. Guo, 2007 Dopamine-Mushroom Body Circuit
Regulates Saliency-Based Decision-Making in Drosophila. Science (80-) 316: 1901–1904.
https://doi.org/10.1126/SCIENCE.1137357

Zhang S., J. Qi, X. Li, H.-L. Wang, J. P. Britt, *et al.*, 2015 Dopaminergic and glutamatergic
microdomains in a subset of rodent mesoaccumbens axons. Nat Neurosci 18: 386–396.
https://doi.org/10.1038/nn.3945

Zheng Z., J. S. Lauritzen, E. Perlman, C. G. Robinson, M. Nichols, *et al.*, 2018 A complete
electron microscopy volume of the brain of adult Drosophila melanogaster. Cell 174: 730-
743.e22. https://doi.org/10.1016/j.cell.2018.06.019

Zhou C., Y. Rao, and Y. Rao, 2008 A subset of octopaminergic neurons are important for
Drosophila aggression. Nat Neurosci 11: 1059–1067. https://doi.org/10.1038/nn.2164

Discussion

To understand how neurotransmission is controlled within individual neurons, how neuronal control of transmitter release impacts circuit activity, and/or how circuit activity alters behavior of the unique functional capabilities of dual transmission must be included (Nusbaum *et al.* 2001; Burnstock 2004; Nässel 2018; Trudeau and El Mestikawy 2018; Svensson *et al.* 2019). While significant progress has been made characterizing both the neurotransmitters, neuromodulators, and neuropeptides that colocalize within individual neurons and the mechanisms of co-release and co-transmission (Hökfelt *et al.* 2003; Vaaga *et al.* 2014), the functional properties at the cellular level of dual transmitting neurons that result in changes to behavior in the organism are not understood.

The experiments in Aim 1 demonstrated that OA neurons express dVGLUT and utilized a new genetic tool to remove dVGLUT in OA-glutamate neurons (Sherer *et al.* 2020). We quantified changes in aggressive behaviors resulting from a loss of dVGLUT and determined that dVGLUT in brain OGNs is required to promote male aggression. When encountering another fly, males determine its sex via pheromonal information, and subsequently decide to fight or court. Previous work has shown that OA neurons are critical in facilitating this decision (Certel *et al.* 2010; Andrews *et al.* 2014), raising the question of whether dVGLUT is required from OGNs for courtship. Males lacking dVGLUT did not exhibit an increase in unilateral wing extensions, indicating that dVGLUT is not required in the decision to court. These results establish a previously undetermined role for dVGLUT in brain OA neurons and reveal glutamate uncouples aggression from inter-male courtship. Secondly, we used MiMIC Trojan-Gal4 lines to characterize expression of the alpha and beta OA receptors and identified possible OA and glutamate autoreceptors within OA neurons (McKinney *et al.* 2020). Lastly, we demonstrate expression of OAα2R and DmGluRA in VPM4 and examine the role of these autoreceptors in constraining mid-intensity and high-intensity aggressive behaviors. RNAi-mediated knockdown of either OAα2R or DmGluRA in males results in a significant increase in the number of boxing and holding bouts (high-intensity aggressive behavior) without changing the number of lunges (medium-intensity aggressive behavior) performed. Moreover, RNAi reduction of either the rate-limiting enzyme in OA synthesis TβH (i.e., decreasing OA release) or OAα2R (i.e., increasing

OA release) demonstrate a secondary role for OA release from VPM4 in inhibiting inter-male courtship and suggest the involvement of VPM4 within multiple decision-making circuits.

Our results demonstrated that dual transmission within OGNs is a significant factor in the behavioral outputs that occur as a result of dual transmission of fast-acting glutamate and a slow-acting monoamine. Several studies have suggested that the expression of glutamate in monoaminergic neurons serves only to modulate the quantal level of the monoamine in SVs (El Mestikawy *et al.* 2011; Münster-Wandowski *et al.* 2016; Aguilar *et al.* 2017). In this interpretation, glutamate release from OA neurons would not serve to alter behavior, and a lack of glutamate in OA neurons would only reduce the strength of aminergic signaling. In contrast to these studies, we have demonstrated a functional role for glutamate release from OA neurons. We have determined that the release of both OA and glutamate are required from OGNs for aggressive behavior. Notably, we also identified a functional role for glutamate in uncoupling OA-dependent promotion of aggression and OA-dependent inhibition of courtship. Our lab and others have demonstrated that OA release is required to promote aggression and inhibit courtship (Hoyer *et al.* 2008; Certel *et al.* 2010; Andrews *et al.* 2014). If the only role of glutamate in OGNs were to enhance OA release, we would have expected to see an increase in courtship when dVGLUT was reduced only in brain neurons equal to the increase in courtship when both OA and dVGLUT were reduced. However, we saw wild-type levels of courtship when VGLUT expression was reduced in brain neurons, indicating that OA was still capable of being loaded into vesicles and released despite the lack of vesicular synergy. Furthermore, we saw no further increase in courtship between males lacking both OA and VGLUT relative to males lacking only OA, indicating that only OA release functions to inhibit courtship. These changes in courtship suggest differences in signaling between OA and glutamate from OGNs on courtship-related circuitry (likely through spatial segregation) and indicate that regardless of any vesicular synergy within OGNs, dVGLUT co-expression serves a functional role in promoting aggression.

In vertebrates, it has been proposed that co-transmission from dopamine-glutamate neurons in the nucleus accumbens medial shell might facilitate shifts in behavioral responses (Mingote *et al.* 2017, 2019) This behavioral switching was attributed to differences in postsynaptic neurons. Our work with glutamate and OA autoreceptors in VPM4 suggests a possible presynaptic mechanism for shifts between mutually-exclusive behaviors. Our data show that decreased OA release from

VPM4 results in increased courtship, and that increased OA release due to the loss of autoreceptor-facilitated negative feedback results in increased aggression. This result demonstrates a switch between two mutually-exclusive behaviors mediated by a single autoreceptor that is able to inhibit OA release. An interesting investigation might involve examining whether specific autoreceptors are uniformly present at all synaptic boutons by using antibodies specific to autoreceptors or conditionally-expressed, fluorescently labeled autoreceptor genetic tools (as in Aim 1). Many studies have indicated that postsynaptic neurons can modulate their responses to transmitter release through selective expression of receptors (Dugué *et al.* 2005; Kapoor *et al.* 2016; Nässel 2018; Brewer *et al.* 2019; Cai *et al.* 2021). Could presynaptic neurons modulate their local transmitter outputs in the same way via selective trafficking of inhibitory autoreceptors to presynaptic terminals? Such a specialized mechanism would provide further explanation of how dual transmitting neurons are able to elicit diverse responses and would provide insight into how the neuronal mechanisms that constrain and promote aggressive behavior might be (dys)regulated.

References

Aguilar J. I., M. Dunn, S. Mingote, C. S. Karam, Z. J. Farino, *et al.*, 2017 Neuronal depolarization drives increased dopamine synaptic vesicle loading via VGLUT. Neuron 95: 1074-1088.e7. https://doi.org/10.1016/J.NEURON.2017.07.038

Andrews J. C., M. de la P. Fernández, Q. Yu, G. P. Leary, A. K. Leung, *et al.*, 2014 Octopamine neuromodulation regulates Gr32a-linked aggression and courtship pathways in Drosophila males, (T. Clandinin, Ed.). PLOS Genet. 10: e1004356. https://doi.org/10.1371/journal.pgen.1004356

Brewer J. C., A. C. Olson, K. M. Collins, and M. R. Koelle, 2019 Serotonin and neuropeptides are both released by the HSN command neuron to initiate Caenorhabditis elegans egg laying, (A. C. Hart, Ed.). PLOS Genet. 15: e1007896. https://doi.org/10.1371/journal.pgen.1007896

Burnstock G., 2004 Cotransmission. Curr. Opin. Pharmacol. 4: 47–52. https://doi.org/10.1016/j.coph.2003.08.001

Cai Y., B. E. Nielsen, E. E. Boxer, J. Aoto, and C. P. Ford, 2021 Loss of nigral excitation of cholinergic interneurons contributes to parkinsonian motor impairments. Neuron 109: 1137-1149.e5. https://doi.org/10.1016/J.NEURON.2021.01.028

Certel S. J., A. K. Leung, C.-Y. Lin, P. Perez, A.-S. Chiang, *et al.*, 2010 Octopamine neuromodulatory effects on a social behavior decision-making network in Drosophila males, (W. S. Leal, Ed.). PLoS One 5: e13248. https://doi.org/10.1371/journal.pone.0013248

Dugué G. P., A. Dumoulin, A. Triller, and S. Dieudonné, 2005 Target-Dependent Use of Coreleased Inhibitory Transmitters at Central Synapses. J. Neurosci. 25: 6490–6498. https://doi.org/10.1523/JNEUROSCI.1500-05.2005

Hökfelt T., T. Bartfai, and F. Bloom, 2003 Neuropeptides: opportunities for drug discovery. Lancet Neurol. 2: 463–472. https://doi.org/10.1016/S1474-4422(03)00482-4

Hoyer S. C., A. Eckart, A. Herrel, T. Zars, S. A. Fischer, *et al.*, 2008 Octopamine in male aggression of Drosophila. Curr. Biol. 18: 159–167. https://doi.org/10.1016/J.CUB.2007.12.052

Kapoor V., A. C. Provost, P. Agarwal, and V. N. Murthy, 2016 Activation of raphe nuclei triggers rapid and distinct effects on parallel olfactory bulb output channels. Nat. Neurosci. 2016 192 19: 271–282. https://doi.org/10.1038/nn.4219

McKinney H., L. M. Sherer, J. L. Williams, S. J. Certel, and R. S. Stowers, 2020 Characterization of Drosophila octopamine receptor neuronal expression using MiMIC-converted Gal4 lines. J. Comp. Neurol. cne.24883. https://doi.org/10.1002/cne.24883

Mestikawy S. El, Å. Wallén-Mackenzie, G. M. Fortin, L. Descarries, and L.-É. Trudeau, 2011 From glutamate co-release to vesicular synergy: vesicular glutamate transporters. Nat. Rev. Neurosci. 12: 204–216. https://doi.org/10.1038/nrn2969

Mingote S., N. Chuhma, A. Kalmbach, G. M. Thomsen, Y. Wang, *et al.*, 2017 Dopamine neuron dependent behaviors mediated by glutamate cotransmission. Elife 6: e27566. https://doi.org/10.7554/eLife.27566

Mingote S., A. Amsellem, A. Kempf, S. Rayport, and N. Chuhma, 2019 Dopamine-glutamate neuron projections to the nucleus accumbens medial shell and behavioral switching. Neurochem. Int. 129: 104482. https://doi.org/10.1016/j.neuint.2019.104482

Münster-Wandowski A., J.-F. Zander, K. Richter, and G. Ahnert-Hilger, 2016 Co-existence of functionally different vesicular neurotransmitter transporters. Front. Synaptic Neurosci. 8: 4. https://doi.org/10.3389/fnsyn.2016.00004

Nässel D. R., 2018 Substrates for neuronal cotransmission with neuropeptides and small molecule neurotransmitters in Drosophila. Front. Cell. Neurosci. 12: 83. https://doi.org/10.3389/fncel.2018.00083

Nusbaum M. P., D. M. Blitz, A. M. Swensen, D. Wood, and E. Marder, 2001 The roles of co-transmission in neural network modulation. Trends Neurosci. 24: 146–154. https://doi.org/10.1016/S0166-2236(00)01723-9

Sherer L. M., E. Catudio Garrett, H. R. Morgan, E. D. Brewer, L. A. Sirrs, *et al.*, 2020 Octopamine neuron dependent aggression requires dVGLUT from dual-transmitting neurons, (G. Hasan, Ed.). PLOS Genet. 16: e1008609. https://doi.org/10.1371/journal.pgen.1008609

Svensson E., J. Apergis-Schoute, G. Burnstock, M. P. Nusbaum, D. Parker, *et al.*, 2019 General principles of neuronal co-transmission: insights from multiple model systems. Front. Neural Circuits 12: 117. https://doi.org/10.3389/fncir.2018.00117

Trudeau L.-É., and S. El Mestikawy, 2018 Glutamate cotransmission in cholinergic, GABAergic and monoamine systems: contrasts and commonalities. Front. Neural Circuits 12: 113. https://doi.org/10.3389/fncir.2018.00113

Vaaga C. E., M. Borisovska, and G. L. Westbrook, 2014 Dual-transmitter neurons: functional implications of co-release and co-transmission. Curr. Opin. Neurobiol. 29: 25–32. https://doi.org/10.1016/j.conb.2014.04.010